# How the structure and physical chemistry of dietary fibre can help make healthier foods

## Kathrin Haider

A thesis submitted in fulfilment of the

requirements of the degree of

Doctor of Philosophy

July 2022

University of East Anglia

Quadram Institute Bioscience

## Preface

This thesis was submitted to the University of East Anglia (Norwich, UK) for the degree of Doctor of Philosophy. The work presented herein was undertaken at the Quadram Institute Bioscience (Norwich, UK) from April 2018 to July 2022. This research is supported by the UKRI Biotechnology and Biological Sciences Research Council Norwich Research Park Biosciences Collaborative Training Partnership [Grant No. BB/P011640/1] in collaboration with Mondelēz International.

## Access Condition & Agreement

# Abstract

There is substantial evidence supporting the beneficial health effects of dietary fibres. Due to the huge diversity of dietary fibres, it is highly challenging to classify them in a manner to predict health outcomes in humans. The overall aim of this thesis was to link the physico-chemical properties of a range of dietary fibres to their functionality in physiological mechanisms in duodenal digestion.

Cereal brans as well as isolated fibres like β-glucan, inulin and cellulose were characterised in terms of rheological, colligative or binding properties. This information is used to understand the impact of dietary fibre on lipid digestion, dietary fibre interaction with bile acids as well as dietary fibre's effect on starch gelatinisation and digestion in *in vitro* digestion models.

Barley fibres appeared more potent in delaying lipolysis than oat fibres. The presence of insoluble dietary fibre was found to enhance the effects of oat β-glucan. Lipase activity was reduced substantially by both barley and oat brans but not to the same extent by its β-glucan extracts. Barley and oat bran retained bile acids but purified β-glucan did not. Cereal dietary fibre has the potential to slow down lipid digestion via increased viscosity, bile acid and/or lipase interaction. The physico-chemical properties of the isolated fibres β-glucan, inulin and cellulose determined their impact on starch gelatinization via acting as a plasticizer or water competitor. This was tested in a realistic food matrix by incorporating dietary fibre into biscuits, which led to reduced starch digestibility with one of the tested inulins.

This research in combination with the current literature helps to classify the different forms of fibre, their behaviour during digestion, and the resulting physiological benefits. Important properties of dietary fibres for health benefits are physiological solubility, viscosity, interaction with water and physico-chemical binding.

## Outputs from this Project

**Peer-reviewed article:**

Colosimo, R., Mulet-Cabero, A.I., Cross, K.L., **Haider, K.,** Edwards, C.H., Warren, F.J., Finnigan, T.J. and Wilde, P.J., 2021. β-glucan release from fungal and plant cell walls after simulated gastrointestinal digestion. Journal of Functional Foods, 83.

**Book chapter:**

**Haider K**, Wilde P (2020). 'Digestion and Metabolism of Pectin'. In: Kontogiorgos, V. (eds) Pectin: Technological and Physiological Properties. Springer, Cham.

**Conference presentations:**

Poster: 'Interference of dietary fibre with lipolysis: method of administration of barley and oat β-glucans (BG) - intact bran vs extracted BG' at the 7th International Conference on Food Digestion, 3-5 May 2022, Cork, Ireland.

Runner up poster award: 'How understanding the structure and physical chemistry of dietary fibre helps make healthier foods' at the EDESIA Conference: diverse food, healthy people, 17 March 2022, organised by the Wellcome Trust EDESIA PhD programme, Norwich, UK.

Talk: '*In vitro* lipid digestion impacted by dietary fibre β-glucans and intact brans' at the 7th International conference on Food Chemistry and Technology, 8-10 November 2021, organised by the United Scientific Group, online.

**Science communication:**

Quadram institute Bioscience Instagram account takeover in May 2021: 'Fibre Challenge' highlight @quadraminstitute with information about dietary fibre and how to increase dietary fibre intake.

# Table of Contents

**Chapter 4 – Interaction of cereal dietary fibres with bile acids and β-glucan-release kinetics of barley bran and oat bran .....................................150**

## List of Figures

**Appendices**

## List of Tables

---

**Appendices**

# List of Equations

# List of Abbreviations

| | |
|---|---|
| a.u. | Arbitrary units |
| AACC | American Association of Cereal Chemists |
| AOAC | Association of Official Analytical Chemists (now AOAC International) |
| Ara | Arabinose |
| Ara/Xyl | Arabinose to xylose |
| ASBT | Apical sodium-dependent bile acid transporter |
| AX | Arabinoxylan |
| BA | Bile acid |
| BB | Barley bran |
| BG | β-glucan, short for mixed linkage (1→3),(1→4)-β-D-glucan |
| C* | Critical coil overlap concentration |
| CA | Cholic acid |
| cat# | Catalogue number |
| CDCA | Chenodeoxycholic acid |
| CHD | Coronary heart disease |
| CLF | Cholyl-Lysyl-Fluorescein |
| CMC | Critical micellar concentration |
| CV | Cardiovascular |
| CVD | Cardiovascular disease |
| d.m. | dry matter |
| d4-CA | Deuterated cholic acid |
| d4-CDCA | Deuterated chenodeoxycholic acid |
| d4-DCA | Deuterated deoxycholic acid |
| d4-GCA | Deuterated glycocholic acid |
| d4-GCDCA | Deuterated glycochenodeoxycholic acid |
| d4-LCA | Deuterated lithocholic acid |
| DCA | Deoxycholic acid |
| DF | Dietary fibre |

| | |
|---|---|
| DHCA | Dehydrocholic acid |
| DMSO | Dimethyl sulfoxide |
| DP | Degree of Polymerisation |
| DSC | Differential Scanning Calorimetry |
| dw | Dry weight |
| FDA | U.S. Food and Drug Administration |
| FFA | Free fatty acid |
| GCA | Glycocholic acid |
| GCDCA | Glycochenodeoxycholic acid |
| GDCA | Glycodeoxycholic acid |
| GHCA | Glycohyocholic acid |
| GHDCA | Glycohyodeoxycholic acid |
| GI | Gastrointestinal |
| GLCA | Glycolithocholic acid |
| GUDCA | Glycoursodeoxycholic acid |
| HDCA | Hyodeoxycholic acid |
| HPAEC | High-performance anion-exchange chromatography |
| HPLC | High-performance liquid chromatography |
| HPMC | Hydroxypropyl methylcellulose |
| IDF | Insoluble dietary fibre |
| LCA | Lithocholic acid |
| LC-MS/MS | Liquid chromatography-mass spectrometry/mass spectrometry |
| LiBr | Lithium bromide |
| m/z | Mass-to-charge ratio |
| MAG | Monoacylglycerol |
| MCA | Muricholic acid |
| MU | Monomeric units |
| Mw | Molecular weight |
| n.a. | Not applicable |
| n.d. | Not determined |
| n.t. | Not tested |

| | |
|---|---|
| NCP | Non-cellulosic polysaccharide |
| O/W | oil-in-water |
| OB | Oat bran |
| OHF | Oat hull fibre |
| PAD | Pulsed amperometric detection |
| PAHBAH | P-hydroxybenzoic acid hydrazide |
| PBS | Phosphate buffered saline |
| PCW | Plant cell wall |
| RFO | Raffinose family of oligosaccharides |
| RI | Refractive index |
| RPM | Revolutions per minute |
| SCFA | Short chain fatty acids |
| SEC | Size-exclusion chromatography |
| SGF | Simulated gastric fluid |
| SIF | Simulated intestinal fluid |
| SSF | Simulated salivary fluid |
| TAG | Triacylglycerol |
| TAME | P-toluene-sulfonyl-L-arginine methyl ester |
| TCA | Taurocholic acid |
| TCDCA | Taurochenodeoxycholic acid |
| TDCA | Taurodeoxycholate |
| TDHCA | Taurodehydrocholic acid |
| THCA | Taurohyocholic acid |
| THDCA | Taurohyodeocycholic acid |
| TLCA | Taurolithocholic acid |
| TUDCA | Tauroursodeoxycholic acid |
| T-α-MCA | Tauro-α-Muricholic acid |
| T-β-MCA | Tauro- β -Muricholic acid |
| UDCA | Ursodeoxycholic acid |
| $V_h$ | hydrodynamic radius |
| w/o | Without |
| WB | Wheat bran |

| | |
|---|---|
| ww | Wet weight |
| XRD | X-ray diffraction |
| Xyl | Xylose |
| α-MCA | α-Muricholic acid |
| β-MCA | β-Muricholic acid |

# Chapter 1 – Introduction and literature review

## 1.1 Introduction and problem statement

Around 50 years ago, we started to understand that dietary fibre (DF) is not solely an undigestible by-product of our food (Burkitt *et al.* 1972) but rather an essential part of a healthy diet (Stephen *et al.* 2017, Reynolds *et al.* 2019, Larrosa *et al.* 2020). DF is generally defined as carbohydrate polymers with three or more monomeric units, which are neither digested nor absorbed in the human upper intestinal tract (Stephen *et al.* 2017) but may be fermented by commensal bacteria in the lower gut. Early observations of health benefits included gut regularity and laxative effects (Walker 1961); later, the potential of DF to reduce the risk of hyperlipidaemia, type 2 diabetes, obesity, and various types of cancer, was observed (Stephen *et al.* 2017, Reynolds *et al.* 2019).

The DF definition includes a wide range of naturally occurring and synthetically modified compounds with substantial variations in physical and chemical properties and subsequent potential physiological effects (Poutanen *et al.* 2018). The range of compounds is diverse and further work is needed to more closely characterise specific types of DF and link their properties to mechanisms behind specific health benefits. Once we understand the relations between the structure of DF, its physico-chemical properties and physiological benefits, we can start to predict the

health benefits of different DFs and develop healthier ingredients and foods (Poutanen *et al.* 2018).

The aim of this literature review was to determine the current knowledge relating to DF structure-function relationships with a focus on the influence of DF on small intestinal digestion from a fundamental and an applied food science perspective.

## 1.2 The concept of dietary fibre

### 1.2.1 Definition

There is no worldwide harmonized definition for DF. The simplest way to define DF is to say it is the edible part of plants or analogous carbohydrates, which resist hydrolysis by digestive enzymes in the upper GI tract of humans and are described further by The American Association of Cereal Chemists (AACC) as being completely or partially fermented in the large intestine (AACC 2001, Dhingra *et al.* 2012). The European Union definition, is aligned with the CODEX Alimentarius Alinorm definition (Codex Alimentarius Commission 2009) which states that DF means "carbohydrate polymers with three or more monomeric units (MU), which are neither digested nor absorbed in the human small intestine" and are either naturally occurring in the food as consumed or have been shown to have a beneficial physiological effect if obtained from food raw material or are edible synthetic carbohydrate polymers (Regulation (EU) No 1169/2011). The FDA has set up a review process for beneficial

positive health effects and publishes a list of fibres which can be declared on package labelling as DF when the putative health effect is sufficiently documented (see Table 1.1). Similarly, it was suggested by the International Carbohydrate Quality Consortium (ICQC) to distinguish between supplemented fibres and those endogenous to foods on food product labelling (Augustin *et al.* 2020), which has to be done by keeping records of the added ingredients as the analytical methods available to quantify the undigestible fraction of a food, i.e. the total dietary fibre content, do not differentiate them. The most current methods are AOAC 2009.01 and 2011.25 methods which use enzymatic-chemical methods followed by liquid chromatography and measure all DF constituents which fall under the CODEX definition (McCleary *et al.* 2010).

The recommended daily DF intake for adults is approximately 30 g per day for most countries (Stephen *et al.* 2017), but it is under discussion whether this value should be increased to 50 g/day to protect against colon cancer (O'Keefe 2017). However, most people do not consume the currently recommended daily DF intake (Stephen *et al.* 2017), therefore strategies are required to close this gap, e.g. via fortification of commercially manufactured products (Dhingra *et al.* 2012).

*Table 1.1 – Isolated or synthetic carbohydrates approved by the FDA as DF due to their respective health effect (U.S. Food and Drug Administration 2018, U.S. Food and Drug Administration 2021)*

| Dietary fibre | Source | Health effect |
|---|---|---|
| Cellulose | Isolated | Improved laxation |
| Guar gum | Isolated | Attenuating blood cholesterol levels |
| Pectin | Isolated | |
| Locust bean gum | Isolated | |
| Hydroxypropylmethyl-cellulose | Synthetic | |
| Glucomannan | Isolated | |
| β-glucan soluble fibre | Isolated | Reducing the risk of coronary heart disease |
| Psyllium husk | Isolated | |
| Arabinoxylan | Isolated | Beneficial effect on blood glucose and/or insulin levels |
| Alginate | Isolated | |
| High amylose starch (resistant starch 2) | Isolated | |
| Cross linked phosphorylated resistant starch 4 (regardless of source) | Isolated, modified | |
| Acacia (Gum Arabic) | Isolated | |
| Inulin and inulin-type fructans | Isolated | Improving absorption of calcium |
| Galactooligosaccharide | Synthetic | |
| Resistant maltodextrin/dextrin | Synthetic | |
| Polydextrose | Synthetic | Reduced energy intake during subsequent meals |
| "Mixed plant cell wall fibres" | Isolated | Beneficial effect considered for cellulose, pectin, β-glucan, and/or arabinoxylan of which at least two have to be present |

## 1.2.2    Diversity of dietary fibre

The broad definition of DF means that it covers a diverse range of constituents with many different structural and chemical properties including a range of molecular sizes (Dhingra *et al.* 2012). Molecular species include cellulose, arabinoxylans (AX), galactomannans, glucomannans, β-glucan (BG), inulin, lignin, chitin, pectin, resistant dextrins and oligosaccharides. It is important to sufficiently describe the DF characteristics used in nutrition research (Poutanen *et al.* 2018), since the function can differ even if it refers to a fibre sharing the same name. E.g. AX from psyllium are highly branched polymers, although they have a low arabinose-to-xylan ratio (0.30), and therefore show a high gelling property. This is different from the AXs found in e.g. wheat bran which are largely insoluble since they are to a high extent covalently crosslinked to each other or to other constituents of the cell wall as well as having a lower branching density and therefore less likely to form molecular entanglements (Izydorczyk 2009, Parker *et al.* 2005). It is thought that the properties of BG and AX depend on their molecular weight (Mw), which was suggested to be >100 kDa for BG and >20 kDa for AX in order to show an effect on postprandial glucose and insulin response (Biorklund *et al.* 2005, Gemen *et al.* 2011). Increasing fullness or decreasing appetite after a meal has been shown to depend on a low mannuronic:guluronic acids ratio for alginate (Jensen *et al.* 2012)

and the degree of esterification for pectin (Wanders *et al.* 2014), both subject to their gel-forming properties.

The level of purity or presence of associated compounds should also be considered. Most DFs are not pure polymers but rather crude plant constituents and therefore contain also other compounds like protein, phytate, phytochemicals (lignans, stanols and sterols) or vitamins and minerals (Gemen *et al.* 2011). Purified single compound DFs have the advantage of being well defined and quantifiable, which makes them easier to compare. However, they are rarely consumed as such, which was recently acknowledged by the FDA by adding "mixed plant cell wall fibres" to the DF definition (see Table 1.1). This concept refers to ingredients that contain two or more plant cell wall components like cellulose, pectin, lignin, BG and AX, which can be present in varying proportions (U.S. Food and Drug Administration 2018).

The diversity makes it difficult to find a satisfying classification for DFs. Approaches are based on fibre constituents or components, origin or their role in the plant (Stephen *et al.* 2017, Tungland and Meyer 2002). In an attempt to classify DF in a more functional manner, it is assumed that important properties are: solubility, viscosity and fermentability (see Table 1.2). However this classification has the limitation that neither of the three properties is a distinct, exclusive category but should rather be seen as a

continuum with fibre types fitting into several sections on the spectrum depending not only on intrinsic but also on extrinsic conditions (Gidley and Yakubov 2019) as discussed further in section 1.5.

*Table 1.2 – Traditional classification of fibres based on three characteristics which are insufficiently defined (modified according to (Slavin 2013))*

| Physico-chemical property | Fibre types |
|---|---|
| Soluble fibres | β-glucan<br>Gums<br>Wheat dextrin<br>Psyllium<br>Pectins<br>Inulin |
| Insoluble fibres | Cellulose<br>Lignin<br>Some pectins<br>Some hemicelluloses like arabinoxylan |
| Fermentable fibres | Wheat dextrin<br>Pectins<br>β-glucans<br>Guar gum<br>Inulin |
| Less fermentable fibres | Cellulose<br>Lignin |
| Viscous fibres | Pectins<br>β-glucans<br>Some gums (e.g. guar gum)<br>Psyllium |
| Non-viscous fibre | Polydextrose<br>Inulin |

### 1.2.3 Plant cell walls as dietary fibres

Most DFs we consume derive from plant cell walls (PCWs) (McDougall *et al.* 1996). PCWs have highly complex structures to perform a range of specialised functions during the life of the plant (Waldron *et al.* 2003) such as nutrient storage, water transport, providing rigidity (McDougall *et al.* 1996) and acting as the first line of defence from biotic and abiotic stresses (Houston *et al.* 2016).
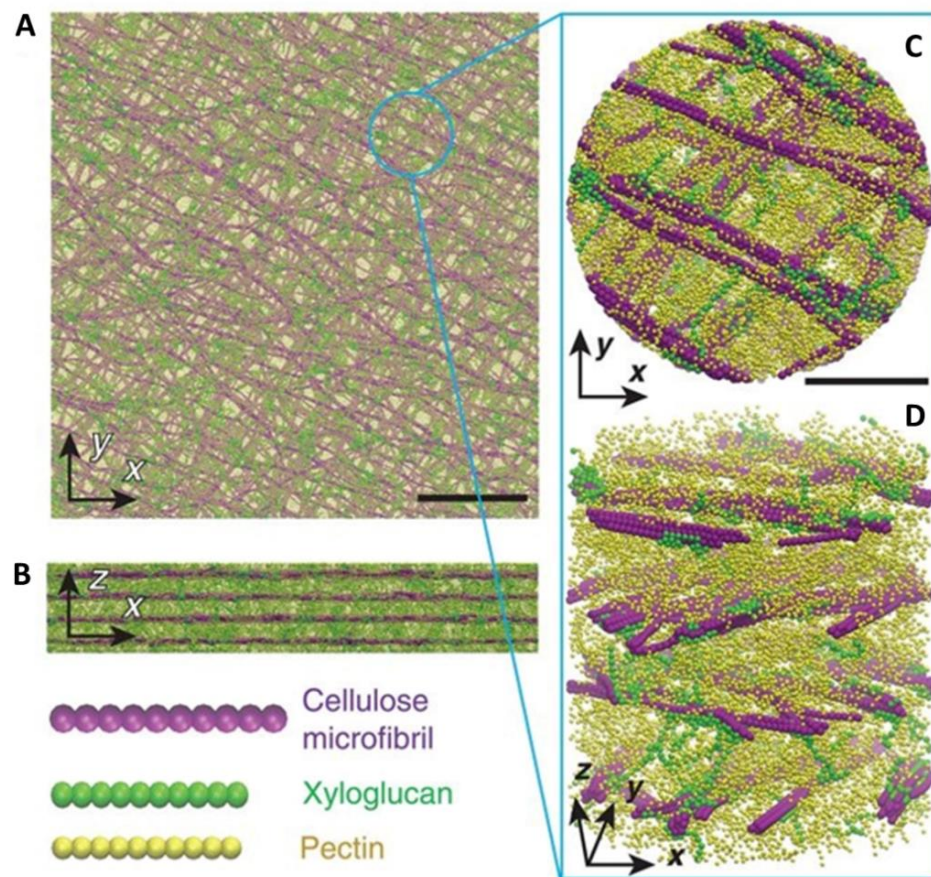


*Figure 1.1 – Plant cell wall structure model of an onion epidermal wall: Top (A) and side (B) views of the four-lamella wall at the same scale and close-ups (C and D) of the top and side views [modified from Zhang et al. (Zhang et al. 2021a)]*

Figure 1.1 shows a diagram of an onion PCW to display the assembly of the structure. The main component categories in PCWs are cellulose, non-cellulosic polysaccharides (NCPs), proteins and polyphenolic compounds. Cellulose consists of β-(1→4)linked glucopyranose residues (see Figure 1.2A); the main NCPs are pectin and hemicelluloses which include AX or mixed linkage BG among others (Figure 1.2). Pectins constitute a heterogenous group of polysaccharides with galacturonic acid units with distinct structures most commonly homogalacturan and rhamnogalacturan (see Figure 1.2C). The degree of substitution with rhamnose residues and the degree of methyl esterification of the acid groups varies and leads to different properties (Tosh and Yada 2010). Pectic polysaccharides form structural components of PCWs but are also intercellular cementing substances (McDougall *et al.* 1996). They often have calcium bridges between non-esterified rhamnogalacturan regions, so solubilisation from the cell wall structure usually requires chelation of $Ca^{2+}$ (Selvendran and Robertson 1990) whereas most hemicelluloses require alkali extraction (McDougall *et al.* 1996). Backbones of hemicelluloses usually consist of β(1→4)linked xylose, mannose or glucose residues (Figure 1.2A+B). There are structural differences in the xylans depending on their origin (McDougall *et al.* 1996). On a molecular architecture level of PCWs, the pattern of xylan substitution seems to be important for interaction with cellulose in PCWs (Grantham *et al.* 2017).

**(A)**

**(B)**
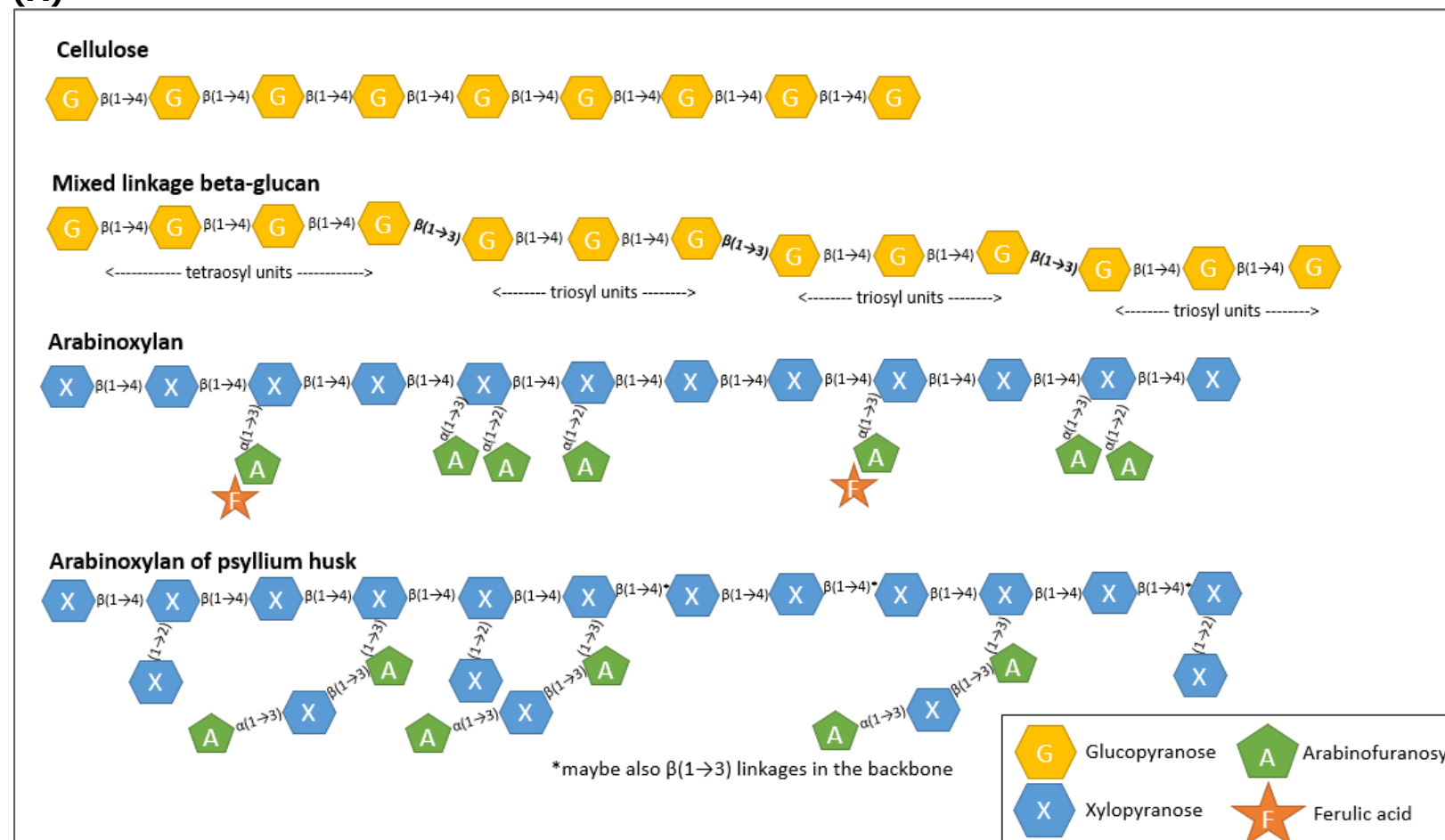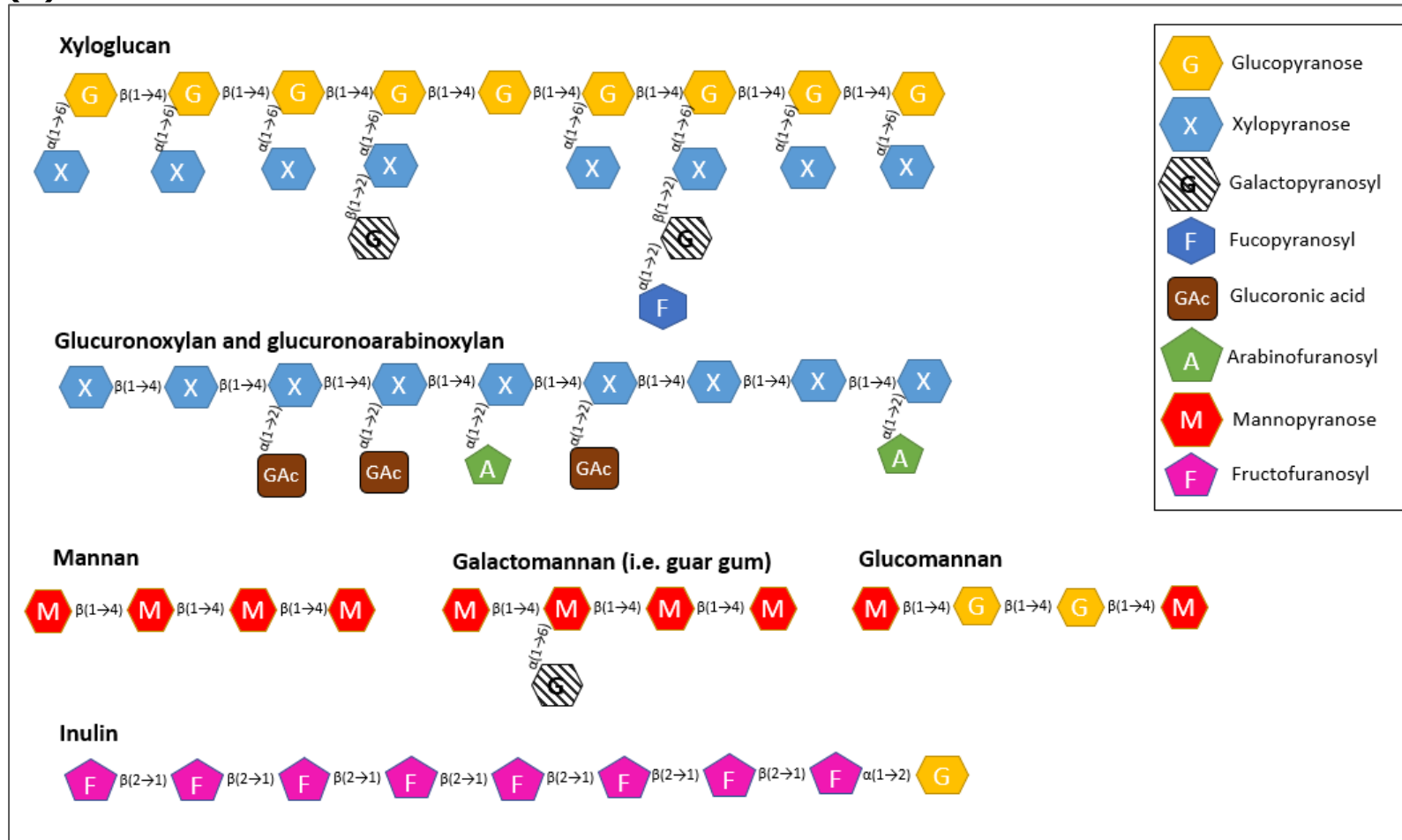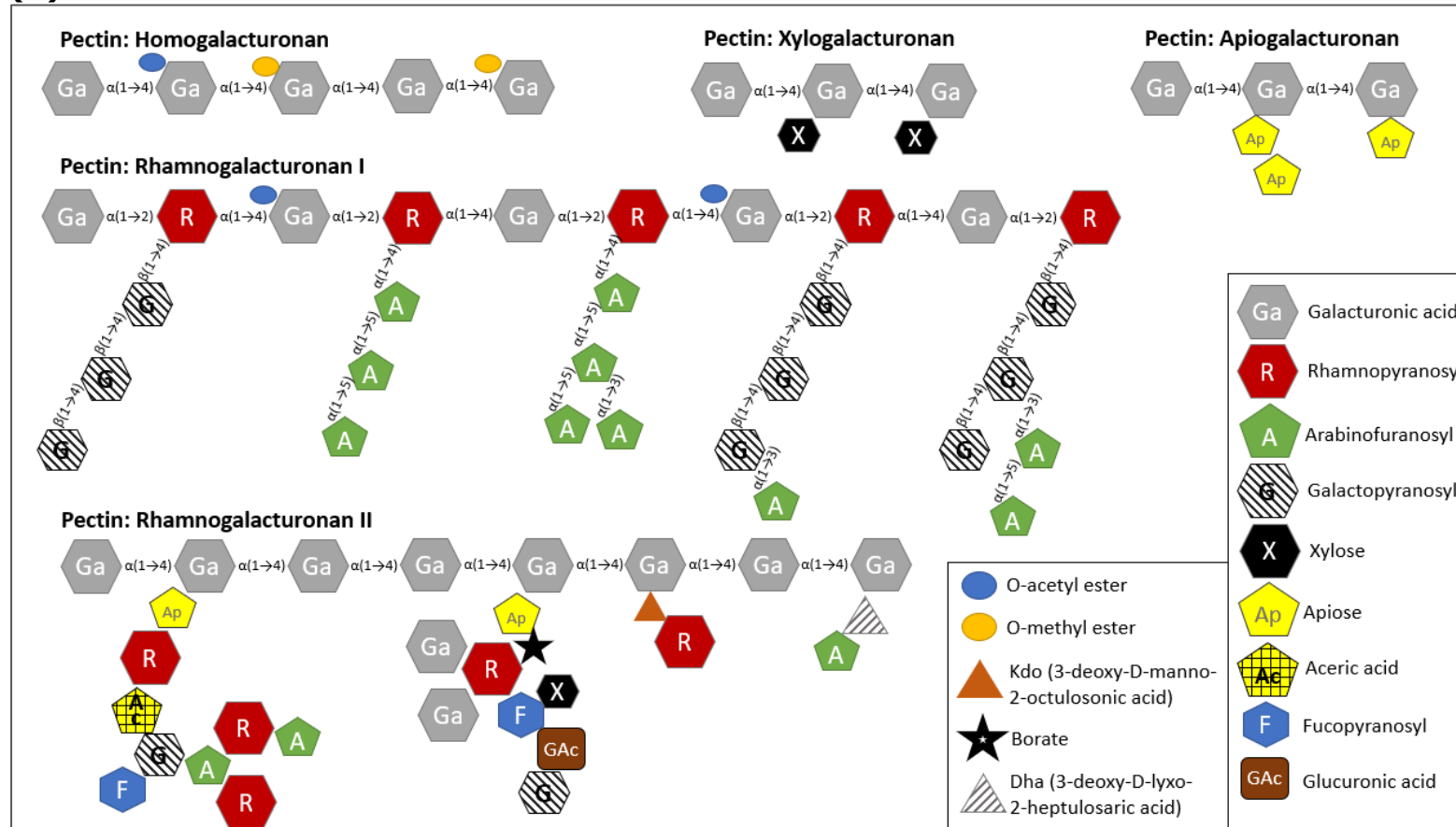
*Figure 1.2 – Schematic representation of the structures of (A) cellulose, mixed linkage β-glucan, arabinoxylans; (B) xyloglucan, glucuronoxylans, mannans, inulin; and (C) pectins; not representative of their chain length (Drawn according to (Stephen et al. 2017) and modified from (Blackman et al. 2014) and (Leclere et al. 2013)).*

AXs (Figure 1.2A) consist of a linear xylan backbone which is either unsubstituted, monosubstituted with arabinofuranosyl at O-2, monosubstituted at O-3 with ferulic acid residue esterified at arabinofuranosyl or disubstituted at O-2,3 (Izydorczyk 2009). Important characteristics of AXs are the arabinose to xylose (Ara/Xyl) ratio, the substitution pattern, and the average degree of polymerization of the xylan backbone (Courtin and Delcour 2002, Izydorczyk 2009). In wheat, the Ara/Xyl ratio of AXs is lower in the bran (0.5 – 0.7) than in the endosperm (1 – 1.2), which means that the former is less branched (Andersson *et al.* 2003, Kamal-Eldin *et al.* 2009, Nilsson *et al.* 1997).

BG (Figure 1.2A) has a structure of D-glucose units linked with a mix of β-(1→4) and β-(1→3)-glycosidic bonds to form a linear polymer. The ratios of tri- to tetramers blocks and of β-(1→4) and β-(1→3) linkages in the polysaccharide chain as well as other structural features appear to be important determinants of their physical properties, such as water solubility, viscosity, and gelation properties and for their physiological action in the gastrointestinal (GI) tract (Lazaridou and Biliaderis 2007). Barley BGs have a ratio of trisaccharides/tetrasaccharides of 3:1 whereas oat and wheat show 2:1 and 4:1 respectively (Wang and Ellis 2014).

Lignin is not a carbohydrate but rather a phenolic compound formed by the polymerisation of coniferyl, p-coumaryl and sinapyl alcohols.

Lignins are usually covalently linked to polysaccharides, especially to hemicelluloses in secondary PCWs (Terrett and Dupree 2019), both directly via sugar residues and indirectly via ferulic acid esterified to polysaccharides, and make the PCW more rigid (McDougall *et al.* 1996). They vary in Mw but show in general greater resistance than any other cell wall polymer in nature due to strong intramolecular bonding including carbon to carbon linkages which makes lignin very inert (Dhingra *et al.* 2012).
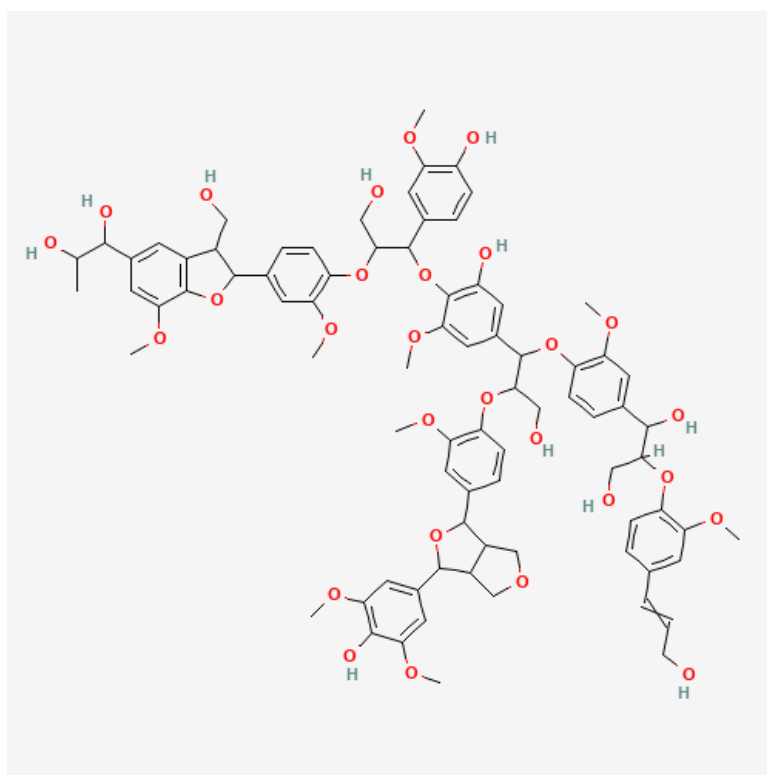


*Figure 1.3 – Chemical structure of lignin [Picture from https://pubchem.ncbi.nlm.nih.gov]*

All these PCW components are assembled to form a cell wall matrix, a certain molecular architecture (Figure 1.1). How the constituents are cross-linked will impact how they maintain their cross-links or

change (e.g. solubilise) under physiological conditions. However, there is still limited information available on the complex supramolecular assemblies of cell wall polymers (Grantham *et al.* 2017, Grundy *et al.* 2016, Selvendran and Robertson 1990, Terrett and Dupree 2019).

### 1.2.4 Resistant starch

Starch is a complex polysaccharide comprised of a glucose homopolymer with α-(1,4) linkages in the form of amylose, an unbranched, linear chain, and amylopectin, a branched form. Uncooked (ungelatinized) starch has a crystalline structure which makes it less digestible for human amylases (Edwards and Warren 2019). This and other structural properties can cause starch to escape digestion in the small intestine and is then called resistant starch (RS). RS  falls under the DF definition of most countries. RS can be inaccessible to digestion for five main reasons: it is physically entrapped by an indigestible plant matrix (type 1 or RS1); the starch granule is naturally resistant such as in an uncooked potato and high amylose maize (RS2); the starch structure is changed during processing such as heating and cooling (RS3); the starch has been chemically modified by esterification, crosslinking, or transglycosylation to resist digestion and is not found in nature (RS4) (Lattimer and Haub 2010); or contains an amylose-lipid complex (RS5) (Hasjim *et al.* 2013).

## 1.2.5    Inulin

Inulin is a plant energy storage carbohydrate (Williams *et al.* 2017) consisting of fructose units (Figure 1.2B), which varies substantially in its degree of polymerisation (DP) (Lattimer and Haub 2010). Inulin is utilised as a functional food ingredient since it can be used as a replacement for fat and soluble carbohydrates (Lattimer and Haub 2010) and especially because it has a pleasant, slightly sweet taste (Chawla and Patil 2010). It is usually derived from chicory roots. Although it is generally regarded as soluble and non-viscous (Table 1.2), its solubility depends on intrinsic and extrinsic factors (Franck 2002) and it can increase the viscosity of a food matrix (Tsatsaragkou *et al.* 2021). Inulin is rapidly and completely fermented by the microbiota in the colon (Lattimer and Haub 2010).

## 1.3    Sources of dietary fibre, food matrix & processing

### 1.3.1    Cereals

Adult populations in Western Europe and the US consume at least two thirds of their DF from cereals (Stephen *et al.* 2017). Cereal DF is mainly contained in the bran, which is comprised of the outer parts of the cereal grain consisting of the pericarp, testa and the aleurone layer. The type of grain, its genetic/agricultural origin and the processing influence the chemical composition of brans (Kamal-Eldin *et al.* 2009).

### 1.3.1.1  Wheat

In wheat bran, AX is the main DF (22-30 wt%) and its content can vary depending on genotype and environmental conditions (Dornez *et al.* 2008, Kamal-Eldin *et al.* 2009). Other DF components of wheat bran are cellulose, lignin and BG in decreasing amounts (Kamal-Eldin *et al.* 2009).

### 1.3.1.2  Oats

According to the definition by AACC (1989) oat bran should consist of at least 5.5% BG and 16% total DF. Generally, oat bran has a total DF content between 10 and 19% with BG as the most abundant fibre (4.7-8.3%), followed by AX (2.3-4.7%) cellulose (1.2-4.2%) and lignin (1.0-2.0%). (Luhaloo *et al.* 1998) Oat flakes consist, like the bran, of the pericarp and the testa but also the endosperm and the germ (Grundy *et al.* 2017b).

### 1.3.1.3  Barley

Compared to wheat and oats, barley is less commonly consumed as flour cereal by humans in western countries (AbuMweis *et al.* 2010) nor has it been roller-milled on a large commercial scale to obtain bran and flour (Bhatty 1993). However, since it is rich in BG like oats, there is increasing interest in barley being used as a food ingredient since the 90s (Bhatty 1993). The BG content however depends on genotype and geographic origin, and was found to range from 2.40 to 7.42 g/100 g in a recent study (Martínez *et al.* 2018). BG may be less soluble from barley compared to oat (Lambo *et al.* 2005).

### 1.3.2    Fruits and vegetables

Fresh fruits and vegetables generally contain only about 1-3.5 g total DF/100 g, mostly due to their very high moisture content (between 85 and 95%) (England 2017). In vegetables, the major fibre type apart from cellulose is xyloglucan, which is found at much lower concentrations in cereals where BGs are more abundant. Also the pectin content is much higher in vegetables than in cereals, with about 35% of primary cell wall dry weight in vegetables compared to 5% in cereals (McDougall *et al.* 1996). In fruits (e.g. apple, citrus) and some vegetables (e.g. beetroot), pectins are the most abundant non-cellulose DF constituents  (Stephen *et al.* 2017) and some fruits and vegetables like onions, garlic, Jerusalem artichoke and bananas are high in inulin (Lattimer and Haub 2010).

### 1.3.3    Legumes

Legume or pulse fibre is used for fibre enrichment in some commercially available products. The cotyledon consists of cell wall polysaccharides of varying degrees of solubility. The seed coat or hull fibre consists mainly of water-insoluble polysaccharides as well as some pectin. Legume fibre usually also contains α-galacto-oligosaccharides known as the raffinose family of oligosaccharides (RFO) in appreciable amounts, most notably in soybeans. RFOs have a somewhat negative reputation due to its association with flatulence, but have also been shown to serve as prebiotics with beneficial effects on the human gut microbiota (Tosh and Yada 2010).

In contrast to fruit and vegetable cells which tend to rupture during mastication, cells of boiled legumes can remain largely intact and tend to separate rather than rupture which prevents the release of their content and makes it unavailable for digestion, especially starch, which can remain entrapped inside intact cells and is then transported to the colon as resistant starch type 1 (RS1) (Lovegrove *et al.* 2017).

### 1.3.4 Food matrix and processing

Processing aims at preserving, transforming, destroying or creating food structure, often defined as microstructure at a microscopic level (Aguilera and Stanley 1999). A part of the microstructure, either as a consequence of processing or by nature (see above defined cell wall matrix, section 1.2.3), is the food matrix. Food matrix is regarded as the physical and spatial domain "that contains and/or interacts with specific constituents of a food (e.g. a nutrient) providing functionalities and behaviours which are different from those exhibited by the components in isolation or a free state" (Aguilera 2019).

Processing can change the physico-chemical properties of DF and includes mechanical (grinding), thermal (cooking) or thermo-mechanical (extrusion, cooked-extrusion) but also chemical or enzymatic methods (Guillon and Champ 2000). During hydration, polysaccharides may be released from the cell wall structure. For example, 25-30% of wheat AXs are water-extractable (Courtin and

Delcour 2002). The extractability of AX and BG increased significantly when the flour slurry was allowed to rest before cooking, whereas the Mw of extracted BG decreased compared to no rest time (Rakha *et al.* 2011). Cooking has a big effect on DF. For example it can decrease BG release from oat flakes and flours (Grundy *et al.* 2017a) and it can cause structural changes in other compounds like pectins, which are relatively process-sensitive (Lovegrove *et al.* 2017). Hydrothermal methods may cause the plant cells to swell, which can rupture its walls (Capuano *et al.* 2018), potentially releasing cell contents or exposing them to digestive enzymes. Other nutrients such as starch compete for available water (Grundy *et al.* 2017a) with protein and the cell wall. As well as changing the cell wall integrity, heating can disrupt the intracellular matrix (Capuano *et al.* 2018).

Mechanical processing like grinding, milling, and puréeing destroys the natural matrices of plant materials. Extrusion and flaking employ both heating and particle size reduction (Capuano *et al.* 2018) and have been shown to affect the extractability of hemicelluloses depending on the conditions used. The AX and BG content released from extruded wheat bran could be increased by 0.6 to 2 wt% and up to 3.3 wt% respectively (Andersson *et al.* 2017), which could make a difference within the digestive tract depending on the amount consumed in relation to other nutrients present. Extruded oat bran cereals produced with varying molecular weight of BG

resulted in differences in solubility, with the lower Mw extrudate showing the highest solubility (Brummer *et al.* 2012). The effect of milling on BG solubility was shown with oat flakes resulting in less extractable BG over time but a more gradual release compared to oat flours. This demonstrates the importance of the particle size, including the amount of intact plant cells and their cell walls (Grundy *et al.* 2017a).

Processing can separate or rupture plant cells depending on the type of processing, time and temperature as well as on the plant tissue matrix, i.e. source used, which has implications on nutrient digestibility due to cell wall entrapment (Edwards *et al.* 2021, Bajka *et al.* 2021, Pälchen *et al.* 2022). During cooking, the cell walls become more permeable, and nutrient digestibility usually increases (Holland *et al.* 2020). However, comparing chickpea with durum wheat cells shows that the latter are more permeable and susceptible to cell rupture during hydrothermal processing (Edwards *et al.* 2021). In this example, chickpea cell walls are thicker and contain pectin in the middle lamellar which is solubilised during hydrothermal processing. This weakens the cell-cell adhesion and makes them more likely to separate rather than rupture (Edwards *et al.* 2021).

## 1.4    Human digestion in general and in presence of DF

Figure 1.4 gives an overview of the different stages of digestion in humans. Whole-gut transit time  can take between 34 or 80 hours comparing a high fibre with low a fibre diet, respectively (Burkitt *et al.* 1972). A reduction in transit time after additional fibre intake was confirmed by a more recent study using a wireless motility capsule (SmartPill®) (Timm *et al.* 2011). The following section describes the digestive process in general as well as highlights potential influences of dietary fibre.



**1. Mouth (oral phase)**
Mastication, mixing
Salivary α-amylase
*Particle size and cell breakage*
*→ Nutrient release*

**2. Stomach (gastric phase)**
Mixing
Protease, lipase
*High viscosity can enhance satiation (fullness) and slow down gastric emptying*

**3. Small intestine (duodenal phase)**
Nutrient digestion & uptake
Pancreatin (mix of digestive enzymes)
Bile salts
*Viscosity can slow down digestion kinetics and diffusion to gut wall*
*→ Gut signalling to maintain satiety*
*Interaction with enzymes or bile*

**4. Large intestine (colon phase)**
Water absorption
Microbial fermentation
Nutrient/metabolite production/signalling
*→ Satiety signals, nutrient metabolism*

*Figure 1.4 – Diagram of the stages of human food digestion highlighting the main functions of each and potential role of DF in italics. Blue arrows indicate gut signalling pathways to the brain [modified from (Haider and Wilde 2020)]*

### 1.4.1    Mouth

In the mouth, food is chewed and mixed with salivary fluid. Mastication alters the texture of food and impacts nutrient release

as well as digestion rate. Usually cell breakage takes place during mastication but some plant food sources have been shown to separate rather than rupture which limits access to the nutrients located within the intact plant cells (Mackie 2019, Minekus *et al.* 2014, McDougall *et al.* 1996, Grundy *et al.* 2015). Digestion of food starts in the oral cavity with degradation of starch by salivary α-amylase, which cleaves α-1-4 glycosidic bonds of starch resulting in maltoses and maltooligosaccharides at a pH optimum at pH 6.8 (Pedersen *et al.* 2002, Minekus *et al.* 2014, Whelan 1960).

### 1.4.2 Stomach

Consumed food is swallowed and passes into the stomach, where it is mixed with gastric fluids containing the protease pepsin and gastric lipase as well as hydrochloric acid, which gradually reduces the pH. Also salivary α-amylase is still active and continues to digest starch in the early gastric phase until its activity is reduced by the pH becoming too low and the proteolytic activity in the stomach. Gastric pH during fasting is usually below 2 which increases to around 5 or even higher after food intake depending on the amount and the buffering capacity of the ingested food (Minekus *et al.* 2014). Digesta viscosity can be increased in presence of DF, which can reduce gastric mixing and therefore slow down the pH change within the food bolus (Marciani *et al.* 2000, Marciani *et al.* 2001) which delays protein digestion (Mulet-Cabero *et al.* 2017, Mulet-Cabero *et al.* 2019) as pepsin is mainly active between pH 2 and 4 (Minekus

*et al.* 2014). In studies with pectin or alginate, their physico-chemical behaviour during digestion led to a slower gastric emptying. This prolonged nutrient absorption in the duodenum and release of appetite-regulating peptides which decreased appetite and energy intake after consumption (Wanders *et al.* 2011, Wanders *et al.* 2013, Wanders *et al.* 2014, Jensen *et al.* 2012). With increasing gastric volume, stretch receptors in the stomach wall are stimulated which induce satiation signals in the brain and initiate a reduction in the circulating levels of the hormone ghrelin which also reduces the feeling of hunger. For an optimal digestion in the intestine, the stomach stores and disintegrates the food. Liquid and particles between < 1 to 2 mm (Dressman 1986, Meyer and Doty 1988, Kong and Singh 2008) are emptied gradually via the pylorus at a rate that is dependent on the nutrient composition (2 to 4 kcal/min) (Kong and Singh 2008, Faas *et al.* 2002, Gentilcore *et al.* 2006, Hellström *et al.* 2006) controlled by signals coming from sensing enteroendocrine cells in the small intestine but also influenced by oro-sensory signals. The structure, gelling behaviour and viscosity in presence of DF can increase gastric volume and prolong contact time with gastric sensors (de Graaf 2012, Guerra *et al.* 2012, Rigaud *et al.* 1998, Guillon and Champ 2000), reduce gastric emptying and prolong satiety (Kong and Singh 2008, Kristensen and Jensen 2011, Wanders *et al.* 2011).

### 1.4.3    Small intestine

The small intestine is the main site of nutrient digestion and absorption. The first part of the small intestine, called the duodenum has a pH around pH 6.5. Acidic chyme arriving from the stomach is mixed with bicarbonate to increase the pH. Factors such as meal type, gastric emptying rate and digesta viscosity will determine the pH. Transit through the small intestine usually takes around 3 hours and over the course of transit, the pH increases slightly to around 7.5 in the distal part called ileum. Digesta and enzyme concentrations change during transit time due to digestion and absorption of digestive products as well as water content (Minekus *et al.* 2014). In the duodenum, chyme is mixed with bile from the liver and enzymes secreted by the pancreas. The pancreatic enzymes can be summarised into three categories, depending on which macronutrient is their substrate. First, the proteases which are primarily trypsin and chymotrypsin but also elastase and carboxypeptidase among other peptidases, which are responsible for protein digestion (Mackie 2019). Secondly, pancreatic α-amylase further digests the majority of the digestible starch reaching the small intestine producing maltose, maltooligosaccharides and dextrins (Edwards and Warren 2019). Thirdly, fats are digested by pancreatic lipases with the help of colipase as well as bile (Mackie

2019). The main functional component of bile juice are bile acids

(BAs)[1] (Macierzanka *et al.* 2019).
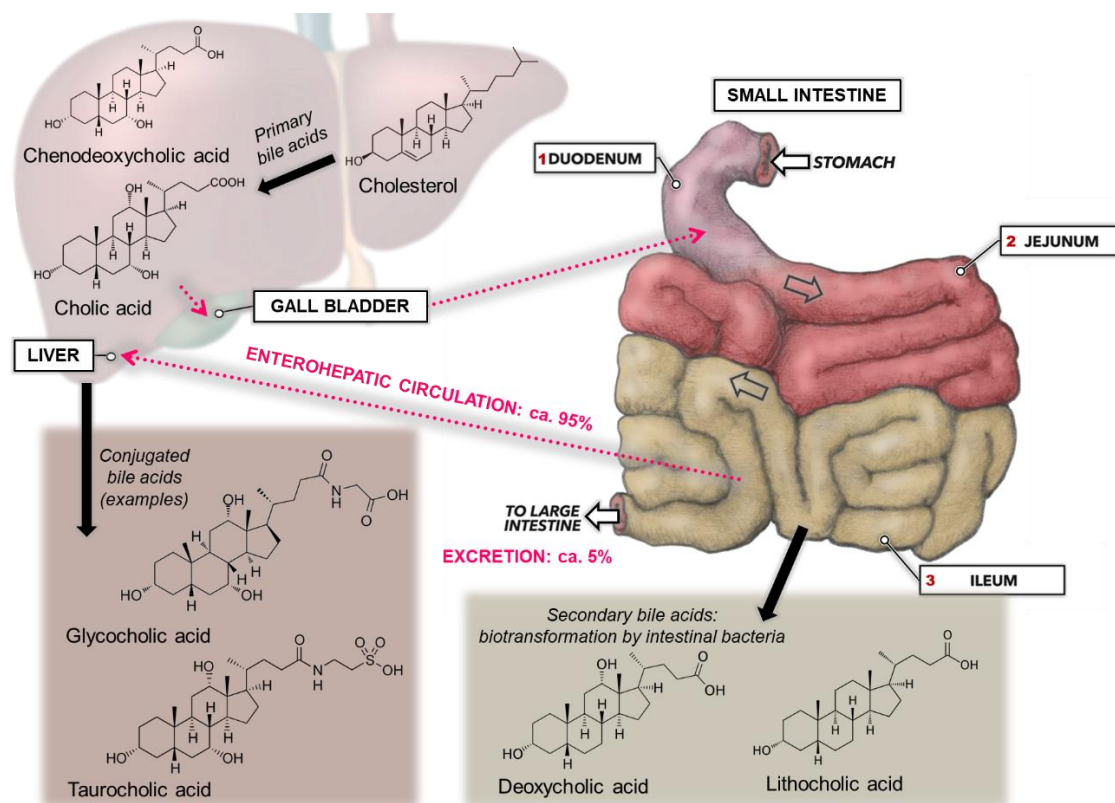


*Figure 1.5 – Schematic representation of bile acid biosynthesis from cholesterol (primary bile acids), conjugation with glycine or taurine on the example of cholic acid and biotransformation into secondary bile acids. and enterohepatic circulation of bile acids. Enterohepatic circulation highlighted in pink: Bile acids are stored in the gall bladder and released into the duodenum during digestion, reabsorbed in the terminal ileum and transported to the liver for ca. 95% of the bile acid pool, ca. 5% are excreted via the faeces [modified from (Urdaneta and Casadesús 2017)]*

---

[1] Conjugated BAs are sometimes called bile salts, however to refer to the total BA pool, the term BAs will be used throughout this thesis, whereas 'BA species' will be used to refer to a specific BA.

BAs have a hydrophilic and a more hydrophobic side which makes them very important in the emulsification of lipids as well as in the removal of hydrolysis products from the lipid interface and solubilisation of free fatty acids into mixed micelles (Mackie 2019). This enables transport to and absorption through the epithelium of the small intestine (Takagaki *et al.* 2018). The primary BAs cholic acid (CA) and chenodeoxycholic acid (CDCA) (Figure 1.5) are synthesised from cholesterol in the liver via a cascade of 14 enzymatic reactions with cholesterol 7α-hydroxylase being the rate limiting enzyme and conjugated with taurine or glycine to make them more water soluble. Bile is stored in the gall bladder and when needed for digestion secreted into the duodenum. Intestinal bacteria metabolise the primary BAs into the secondary BAs deoxycholic acid (DCA) and lithocholic acid (LCA), which can also be reconjugated with taurine or glycine. In a process called enterohepatic circulation, about 95% of BAs are reabsorbed in the distal ileum via the apical sodium-dependent bile acid transporter (ASBT) and transported back to the liver. Usually about 5% of the bile acid pool is lost with faecal excretion and has to be replenished with synthesis from cholesterol (Gunness and Gidley 2010, Mackie 2019, Macierzanka *et al.* 2019).
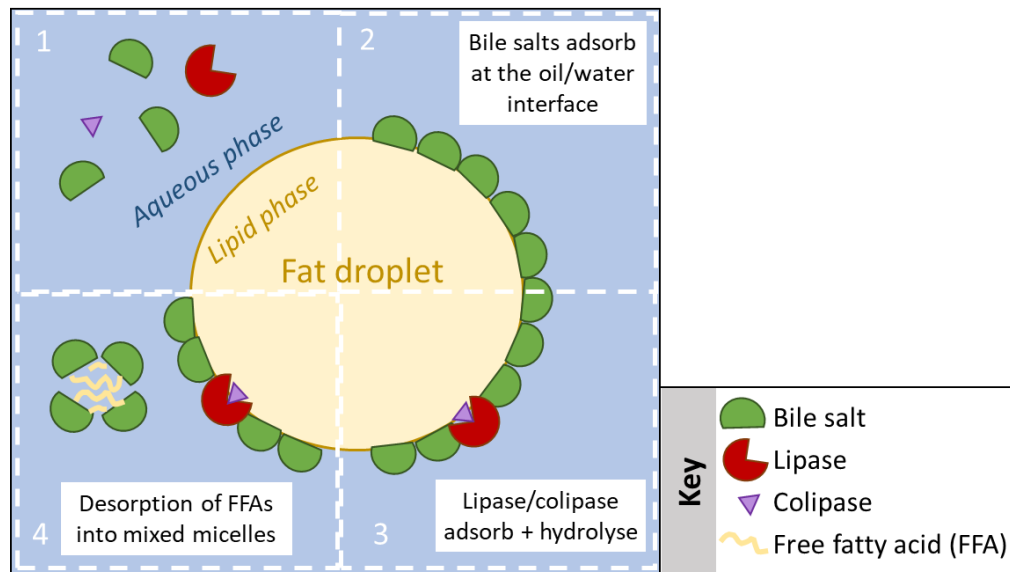
*Figure 1.6 – Diagram of duodenal lipolysis: 1) highlighting the 2-phase system: aqueous/water phase containing digestive agents vs lipid/oil phase, 2) bile salts adsorb at the oil/water interface, 3) the lipase/colipase complex adsorbs at the interface and hydrolyses the lipid into free fatty acids (FFAs), 4) desorption of FFAs from the interface with bile salts into mixed micelles.*

The vast majority of lipid digestion happens in the small intestine where pancreatic lipase hydrolyses one triacylglycerol (TAG) molecule into two free fatty acids (FFAs) and a monoacylglycerol (MAG) with a FA at the sn-2 position (Maldonado-Valderrama *et al.* 2011). However, the main difficulty is to overcome a two-phase system: a lipid phase and an aqueous phase which are not miscible (see Figure 1.6). The aqueous phase contains the water soluble essential digestive enzymes among other important compounds, whereas the lipid phase holds the dietary fats to be digested. In the duodenum, BAs are essential surfactants which adsorb at the oil/water interface. With their lipophilic side they adsorb at the interface and increase the interfacial area, which aids adsorption of

the lipase/colipase complex to hydrolyse the lipid (Maldonado-Valderrama *et al.* 2011, Corstens *et al.* 2017). An accumulation of the formed FFAs and MAGs remove lipase from the interface since they are surface-active, which slows down the hydrolysis. Therefore, BAs are also essential in the desorption and solubilisation of digestion products into mixed micelles and preventing inhibition of lipase activity. Mixed micelles which contain the lipolytic products diffuse through the mucus layer on the luminal side where the FFAs and MAGs are adsorbed by the enterocytes (Golding and Wooster 2010, Pilosof 2017). The available concentration of calcium during the digestion is important as it plays multiple roles in lipolysis. It is needed as a co-factor for pancreatic lipase but also interferes with lipolytic products if it binds long-chain FFAs and precipitates them as soaps. By removing them from the interface (Corstens *et al.* 2017), it prevents the inhibition of lipase by the beforementioned self-regulatory mechanism but on the other hand may make the FAs as insoluble compounds unavailable for uptake (Cervantes-Paz *et al.* 2017). Additionally, calcium levels may influence lipid droplet flocculation and interact with the polymers and BAs which may lead to aggregation or precipitation (Corstens *et al.* 2017).

Human digestive enzymes cannot digest DF, but DF may interfere with the digestive process via different mechanisms. The digestion products have to reach the epithelium of the small intestine for absorption which relies on efficient mixing (Mackie 2019). Some DF

increase viscosity which can decrease mixing of the chyme, form structures or interact with the digestive components (enzymes or BAs) which slow down digestion or absorption steps (Grundy *et al.* 2018b). Presence of DF can reduce the digestion rate of nutrients and promote the transit of nutrients further down the small intestine resulting in stimulation of satiety promoting hormones (Wanders *et al.* 2011). Monosaccharides, FFAs, MAGs and amino acids are detected by sensory proteins located on the plasma membrane of enteroendocrine cells which triggers gut hormone release regulating gastric emptying, appetite and postprandial glucose metabolism (Gribble and Reimann 2022, Xie *et al.* 2020). In addition to nutrient sensing receptors on the cells, there are also different BA sensing receptors, which play important roles in the modulation of hepatic BA biosynthesis, faecal elimination and the rate of BA absorption. There are regional differences regarding nutrient absorption and gastrointestinal hormone secretion in the three sections of the small intestine, duodenum, jejunum and ileum, which are associated with differences in postprandial glycemia and appetite (Xie *et al.* 2020, Gribble and Reimann 2022). The hormones PYY and GLP-1 are mediating the so-called ileal brake, i.e. slowing gastric emptying and promoting digestive activities (Mackie 2019).

The small intestine has microbial populations which may degrade or start to ferment DF. Although they only make up a very small share of the entire microbiome, they are thought to be important for

effects on health and disease but research so far is very limited (Guerra *et al.* 2012). Despite this, the majority of DF has been shown to reach the large intestine relatively intact (Saito *et al.* 2005, Sandberg *et al.* 1983, Stephen *et al.* 2017, Burkitt *et al.* 1972). Nasoenteric tubes which can aspirate samples are a relatively new technique to study the digestive content of the distal small intestine in humans. This will show whether the consumption of minimally-processed high-fibre foods will result in more intact cellular structures and carbohydrate reaching the distal ileum (Byrne *et al.* 2019).

### 1.4.4　Large intestine

Food which is not digested by the human digestive enzymes will pass into the large intestine or colon. This is where the majority of the gut microbiota reside, which ferment and metabolise the remaining compounds, including resistant protein and starch, DFs as well as other compounds such as phytochemicals. The trillions of microbes secrete a wide range of enzymes capable of fermenting complex structures such as DF. This is achieved by working together via cross-feeding in a complex community. DF fermentation produces important metabolites such as short chain fatty acids (SCFAs) which have various systemic effects on the human body leading to health benefits (Haider and Wilde 2020, Williams *et al.* 2017, Makki *et al.* 2018). Another important task of the colon is to adsorb any

remaining water to form stool. Some DFs have a bulking and laxative effect in the colon (McRorie and Chey 2016, Holma *et al.* 2010).

## 1.5 Mechanisms and functionalities underlying health benefits

Depending on the type of DF (section 1.2), and the matrix DF is consumed in (sections 1.2.3 and 1.3.4), as well as how DF is processed (section 1.3), will determine how DF may interact with the digestive processes (section 1.4). Health effects such as lowering blood cholesterol levels, reducing the risk of coronary heart disease, beneficial effect on blood glucose and/or insulin levels, reduced energy intake during subsequent meals, improved absorption of calcium or improved laxation are proposed to depend on DF's behaviour in the GI tract including:

- Undigestible plant cell wall barrier which controls nutrient bioaccessibility and energy absorption (section 1.3.4)

- Effect of DF on the rheological and colloidal state of digesta slowing mixing, digestion and absorption (section 1.4.2, 1.4.3 and 1.5.2)

- Interaction of DF with BAs, digestive enzymes, phenolic compounds, mineral ions (section 1.4.3 and 1.5.3)

- DF fermentation in the large intestine and the effect on gut microbiota composition (section 1.4.4)

- Bulking effect, predominantly in the colon (section 1.4.4)

(Capuano 2017, Cervantes-Paz *et al.* 2017, Eastwood and Morris 1992, Grundy *et al.* 2016).

Physico-chemical characteristics which underpin many of these behaviours are solubility and hydration, rheological as well as binding properties of DFs, hence were investigated in this thesis.

## 1.5.1　Solubility and hydration properties

DF solubility appears to have a big effect on fibre functionality (Guillon and Champ 2000) but has limitations as an indicator of type of functionality (Gidley and Yakubov 2019). Constraints of a classification of DF depending on solubility include 1) lack of a definition, 2) the physical continuum of solubility, and 3) it overlooks other potentially important hydration properties.

First, solubility of DF in the current literature is not clearly defined. It is commonly regarded as the property of a purified polysaccharide to solubilise or used synonymously with extractability if the polysaccharide disperses from a solid food matrix in a liquid medium and is usually separated from insoluble fibre by filtration or centrifugation (Gidley and Yakubov 2019, Wang and Ellis 2014). One can argue though that polymers are hydrated rather than truly solubilised (Wang *et al.* 2008). There is no standardized method measuring solubility so the conditions vary, including the solvent used, which is usually aqueous, temperature and pH (Chawla and

Patil 2010). Most importantly though is the solubility under physiological conditions, i.e. the proportion of fibre that is solubilised in the upper GI tract which can be different from analytical solubility (Rieder *et al.* 2017). In the example of BG found in cereals, the polymers have to dissolve from the PCW structure into the solvent and be hydrated to increase the viscosity of the digesta. The level of extractability depends on particle size, processing and Mw of the polymer (Grundy *et al.* 2017a), which leads us to the second constraint of a classification based on solubility.

A food may contain a range of fibre compounds of which only some are solubilised during the digestion. Although having a long tradition, a two category system to predict potential health effects is insufficient, as we find a range of solubilities creating a physical continuum from easily soluble fibres, to poorly soluble, swollen gel-like fibre networks to insoluble fibres (Gidley and Yakubov 2019, Holland *et al.* 2020). It leads to inconsistent conclusions as for example, fibres which are regarded to fall into the soluble fibre category are thought to lower cholesterol and insoluble fibres to increase stool weight. There are exceptions on a fibre type level like inulin for example is mostly soluble, but does not appear to lower blood cholesterol and psyllium which is also soluble but can enlarge stool weight (Slavin 2013). A series of systematic reviews and meta-analyses of prospective cohort studies and clinical trials found a lower risk of all-cause and cardiovascular disease (CVD) related

mortality, and incidence of coronary heart disease (CHD), stroke incidence and mortality, type 2 diabetes, and colorectal cancer among high DF consumers. When split into soluble and insoluble DF intake, risks of CVD mortality as well as incidence of CVD, CHD stroke and type 2 diabetes were significantly reduced in both categories (Reynolds *et al.* 2019).

Thirdly, hydrated but overall insoluble fibres like oat bran or fruit and vegetable pulps become swollen, hydrated, sponge-like networks of food particles (Eastwood and Morris 1992) which can change the rheological behaviour of digesta (Moelants *et al.* 2014, Gidley and Yakubov 2019, Wang and Ellis 2014). Insoluble fibre's interaction with water is usually measured and categorised as absorption, uptake, holding and binding as well as swelling but meanings of these can vary. An attempt to harmonize and define hydration properties has been made by the PROFIBRE action group in 1998 with swelling being "the volume occupied by a known weight of fibre under the condition used", water retention capacity (rather than water holding capacity or water binding capacity) as "the amount of water retained by a known weight of fibre under the condition used" and water absorption as "the kinetics of water movement under defined conditions" with conditions defined in the PROFIBRE protocols (Robertson *et al.* 2000, Guillon and Champ 2000).

## 1.5.2 Digesta viscosity and entrapment of compounds: Rheological properties

An important property of some DFs is thought to be the development of viscosity or resistance to flow. The viscous DFs BG (Queenan *et al.* 2007, Wang *et al.* 2017b), psyllium (Anderson *et al.* 2000), pectin (Brouns *et al.* 2011) and guar gum (Jenkins *et al.* 1979) were shown to lower serum LDL cholesterol concentrations. Vuksan *et al.* showed that viscosity rather than quantity explains the cholesterol lowering effect of DF however the physiological mechanisms and the role of viscosity are still not entirely understood, as comparisons of different viscous fibres have shown inconsistent results (Vuksan *et al.* 2011).

With increasing polymer concentration, viscosity increases and changes from a liquid 'dilute regime' at low concentrations, to a viscous solution at the critical coil overlap concentration (C*) (Figure 1.7). From this concentration onwards, physico-chemical interactions, entanglement and overlap of polymer chains occur, which can be enhanced by the polymer's side groups on its back bone as observed for galactomannans (i.e., guar and locust bean gum) (Rayner *et al.* 2016).
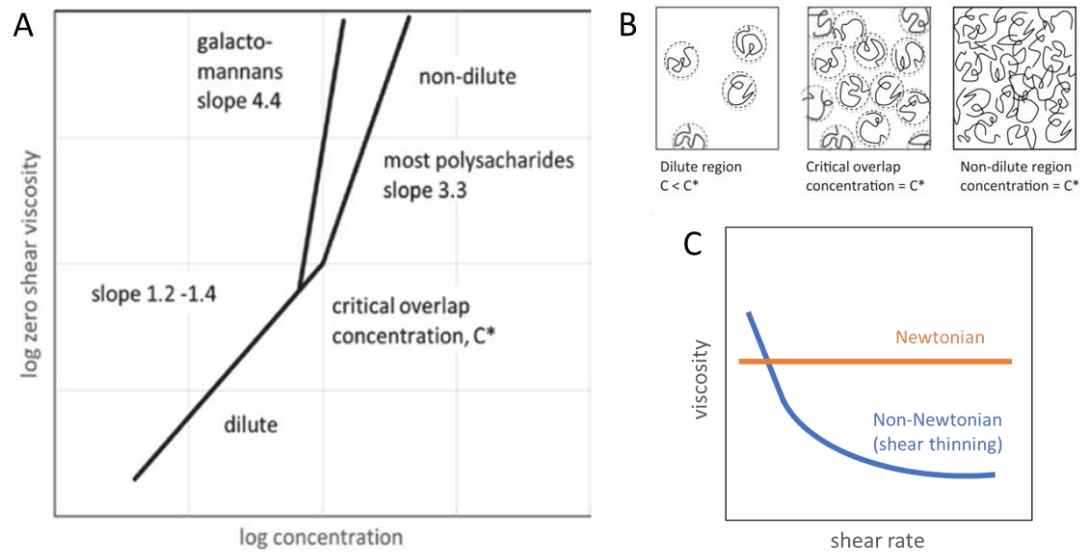
*Figure 1.7 – Rheological properties: (A) Effect of polymer concentration on viscosity and the concept of critical overlap concentration C\*, (B) schematic of random coil overlap, (C) Newtonian vs Non-Newtonian (shear thinning) fluid behaviour [modified from (Rayner et al. 2016)]*

Hence the viscosity of a polysaccharide solution depends on the molecular structure (i.e. branching), Mw, concentration and environmental conditions including shear rate and temperature (Wang and Ellis 2014). In the 'dilute regime' the coils move independently showing Newtonian flow behaviour, which means that viscosity is independent of the applied shear rate and increases approximately directly proportional with concentration, whereas from C\* onwards, viscosity decreases with increasing shear which is called shear thinning behaviour (Figure 1.7C) (Morris *et al.* 1981, Rieder *et al.* 2017). To translate peristalsis in the GI tract *in vivo* into *in vitro* measurements, different shear rates may be applied although GI flow patterns are much more complex (Wang and Ellis

2014). Viscosity, i.e. thickening of the digesta, is thought to slow down gastrointestinal transit, reduce mixing, and limit the diffusion of nutrients and enzymes, thus slowing down the rate of digestion and absorption (McRorie and McKeown 2017, Wanders *et al.* 2011). This has been demonstrated for the viscous fibres pectin and alginate, both of which have high water-holding capacities (Guillon and Champ 2002, Rigaud *et al.* 1998, Guillon and Champ 2000). Their physico-chemical behaviour has been shown to lead to a reduction in both appetite and energy intake (Jensen *et al.* 2012, Wanders *et al.* 2014, Wanders *et al.* 2011). A decelerated sugar absorption from the small intestinal lumen due to increased viscosity could not be confirmed by the *in vitro* study of Repin *et al.* nor by Dhital *et al.* (Repin *et al.* 2017, Dhital *et al.* 2015). Inconsistencies in the glucose lowering effect of BG *in vivo* can partially be explained by a lack of sufficient level of viscosity. When compared with *in vitro* viscosity data, an effect in reduction in post-prandial glycaemic response was more likely to be seen when the viscosities from six human intervention studies were at or above the C* (Rieder *et al.* 2017).

Viscous fibre could also entrap BAs or mixed micelles, in a viscous network at different stages of the digestive pathway and therefore either reduce lipid absorption or the enterohepatic circulation pathway of BAs which are then produced *de novo* from cholesterol (Grundy *et al.* 2018a, Gunness and Gidley 2010). Whether this is

solely a rheological mechanism is still to be elucidated since several *in vitro* studies have shown that some DFs may show a BA binding effect not related to viscosity (Naumann *et al.* 2018). The influence on lipid metabolism seems to depend on the Mw and quantity of BGs and thereof resulting digesta viscosity, but also on the type of administration with unrefined BG-rich foods showing higher reductions of cholesterol than BGs consumed in liquid form (Grundy *et al.* 2018a).

Depending on the DFs structural composition, some DFs have an additional key property of being able to form gels. A gel is formed via association or crosslinking of polymer chains, hence creating a three-dimensional network trapping water within it to form a semi-rigid structure being resistant to flow (Rayner *et al.* 2016), which requires a highly soluble polymer (Lovegrove *et al.* 2017).

### 1.5.3 Association of dietary fibre with components of digestion: Binding properties

Another mechanism of interference with the digestive process is binding or association of DFs with digestive components. Digestive enzymes could be bound in a complex or precipitated in a way that inhibits their catalytic activity (Capuano *et al.* 2018). A reversible and non-specific binding of cellulose to α-amylase was shown during *in vitro* hydrolysis of starch. The enzyme appeared to absorb to the surface of the insoluble fibre, hence inhibiting its activity by depleting it from solution (Dhital *et al.* 2015). Slaughter *et al.* found

that guar gum has a direct, non-competitive inhibitory effect on α-amylase, which is a different mechanism from that found with cellulose (Slaughter *et al.* 2002). Another way of reducing α-amylase enzymatic activity resulting in a reduced starch hydrolysis was found by entrapment of the enzyme within the fungal cell wall of mycoprotein (Colosimo *et al.* 2020b).

Interference of DF with lipid hydrolysis or lipid uptake has also been proposed (Takagaki *et al.* 2018). DFs are thought to interact with the enzyme's substrates or the products of hydrolysis (Capuano *et al.* 2018) or form complexes with BAs (Davison and Temple 2018, Gunness and Gidley 2010). A consequence of binding to these components would be a reduction in the rate of hydrolysis and/or absorption of lipids (Takagaki *et al.* 2018). Some DFs, like isomaltodextrin and chitosan have been shown to change the properties of mixed micelles, slowing their diffusion through the mucin layer and thus potentially slowing lipid absorption (Takagaki *et al.* 2018). Interference with colloidal stability was shown via another mechanism in an *in vitro* study with guar gum and BG. Depletion flocculation, i.e. aggregation of emulsion droplets, was induced by both polysaccharides but even more by a water-soluble extract of BG from oat flakes (Grundy *et al.* 2018b). However, the flocculation only occurred at a certain range of Mws and concentrations and lipolysis inhibition was not linearly related to the viscosity of the samples, which may explain some of the

inconsistencies in relating fibre viscosity to rates of digestion. This optimal Mw range is still to be found which probably explains why BG is only described in very general terms in the Scientific Opinions on EU health claims as having a Mw between 50 kDa (EFSA Panel on Dietetic Products and Allergies 2011a, EFSA Panel on Dietetic Products and Allergies 2009, EFSA Panel on Dietetic Products and Allergies 2010b, EFSA Panel on Dietetic Products and Allergies 2011b) or 100 kDa and 2000 kDa without specifying the measurement method (EFSA Panel on Dietetic Products and Allergies 2010a).

If DF forms a complex or association with BAs during digestion and reduces their reabsorption and enterohepatic circulation, the loss has to be compensated for by *de novo* synthesis from cholesterol in the liver (Mertens *et al.* 2017). This is thought to lead to the cholesterol lowering effect of some DFs. In an ileostomy study with nine subjects, an oat bran-rich bread intervention led to a decrease in total cholesterol, LDL and apolipoprotein B in plasma, and to an increased excretion of total BAs in ileal effluents. However, this was only the case if the subjects had a low daily excretion of BAs at baseline (Zhang *et al.* 1992). It is still under debate if the re-uptake is impeded for mixed micelles formed of BAs, cholesterol, FFAs and MAGs or for BAs only. Two other ileostomy studies showed that the BA to cholesterol ratio in the ileal effluents was similar to that found in mixed micelles (Ellegard and Andersson 2007, Lia *et al.* 1997).

Several *in vitro* BA to DF binding experiments are reported in the literature. Most used a centrifugation method after simulated digestion and incubation of either single or mixed BA solutions with the DF, resulting in some binding in the vast majority of the studies (Drzikova *et al.* 2005, Kahlon *et al.* 2006, Kahlon and Woodruff 2003, Li *et al.* 2017, Naumann *et al.* 2018). Dialysis may mimic the physiological mechanism better than centrifugation but has also the limitation that it is a passive transport in contrast to the gut. With the dialysis method only small retention is usually seen, especially when purified DFs like AX, BG (Gunness *et al.* 2012), citrus or potato fibre (Naumann *et al.* 2018) are used whereas with a more complex high-fibre barley product, more significant retention was seen, which could be further confirmed with an inverse dialysis model (Naumann *et al.* 2018). It is likely, that the two methods show different types of interaction between BAs and different kinds of DF depending on surface porosity, particle size, Mw of soluble fractions and viscosity.

The interaction between the DFs BG and AX with BAs was studied by Gunnes *et al.* using $^{13}$C NMR and small angle X-ray scattering (SAXS). The DFs showed evidence of both dynamic molecular interactions and network formation indicating that the DFs interact either directly with the micelle or change the internal micelle organisation. However, all potential binding effects were readily reversible and weak (Gunness *et al.* 2016, Gunness *et al.* 2010).

## 1.6   Summary

Epidemiologically, the beneficial effects of DF intake on lipid metabolism, i.e. prevention of CV-related diseases, as well as on glucose metabolism, i.e. prevention of diabetes, are well established (Reynolds *et al.* 2019, Stephen *et al.* 2017). Cereal DFs are generally superior in their health benefits compared to other DFs (Davison and Temple 2018, Reynolds *et al.* 2019), however it is unclear if this is due to a specific fibre type or the particular mechanism(s) whereby DFs affect digestion and metabolism.

Whilst DFs are not affected by human digestive enzymes, their properties may change on their journey through the GI tract. For example, when components of the cell wall matrix, considered initially as insoluble fibre, are solubilised during digestion (e.g. BG of oat cell walls). It is still under debate if the physiological effects are mediated solely by a specific fibre component (e.g. BG) or if there is a synergistic effect between the different DF components as DFs are usually not consumed as isolated, purified compounds but rather in their natural form as PCW constituents and together with other components of food (Grundy *et al.* 2016, Holland *et al.* 2020). More research is therefore needed to fully understand how DFs in a natural matrix like cereal brans as well as specific isolated fibres with structural differences, interact with other components and change within a food matrix and digesta matrix during processing and digestion, respectively. DF's physiological functions and behaviour in

the upper GI tract are influenced by a combination of their hydration, rheological and binding properties (Gidley and Yakubov 2019), which need further research to translate into structure-function relationships.

## 1.7  Aim

This project aimed to understand which physico-chemical properties of a range of DFs are important to underpin mechanisms which influence small intestinal duodenal digestion of lipids and starch.

## 1.8  Objectives

The key objectives were to determine the physico-chemical properties of PCW fibres of cereals as well as isolated fibres (BG, inulin and cellulose) in terms of their rheological and/or hydration and/or binding properties and to investigate whether these underpin their effect on *in vitro* simulated digestion models of

a) **Lipid digestion** [based on (Grundy *et al.* 2018b, Grundy *et al.* 2017b)], Chapter 3;

b) **BA interaction** [based on (Naumann *et al.* 2018, Gunness *et al.* 2012)], Chapter 4; and

c) **Starch digestion** [based on (Perry and Donald 2002, Lai *et al.* 2012, Woodbury *et al.* 2021, Hou *et al.* 2020, Edwards *et al.* 2019)], Chapter 5.

# Chapter 2 – General Materials and Methods

## 2.1 Sourced Materials

### 2.1.1 Fibre ingredients for lipid digestion and bile acid interaction studies

The cereal flour DF ingredients barley bran, wheat bran, oat hull fibre and oat bran were sourced from the respective suppliers and provided with the composition data as outlined in Table 2.1. They were used in Chapter 3 and Chapter 4. Bran flours are made from the bran layer, the first layer of the cereal grain. Hull fibre flour is from the outermost protective layer of the oat grain, sometimes also called husk.

Purified BG from oat (high viscosity, cat# P-BGOH) was purchased from Megazyme (Ireland) and used in Chapter 4.

*Table 2.1 – DF ingredients for lipid digestion and BA interaction studies: product names, suppliers, particle sizes (from technical data sheet) and composition [%], AOAC 2011.25 dietary fibre analysis.*

| Fibre material | Product name; supplier | Particle size | Total DF | High Mw Insoluble DF | High Mw Soluble DF | Low Mw DF | Carbohydrate | Protein | Fat | Ash | Moisture |
|---|---|---|---|---|---|---|---|---|---|---|---|
| Barley Bran (BB) | Barley Balance (variety Hordeum vulgare); Poly-Cell Technologies | < 595 µm | 39.5 | 10.0 | 25.1 | 4.5 | 78.49 | 9.37 | 2.04 | 1.18 | 8.92 |
| Wheat Bran (WB) | Stabilized Red Wheat Bran, medium, Canadian Harvest; J. Rettenmaier | 71% 1000-250 µm | 54.6 | 48.5 | 4.4 | 1.6 | 64.76 | 16.72 | 6.91 | 6.62 | 4.99 |
| Oat Hull Fibre (OHF) | HF 200 Oat Fiber Vitacel; J. Rettenmaier | 60-75% 100-30 µm | 93.8 | 88.2 | 5.7 | 0.0 | 89.70 | 0.30 | 0.33 | 2.76 | 6.91 |
| Oat Bran (OB) | Sweoat Bran BG28 (variety Avena sativa L.); Naturex/ Swedish Oat Fiber AB | < 250 µm | 50.4 | 30.1 | 17.1 | 3.2 | 62.00 | 25.54 | 3.80 | 3.30 | 5.36 |

## 2.1.2   Fibre ingredients for starch interaction studies

Table 2.2 lists the DF ingredients used in Chapter 5, with the respective suppliers and DF content. For ease of differentiation of the two inulin fibres, they were termed for the purpose of this thesis as 'soluble inulin' and 'insoluble inulin' despite solubility of both depending on conditions like solvent, temperature and concentration.

*Table 2.2 – DF ingredients for starch interaction studies: product names, suppliers and DF content (from technical data sheet).*

| Fibre material | Product name; supplier | DF content |
|---|---|---|
| Soluble inulin | Orafti GR (chicory inulin); Beneo-Orafti S.A. | 89% (AOAC 997.08)* |
| Insoluble inulin | Orafti HPX (chicory inulin); Beneo-Orafti S.A. | 97% (AOAC 997.08) |
| Cellulose | Cellulose microcrystalline (extra pure); Acros Organics via Thermo Fisher Scientific | 100% purity |
| BG | β-Glucan (Oat Medium Viscosity, P-BGOM); Megazyme | > 94% purity |

\* max 10 g/100 g (d.m.) glucose, fructose and sucrose

## 2.1.3   Other sourced materials

The reagents used throughout the thesis are listed below [including their catalogue number (cat#) where applicable]. Materials used for specific experiments are reported in the Materials section of the corresponding chapter. Ultra-pure, deionised water (18.2 MΩ·cm @25 °C) was prepared daily using an Avidity Science Duo™ water purification system (Bucks, UK) and used for preparing solutions unless specified otherwise.

The following chemicals and reagents of standard analytical grade were purchased from Merck (UK): Human salivary α-amylase (cat# A0521), pepsin from porcine gastric mucosa (cat# P7012), pancreatin from porcine pancreas (cat# P7545), α-amylase from porcine pancreas (cat# A3176), bovine bile extract (ox gall powder) (cat# B3883), NaOH (cat# 06203), NaCl (cat# S7653), KCl (cat# P3911), $KH_2PO_4$ (cat# P0662), $NaHCO_3$ (cat# S6014), $MgCl_2(H_2O)_6$ (cat# M2670), $(NH_4)_2CO_3$ (cat# 207861), $CaCl_2(H_2O)_2$ (cat# 223506), cholic acid (CA) (cat# C1129), glycocholic acid (GCA) (cat# G7132), taurocholic acid (TCA) (cat# 86339), chenodeoxycholic acid (CDCA) (cat# C9377), deoxycholic acid (DCA) (cat# D2510) and taurodeoxycholate (TDCA) (cat# T0875), tributyrin (cat# T8626), Calcofluor White Stain (containing 1 g/L Calcofluor White M2R and 0.5 g/L Evans blue) (cat# 18909), p-hydroxybenzoic acid hydrazide (PAHBAH) (cat# 240141), maltose monohydrate (cat# 1375025), dimethyl sulfoxide (DMSO) (cat# 472301), lithium bromide (LiBr) (cat# 451754), D-fructose (cat# F2793), D-glucose (cat# 47249), D-mannitol (cat# 78513), maltose (cat# 47288), D-raffinose (cat# 95068), 1-kestose/ kestotriose (cat# 72555), nystose/1,1-kestotetraose (cat# 56218), sucrose (cat# 47289), haemoglobin (bovine blood haemoglobin) (cat# H2500), LightSafe micro centrifuge tubes (black, 5 mL) (cat# Z688290) and Mini UniPrep Syringeless Filter autosampler (0.2 μm PTFE) (cat# WHAUN203NPEORG).

LC-MS/MS BA standards CDCA (cat# C9377), DCA (cat# D2510), DHCA (cat# 30830), GCA (cat# G2878), GCDCA (cat# G0759), GDCA (cat# G9910), LCA (cat# L6250), TCA (cat# T4009), TCDCA (cat# T6250), TDCA (cat# T0875), UDCA (cat# U5127) and TLCA (cat#T7515) were purchased from Merk (UK).

LC-MS/MS BA standards α-MCA (cat# C1890-000), β-MCA (cat# C1895-000), CA (cat# C1900-000), GLCA (cat# C1437-000), HDCA (cat# C0860-000), MCA (cat# C1850-000), T-α-MCA (cat# C1893-000), T-β-MCA (cat# C1899-000), GHCA (cat# C1860-000), GUDCA (cat# C1025-000), THCA (cat# C1887-000), THDCA (cat# C0892-000), TUDCA (cat# C1052-000), GHDCA (cat# C0867-000), TDHCA (cat# C2047-000), d4-DCA (cat# C1070-015), d4-LCA (cat# C1420-015), d4-CA (cat# C1900-015), d4-GCA (cat# C1925-015), d4-CDCA (cat# C0940-015) and d4-GCDCA (cat# C0960-015) were purchased from Steraloids (U.S.).

The following reagents were purchased from Megazyme (Ireland): β-Glucan Assay Kit (Mixed Linkage) (cat# K-BGLU), thermostable amylase (cat# E-BLAAM), protease (cat# E-BSPRT), lichenase (cat# E-LICHN), 1,1,1-kestopentaose (cat# O-KPE), Total Starch Assay (cat# K-TSTA-100A).

Absolute ethanol (HPLC grade), sodium acetate trihydrate (HPLC electrochemical detection), sodium hydroxide (46-51%, analytical reagent grade), isopropanol (propan-2-ol, isopropyl alcohol) (cat# 10628143), fluorescein (cat# 173241000) and bolting cloth

("Spectra/Mesh woven filter" nylon, mesh size 53 μm) were purchased from Fisher Scientific (UK).

Cholyl-Lysyl-Fluorescein was obtained from Corning BV Life Science (Netherlands). Total BA colorimetric assay was purchased via Alpha laboratories (UK) from Dialab (Austria). 0.45 μm syringe filter (Sartorius Minisart) (cat# SM16555K) were purchased from Sartorius UK Ltd. (UK).

From VWR International GmbH (UK) were ethanol absolute (cat# 20821.330) and spectra/Por 1 dialysis membrane (Spectrum, U.S.) with a molecular weight cut off (MWCO) of 6-8 kD (cat# 734-0665). Before use, dialysis tubings were pre-hydrated in distilled water by rinsing them three times in deionised water at room temperature, followed by heating to 80ºC (repeated 3 times in total) to remove the preservative.

## 2.2 Dietary fibre soluble extracts and insoluble fraction materials

### 2.2.1 BG extracts and insoluble dietary fibre for lipid digestion interaction studies

The extraction method was based on (Wood *et al.* 1989) with modifications as follows. Deactivation of intrinsic glucanases in barley or oat bran flour included heat treatment of 60 g bran flour in 600 mL 70% ethanol under reflux for 3 hours. After cooling to room temperature, the mixture was centrifuged at 9,000xg for 15 min (Beckman Coulter J6MI centrifuge) and the supernatant

discarded. The residue was dried in the oven at 60-70°C overnight and stored in the freezer until further use.

For BG extraction and starch removal, 12.5 g deactivated bran flour was combined with 500 mL MES/Tris buffer and 0.25 mL thermostable amylase and stirred at 90°C. After 2 hours, the mixture was left to cool to 60°C. For protein removal, 1.0 mL of protease was added and stirred for 60 min at 60°C. The mixture was left to cool to room temperature and once cool, centrifuged at 9,000xg for 15 min (Beckman Coulter J6MI centrifuge) and the residue separated from the supernatant. BG from the supernatant was precipitated with an equal volume of isopropyl alcohol (IPA) of undiluted supernatant for barley bran supernatant and of a 1:1 diluted supernatant in deionised water for oat bran. The IPA/supernatant mixture was left in the fridge overnight. The residue of insoluble fibre was dried in the oven overnight. The IPA/supernatant was centrifuged at 4,200 rpm for 20 min (Beckman Coulter J6MI centrifuge) and the supernatant was discarded. The pellet was mixed with fresh IPA to de-water it further. A spatula was used to break the pellet into smaller pieces. The mixture was put again in the fridge overnight. It was centrifuged at 4,200 rpm for 20 min (Beckman Coulter J6MI centrifuge) and the supernatant discarded. Using a mortar and pestle, the BG pellet was ground to small particles and dried in the oven at 65°C oven until dry (a few

hours or overnight). Using the residue of insoluble fibre, the BG extraction procedure was repeated in the same way.

The dried insoluble fibre residue (after extracting BG twice) was stored in sealed containers at room temperature. IDF residue was ground and sieved to <600 μm. For removal of potentially remaining BG, 200 mg of IDF residue was incubated in 8 mL 20 mM Na phosphate buffer (pH 6.5) for 30 min at 50°C in an incubator on a rotary mixer. 0.4 mL lichenase (50 U/mL in 20 mM Na phosphate buffer) was added and incubated for 2 hours at 50°C. The mixture was left to cool to room temperature and centrifuged at 4,000xg for 20 min and the supernatant discarded. The pellet was dried in the oven at 65°C overnight. IDF was heat treated for ~1h in the oven at 120°C on the day of simulated digestion before use to ensure that any remaining lichenase is inactivated (Wang *et al.* 2016).

## 2.2.2 Analytical BG extraction protocols for determination of BG Mw

### 2.2.2.1 BG extraction protocol code 'P1'

Solutions of oat or barley bran of 2.5% (w/w) in deionised water (containing 0.02% sodium azide to avoid microbiological growth) were hydrated overnight under stirring at room temperature. On the next day, the hydrated oat or barley bran was centrifuged to remove insoluble material. The pH of the supernatant was decreased to 4.5 with 1 M HCl to precipitate proteins. The mixture was centrifuged and the solubilised BGs in the supernatant precipitated with an equal

amount of ethanol (abs) and the precipitate washed again with ethanol (abs).

### 2.2.2.2  BG extraction protocol code 'P2'

Solutions of oat or barley bran of 2.5% (w/w) in deionised water (containing 0.02% sodium azide to avoid microbiological growth) were hydrated overnight under stirring at 37°C and centrifuged to remove insoluble material on the next day. The pH of the supernatant was decreased to 4.5 with 1 M HCl to precipitate proteins. The mixture was centrifuged and the solubilised BGs in the supernatant precipitated with an equal amount of either A) ethanol abs. or B) 50% ethanol followed by mixing and another aliquot of ethanol (abs).

### 2.2.2.3  BG extraction protocol code 'P3'

To deactivate endogenous β-glucanases, oat bran or barley bran were pre-treated in 70% boiling ethanol for 3 hours. The brans were hydrated in MES/Tris buffer and treated with thermostable amylase for 2 hours at 90°C followed by a 1 h treatment with protease at 60°C. The solubilised BGs were precipitated from the supernatant with IPA and left in the fridge overnight, centrifuged the following day and washed again with IPA.

Extracts from all extraction protocols were ground while still wet using a mortar and pestle and left to dry at room temperature as well as stored in a closed container at room temperature after.

## 2.3   Methods

**In vitro simulation of human digestion:**

**Start:** fibre samples normalised for e.g. particle size, nutrient or fibre content

**Oral phase**
+ simulated salivary fluid (1:1)
+/- salivary α-amylase
2 min @ 37 °C on rotator

**Gastric phase** (pH 3)
+ simulated gastric fluid (1:1)
+/- pepsin
2 h @ 37°C on rotator

**Duodenal phase** (pH 7)
+ simulated intestinal fluid (1:1)
+ bile
+/- pancreatin or α-amylase
2, 4 or 20 h @ 37°C while mixing

**Duodenal phase variations and investigated mechanism:**

*Chapter 3*

**Fibre interference with lipid digestion**
❖ Lipid digestion measured over time using a pH-stat titrator
❖ Rheology of whole digesta

*Chapter 4*

**Fibre/bile acid interaction**
❖ Quantification of total bile acid release over time
❖ Bile acid species analysis
❖ Rheology of digesta supernatant

**β-glucan release kinetics**
❖ β-glucan quantification and Mw distribution
❖ Rheology of digesta supernatant
❖ Quantification of total bile acids
❖ Microscopy of pellet

**Fibre interaction with a fluorescein labelled bile acid**
❖ Fluorometer measurement
❖ Confocal microscopy

*Chapter 5*

**Starch digestion in presence of fibre**
❖ Digestion of starch in inulin biscuits
❖ Quantification of reducing sugars

*Figure 2.1 – Overview of in vitro digestion experiments and duodenal phase variations with measurements taken grouped by investigated mechanism and respective chapter in this thesis.*

## 2.3.1 *In vitro* simulation of human digestion

In general, *in vitro* digestions simulating physiological conditions in humans were based on the harmonised protocol of the INFOGEST consortium (Minekus *et al.* 2014) and adapted/modified where necessary as described in the respective chapters (see Figure 2.1). Simulated digestive fluids were prepared according to Minekus *et al.* (Minekus et al., 2014). Food and DF materials were weighed in either normalised for their total DF (based on the composition table provided, see Table 2.1), BG (measured using BG assay, see section 2.3.12) or starch (measured using total starch assay, see section 2.3.13) content. The *in vitro* digestion followed three compartmental steps of an oral, gastric and duodenal phase, each with a final 1:1 dilution of food/bolus/chyme with simulated fluids and other fluids containing e.g. enzymes or BAs. Digestion simulation involved first, a 2 minute oral phase at a pH of ~7, then a 2 hour gastric phase at a pH of 3, followed by an at least 2 hour duodenal phase at pH 7 as suggested as standardised conditions by Minekus *et al.* (Minekus *et al.* 2014). Digestive enzymes were added in the respective phases as determined according to the nutrient under study (see section 2.3.2).

## 2.3.2 Digestive enzyme activity assays

### 2.3.2.1 Pepsin activity

Pepsin activity was measured according to pepsin activity assay EC 3.4.23.1, INFOGEST 2.0 supplementary material (Brodkorb *et al.* 2019). The assay is based on the principle that pepsin digests

haemoglobin resulting in tyrosine containing peptides which are soluble in trichloroacetic acid.

A haemoglobin solution was prepared by dispersing 0.5 g haemoglobin in 20 mL deionised water, adjusted to pH 2 with 300 mM HCl and made up to a volume of 25 mL to obtain a solution at 2% w/v haemoglobin at pH 2. A stock solution of 1 mg/mL pepsin in 10 mM Tris buffer (containing 150 mM NaCl at pH 6.5) was prepared and stored on ice until use. From this, a range of 5 concentrations of pepsin in 10 mM HCl were prepared: 10, 15, 20, 25, 30 µg/mL.

500 µL of haemoglobin solution was incubated in a 1.7 mL Eppendorf tube in an incubator at 37°C on a rotator for 3-4 minutes to reach the assay temperature. 100 µL of pepsin solution (repeated for each concentration) added and incubated at 37°C for exactly 10 minutes. To stop the reaction, 1 mL of 5% w/v trichloroacetic acid was added to each tube. The sample was centrifuged at 6,000×g for 30 min. Using quartz cuvettes, the absorbance of the supernatant was measured at 280 nm (Biochrom Libra S80 UV/Vis Spectrophotometer, Biochrom Ltd., UK). For blank tests, the same procedure was followed with the difference that pepsin was added after the addition of trichloroacetic acid. Pepsin activity was calculated for each pepsin concentration using Equation 2.1, which resulted in similar activities of which the mean was used.

$$\text{Units/mg} = \frac{(A_{Test} - A_{Blank})*1000}{(\Delta t*x*0.001)}$$

*Equation 2.1 – Pepsin activity (units/mg): $A_{Test}$ is the absorbance of the pepsin test solution, $A_{Blank}$ is the absorbance of the blank, 1000 is a dilution factor to convert µg to mg, Δt: duration of the reaction, i.e. 10 minutes, X is the amount of pepsin powder (µg) in 1mL in the assay solution and 0.001 is the ΔA per unit of pepsin.*

## 2.3.2.2 Trypsin activity (TAME assay)

Trypsin activity in pancreatin was using the Trypsin Activity Assay EC 3.4.21.4, INFOGEST 2.0 supplementary material (Brodkorb *et al.* 2019). The assay is based on the principle that one unit trypsin hydrolyses 1 µmol of p-toluene-sulfonyl-L-arginine methyl ester (TAME) per minute to p-Toluene-Sulfonyl-L-Arginine and methanol.

The spectrophotometer was set to 247 nm at room temperature. Two quartz cuvettes (one for the enzyme reaction and one for the no enzyme reference) were prepared with 1.3 mL of Tris-HCl buffer (pH 8.1) and 150 µL of the substrate (10 mM TAME: 18.9 mg of TAME and dilute it in 5 mL with dionised water) and mixed. The mixture was incubated for 3-4 minutes at room temperature. 50 µL of the pancreatin solution in 0.25 mg/mL or 0.5 mg/mL was added to the sample cuvette or 50 µL of 1 mM HCl solution to the reference cuvette, and mixed. The absorbance at 247 nm was recorded every 10 seconds for at least 10 minutes. This was repeated with the other pancreatin concentration. The absorption (y-axis) was plotted versus the time (x-axis) in minutes. The slopes $\Delta A_{247}$ [unit absorbance/minute] were calculated for both the blank and test

assays using the maximum linear rate and over at least 5 minutes

and trypsin activity per mg pancreatin calculated according to

Equation 2.2.

$$Units/mg = \frac{[\,(\Delta A247\ Test - \Delta A247\ Blank) * 1000 * 1.5]}{(540 * X)}$$

*Equation 2.2 – Trypsin activity (units/mg): $\Delta A_{247}$ is the slope of the initial linear portion of the curve, [unit absorbance/minute] for the Test (with enzyme) and Blank, 540 is the molar extinction coefficient of TAME at 247 nm, 1.5 is the volume (in mL) of the reaction mix (Tris-HCl + TAME + enzyme), X is the quantity of trypsin in the final reaction mixture (cuvette) (in mg).*

### 2.3.2.3  Pancreatic α-amylase activity assay

The method defines one unit of amylase activity as the amount that

liberates 1 mg maltose from starch in 3 min at 37°C. 100 mg of

potato starch in a 5 mg/mL suspension in PBS was gelatinised by

immersion into a 90°C water bath for 20 min. Stock solutions of

pancreatin (containing pancreatic α-amylase) or pancreatic α-

amylase were freshly prepared at a concentration of 1 mg/mL before

use and kept on ice. 100 µl of α-amylase stock solution was added

to three replicates of 15 mL gelatinised starch substrate with

samples taken at 0, 3, 6, 9 and 12 minutes timepoints. The amount

of maltose in the samples was determined using a PAHBAH assay as

described in section 2.3.14 and the activity calculated from the slope

of maltose release.

## 2.3.2.4 Pancreatic lipase activity assay (in presence of BAs)

Pancreatic lipase activity was determined according to assay EC 3.1.1.3 as described in the INFOGEST 2.0 supplementary material (Brodkorb *et al.* 2019). The assay principle is based on FFA release from tributyrin due to lipase hydrolysis which is measured by pH titration.

The assay solution (pH 8) contained 9000 mg/L NaCl, 200 mg/L $CaCl_2$ and 36 mg/L mg Tris-(hydroxymethyl)-aminomethane and 400 mg sodium taurodeoxycholate. 14.5 mL of the assay solution was mixed with 0.5 mL tributyrin in a pH-stat titration vessel (jacketed and capped reaction vessel, number 6.1418.150, 5-70 mL volume, Metrohm AG, Switzerland) at 37°C with a X-shaped magnetic stirrer bar at 700 RPM for 3-5 minutes. A pH probe (8172BNWP, Thermo Scientific, UK) connected to a pH-stat device KEM AT-700 (Kyoto electronics, Japan) was immersed in the tributyrin in water emulsion. The pH was adjusted to 8 using 0.1 M NaOH if necessary. RPMs were set to the reaction mixing speed and the assay reaction was started by adding 100 µL of a 2 mg/mL pancreatin in water solution and simultaneously starting the programme to titrate 0.1 M NaOH to keep the pH constant at 8 and volume of NaOH dispensed recorded over 15 minutes. To test the influence of mixing regime on the lipase activity assay, mixing speed during the reaction was tested at 200, 350, 520 and 700 RPM each at least in triplicate. Linear kinetics of FFA release of at least 5 minutes were fitted to Equation 2.3.

$$\frac{\text{Units}}{\text{mg powder}} = \frac{\text{R(NaOH)} * 1000}{\text{v} * [\text{E}]}$$

*Equation 2.3 – Lipase activity (units/mg): R(NaOH) is the rate of NaOH delivery in µmol NaOH per minute which equals µmol free fatty acid titrated per minute, v is the volume [µL] of enzyme solution added to the pH-stat vessel, [E] is the concentration of the enzyme solution [mg powder/mL].*

### 2.3.3 Bile acid analysis

A colorimetric assay was used to determine total BA concentration whereas BA analysis with LC-MS/MS provided additional information on individual species of BA and their concentration.

### 2.3.3.1 Enzymatic colorimetric assay to determine total bile acids

A total BAs kit manufactured by Dialab, Austria (Alpha Laboratories, Eastleigh, UK) was used and modified for use in a 96-well plate. The assay is an enzymatic recycling method measured colorimetrically. In presence of Thio-NAD, the enzyme 3-hydroxysteroid dehydrogenase converts BAs to 3-keto steroids and Thio-NADH, which is reversible. The presence of excess NADH efficiently promotes the enzyme cycling and the rate of formation of Thio-NADH is determined by following the reaction kinetics at 405 nm over 20 min. Samples were diluted in SIF, a standard curve from 5 to 200 µM using 5 mM sodium GDCA was run with every 96-well microplate. 5 µL of sample or standard in duplicate were added to a 96-well microplate, 240 µL Reagent 1 (> 0.1 mM thio-nicotinamide adenine dinucleotide [thio-NAD] in buffer) and 80 µL Reagent 2 (>

2 kU/L 3-α-hydroxysteroid dehydrogenase, > 0.1 mM NADH in buffer) were added. A kinetic profile was determined at 37°C with single measurements at 405 nm, 40 readings every 30 second using a Benchmark Plus™ spectrophotometer (Bio-Rad, Watford, UK). A sample's BA concentration was calculated from the reaction velocity based on the standard curve of GDCA concentration velocities.

### 2.3.3.2  Bile acid species analysis with LC-MS/MS

Liquid chromatography-mass spectrometry/mass spectrometry (LC-MS/MS) combines HPLC separation with a tandem MS for analyte detection. HPLC was based on reversed-phase HPLC which separates molecules on their hydrophobicity. The analytes in the mobile phase bind to hydrophobic ligands in the stationary phase, i.e. the sorbent, and are immobilized in the presence of aqueous buffers. By addition of an organic solvent to the mobile phase, the analytes are eluted. The elution can either be under isocratic conditions, i.e. the concentration of organic solvent is constant, or under gradient conditions, i.e. increasing the amount of organic solvent over time (Aguilar 2004). MS measures the relative abundance of ionic species according to their mass-to-charge ratios (m/z) after producing a beam of gaseous ions from the analyte. Coupling together two mass analysers (MS/MS) has the advantage of identification and separation of ions with very similar m/z. The first MS ionises the analytes and separates them by their m/z, then ions with a similar m/z are selected to be split into smaller fragments which are analysed for their m/z and detected by the second MS. MS

instruments are usually classified based on how mass separation is achieved, either by electric and/or magnetic force fields. In this study a quadrupole ion trap MS was used. An electrospray ionisation was used to assist the transfer of ions from solution into the gas phase. In a quadrupole mass analyser, ions are created and trapped in a radio frequency (RF) quadrupole field. It uses oscillating electrical fields to selectively stabilize or destabilize the paths of ions passing through the RF field, which serves as a mass-selective filter with only a single m/z passing through the system at any time. This is either done non-destructively or destructively as isolated ions can be fragmented by collisional activation and the fragments detected (Kang 2012).

The method was based on (Han *et al.* 2015) and modified as follows. Samples taken from dialysate were diluted either 1:20 or 1:50 with methanol to a total volume of 400 µL. 20 µL d4-GCA (40 µg/mL) and 20 µL d4-LCA (40 µg/mL) were added as internal standard to the sample and filtered with Whatman Mini UniPrep Syringeless Filter autosampler (0.2µm PTFE). Of the internal standards added, d4-GCA was the primary reference internal standard with the other monitored as checks in the extraction procedure. The final sample was submitted for analysis by LC-MS/MS.

Calibration standards of 1 mg/mL of each BA in MeOH were prepared and stored refrigerated. A 10 µg mix of the BA standards was prepared in 70% methanol by taking 100 µl of each individual BA

(at 1 mg/mL) into a pooled vial and making to 10 mL total volume. A series of dilutions was prepared ranging from 4000 ng/mL to 10 ng/mL as well as a methanol blank. Deuterated internal standards were added to each of the calibration standards by adding 25µl of d4-internal standard mix (containing 40 µg/mL of each internal d4 standard: d4-DCA, d4-CDCA, d4-CA, d4-GCA and d4-LCA) to give 2000 ng/mL each.

Each sample or standard was analysed using an Agilent 1260 binary HPLC coupled to an AB Sciex 4000 QTrap triple quadrupole mass spectrometer. HPLC was achieved using a binary gradient of solvent A (Deionised water + 5mM Ammonium acetate + 0.012% Formic acid) and solvent B (Methanol + 5mM Ammonium acetate + 0.012% Formic acid) at a constant flow rate of 600 µl/min. Separation was made using a Supelco Ascentis Express C18 150 x 4.6, 2.7µm column maintained at 40°C. Injection was made at 50% B and held for 2 min, ramped to 95% B at 20 min and held until 24 minutes. The column equilibrated to initial conditions for 5 minutes.

The mass spectrometer was operated in electrospray negative mode with capillary voltage of -4500V at 550°C. Instrument specific gas flow rates were 25 mL/min curtain gas, GS1: 40 mL/min and GS2: 50 mL/min. Mass fragmentation was monitored according to defined BA Mw. Quantification was applied using Analyst 1.6.2 software to integrate detected peak areas relative to the deuterated internal standards.

## 2.3.4 Size-exclusion chromatography

Size-exclusion chromatography (SEC) was used to determine the BG molecular weight distribution. This high-performance liquid chromatography (HPLC) technique employs an 'inverse-sieving' technique based on the molecule's size and hydrodynamic radius ($V_h$). An analyte is injected onto an SEC column packed with an inert, porous substrate. Depending on the size and $V_h$ of the analyte and the substrate's pore sizes, the analyte diffuses into the pores. Larger molecules elute faster from the column, whereas smaller molecules enter the pore volume and elute later. Therefore, elution in SEC is in the reverse order of the analyte size. Specifically, in this instance the type of SEC utilized is gel permeation chromatography because the analytes were separated using a non-aqueous mobile phase, DMSO.

Once separated, quantitative measurements of the polymers are possible using a refractometer as the detector. Detection measured as refractive index is based on the measurement of refraction of light and angle of incidence at a boundary between the analyte and another material with a known refractive index, usually quartz. Refractive index increases with increasing concentration of the analyte (Striegel 2017).The method used for the separation of BG polymers was adapted from Tuncel *et al.* (Tuncel *et al.* 2019). Dried BG extracts (2 or 4 mg/mL) were dissolved in DMSO + 0.5% LiBr (w/w) (Samples with higher viscosity would have been too viscous and had to be diluted to a concentration of 2 mg/mL). The samples

and standards were incubated in the oven at 80°C overnight. The HPLC-SEC system used was a Perkin-Elmer Series 200 HPLC (Llantrisant, UK) fitted with two columns (8x300 mm, GRAM; Polymer Standard Service, Mainz, DE) in series (10 µm; 300 Å followed by 30 Å) and affixed to a guard column (8x50 mm, GRAM; Polymer Standard Service, Mainz, DE), equipped with refractive index detector (RI), autosampler (35°C), and column heater (80°C). The HPLC ran isocratically at a flow rate of 0.6 mL/min using DMSO/LiBr (0.5% w/w) as the eluent with the column oven set at 80°C. Initially, a series of standards dissolved at 1 mg/mL in DMSO/LiBr were injected using the instrument autosampler. Samples were then injected onto the column in series, at a concentration of 2 mg/mL or 4 mg/mL, depending on the viscosity. β-glucan Mw standards were purchased from Megazyme (P-MWBGS) and analysed. Pullulan standards (PSS-pulkit; Polymer Standard Service, Mainz, Germany) having a range of peak molecular weights from 342 to 708,000 Da were used for calibration. Correlation coefficients of calibration curves generated from pullulan standards were $R^2=0.99995\pm0.00003$. Pullulan is a linear d-anhydroglucose polysaccharide with two $(1{\rightarrow}4)$-α linkages per $(1{\rightarrow}6)$-α linkage. $V_h$ was calculated using Equation 2.4 based on Mark-Houwink parameters of $K = 0.0002427\,dL\,g^{-1}$ and $a = 0.6804$ for pullulan in DMSO at 90 °C. Elution volume ($V_{el}$) was plotted against $V_h$ to obtain a calibration curve for the pullulan standards as described by Cave *et al.* (Cave *et al.* 2009). The RI elution profiles of the BG samples

were converted to SEC weight distributions $w(\log V_h)$ and the calibration parameters using Equation 2.5. The chain length distributions were normalised using standard normal variate normalisation. A number distribution ($N_{de}(X)$) was obtained from the corresponding weight distribution of linear polymers, such as BG, using Equation 2.6 (Cave *et al.* 2009, Perez-Moral *et al.* 2018).

$$V_h = \frac{2}{5} \frac{KM^{1+\alpha}}{N_A}$$

*Equation 2.4 – Calculation of hydrodynamic volume $V_h$ for linear polymers based on the Mark-Houwink relation with K and α Mark-Houwink parameters as reported above, M as the known molecular weight of the pullulan standard and the Avogrado's constant $N_A$.*

$$w(\log V_h) = S_{RI}(V_{el}) \frac{dV_{el}}{d\log V_h}$$

*Equation 2.5 – SEC weight distribution $w(\log V_h)$ calculation, $S_{RI}(V_{el})$ is the signal obtained from RI elution, $V_{el}(V_h)$ is obtained from the pullulan calibration curve.*

$$w(\log V_h) = X^2 \, N_{de}(X)$$

*Equation 2.6 – Number distribution ($N_{de}(X)$) calculation based on $w(\log V_h)$ derived from Equation 2.5.*

### 2.3.5 High-performance anion-exchange chromatography

Inulin and sugar analysis was performed by high-performance anion-exchange chromatography (HPAEC) with pulsed amperometric detection (PAD). This liquid chromatographic technique relies on a high pH as most carbohydrates are not negatively charged at neutral pH but start to ionize at their hydroxyl groups at high pH (>11). This charge is needed to bind to a pellicular

anion-exchange resin in the column. Separation takes place on an ethylvinylbenzene divinylbenzene core particle of 4–10 µm diameter that is surface sulfonated to allow smaller particles containing strong anion-exchange groups to be electrostatically attached as well as small latex particles. The carbohydrate's acidity directly determines its retention with more acidic carbohydrates, being more tightly bound to the column. After the carbohydrates exit the column, they are detected by oxidizing them on a gold working electrode. This produces electrons which flow to the working electrode and this current can be measured to detect the eluting carbohydrate. PAD uses a series of potentials, called waveform, to detect the carbohydrate, clean and restore the gold working electrode surface. The current measured during detection of the carbohydrate is integrated to yield a charge which can be plotted as a function of separation time resulting in a HPAEC-PAD chromatogram (Rohrer 2021).

The method was adapted from Ziegler *et al.* (Ziegler *et al.* 2016) using a Dionex ICS-3000 system (Sunnyvale, CA, USA) equipped with an autosampler at 25°C. A CarboPac-PA100 guard column (4 × 50 mm) and a CarboPac-PA100 analytical column (4 × 250 mm) at 30°C was the stationary phase and purchased from Thermo Fisher Scientific (UK). Detection was facilitated by PAD with a gold working electrode and an Ag/AgCl reference electrode. Integration was performed using the Chromeleon 6.8 chromatography data system.

The mobile phase included 85 mM NaOH with 25 mM sodium acetate (eluent A) and 300 mM NaOH with 100 mM sodium acetate (eluent B). Eluents were degassed using helium and maintained under helium atmosphere. Gradient elution began with binary eluents (A:B) at 100:0, progressed linearly to 85:15 in 20 min and then to 0:100 at 60 min, and returned to 100:0 at 85 min. Total run time was 85 min at a flow rate of 0.25 mL/min with an injection volume of 2 uL. All extracts were analysed in triplicate.

Sugar standards were analysed to act as a reference for retention times of peaks found in samples. This then were reported as the tentative identities of compounds found in the samples. Primary stock solution of each single sugar standard was prepared by dissolving myo-inositol, mannitol, glucose, and fructose at 2 mg/mL and the remaining sugars (maltose, raffinose, kestose, 1,1,1-kestopentaose, nystose, and sucrose) to 8 mg/mL. All stock solutions were stored in the freezer at -25°C until required for analysis. Retention times for each sugar were determined individually in concentrations of 10 mg/L for myo-inositol, 10 mg/L for mannitol, 20 mg/L for glucose, 20 mg/L for fructose, 100 mg/L for sucrose, 100 mg/L for raffinose, 100 mg/L for 1-kestose, 60 mg/L for maltose, 120 mg/L for nystose and 100 mg/L for kestopentose.

## 2.3.6    Microscopy

Samples were imaged using a BX60 wide-filed microscope (Olympus, Germany) in brightfield (BF) and/or fluorescence mode. Fresh samples were transferred to a glass slide, either unstained or stained with Calcofluor (containing 1 g/L Calcofluor White M2R and 0.5 g/L Evans blue) and covered with a cover slip.

A stereomicroscope M165c (Leica, Germany) was used to image a representative sample of fresh digesta pellet on a glass petri dish.

A confocal microscope LSM880 Airyscan (Zeiss, Germany) was used for imaging CLF together with the fibre digesta described in section 4.2.2.3. The settings included two tracks to image the FITC channel (for CLF) separately from the DAPI channel (for Calcofluor). Track 1 included a FITC (filter specification and wavelength: 470/40 FT495 BP525/50) and a transmitted light channel. Track 2 was a DAPI channel (filter specification and wavelength: BP420/40 BS 465 LP470nm).

## 2.3.7    Rheology

Rheology studies the deformation and flow of matter when subjected to normal and tangential stresses. Viscosity ($\eta$) is defined as the internal friction of a fluid or its tendency to resist flow as expressed by Equation 2.7. A rheometer determines the viscosity of a sample by applying a shear rate and measuring the torque to calculate shear stress. Torque is a measure how much force is acting on an object during deformation and is multiplied by a stress constant dependent

on the measurement geometry to determine shear stress. Shear rate is a calculated parameter determined by an angular velocity multiplied by a strain constant which again depends on the measurement geometry.

$$\text{Apparent viscsosity } (\eta) = \frac{shear\ stress}{shear\ rate}$$

*Equation 2.7 – Calculation of apparent viscosity (η) in units of Pa.s from shear stress and shear rate.*

For dilute polymer solutions, viscosity depends on solvent viscosity, the intrinsic viscosity of the polymer in solution and the concentration of the polymer in solution. The intrinsic viscosity depends on structural properties of the polymer, conformation in solution and Mw. With increasing polymer concentrations, entanglement and overlap of polymers occurs as shown in Figure 1.7, with additional increase of the viscosity (Moelants *et al.* 2014, Rao 2007).

An Advanced Rheometer AR 2000 (TA instruments, Elstree, UK) controlled with the software Rheology Advantage Instrument Control AR V5.8.2 (UK) was used to measure the viscosity of whole digesta samples or digesta supernatants. For whole digesta, the rheometer was equipped with a cup at 37°C and vane rotor (stator inner radius: 15.00 mm, rotor outer radius: 14.00 mm) with a gap of 2 mm on a continuous shear ramp from 0.1 to 31 s$^{-1}$ on a log scale with 10 points per decade for 10 minutes, after 1 minute

equilibration time. For digesta supernatants, the digesta was centrifuged at 3,000xg for 20 min (Centrifuge Megafuge 16 Heraeus, Thermo Fisher Scientific, US) and the supernatant decanted into a fresh tube. The measurement geometry was a 40 mm 1 degree acrylic cone at a truncation gap of 28 µm and heating plate at 37°C. Conditions used were continuous ramp from a shear rate of 10 to 1000 s$^{-1}$ with 10 points per decade on a log scale up and down for 2 minutes each.

Before a set of rheological measurements, the geometry inertia was calibrated, a mapping of the geometry performed and zero gap determined.

### 2.3.8 Particle size distribution analysis using laser diffraction

A particle size analyser LS13-320 (Beckman Coulter, USA) based on laser diffraction was used to determine the droplet size of emulsions.

This static light scattering method determines particle size distribution from the scattering intensity after a laser beam illuminated a particle in the scattering volume. The size, shape and refractive index of the particle generate unique angular scattering patterns which are transformed into a spatial intensity pattern and detected by a photon detector under the assumption that the refractive index of the media and density of the particles are uniform throughout the particulate system. Using the Mie scattering theory allows the calculation of a particle size based on the relative intensity

of scattered light, angle of observation, wavelength and polarization of the incident beam, by taking into account optical properties (refractive index, absorptivity and reflectivity) of the particle and the refractive index of the medium. The theory assumes the particles are homogeneous spheres. Due to tumbling and rotation of sample circulation during the measurement, scattering effects from corners and edges of non-spheric particles are smoothed. Hence by assuming a volume-equivalent sphere model, the volume weighted distribution where the contribution of each particle in the distribution relates to the volume of that particle can be determined (=volume-equivalent sphere diameter) (Beckman Coulter Accessed 02/07/2022).

Measurements were taken by using optical parameter settings in the instrument software based on a particle (sunflower oil) and dispersant (water) refractive index of 1.473 and 1.333, respectively. Results are reported as volume-equivalent sphere diameter mean.

### 2.3.9   Differential Scanning Calorimetry

Starch gelatinisation is an endothermic process which takes up heat upon cleavage of the non-covalent bonding interactions which maintain the granule structure of starch. These inter- and intra-molecular non-covalent interactions are higher in crystalline structures as opposed to their disordered, amorphous counterparts. Therefore, the enthalpy required to disrupt this structure can be measured and the enthalpy change associated with gelatinisation

can be related to relative amounts of crystalline and amorphous material (Craig *et al.* 1999). A DSC instrument compares a thermal cycle applied to a sample cell with the one applied to a reference cell which has a heat capacity that is closely matched to the sample. Both cells are hermetically sealed and placed in an adiabatic chamber, where they are heated at a precisely controlled rate. If the sample undergoes an endothermic process, the additional energy that must be applied to the sample cell compared to the reference cell to maintain the same heating rate is recorded. This is achieved either via heat flux or power compensation. For the former, a metal plate is used as a thermally conducting material to connect the sample and reference pans to measure the heat flow between the sample and the reference. In power compensation instruments, sample and reference cells are each heated in thermally insulated furnaces. By controlling the temperature of both chambers to reach the same temperature in the sample as well as the reference, differences in electrical power to achieve and maintain this are recorded. Calibration ensures that the heat capacity of the sample can be measured as a function of temperature, where heat flow is considered proportional to the heat capacity of the sample. By plotting heat flow against temperature, enthalpy changes can be determined as a stepwise change in the heat flow with temperature. DSC was used to measure the endothermic heat flow due to the enthalpy change during starch gelatinisation by integrating the peak in heat flow [J/s or W], normalised to the mass of starch in the

sample pan [J/g starch] and the corresponding temperatures of onset, peak and end of gelatinisation.

DSC experiments were performed using a TA Instrument (TA Instruments Ltd., New Castle, USA) multicell differential scanning calorimeter (MC-DSC), which has three sample cells and one reference cell containing 1 mL degassed, deionised water (Hastelloy ampoules with 1 mL volume). The furnace was continuously flushed with dry Nitrogen at a rate of $50\,mL.min^{-1}$. Synthetic sapphire crystals (NIST SRM 720) were used for heat capacity calibration.

### 2.3.10  X-ray diffraction

X-ray diffraction (XRD) is a technique to determine the degree of crystallinity in polymers by using x-ray beams, high-energy electromagnetic waves, and measuring their diffraction by the tested material (Figure 2.2). When X-ray photons reach a material, an elastic, coherent scattering takes place between the photons and the electrons surrounding the atomic nuclei. As a consequence, the energy of the scattered wave remains unchanged which means it retains its phase relationship to the incident wave. Therefore, the X-ray photons impinging on all atoms of an irradiated volume are scattered in all directions. Crystalline structures with their periodic nature, scatter radiation in a constructive or destructive manner which leads to characteristic diffraction patterns.
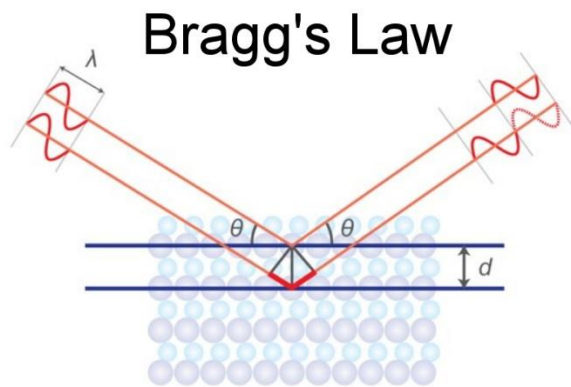
Bragg's Law

$$n\lambda = 2d \cdot \sin\theta$$

*Figure 2.2 – Geometrical condition for diffraction from atomic planes, described by Bragg's law and equation [Picture from www.ridaku.com]*

Bragg's law with the equation $n\lambda = 2d\sin\theta$ underpins the principle based on the diffraction of X-rays by periodic atomic planes and detection of the angle of the diffracted signal. The geometrical interpretation was described by W.L. Bragg in 1913, where n is the order of diffraction, $\lambda$ is the wavelength of the X-rays impinging on the crystalline sample, d is the interplanar spacing between rows of atoms, and $\theta$ is the angle of the X-ray beam with respect to these planes. When this equation is satisfied, X-rays scattered by the atoms in the plane of a periodic structure are in phase and diffraction occurs in the direction defined by the angle $\theta$. (Epp 2016). Diffraction intensity together with the angles at which they are observed are measured and diffraction patterns can be compared to a database of known material diffractograms.

## 2.3.11 Moisture content determination

AACC International method 44-15.02 determines moisture content as loss in weight of a sample when heated under specified conditions. An oven (ED23 Classic, Binder GmbH, Germany) was set to 103°C. Empty aluminium pans were weighed with weight recorded, samples weighed in in triplicate (~300 mg) and the exact weight recorded. The samples were dried in the oven overnight, taken out of the oven, left to cool to room temperature for about 10 min and weighed. This was repeated till continuous weight. Moisture was calculated using Equation 2.8.

$$Moisture\ content\ \% = \frac{sample\ wet\ weight - sample\ dry\ weight}{sample\ wet\ weight} * 100$$

*Equation 2.8 – Moisture content calculation.*

## 2.3.12 β-glucan determination assay

An assay kit from Megazyme (Ireland) was used to determine the BG content. The assay principle involves suspension and hydration of an accurately weighed sample in a buffer solution of pH 6.5 which is then incubated with purified lichenase enzyme (specifically endo-(1-3)(1-4)-β-D-glucan4-glucanohydrolase purified from *Bacillus subtilis*). An aliquot is further hydrolysed with purified β-glucosidase. The D-glucose produced is assayed using a glucose oxidase/peroxidase (GOPOD) reagent which oxidises the released D-glucose to D-gluconate and releases equimolar amounts of hydrogen peroxide ($H_2O_2$) which in turn reacts with p-hydroxybenzoic acid and

4-aminoantipyrine to form quinoneimine dye which can be measured using a spectrophotometer at 510 nm

AOAC Method 995.16 according to the assay kit instructions referred to as method (A) with dilution before β-glucosidase treatment for dry flour or BG extracts were followed with modifications as follows: 5 mg BG extract was weighed in accurately and the weight noted. 20 µL 50% Ethanol was added to aid solubilisation in 4 mL sodium phosphate buffer (20 mM) and vortexed. The mixture was heated in a 99°C water bath for 60 sec and vortex mixed vigorously and heated again in a 99°C water bath for 2 min and vortexed. The tubes were put in a 50°C water bath for 5 min and 0.2 mL lichenase added, vortex mixed and incubated in a 50°C water bath for 2.5 h with regular vortex mixing. After 2.5 hours, 5 mL sodium acetate buffer was added and vortex mixed vigorously. The tubes were left to equilibrate to room temperature for about 5 min before centrifugation. 200 µL of the supernatant was diluted 1:3 with 200 mM sodium acetate buffer. Three times 0.1 mL of this was dispensed in 3 fresh test tubes, 0.1 mL β-glucosidase added to two test tubes (reaction) and 0.1 mL 50 mM acetate buffer to the other tube (control). Glucose standard and blank tubes were prepared according to the Megazyme protocol. All tubes were added to a 50°C water bath for 10 min, followed by addition of 3.0 mL GOPOD and incubation in a 50°C water bath for 20 min. The absorbance at 510 nm against blank was measured within 1 h. BG content was

calculated according to Equation 2.9. The samples were analysed at least in duplicate.

$$BG \%\, w/w = \Delta A * F * \frac{FV}{0.1} * \frac{1}{1000} * \frac{100}{W} * \frac{162}{180} * D$$

*Equation 2.9 – Calculation of BG content (%w/w) wet weight from absorbance at 510 nm. ΔA is the mean of absorbances of sample solution after β-glucosidase treatment (reaction) minus reaction blank absorbance, F is the factor to convert absorbance values to µg glucose (100 µg glucose divided by the GOPOD absorbance value obtained for 100 µg of glucose), FV is the final volume, W is the sample weight in mg (100/W to convert to 100 mg sample), 162/180 is the factor to convert from free glucose as determined to anhydroglucose which occurs in BG, D is a dilution factor prior to incubation with β-glucosidase.*

### 2.3.13  Total starch assay

The total starch determination method used involves an enzymatic hydrolysis of gelatinised starch and colorimetric measurement of released glucose. Starch in the sample is gelatinised at 100°C in DMSO and heat stable α-amylase added which hydrolyses starch into soluble, branched, and unbranched maltodextrins. These are quantitatively hydrolysed by amyloglucosidase into D-glucose. Glucose oxidase/peroxidase (GOPOD) reagent is added which oxidises the released D-glucose to D-gluconate and releases equimolar amounts of hydrogen peroxide ($H_2O_2$) which in turn reacts with p-hydroxybenzoic acid and 4-aminoantipyrine to form quinoneimine dye which can be measured using a spectrophotometer at 510 nm.

The Megazyme total starch assay kit (K-TSTA) with procedure d), DMSO format (AOAC Official Method 996.11) including an alcohol

wash (procedure e) was used to determine total starch in biscuits, ground to a particle size <600>500 µm. About 100 mg of sample was accurately weighed into glass tubes, 5.0 mL of 80% ethanol added and incubated at 80-85 °C in a water bath for 5 min. The tube was removed from the water bath and another 5.0 mL 80% ethanol added and centrifuged for 10 min at 3,900 rpm (Eppendorf Centrifuge 5810R) and the supernatant discarded. The pellet was resuspended in 5 mL 80% ethanol and vortex mixed after which another 5 mL of 80% ethanol were added, mixed by inversion and again centrifuged for 10 min at 3,900 rpm (Eppendorf Centrifuge 5810R) and the supernatant discarded. Then immediately 2 mL DMSO was added, vortex mixed and placed in a vigorously boiling water bath for 5 min. In the meantime, the α-amylase was diluted 30-fold in MOPS buffer (50 mM, pH 7.0). The tubes were taken out from the water bath, 3 mL of diluted α-amylase was added immediately, and vortex mixed vigorously for 20 sec, put back in a boiling water bath and incubated for 6 min with vortex mixing after 2, 4 and 6 min. Then the tubes were placed in a 50 °C water bath and 4 mL sodium acetate buffer (200 mM) as well as 0.1 mL amyloglucosidase added. The mixture was vortex mixed and incubated for 30 min. The entire contents of the tube were transferred to a 100 mL volumetric flask with a funnel to assist and a wash bottle containing deionised water was used to rinse the tube contents thoroughly. The volume was adjusted to 100 mL with

sodium acetate buffer (200 mM) and mixed by inversion. 1.5 mL from the volumetric flask was transferred to Eppendorf tubes and centrifuged at 13,000 rpm for 5 min (Eppendorf Centrifuge 5810R). 0.1 mL supernatant was transferred into two glass test tubes each (duplicate), 0.1 mL deionised water was used for blank and 0.1 mL glucose standard (duplicate). 3.0 mL of GOPOD reagent was added to each glass test tube and incubated at 50 °C for 20 min. The absorbance was measured at 510 nm (Biochrom Libra S80 UV/Vis Spectrophotometer, Biochrom Ltd., UK) against the blank. Starch content was calculated using Equation 2.10 on a 'as is' basis. Equation 2.11 was used to calculate total starch on a dry weight basis using the moisture content analysis as described in section 2.3.11. The samples were analysed at least in duplicate.

$$Starch\ \%\ w/w\ (wet\ weight\ basis) = \Delta A * F * \frac{100}{0.1} * \frac{1}{1000} * \frac{100}{W} * \frac{162}{180}$$

*Equation 2.10 – Calculation of total starch from absorbance at 510 nm. ΔA is the mean of absorbances of sample solution against reagent blank, F is the factor to convert absorbance values to µg glucose (100 µg glucose divided by the GOPOD absorbance value obtained for 100 µg of glucose), W is the sample weight in mg (100/W to convert to 100 mg sample), 162/180 is the factor to convert from free glucose as determined to anhydroglucose which occurs in starch.*

$$Starch\ \%\ w/w\ (dry\ weight\ basis)$$
$$= Starch\ \%\ w/w\ (wet\ weight\ basis)$$
$$* \frac{100}{100 - moisture\ content\ (\%\ w/w)}$$

*Equation 2.11 – Calculation of starch per dry weight basis.*

## 2.3.14  Reducing sugar analysis (PAHBAH assay)

P-hydroxybenzoic acid hydrazide (PAHBAH) reacts with reducing sugars, e.g. maltose, in an alkaline media and forms aromatic acid hydrazides, such as p-hydroxybenzoic acid. The yellow colour of these reaction products can be measured at 405 nm with a spectrophotometer (Lever 1972).

A solution of 5% (w/v) PAHBAH in HCl 0.5 mM was prepared and then diluted 1:10 with 0.5 mM NaOH, prepared freshly before use. 100 µL of sample was mixed with 1 mL PAHBAH solution and incubated in a boiling water bath for 5 minutes. Maltose standards ranging from 50 to 1000 µM as well as a water blank were analysed in parallel. The solutions were allowed to cool to room temperature, 200 µL was transferred to a 96-well plate in duplicate and the absorbance was measured at 405 nm using a plate reader (VersaMax Absorbance Microplate Reader, Molecular Devices, US). Concentrations of maltose in the sample were calculated from the maltose standard curve.

## 2.4  Data analysis

### 2.4.1  Fitting a non-linear regression model

The *nlme* package (Pinheiro *et al.* 2017) in R (version 4.0.2) (Team 2013) was used to calculate coefficients using a non-linear mixed effects regression with fixed effects over treatment and random effects over replicate. Coefficient random effect variances were checked for random distribution. The models used depended on the

nature of the data and literature references (Naumann *et al.* 2018, Grundy *et al.* 2017b, Edwards *et al.* 2019) and are described in the respective chapters. Model fit was assessed by calculating the predicted parameter over time based on the model and comparing how closely they resemble the measured data by plotting both.

## 2.4.2   Statistical analysis

Statistical analyses were performed with R (version 4.0.2) (Team 2013) at a statistical significance level set at p-value ≤ 0.05 using the *emmeans* package (Lenth 2020). Graphs were made either using Microsoft Excel or *ggplot2* package (Wickham *et al.* 2016) in R. Further details of data analysis and statistical tests are described for each experiment in the respective chapters.

# Chapter 3 – Interference of β-glucan-rich cereal fibres with lipid digestion

## 3.1 Introduction

Increasing the population's DF intake holds the potential to combat obesity and hyperlipidaemia (Chambers *et al.* 2015, Jovanovski *et al.* 2020, Reynolds *et al.* 2019). There are several suggested physiological checkpoints at which fibres can positively influence digestive and biochemical processes, examples include gastric emptying and intestinal motility; appetite, satiety and satiation regulation; SCFA production and signalling, as well as reduced lipid hydrolysis during food digestion (Grundy *et al.* 2018a, Grundy *et al.* 2016, Weitkunat *et al.* 2017). Certain DFs like oat bran, barley fibre, pectins, gums and wheat germ have been shown to reduce lipolysis in ileostomy patients as well as animal studies (Lia *et al.* 1997, Lairon *et al.* 2007). The suggested underlying mechanism or combination of mechanisms in human studies seem to be fibre-type specific and include viscosity for gum arabic supplements in healthy adult females in which pectin was used as control (Babiker *et al.* 2012) or an interaction of fibre with BAs for guar gum in a high-fat test meal with 10 g fibre whereas sugar-beet fibre and wheat bran were without effect (Morgan *et al.* 1993). Oat bran also led to an increased excretion of BAs in an ileostomy study with an oat bran enriched bread intervention (Zhang *et al.* 1992). Additional potential interference mechanisms are reduction in lipid hydrolysis rate or

extent as shown with pectin and whole wheat bran but not cellulose (Dutta and Hlasko 1985) or reduced absorption rate of lipids as shown in a high fibre meal with psyllium husk (Khossousi *et al.* 2008). Interestingly in the latter study, the postprandial lipid alterations were independent of glycaemic and insulinaemic responses (Khossousi *et al.* 2008).

Oat bran and barley bran are rich in the soluble fibre BG which has health claims approved about maintenance of normal blood cholesterol levels. The use of the health claim is allowed if a specific amount of BG is contained per quantity of food, but this amount does not seem to provide a consistent answer in terms of whether a cholesterol lowering effect is seen or not (Rieder *et al.* 2017, Grundy *et al.* 2018a). Natural BG-rich foods seem more efficient in their ability to lower blood cholesterol than purified BG added to food if an effect is achieved which makes natural food sources less consistent (Grundy *et al.* 2018a). The functionalities of BG are linked to the molecular composition and Mw (Wang and Ellis 2014) but seem also to depend on the occurrence C*, i.e. a combination of concentration and Mw (Rieder *et al.* 2017). Solubility of BG under simulated digestion conditions is lower than under analytical extraction conditions (Rieder *et al.* 2017, Rosa-Sibakov *et al.* 2020) but it may be important that the solubilisation occurs during the digestive process (Henrion *et al.* 2019) and BG may not be the only important component but rather a synergistic effect and interaction

between the cereal constituents which lead to hypocholesterolaemia (Grundy *et al.* 2018a).

Therefore, it was investigated whether the physical form of cereal DF, the DF composition and the botanical origin change the influence on intestinal lipid digestion *in vitro*. Barley bran and oat bran were tested to compare two botanical origins of samples with the cell wall matrix still intact. These were compared with BG extracts of either barley bran or oat bran , either pre-solubilised before or solubilised during the *in vitro* digestion. Additionally, re-combined extracted BG together with the respective insoluble fibre fraction from oat or barley were tested. The digestion rates and extents of an oil-in-water (O/W) emulsion in the presence of the different cereal fibres were compared to O/W emulsion without fibre.

## 3.2 Materials and Methods

### 3.2.1 Materials

Oat bran and barley bran were used as described in section 2.1.1, see Table 2.1. BG extracts and insoluble dietary fibre (IDF) thereof were made as described section 2.2.1.

Whey protein isolate (WPI) BiPRO, was purchased from Davisco Foods international INC(USA). Sunflower seed oil (SFO) was purchased from a grocery store. Polar and surface-active compounds in the SFO were removed using a glass column filled with Florisil® (cat# 288705, Merck).

All other materials are described in section 2.1.3.

### 3.2.2 Methods

#### 3.2.2.1 Oil-in-Water emulsion preparation

1.8 g SFO was mixed with 28.2 g of 1% WPI in water (which was hydrated for 1 hour) using an Ultra-turrax T-25 (IKA, Germany) at 13,500 rpm for 1 minute to produce a coarse pre-emulsion. To reduce the droplet size further, the emulsion was sonicated using a Branson Digital Sonifier® (Marshall Scientific, USA) at 30% amplitude for 2 minutes, 10 seconds on, 10 seconds off. The emulsion's particle size was measured using a laser diffraction instrument (LS13-320 Beckman Coulter, USA) as described in section 2.3.8. The emulsion was used on the same day if the mean particle diameter ($D_{4,3}$) was in a range of 1.4 +/- 0.3 µm.

## 3.2.2.2 Fibre and control samples investigated using a pH-stat

| Sample name and information | Intact bran: contains BG*, IDF*, intrinsic lipid & protein | BG: extracted from intact bran | IDF: extracted from intact bran | BG + IDF: extracted from intact bran | Emulsion control: no fibre added | Intact bran: contains BG*, IDF*, intrinsic lipid & protein |
|---|---|---|---|---|---|---|
| Fibre diagram | | | | | X | |
| Emulsion added | + emulsion | + emulsion | + emulsion | + emulsion | emulsion | X |
| Investigation | How intact bran fibre impacts the digestion kinetics of the emulsion. | Can the impact on the digestion of the emulsion be attributed to the soluble fibre BG. | Can the impact on the digestion of the emulsion be attributed to the insoluble fibre component. | Do the extracted components BG and IDF impact the digestion of the emulsion in the same way as the intact bran*. | What are the digestion kinetics of emulsion in absence of fibre. How do the kinetics change if lipid content is increased or decreased. | What are the digestion kinetics of intrinsic lipid content in absence of the emulsion. |

*BG and IDF in an intact PCW matrix structure

*Figure 3.1 – Sample overview with investigation reason as investigated for barley bran and oat bran using the pH-stat technique.*

Figure 3.1 gives an overview on the samples investigated together with the aim of the investigation. The fibre materials intact barley or oat bran (with intrinsic lipid and protein content as listed in Table 3.1) or extracted BG with or without IDF based on their BG content (see Table 3.2) or IDF without BG, were digested *in vitro* together with the above described O/W emulsion (see 3.2.2.1) as described in section 3.2.2.3. Controls included either replacing the emulsion and/or the fibre material with 2 mL water, emulsion controls ranged from 9 mg to 150 mg lipid, with 120 mg lipid as the main control termed 'Emulsion control' (see Table 3.2). This range of lipid content was used to cover a range of the lowest lipid content of barley bran

(0.1g BG) in absence of emulsion and the highest lipid content of

oat bran (0.2g BG) in presence of emulsion (see Table 3.1).

*Table 3.1 – Bran intrinsic lipid and protein content and calculated respective quantities in digestion vessel*

| Material | Quantity used for digestion (mg) | Intrinsic lipid (%) | Total intrinsic lipid (mg) | Protein (%) | Total intrinsic protein (mg) |
|---|---|---|---|---|---|
| Barley bran (0.2g BG) | 901 | 2.04 | 18.38 | 9.37 | 84.42 |
| Barley bran (0.1g BG) | 451 | 2.04 | 9.19 | 9.37 | 42.26 |
| Oat bran (0.2g BG) | 746 | 3.80 | 28.35 | 25.54 | 190.53 |
| Oat bran (0.1g BG) | 373 | 3.80 | 14.17 | 25.54 | 95.26 |

*Table 3.2 – Sample overview pH-stat experiments: brans, BG, BG + IDF were either from barley or from oat as well as controls and their respective BG (mg), IDF (mg) and lipid (mg) content.*

| Material | BG (mg) | IDF (mg) | Lipid* (mg) |
|---|---|---|---|
| Barley bran (0.2g BG) | 200 | 90 | 120 |
| Barley bran (0.2g BG) | 200 | 90 | 0 |
| Barley bran (0.1g BG) | 100 | 45 | 120 |
| Barley bran (0.1g BG) | 100 | 45 | 0 |
| Barley BG (dry) | 100 | 0 | 120 |
| Barley BG (solubilised) | 100 | 0 | 120 |
| Barley BG + IDF | 100 | 45 | 120 |
| Barley IDF | 0 | 45 | 120 |
| Oat bran (0.2g BG) | 200 | 225 | 120 |
| Oat bran (0.2g BG) | 200 | 225 | 0 |
| Oat bran (0.1g BG) | 100 | 112 | 120 |
| Oat bran (0.1g BG) | 100 | 112 | 0 |
| Oat BG (dry) | 100 | 0 | 120 |
| Oat BG (solubilised) | 100 | 0 | 120 |
| Oat BG + IDF | 100 | 112 | 120 |
| Oat IDF | 0 | 112 | 120 |
| Emulsion control | 0 | 0 | 120 |
| Emulsion ctrl (150 mg) | 0 | 0 | 150 |
| Emulsion ctrl (135 mg) | 0 | 0 | 135 |
| Emulsion ctrl (60 mg) | 0 | 0 | 60 |
| Emulsion ctrl (30 mg) | 0 | 0 | 30 |
| Emulsion ctrl (9 mg) | 0 | 0 | 9 |

*Lipid from emulsion

All lipid digestions in presence and absence of fibre were carried out in triplicate, except barley BG (solubilised) which was repeated in duplicate per solubilised BG batch (i.e. 6 times in total) due to batch effects of the pre-solubilisation of barley BG.

### 3.2.2.3 Static gastric digestion followed by duodenal digestion using a pH-stat

The fibre material (see Table 3.2) was weighed in dry (except for solubilised BG, see below) in the respective amount to have 100 or 200 mg BG and water added to a total of 2 g. This was mixed with 2 g 6% O/W emulsion (see 3.2.2.1) and together made 4 g starting material for the simulated digestion calculations according to Minekus *et al.* (Minekus *et al.* 2014), resulting in a BG concentration in the duodenal phase of 0.313 or 0.625%, respectively. Barley or oat IDF (in absence of BG) were digested together with the emulsion in the same manner.

Simulated fluids were prepared according to Minekus *et al.* (Minekus *et al.* 2014) but replacing $NaHCO_3$ with NaCl in the SIF to avoid $CO_2$ formation, which would have introduced undesirable pH changes as described by Mat *et al.* (Mat *et al.* 2016), and recommended in the latest INFOGEST protocol (Brodkorb *et al.* 2019).

For the oral phase, the starting material was diluted with simulated salivary fluids (SSF) (α-amylase replaced by SSF) and $CaCl_2$, followed by the gastric phase, the mixture was again diluted 1:1 with simulated gastric fluid (SGF), pepsin (2000 U/mL), $CaCl_2$, 1 M HCl to reach a pH of 3 and deionised water and digested for 2 hours at 37°C on a rotary mixer. The gastric digesta was mixed with the required amount of simulated intestinal fluid (SIF) and transferred into a pH-stat titration vessel (jacketed and capped reaction vessel, number 6.1418.150, 5-70 mL volume, Metrohm AG, Switzerland) at

37°C which was connected to a pH-stat device KEM AT-700 (Kyoto electronics, Japan). Bovine bile (10 mM final concentration in digestion vessel) and $CaCl_2$ were added as well as the required amount of 1 M NaOH to reach a stable pH of 7. A pH probe (8172BNWP, Thermo Scientific, UK) connected to a pH-stat device KEM AT-700 (Kyoto electronics, Japan) was immersed in the digesta. Duodenal digestion and titration was started by adding 1 mL of a freshly prepared pancreatin solution (see below for digestive enzyme activities) in SIF which resulted in a final volume of 32 mL. The pH-stat maintained the pH at 7 by titration of 0.1 M NaOH for 2 hours and recorded the added volume. The digesta was stirred in the digestion vessel using a x-shaped magnetic stirrer bar and the speed was adjusted according to the viscosity of the digesta to ensure mixing and pH measurement across the digesta.

Solubilised oat or barley BG was weighed in to make a batch of 3 or 6 replicates, mixed with the respective amounts of warmed water, warmed SSF and $CaCl_2$ equivalent to the starting and oral hydration to keep the amount of BG in the intestinal phase at 0.313%. This was mixed using a magnetic stirrer in an incubator at 37°C two times overnight. Then, the respective amount of solubilised BG was weighed in and mixed with 2 g emulsion and digested the same way as the other DF materials but omitting the oral phase.

The INFOGEST consortium recommends a pancreatin concentration based on the trypsin activity of 100 TAME units/mL intestinal volume

and 2000 U/mL of porcine pancreatic lipase (Minekus *et al.* 2014). Pancreatin (LOT#SLCG6869) had a trypsin activity of 3.9 U (TAME)/mg solid and a lipase activity of 78.3 U/mg pancreatin at a mixing speed of 700 RPM. 820.5 mg pancreatin were added to 32 mL simulated duodenal phase volume which makes 100 U/mL trypsin and 2008 U/mL lipase in the digestion vessel.

### 3.2.2.4  Rheology

An additional set of digestions was performed as described in section 3.2.2.3. After the gastric phase, the digesta was mixed with simulated intestinal fluid, $CaCl_2$, water and NaOH added to reach a pH of 7 to mimic the same dilution conditions for determination of the viscosity at the beginning of the duodenal phase. Water was used to substitute bovine bile as bile was assessed as having no impact on whole digesta viscosity (data not shown). Rheological properties were measured as described in section 2.3.7 for whole digesta.

Shear thinning index was calculated by dividing the viscosity at the highest measured shear rate (31 $s^{-1}$) by the viscosity measured at a low shear rate (0.15 $s^{-1}$) to compare shear thinning behaviours across samples.

### 3.2.2.5  Lipase activity

Lipase activity in presence of BAs was assayed as described in section 2.3.2.4.

### 3.2.2.6 Lipase activity assay in absence of bile acids

The protocol is based on the pancreatic lipase activity assay (EC 3.1.1.3), INFOGEST 2.0 supplementary material (Brodkorb *et al.* 2019) with modifications as follows:

Assay stock solutions were made as follows: 200 mL assay solution contained 1,800 mg NaCl, 40 mg $CaCl_2$ and 7.2 mg Tris-(hydroxymethyl)-aminomethane and was adjusted to pH 8 with 0.1 M HCl. The titration solution was a 0.1 M sodium hydroxide (NaOH) which was made by dissolving 2 g NaOH in 500 mL of deionised water.

Fibre samples (4 g start weight) were pre-digested in a simulated oral phase (α-amylase replaced by SSF as starch digestion was not the aim of the investigation) and 2h gastric phase using pepsin as described in section 3.2.2.3. Controls were analysed by replacing fibre with the equivalent mass of water and pepsin with SGF to mimic the same dilution conditions as in presence of fibre. This allowed to determine the impact of fibre and/or pepsin on the lipase activity.

14.5 mL assay solution and 0.5 mL of tributyrin, as the lipid substrate, were mixed in a pH-stat titration vessel (jacketed and capped reaction vessel, number 6.1418.150, 5-70 mL volume, Metrohm AG, Switzerland) connected to a pH-stat device KEM AT-700 (Kyoto electronics, Japan). The titration vessel was kept at 37°C and had a cross-shaped magnetic stirrer bar of 0.9 cm length on the

bottom of the vessel, which was placed on a magnetic stirrer (Stuart Digital Stirring Hot Plate) to mix at 700 RPM for 3-5 min to disperse the tributyrin and form a fine oil-in-water emulsion. The gastric digesta (16 mL) was added at a mixing speed of 200, 350, 520 or 700 rpm to the assay solution and tributyrin and pH adjusted to pH 8 with 0.1 M HCl or 0.1 M NaOH with the volume recorded. Deionised water was added for a consistent final volume of 32 mL in the pH-stat vessel in all samples. Following the addition of 100 µL of 2 mg/mL pancreatin solution in deionised water (prepared fresh and kept on ice), the titration program was started. Constant pH was maintained at 8 through addition of the titration solution to counter the release of FFAs, the volume of titration solution was recorded over 15 min. The linear kinetics of free fatty acid release was used to calculate the lipase activity using Equation 3.1 (Brodkorb *et al.* 2019).

$$\frac{Units}{mg\ powder} = \frac{R(NaOH) \times 1000}{v\ \times [E]}$$

*Equation 3.1 – Calculation of lipase activity: R(NaOH): Rate of NaOH delivery in µmol NaOH per minute, i.e., µmol free fatty acid titrated per minute, v: volume [µL] of enzyme solution added in the pH-stat vessel, [E]: concentration of the enzyme solution [mg powder/mL].*

### 3.2.2.7 Data and statistical analysis

Statistical analyses were performed with R (version 4.0.2) (Team 2013) as described in section 2.4.2 with specifics as follows.

A non-linear regression model was fitted to the lipolysis data as described in section 2.4.1 using Equation 3.2 for data on volume NaOH consumption over time. FFA release (%) data calculated using Equation 3.3 over time was also fitted to Equation 3.2 with sub-zero values set to NA for model fit and to 0 for figures. Coefficients as well as lipid digestion results after 2 hours (Volume NaOH or % FFA, data subset: timepoints [sec] > 7194) in presence of fibre were compared with emulsion control using Dunnett's test comparing several treatments with a control.

Lipase activity results in presence and absence of fibre at different mixing speeds were analysed using a pairwise comparison with Tukey correction.

$$x = \frac{a * time}{\log(b) + time}$$

*Equation 3.2 – Lipid digestion kinetics model with coefficient 'a' representing the final extent of lipid digestion and coefficient 'b' the rate of lipid digestion, 'x' is the extent of lipid digestion at a given timepoint (i.e. Volume NaOH consumed or % FFA released) and 'time' is the respective timepoint (i.e. time in seconds) (Grundy et al. 2017b).*

$$\% FFA(t) = 100 \times \frac{\left(V_{\text{NaOH sample}}(t) - V_{\text{NaOH water ctrl}}(t)\right) \times [NaOH] \times M_{\text{Lipid}}}{2 . m_{\text{Lipid}}}$$

*Equation 3.3 – % FFA release: $V_{NaOH\ sample}$ is the volume of NaOH (in litre) required to neutralise the FFA produced per timepoint, $V_{NaOH\ water\ ctrl}$ the volume of NaOH (in litre) of water control per timepoint, [NaOH] the concentration of the NaOH solution used, i.e. 0.1 M, $M_{Lipid}$ the molecular weight of the oil employed in this experiment (for sunflower oil = 876 g/mol (Sánchez et al. 2012)), divided by 2 due to the assumption that one triglyceride releases two FFAs and $m_{Lipid}$, the mass of triacylglycerol (TAG) initially present in the digestion vessel (in gram), i.e. 0.12 g lipid (digestion of 2 g of a 6% O/W emulsion).*

## 3.3   Results

### 3.3.1   Lipid digestion interference in presence of certain types of cereal DFs

Initial experiments investigated the impact of the form of the DF matrix on lipid digestion. As not all BG found in a matrix may solubilise during an *in vitro* digestion (Rieder *et al.* 2017) intact brans with double the BG concentration were also tested. Figure 3.2 shows the consumption of sodium hydroxide to neutralise digestion products (i.e. free fatty acids) over two hours intestinal phase of a 6% O/W emulsion in the presence of the tested cereal fibres compared to emulsion control. The digestion profile exhibited a fast lipolysis in the beginning followed by a slower phase and plateau in line with other studies (Pabois *et al.* 2020, Grundy *et al.* 2017b, Li *et al.* 2011). Digestion kinetics parameters determining lipolysis rate and lipolysis extent were calculated by fitting Equation 3.2, with good fits as shown in Figure 3.3.

Lipolysis rates were statistically significantly slower in presence of barley bran (0.1g and 0.2g BG), barley BG (dry), barley BG + IDF, oat bran (0.1g and 0.2g BG), and oat BG (dry) (p≤0.05, Dunnett's test comparing several treatments with a control, see Table 3.3) compared to the emulsion control.
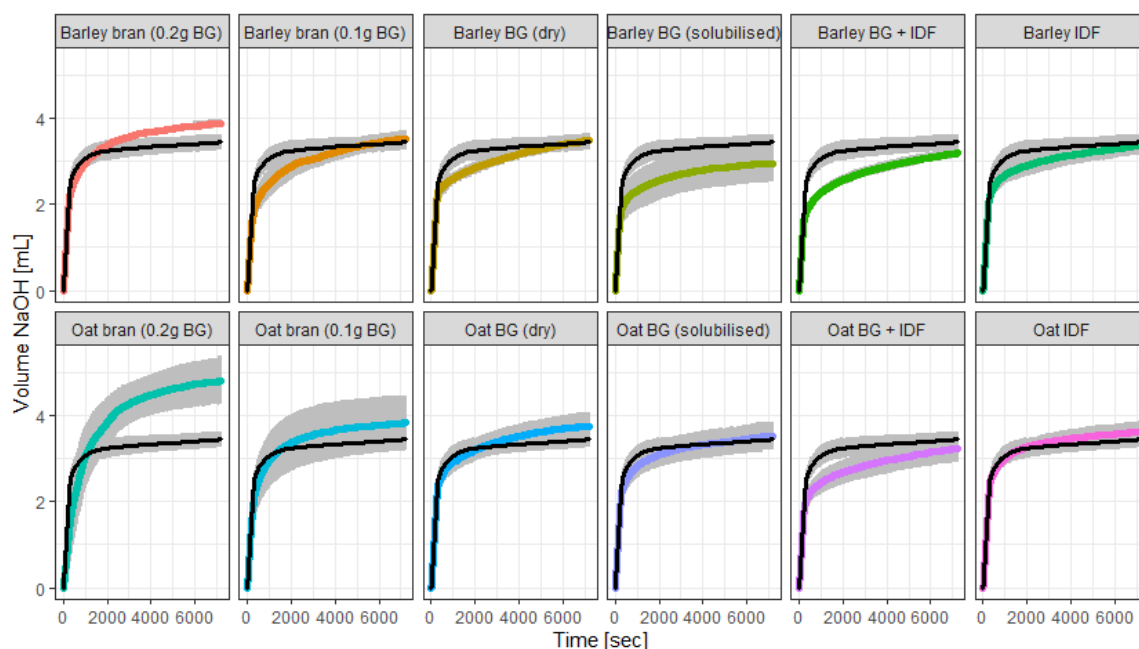
Figure 3.2 – Volume of NaOH [mL] consumption over 2 hours lipid digestion of a 6% O/W emulsion in absence of fibre (black) or in presence of fibre (colour):- barley (upper panel) or oat (lower panel) in order of BG concentrations: bran (intact) with 200mg BG, bran (intact) with 100 mg BG, BG (extracted) with 100 mg BG, BG (extracted and pre-solubilised) with 100 mg BG, extracted BG with insoluble dietary fibre (IDF) with 100 mg BG, or IDF alone (0 mg BG). SD error bars in grey, n=3 (except barley BG (solubilised) n=6).
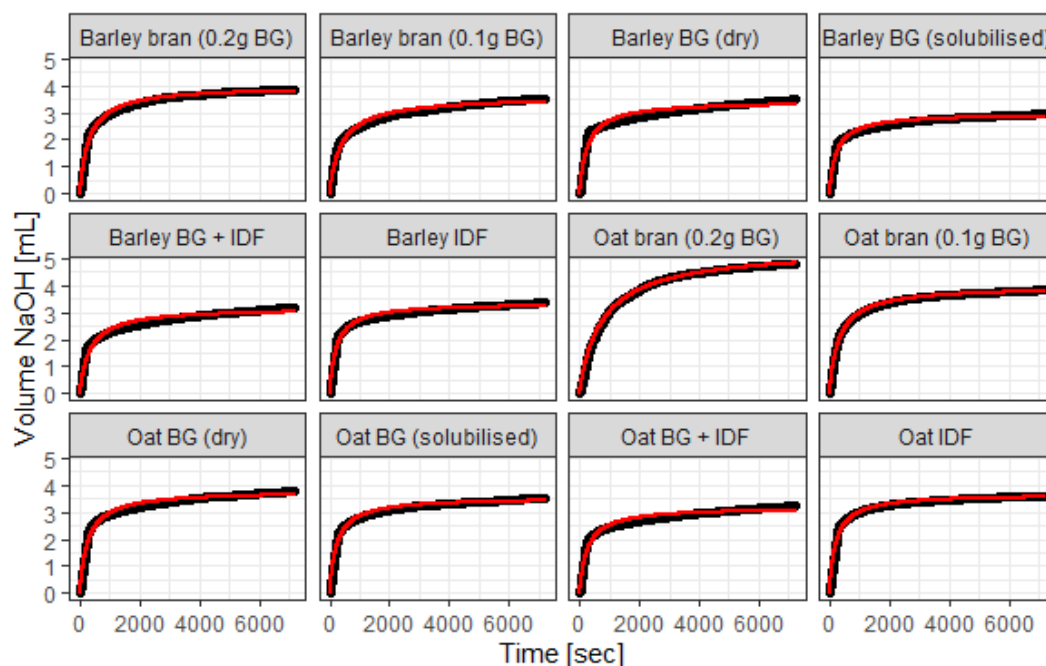


Figure 3.3 – Volume of NaOH [mL] consumption over 2 hours. Mean of measured data in black vs mean of predicted data after fitting to Equation 3.2 in red for comparison of data fit, n=3.

*Table 3.3 – Emulsion control (120mg lipid) in absence and presence of different cereal fibres, as well as cereal fibres in absence of emulsion 2h lipid digestion data fitted to Equation 3.2: Coefficients mean [lower and upper 95% confidence interval (CI)] representing lipolysis extent in volume NaOH (mL) (coefficient a) and lipolysis rate (coefficient b) and results of statistical significance test compared to emulsion control: Dunnett's test p-value adjustment for comparing several treatments with a control, significance level: p≤0.05.*

| Material | Lipolysis extent [95% CI] | p-value | Lipolysis rate [95% CI] | p-value |
|---|---|---|---|---|
| Emulsion control | 3.51 [3.20, 3.81] | n.a. | 5.16 [4.94, 5.37] | n.a. |
| Barley bran (0.2g BG) | 3.98 [3.67, 4.28] | 0.2920 | 5.76 [5.55, 5.97] | 0.0010 |
| Barley bran (0.1g BG) | 3.59 [3.29, 3.90] | 0.9993 | 6.01 [5.80, 6.22] | <0.0001 |
| Barley BG (dry) | 3.42 [3.11, 3.72] | 0.9990 | 5.62 [5.41, 5.83] | 0.0287 |
| Barley BG (solubilised) | 2.97 [2.75, 3.19] | 0.0586 | 5.51 [5.36, 5.66] | 0.0868 |
| Barley BG + IDF | 3.16 [2.86, 3.47] | 0.6561 | 5.85 [5.64, 6.07] | 0.0001 |
| Barley IDF | 3.34 [3.04, 3.65] | 0.9809 | 5.45 [5.24, 5.66] | 0.4009 |
| Oat bran (0.2g BG) | 5.38 [5.07, 5.68] | <0.0001 | 6.67 [6.46, 6.88] | <0.0001 |
| Oat bran (0.1g BG) | 3.97 [3.66, 4.27] | 0.3108 | 5.82 [5.61, 6.04] | 0.0002 |
| Oat BG (dry) | 3.78 [3.48, 4.09] | 0.8277 | 5.62 [5.41, 5.83] | 0.0302 |
| Oat BG (solubilised) | 3.54 [3.24, 3.85] | 1.0000 | 5.50 [5.29, 5.71] | 0.2317 |
| Oat BG + IDF | 3.18 [2.88, 3.49] | 0.7111 | 5.59 [5.38, 5.80] | 0.0541 |
| Oat IDF | 3.67 [3.37, 3.98] | 0.9801 | 5.39 [5.18, 5.60] | 0.6759 |
| Barley bran (0.2g BG) w/o emulsion | 1.85 [1.55, 2.16] | <0.0001 | 4.55 [4.34, 4.76] | 0.0011 |
| Barley bran (0.1g BG) w/o emulsion | 1.71 [1.40, 2.01] | <0.0001 | 4.32 [4.11, 4.53] | <0.0001 |
| Oat bran (0.2g BG) w/o emulsion | 2.93 [2.63, 3.24] | 0.1020 | 6.45 [6.24, 6.66] | <0.0001 |
| Oat bran (0.1g BG) w/o emulsion | 2.11 [1.80, 2.41] | <0.0001 | 4.78 [4.57, 4.99] | 0.1401 |

Although BG is generally regarded as a soluble fibre, its solubility depends on concentration, solvent quality, and may be different between extracted BG and solubilisation from a PCW matrix (Grundy *et al.* 2017b, Henrion *et al.* 2019). Extracted BG from barley or oat, was tested with pre-solubilisation (solubilised) and without pre-solubilisation (dry), the latter forming BG aggregates which did not dissolve during the time course of the *in vitro* digestion. Barley BG (solubilised) had a 0.5 mL lower NaOH response after 2 hours lipid digestion than the control ($p<0.0001$, Dunnett's test). Interestingly, neither barley BG (solubilised) nor oat BG (solubilised) slowed down the lipolysis rate compared to the control, whereas both barley BG (dry) and oat BG (dry) did (Table 3.3). When IDF particles were present and mixed together with BG, the IDF seemed to aid solubilisation of BG hence only very small aggregates were found when both fibre components were present, both in barley and oat. Barley BG + IDF slowed down the lipolysis rate significantly ($p=0.0001$, Dunnett's test) whereas in the presence of oat BG + IDF the reduction was not statistically significant ($p=0.0541$, Dunnett's test). To rule out a potential influence of the IDF on its own, IDF was tested without soluble fibre which resulted in lipolysis extents as well as rates comparable to control with both, barley IDF as well as oat IDF ($p>0.05$, Dunnett's test, see Table 3.3).
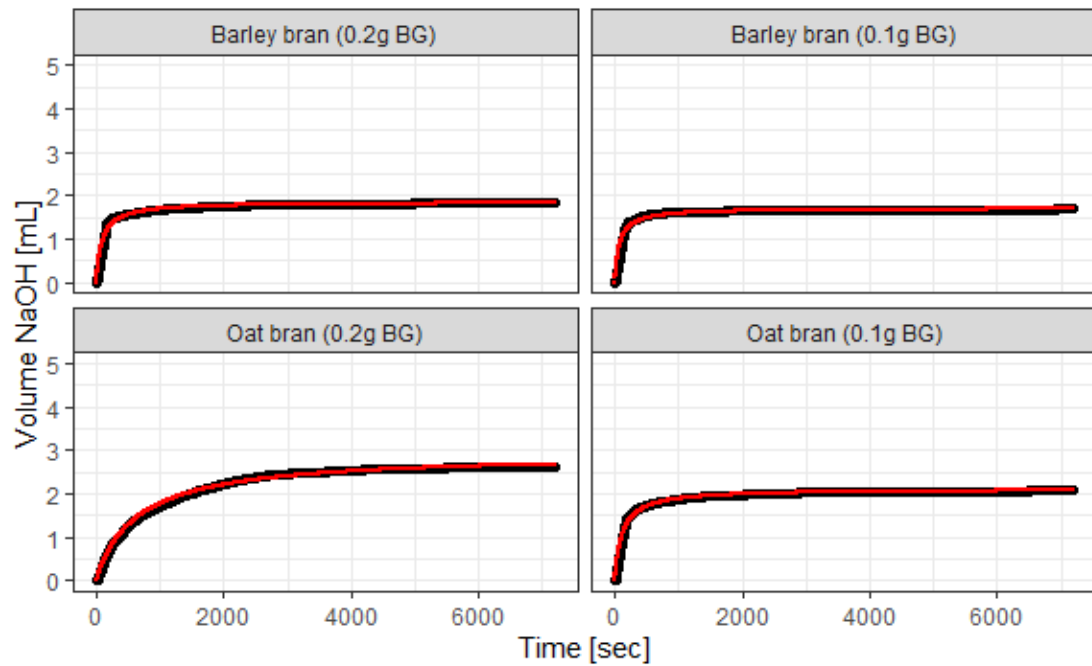
*Figure 3.4 – Intact brans without emulsion: Volume of NaOH [mL] consumption over 2 hours lipid digestion of intact brans digested in absence of emulsion. Mean of measured data in black vs mean of predicted data after fitting to Equation 3.2 in red for comparison of data fit, n=3.*

A statistically significantly higher NaOH response after 2 hours compared to control was found with oat bran (0.2g BG) ($p<0.0001$), oat bran (0.1g BG) ($p=0.0059$) as well as barley bran (0.2g BG) ($p=0.0012$, Dunnett's test). However, the digestion extent modelled using Equation 3.2 (see Table 3.3) was only higher in oat bran (0.2g BG) compared to emulsion control ($p<0.0001$, Dunnett's test). 40% of barley bran and 50% of oat bran, are fibre (Table 2.1) of which the other nutrients include lipids. Oat bran (0.2g BG) had with 28.35 mg intrinsic lipids the highest additional lipid content (see Table 3.1 for calculation). This suggested that the intrinsic lipids in the brans may contribute to the overall lipid digestion. To measure the extent of contribution of intrinsic bran lipids to the overall digestion, the

intact brans were digested without added emulsion and digestion kinetics calculated (Figure 3.4, Table 3.3).

The lipolysis extent in the absence of an emulsion was lower in barley bran (0.2g BG and 0.1g BG) and oat bran (0.1g BG) compared to emulsion control (all p<0.0001, Dunnett's test), as expected due to the lower amount of lipid (see Table 3.2) compared to 120 mg lipid in the emulsion control (Figure 3.4, Table 3.3). However, oat bran (0.2g BG) had with 2.93 mL NaOH [95% CI 2.63, 3.24] a similar lipolysis extent as the control with 3.51 mL NaOH [95% CI 3.20, 3.81] (p=0.1020, Dunnett's test). Compared to emulsion control, barley bran (0.2g BG) and barley bran (0.1g BG) both in absence of emulsion had a faster lipolysis rate (p≤0.05, Dunnett's test), whereas oat bran (0.1g BG) had a lipolysis rate comparable to emulsion control (p=0.1401, Dunnett's test). The lipolysis rate of oat bran (0.2g BG) without emulsion was statistically significantly slower than emulsion control (p<0.0001, Dunnett's test). Considering the bran's intrinsic lipid contents were very low (see Table 3.2) in relation to the emulsion control, there was quite an extensive consumption of NaOH, i.e. liberation of FFAs.

To further investigate this, different amounts of 6% O/W emulsion were digested from 9 to 150 mg total lipid as well as a water only control (Figure 3.5, Table 3.4) and compared to the standard emulsion control containing 120 mg total lipid. There was an unexpected high baseline without any lipid present (Figure 3.5, Table

3.4) This could be due to the pancreatin digestive enzymes digesting the added enzymes and potentially bile tissue from the bovine bile as there were no other digestion substrates added. However, this was not investigated and the result was accepted as baseline for the calculation of FFA released (see Equation 3.3).
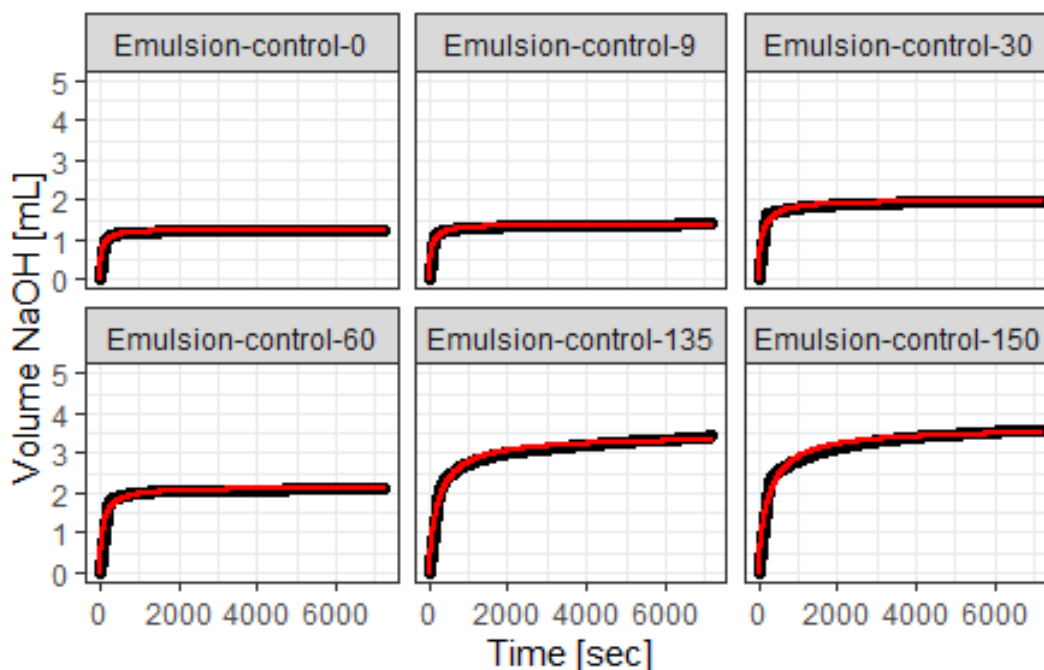


*Figure 3.5 – Volume of NaOH [mL] consumption over 2 hours lipid digestion of emulsion controls with different lipid content of 0, 9, 30, 60, 135 and 150 mg. Mean of measured data in black vs mean of predicted data after fitting to Equation 3.2 in red for comparison of data fit, n=3.*

*Table 3.4 – Controls containing different amount of lipid fitted to Equation 3.2: Coefficients mean [lower and upper 95% confidence interval (CI)] representing lipolysis extent in volume NaOH (mL) (coefficient a) and lipolysis rate (coefficient b). P-values are results of statistical significance test compared to emulsion control (120mg). Different letters represent significant difference, pairwise comparison, Tukey correction, significance level: p≤0.05.*

| Controls lipid levels (mg) | Lipolysis extent [95% CI] | p-value | | Lipolysis rate [95% CI] | p-value | |
|---|---|---|---|---|---|---|
| 0 | 1.25 [0.99, 1.52] | <0.0001 | b | 4.05 [3.86, 4.24] | <0.0001 | b |
| 9 | 1.39 [1.12, 1.65] | <0.0001 | b | 4.20 [4.01, 4.39] | <0.0001 | bc |
| 30 | 1.99 [1.73, 2.26] | <0.0001 | c | 4.58 [4.39, 4.77] | 0.0005 | c |
| 60 | 2.14 [1.88, 2.41] | <0.0001 | c | 4.50 [4.31, 4.69] | <0.0001 | c |
| 135 | 3.43 [3.17, 3.70] | 0.9998 | a | 5.49 [5.30, 5.68] | 0.1769 | a |
| 150 | 3.64 [3.38, 3.91] | 0.9922 | a | 5.53 [5.35, 5.72] | 0.0811 | a |

Only controls containing 60 mg or less total lipid had a statistically significantly lower digestion extent and rate (p≤0.05, Dunnett's test, Table 3.4) than the standard emulsion control. When compared against each other, emulsions with total lipids of 150, 135 and 120 mg had a similar digestion extent and rate, whereas 60 mg was comparable with 30 mg (see Table 3.4). 9 and 0 mg total lipid content had a comparable lipid digestion extent and rate, whereas 9 mg lipid had a similar digestion rate as 30 and 60 mg lipid. The more lipid substrate was available for digestion, the slower the lipolysis rate, except for 60 mg total lipid which was faster than

expected. This relationship partly explained the out of proportion response of the brans digested without emulsion. Additionally, the two pools of lipid, the intrinsic cereal lipid vs the sunflower oil in the emulsion, could potentially be digested at different rates and extents, which makes determination of whether the bran is affecting the digestion of the extrinsic lipid more difficult.
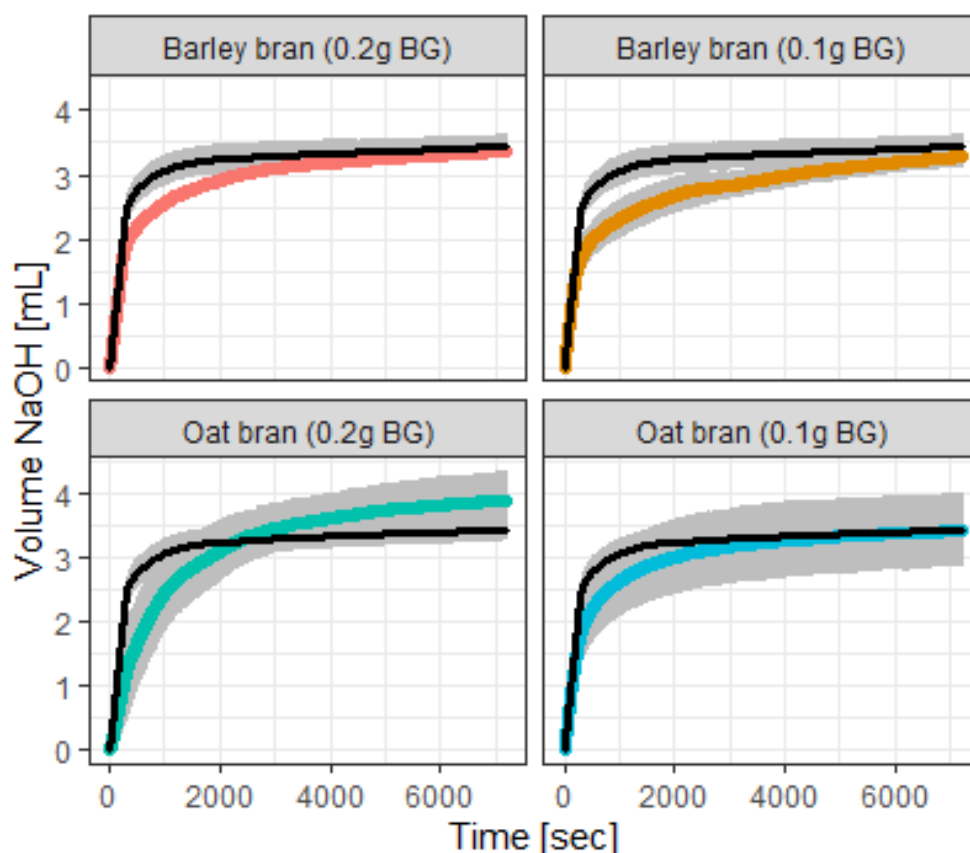


*Figure 3.6 – Volume NaOH for brans normalised for their respective total lipid contents (mean of replicates in colour) vs emulsion control (mean of replicates in black), SD error bars in grey.*

To account for the higher amounts of lipid present from intact brans, the NaOH response was normalised for total lipid by dividing the volume NaOH per timepoint by the total lipid content (= 120 mg lipid in the emulsion + total intrinsic lipid content per bran, see Table

3.2) and multiplying it by 120 (mg) representing the lipid content of the emulsion. Figure 3.6 shows the intact bran digestion results normalised to their respective total lipid content. After normalisation, oat bran (0.2g BG) had still a statistically significantly higher NaOH consumption than emulsion control (p<0.0003, Dunnett's test). However, this was assessed as a good conservative approach to account for intrinsic lipids, hence the normalised data were used for subsequent analysis of % FFA release.

### 3.3.2 Free fatty acid release reveals differences between barley and oat

It is common practice to convert the NaOH consumption into FFAs released (Pabois *et al.* 2020, Guo *et al.* 2017, Dias *et al.* 2019, Torcello-Gómez and Foster 2016, Li and McClements 2010, Grundy *et al.* 2015), assuming the ideal case in which the hydrolysis of one molecule of TAG leads to the formation of one molecule of MAG and two molecules of FFA following Equation 3.3. Figure 3.7A shows FFA release for the digestions of an emulsion in the absence and presence of the fibre materials. Subtraction of the water control led to a lag phase in the very beginning of the lipid digestion. The data were fitted to Equation 3.2 with derived lipid digestion kinetics listed in Table 3.5. Assessment of the data fit by comparing predicted versus measured data (Figure 3.8) showed that measured individual component fibres including BG, BG + IDF and IDF plateaued quickly and deviated slightly from the predicted values whereas intact brans

had a smoother transition to the plateau with good fit with the predicted results. Despite the fact that Equation 3.2 seemed to fit better with data with a smooth transition, the data fit overall was assessed as acceptable.
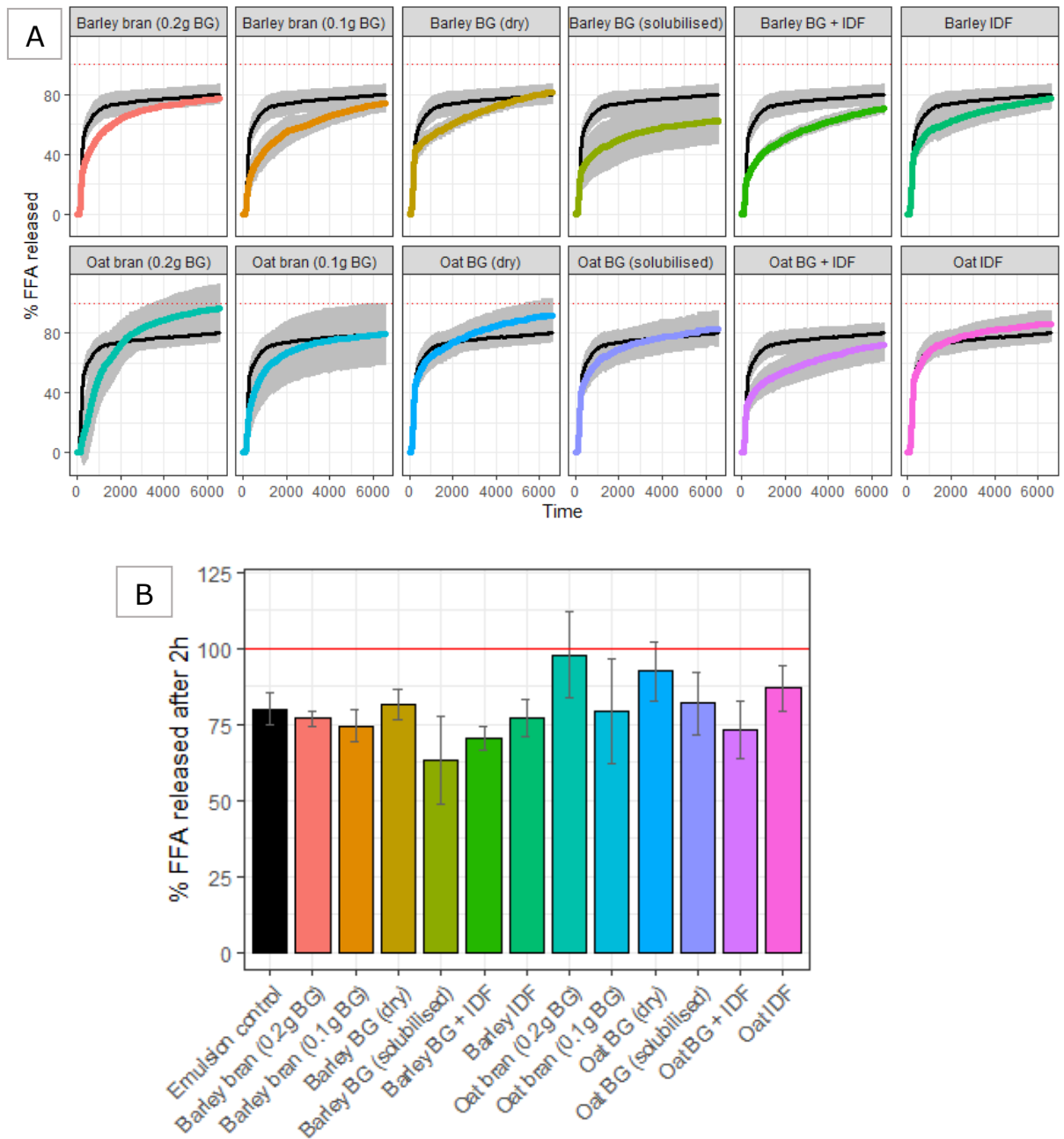


*Figure 3.7 – Mean FFA released [%] A) over time [sec] for 2 hours and B) at the end of 2 hours lipid digestion of the O/W emulsion control (120 mg) in absence of fibres [in black] and in presence of different cereal fibres [in colour] calculated using Equation 3.3, SDs are error bars in grey, 100% is marked with a red horizontal line.*
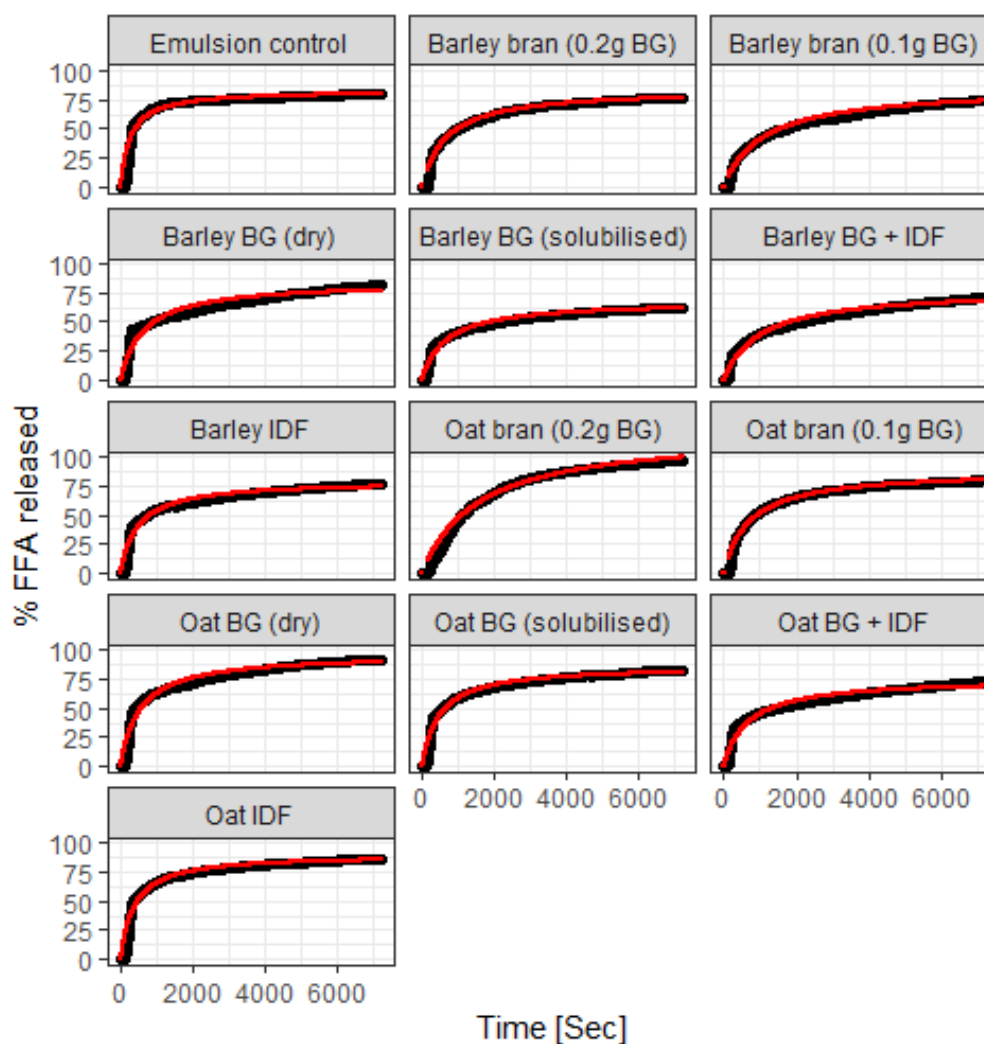
*Figure 3.8 – FFA release [%] calculated using Equation 3.3 of lipid digestion of the O/W emulsion control (120 mg) in the absence and presence of different cereal fibres. Mean of measured data in black vs mean of predicted data after fitting to Equation 3.2 in red for comparison of data fit, n=3 (except for barley BG (solubilised) n=6).*

In the absence of fibre, 80% of the total FFAs were released after 2 hours intestinal digestion (Figure 3.7B) which is comparable to 71% reported in a similar study (Zhai *et al.* 2021). As previously noted with NaOH consumption results, presence of barley BG (solubilised) led to a 17% lower mean release of FFAs after 2 hours digestion compared to control (p<0.0001, Dunnett's test). Only oat bran (0.2g BG) reached almost 100% FFA released after 2 hours of lipid

digestion which was statistically significantly higher than the control (p<0.0001, Dunnett's test). Also oat BG (dry) had a 12% higher FFA release than the control (p=0.0077, Dunnett's test), whereas all other fibres had a FFA release comparable to the control after 2 hours (p>0.05, Dunnett's test). FFA release data fitted to Equation 3.2 (Table 3.5) showed that modelled lipolysis extent was only significantly different in oat bran (0.2g BG), which was 38.5% higher than emulsion control (p<0.0001, Dunnett's test, Table 3.5). This indicated that the lipid digestion may not have come to an end after 2 hours, which is theoretical as oat bran (0.2g BG) reached a lipolysis extent of 121% FFA release. Lipolysis rates were all statistically significantly slower than control (p≤0.05, Dunnett's test) except barley IDF, oat IDF, oat BG (dry) and oat BG (solubilised) (see Table 3.5).

In summary, this highlights important differences between barley and oat. Whereas for barley, only presence of BG (irrespective whether on its own, together with IDF or from an intact bran) was necessary to reduce lipolysis, for oat fibre presence of both, BG and IDF, was important for exerting an effect. Whether lipid digestion might be impacted by different digesta viscosities was investigated further.

*Table 3.5 – FFA release (%) calculated using Equation 3.3 fitted to Equation 3.2: Coefficients mean [lower and upper 95% confidence interval (CI)] representing lipolysis extent in FFA release (%) (coefficient a) and lipolysis rate (coefficient b) and results of statistical significance test compared to emulsion control: Dunnett's test p-value adjustment for comparing several treatments with a control, significance level: p≤0.05.*

| Material | Lipolysis extent [95% CI] | p-value | Lipolysis rate [95% CI] | p-value |
|---|---|---|---|---|
| Emulsion control | 82.87 [72.29, 93.45] | n.a. | 5.60 [5.22, 5.99] | n.a. |
| Barley bran (0.2g BG) | 83.71 [73.13, 94.29] | 1.0000 | 6.51 [6.13, 6.90] | 0.0111 |
| Barley bran (0.1g BG) | 85.01 [74.43, 95.59] | 0.9994 | 7.02 [6.63, 7.40] | <0.0001 |
| Barley BG (dry) | 83.89 [73.31, 94.47] | 1.0000 | 6.47 [6.08, 6.85] | 0.0188 |
| Barley BG (solubilised) | 67.40 [59.92, 74.88] | 0.1565 | 6.51 [6.24, 6.78] | 0.0018 |
| Barley BG + IDF | 77.41 [66.83, 87.99] | 0.9701 | 6.94 [6.56, 7.33] | <0.0001 |
| Barley IDF | 78.91 [68.33, 89.49] | 0.9919 | 6.17 [5.79, 6.56] | 0.2826 |
| Oat bran (0.2g BG) | 121.37 [110.79, 131.95] | <0.0001 | 7.37 [6.99, 7.76] | <0.0001 |
| Oat bran (0.1g BG) | 87.89 [77.31, 98.47] | 0.9786 | 6.58 [6.20, 6.97] | 0.0045 |
| Oat BG (dry) | 95.86 [85.28, 106.44] | 0.4921 | 6.28 [5.89, 6.66] | 0.1228 |
| Oat BG (solubilised) | 85.96 [75.38, 96.54] | 0.9971 | 6.15 [5.77, 6.54] | 0.3190 |
| Oat BG + IDF | 74.99 [64.41, 85.57] | 0.8824 | 6.52 [6.13, 6.90] | 0.0104 |
| Oat IDF | 89.86 [79.29, 100.44] | 0.9231 | 5.92 [5.54, 6.31] | 0.8271 |

### 3.3.3 Impact of mixing rate, shear and viscosity

Figure 3.9 shows whole digesta apparent viscosity at the start of the duodenal phase in presence or absence (emulsion control) of the different cereal fibres. Viscosities of all digesta were dependent on the applied shear and showed non-Newtonian behaviour with shear thinning as the apparent viscosity decreased with increasing shear rate. This is expected behaviour for polymer solutions whereas swollen particulate systems may result in Newtonian behaviour, i.e. that viscosity is independent of shear rate (Picout and Ross-Murphy 2003). Oat fibres showed much less shear thinning compared to the barley fibres. Sorting the digesta containing BG by their shear thinning index from low to high puts them in the following order: oat bran (0.1g BG) < oat bran (0.2g BG) < oat BG < barley bran (0.2g BG) < barley BG + IDF < oat BG + IDF < barley BG < barley bran (0.1 g). Differences in shear thinning behaviour between bran with different botanical origin also meant that oat bran (0.2 g BG) and barley bran (0.2 g BG) only had a similar viscosity at low shear rates. Due to more shear thinning of the latter, the apparent viscosity of barley bran (0.2 g BG) decreased to become more comparable to the viscosity of oat bran (0.1g BG) at a shear rate of 31 s$^{-1}$. Doubling the concentration of the brans had a huge impact on viscosity with a 2- to 13-fold increase with barley bran and a 7- to 15-fold increase in digesta viscosity with oat bran. Oat bran (0.1g BG) and oat BG (solubilised) in the digesta gave similar viscosity results which was surprising as usually not all BG is solubilised from the PCW under

simulated digestion conditions (Rieder *et al.* 2017, Rosa-Sibakov *et al.* 2020). This observation demonstrated that particles from a bran matrix can contribute to the overall viscosity of the digesta (see also Appendix figure A3.2 for a comparison between whole digesta and supernatant). Barley BG (solubilised) showed very comparable viscosity and shear thinning behaviour as barley bran (0.2g BG) in line with BG being the main driver for generating viscosity in these samples.
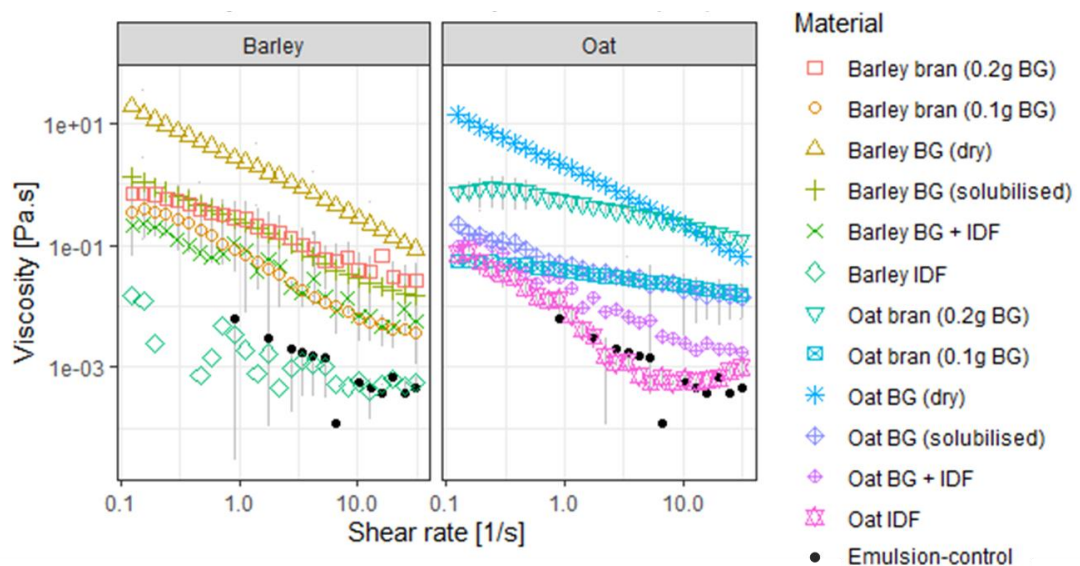


*Figure 3.9 – Log viscosities [Pa.s] over log shear rate [s⁻¹] from 0.1 to 31 s⁻¹ of the fibre whole digesta at the start of the duodenal phase, grouped according to their botanical origin in barley and oat fibres, emulsion control from 0.9 to 31 s⁻¹ on both plots in black dots.*

Barley BG (dry) and oat BG (dry) had a very high apparent viscosity of around 10 Pa.s at the start of the shear ramp. This was probably because of gel-like aggregates which were observed in the digesta, it is likely that the rheometer measured the viscosity of the gel

aggregates rather than the bulk, hence the results are unlikely representative of the presumably lower digesta bulk viscosity.

Comparing the viscosity with the lipolysis rates across the different samples does not suggest increased viscosity as the main mechanism for a lower lipolysis rate (see Figure 3.10).
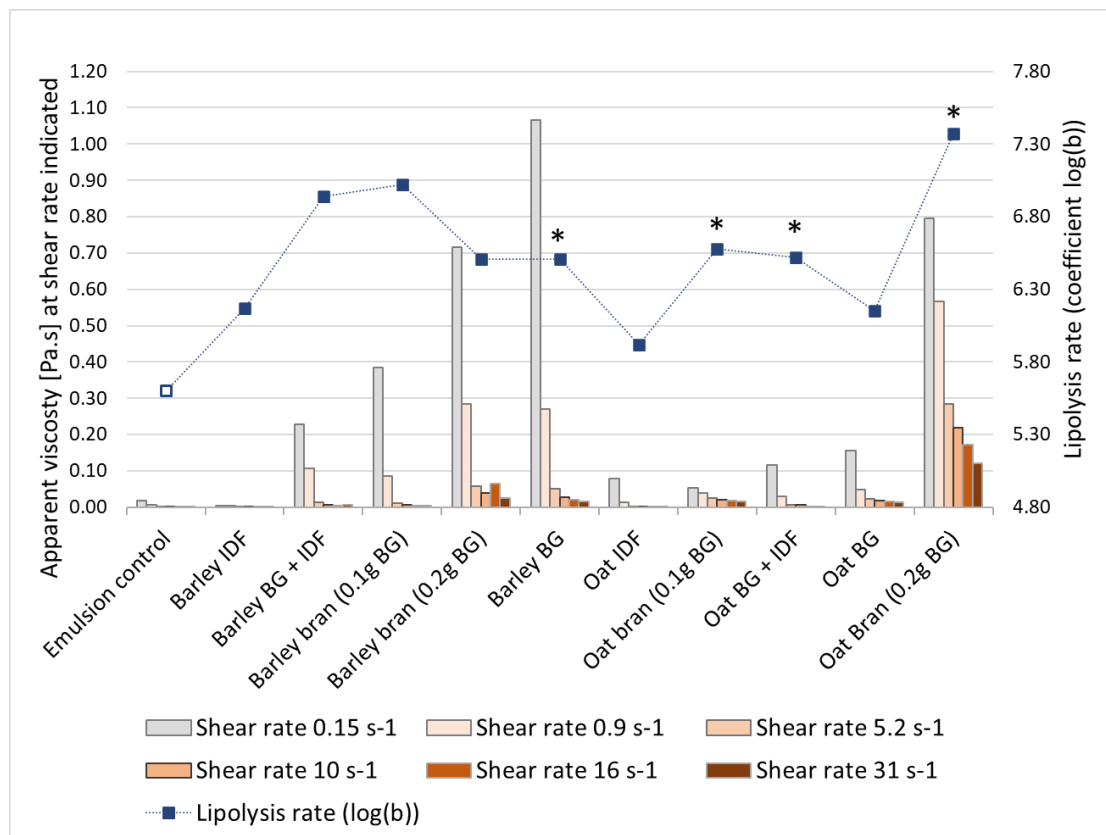


*Figure 3.10 – Apparent viscosities [Pa.s] at selected shear rates [s⁻¹] of intestinal digesta of O/W emulsion in presence and absence of different cereal dietary fibres on the primary y-axis and their respective lipolysis rates (coefficient log(b)) calculated from % FFA released data on the secondary y-axis, stars (\*) indicate statistical difference of lipolysis rates compared to emulsion control, p≤0.05 (Dunnett's test).*

### 3.3.4    Lipase activity and effect of mixing rate

Lipase activity was tested and compared in the absence and presence of fibre material at different mixing rates (see Figure 3.11, Table 3.6). In the absence of DFs, lipase activity linearly increased with mixing speed.
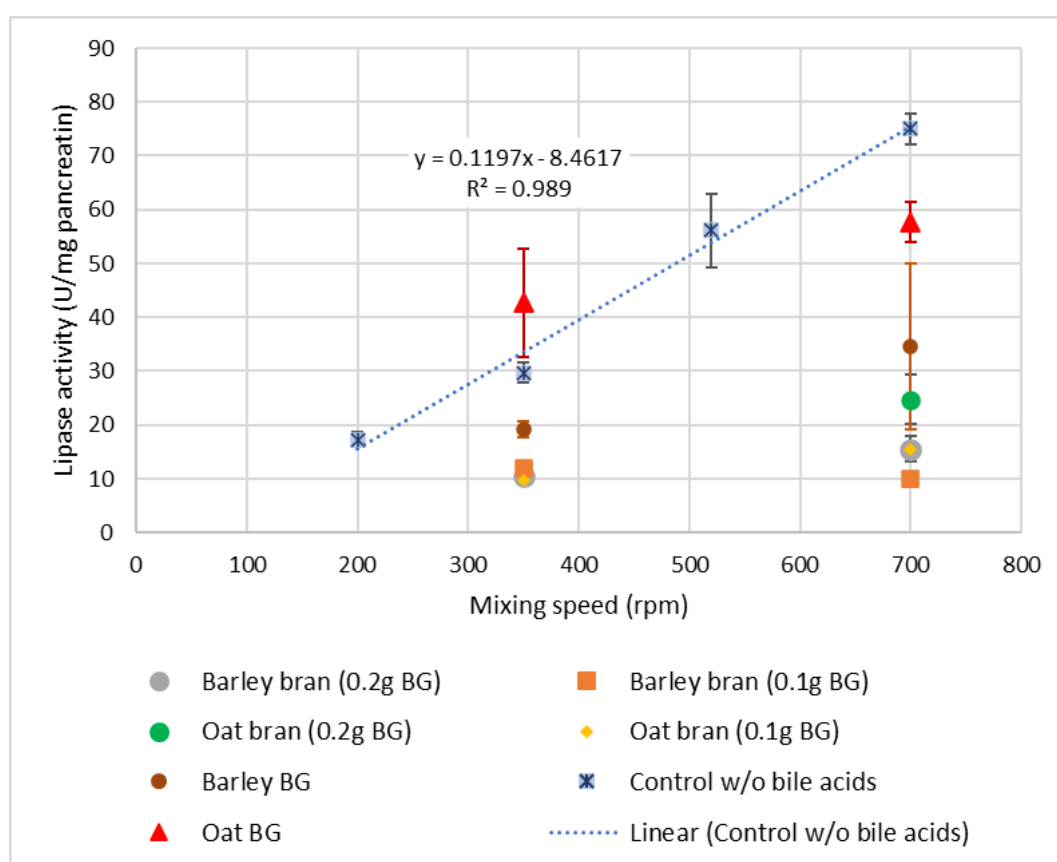


*Figure 3.11 – Lipase activity of pancreatic lipase in absence and presence of digesta containing bran or BG (all in absence of bile acids). Error bars are SDs, for SDs of bran fibre samples please refer to Table 3.6.*

*Table 3.6 – Lipase activity of pancreatic lipase in absence and presence of digesta containing bran or BG (all in absence of bile acids), values are mean and standard deviations, p-value reflects comparison of mixing at 350 with 700 RPM for same material.*

| Material | Lipase activity ± SD (U/mg pancreatin) at mixing rate (RPM) | | | | p-value |
|---|---|---|---|---|---|
| | 200 | 350 | 520 | 700 | |
| Control | 17.25 ± 1.32 | 29.75 ± 1.89 | 56.10 ± 6.90 | 75.00 ± 2.88 | <0.0001 |
| Barley bran (0.1g BG) | n.d. | 11.92 ± 1.01 | n.d. | 10.08 ± 0.80 | 0.7442 |
| Barley bran (0.2g BG) | n.d. | 10.42 ± 1.01 | n.d. | 15.58 ± 0.58 | 0.3608 |
| Oat bran (0.1g BG) | n.d. | 9.83 ± 0.38 | n.d. | 15.58 ± 2.31 | 0.3100 |
| Oat bran (0.2g BG) | n.d. | n.d. | n.d. | 24.75 ± 4.60 | n.a. |
| Barley BG (solubilised) | n.d. | 19.17 ± 1.42 | n.d. | 34.65 ± 15.42 | 0.0042 |
| Oat BG (solubilised) | n.d. | 42.75 ± 10.03 | n.d. | 57.75 ± 3.68 | 0.0074 |

Lipase activity in the presence of fibre at 350 RPM mixing was different from control for all tested fibres (p≤0.05, Tukey correction) except barley BG (p=0.8104, Tukey correction). All DFs lowered the activity whereas the presence of solubilised oat BG increased the activity compared to control (p=0.0399, Tukey correction). At 700 RPM all fibres significantly lowered the lipase activity compared to control except oat BG (p=0.1797, Tukey correction). There was a significant difference in lipase activity between 350 and 700 RPM mixing speed for barley BG (p=0.0042, Tukey correction), oat BG

(p=0.0074, Tukey correction) and control (p<0.0001, Tukey correction). No difference between mixing regimes was found for intact barley bran (0.1g BG) (p=0.7442, Tukey correction), intact barley bran (0.2g BG) (p=0.3608, Tukey correction) and intact oat bran (0.1g BG) (p=0.3100, Tukey correction). This could not be tested for intact oat bran (0.2g BG) as lipolysis was very slow under the tested conditions which did not meet the assay criteria of a linear NaOH consumption response. However, viscosity of the digesta did not correlate with lipase activity results. This suggests that slower or impaired mixing in the presence of DF has the potential to impact lipid digestion kinetics but is not the main mechanism controlling lipid digestion rate in the presence of fibres with intact bran matrix.

## 3.4   Discussion

### 3.4.1   Bile acids as important factors influencing lipid digestion kinetics

The pH-stat method has been used for lipid digestion experiments for many years (Li and McClements 2010, Li *et al.* 2011) and has also been used to determine which digestion conditions influence the rate and extent of lipid digestion. Li, Hu and McClements reported that the concentration of lipase determines the reaction kinetics. The highest concentration of lipase resulted in a digestion profile with a very rapid release of FFAs immediately after the digestion started and reaching a plateau after some time (Li *et al.* 2011) similarly to the *in vitro* digestion results in presence and absence of fibre reported in this thesis. The lipolysis rate was faster with a lower amount of lipid in the digestions without fibre. This is in line with Li and McClements who demonstrated that the rate of lipid digestion increased with decreasing lipid content (Li and McClements 2010). According to Li and McClements, this seems to be due to an increased ratio of lipase-to-lipid substrate in the digestion vessel. As the lipid content decreases, the initial rate of lipolysis increases due to the higher presence of lipase molecules per lipid droplet surface area (Li and McClements 2010).

Rate and extent of lipid digestion increase with increasing bile concentration (Ye *et al.* 2018, Sarkar *et al.* 2016). This is expected due to their role in facilitating the adsorption of the lipase/colipase complex as well as in desorption of FFAs to avoid to the negative

feedback mechanism on lipase activity (Bellesi *et al.* 2016, Pabois *et al.* 2020, Pilosof 2017). Presence of colipase is important, because in absence of colipase, the rate and extent of FFA release decreased with increasing concentrations of bile extract (Li *et al.* 2011). Pabois *et al.* argue that an initial rapid rate of lipolysis, demonstrates the immediate adsorption of lipase/colipase onto the oil/water interface and hydrolysis of the fat droplets. This is followed by a slower digestion phase until it reaches almost a plateau, which is due to accumulation of lipolysis products at the interface (Pabois *et al.* 2020). However, the lipid digestion results presented in this thesis follow regular enzyme kinetics (Equation 3.2) with good fits as modelled in Figure 3.8. Sufficient concentrations of unadsorbed BAs in the continuous phase are essential as they remove FFAs from the interface (Pabois *et al.* 2020, Sarkar *et al.* 2016, Ye *et al.* 2018). However DFs have been shown to interact with BAs, which can make BAs unavailable for this process (Pilosof 2017) resulting in a lower lipid digestion.

### 3.4.2 Reduced mixing due to viscosity and/or viscous entrapment

Viscosity can have several impacts on lipid digestion. Firstly, increased digesta viscosity decreases the mixing rate and hence the contact of lipase, colipase and BA with the lipid substrate as shown in Figure 3.11 (control). Secondly, viscous fibres can create viscous networks which could physically entrap digestive components or emulsion droplets (Grundy *et al.* 2016, Lin and Wright 2018). Thirdly,

with increasing concentration and Mw of a polymer, the viscosity increases but at the same time an osmotic driving force in favour of droplet aggregation (depletion flocculation) builds up as well. Hence there can be an effect on emulsion stability (McClements 2000). Flocculated, i.e. bigger, droplets have a lower surface area to volume ratio and therefore digest slower than smaller lipid droplets (Li *et al.* 2011).

Several researchers tested whether viscosity measurements in presence of fibres can be correlated with a reduced lipid digestion *in vitro*. Only one of the *in vitro* studies found a correlation. The higher the viscosity of the digesta containing pectin both in gastric and duodenal phase, the lower was the overall lipid digestion after 2 hours (Lin and Wright 2018). All other studies either ruled out viscosity as a mechanism (Zhai *et al.* 2020, Grundy *et al.* 2018b), or acknowledged viscosity as additional effect promoting droplet flocculation (Zhai *et al.* 2016, Zhai *et al.* 2021, Pasquier *et al.* 1996). This was in line with the results presented in this thesis as no clear correlation was found despite the digesta covering a range of viscosities from water-like to very viscous. All cereal fibres showed shear thinning behaviour so it would be important to select a shear rate which reflects physiological mixing in the gut. However this can be challenging as mixing in the gut will vary greatly depending on location, physiology and gut signalling (Lentle and Janssen 2010). Depending on the digesta content, faster mixing speed led to an

increased lipase activity as shown in this thesis. Hence impaired digesta mixing due to increased viscosity may affect lipolysis kinetics. However high mixing can negate the hindering effect of increased viscosity as shown in an *in vitro* starch digestion study in the presence of BG (Dhital *et al.* 2014a).

The particle size of the emulsion was measured at the beginning of the *in vitro* digestion to start with a standardised particle size but was not measured at different stages of the digestion. The presence of DF may have caused flocculation or coalescence leading to a reduced lipid digestion as suggested by other studies (Zhai *et al.* 2016, Pasquier *et al.* 1996, Zhai *et al.* 2021). Applying shear by mixing at different mixing speeds at different digesta viscosities may have affected the emulsion stability further. In future experiments, emulsion droplet size should be determined at different stages of the *in vitro* digestion.

### 3.4.3    Decreased lipase activity in presence of bran fibres

As pancreatic lipase activity will be influenced by the presence of BAs, calcium and colipase (Macierzanka *et al.* 2019, Hur *et al.* 2011, Kimura *et al.* 1982, Zangenberg *et al.* 2001), it is important but challenging to differentiate the contributions from these components. Lipase activity measurements in the presence of fibre digesta presented in this thesis were conducted in the absence of BAs to exclude the variable of cereal fibres interacting with BAs. The presence of a bran matrix had a big impact on the lipase activity

with a large inhibition effect of both oat and barley bran unlike the extracted BGs from both sources. This contrasts with Zhai *et al.* who found a stronger inhibitory effect of the high Mw BG from oat compared to medium oat BGs on lipase activity which was concentration dependent (Zhai *et al.* 2016). Similarly, BG extracts from different Qingke varieties, which is a cultivar of hulless barley, had a pancreatic lipase inhibitory effect which was positively correlated with increasing Mw and viscosities (Guo *et al.* 2018). The extraction method of the soluble fibre can also have an effect as shown with pectins as one of the aspects that influenced lipase inhibition (Ahmadi *et al.* 2022). The large inhibition effect of both oat and barley bran could however be a synergistic effect of fibre together with other cereal components like for example proteins. Cara *et al.* found that milling and processing decreased the inhibitory effect on lipase activity in wheat samples and suggested that the intrinsic proteins were responsible for the inhibitory effect (Cara *et al.* 1992). Work by Esfandi *et al.* showed that hydrolysed proteins and peptides from oat bran reduced lipase activity (Esfandi *et al.* 2022).

To investigate interactions between bran fibres and lipase further, molecular binding between the two could be tested. An enzyme activity assay based on the solution depletion method similar to the amylase assay by Dhital *et al.* could be developed for lipase at different bran fibre digesta concentrations (Dhital *et al.* 2015).

### 3.4.4  Conclusions on differences in oat and barley fibres

Cereal DF has the potential to interfere with lipid digestion but the effect is not determined by BG quantity. Barley fibres behaved differently in simulated lipid digestions than oat fibres. Reduced lipolysis was seen in presence of barley fibres as long as BG was present in any form, but with no correlation with viscosity. The oat fibres on the other hand required presence of BG together with IDF, either as a whole bran matrix or added separately, to exert a reduction on lipolysis rate. Hence insoluble oat DF is hypothesized to play a role in solubilisation differences of oat BG and consequential effects of the soluble fibre BG. Hence the solubilisation kinetics of BG were investigated further and are presented in Chapter 4.

Different interaction mechanisms may further play a role depending on the DF and preparation. BG solubilisation processes during digestion and the matrix are clearly important factors. The lipase activity assays in absence of BA showed lipase reduction effects with intact brans and barley BG which should be investigated further for molecular interactions with pancreatic lipase. However, the interference of the cereal fibres in the simulated lipid digestion in presence of BAs could have been due to a fibre/BA interaction mechanism which was investigated further as discussed in Chapter 4.

# Chapter 4 – Interaction of cereal dietary fibres with bile acids and β-glucan-release kinetics of barley bran and oat bran

## 4.1 Introduction

BAs are very important components in duodenal digestion, transport and uptake of lipids (Macierzanka *et al.* 2019). Unlike other surfactants, BAs do not have a hydrophobic head and a hydrophilic tail group, but rather a facial amphilicity due to their steroidal structure, with polar hydroxyl groups on the concave side and methyl groups on the convex side (see Figure 1.5) (Sarkar *et al.* 2016, Euston *et al.* 2013, Galantini *et al.* 2015, Maldonado-Valderrama *et al.* 2014). This feature gives them a high surface activity displacing adsorbed materials, i.e. emulsifiers and proteins, from the interface and helping the lipase/colipase complexes to anchor and hydrolyse the TAGs in the lipid droplet (Sarkar *et al.* 2016). Non-adsorbed BAs also play an important role in lipid digestion as they remove digestion products from the interface which would otherwise inhibit lipase activity (Sarkar *et al.* 2016). BAs have a complex self-assembly behaviour upon reaching critical micellar concentration (CMC) which are different for primary, secondary, conjugated and unconjugated BA species (Madenci and Egelhaaf 2010, Macierzanka *et al.* 2019).

The viscous DFs BG (Queenan *et al.* 2007, Wang *et al.* 2017b), psyllium (Anderson *et al.* 2000), pectin (Brouns *et al.* 2011), guar

gum (Jenkins *et al.* 1979) and glucomannan and the non-viscous chitosan (Stephen *et al.* 2017) have been shown to lower serum LDL cholesterol concentrations and have health claims approved e.g. "contributes to maintenance of normal blood cholesterol levels" (Stephen *et al.* 2017). A potential mechanism may be the interference with the enterohepatic circulation of BAs and/or mixed micelles (Gunness and Gidley 2010, Grundy *et al.* 2018a). Whether this is solely a rheological mechanism is still to be elucidated since several *in vitro* studies have shown that some DFs may show a BA adsorptive effect not related to viscosity (Naumann *et al.* 2018) and comparisons of different viscous fibres have shown inconsistent results (Vuksan *et al.* 2011). Many intervention trials tested BG with regards to their cholesterol lowering effect, however, not all of them show an effect as it seems the concentration and Mw of BG are important (Grundy *et al.* 2018a, Rieder *et al.* 2017). Studies using isolated, purified BG have a more consistent effect on lowering plasma cholesterol but natural BG-rich foods seem more efficient (Grundy *et al.* 2018a).

This chapter tests the hypothesis that the DF/BA interaction is a synergistic effect of the soluble DF constituents and the insoluble DF. To investigate this, different cereal-based ingredients were tested because cereals are the main source of DF in adult populations in Western Europe and the US (Stephen *et al.* 2017). Interaction mechanisms were studied using a centrifugation method as well as

a dialysis model. Barley bran and oat bran were investigated further with regards to their BG release kinetics based on differences observed as described in Chapter 3.

## 4.2 Materials and Methods

### 4.2.1 Materials

Cereal fibre flours from barley bran, wheat bran, oat hull fibre, oat bran as well as purified BG from oat were used as described in section 2.1.1, see Table 2.1.

All other materials are described in section 2.1.3.

### 4.2.2 Methods

### 4.2.2.1 Static oral and gastric digestion followed by duodenal bile acid dialysis

The method is based on (Gunness *et al.* 2012, Naumann *et al.* 2018, Zacherl *et al.* 2011) and was developed and modified as follows: The small scale simulated digestion protocol (Minekus *et al.* 2014) was adapted for use in modified 20 mL syringes. The end of syringes was cut off to be able to transfer the entire digesta content into the dialysis membrane after the gastric phase (see Figure 4.1).

It was decided to normalise the different fibre sample on their total DF content. Due to the fibre samples having a different water-holding capacity, 0.4 g total DF was assessed as practical and doable across all samples. Hence, 2 g starting weight (0.4 g total DF content + adjusted to 2 g total weight with water) was digested in a 2 min oral phase (α-amylase activity 75 U/mL) and 2 hours gastric phase (pH 3, pepsin activity 2000 U/mL) in the modified syringes sealed with parafilm on a rotary mixer in an incubator at 37°C. After the oral and gastric phase, the intestinal phase was initiated with pH adjustment to 7, adding SIF, $CaCl_2$ and bovine bile extract to reach

a concentration of 10 mM bile in the final volume. The digesta was transferred to a pre-hydrated dialysis membrane and pancreatin (100 TAME U/mL) was added. The dialysis membrane was closed and transferred into a 200 mL Duran bottle containing SIF so that the inner volume (IV) containing 10 mM bovine bile and the outer volume dialysate were present in a 1:10 ratio (see Figure 4.1). The Duran bottle containing the digesta in the dialysis bag was kept in an incubator at 37°C, at 170 RPM orbital shaking for 20 h. Samples were taken from the outer volume at 0.5, 1, 2, 4, 6, 8 and 20 hours (Figure 4.1), and stored at -18°C until analysed for BA content (see section 2.3.3). Negative controls were tested in the same manner by replacing the fibre material with 2 mL water. All fibre materials and negative control were tested in quadruplicate.
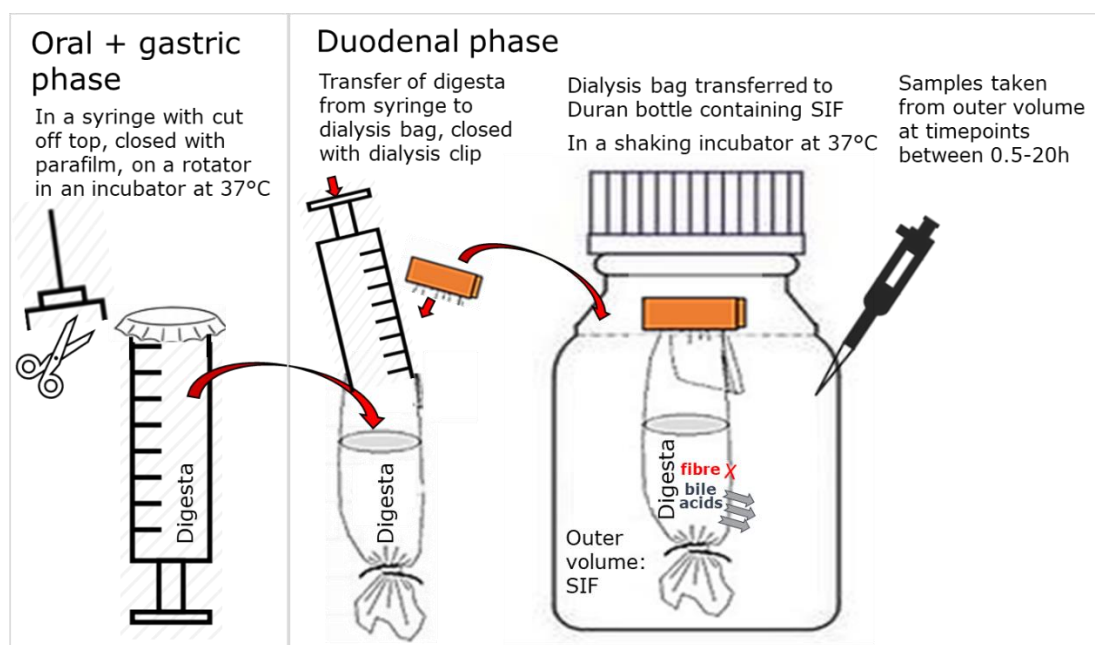


*Figure 4.1 – Schematic setup of the static oral and gastric digestion in a modified syringe followed by duodenal bile acid dialysis*

In the same manner, 1% (w/v) and 8.5% (w/v) purified BG solutions were digested, using 2 g starting weight. While BG can be difficult to solubilise, these concentrations were selected as a 1% BG solution was suggested by the supplier and a 8.5% solution was tested as the highest achievable given BG's water-holding capacity. BG solutions were made the day before use by sprinkling 0.5 g or 0.85 g BG, respectively, onto the surface of 50 mL or 10 mL, respectively, simulated intestinal fluid while stirring on a hot plate magnetic stirrer and slowly heating the mixture to 100°C. When 100°C was reached the mixture was stirred vigorously for 1 hour, cooled to room temperature and stored at 4°C overnight. Each purified BG concentration was analysed in duplicate.

Before use in the *in vitro* model, the bovine bile stock solution was filtered through a 0.45 μm syringe filter (Sartorius Minisart) to remove any bovine gall extract tissue material.

To simulate hydration effects in absence of digestive enzymes, another set of replicates was done replacing the enzymes with simulated digestive fluids to keep the same dilution ratio. Traditionally these would be differentiated as 'digested' and 'undigested', however, as DFs are not digested by the digestive enzymes used in the *in vitro* digestion, they are termed 'with enzymes' and 'no enzymes'.

### 4.2.2.2 Static digestion with and without digestive enzymes to determine BG release and bile acid interaction

The method is a continuation of the *in vitro* digestion as described in section 4.2.2.1, however uses the static method (closed tubes) throughout all three digestion phases. Starting weight was based on 0.4 g total DF content (2.5 % total DF concentration in the intestinal phase) resulting in a BG content as outlined in Table 4.1. After an oral phase (ɑ-amylase activity 75 U/mL, 2 min, 37°C) and gastric phase (pH 3, pepsin activity 2000 U/mL,2 h, 37°C), a duodenal phase was carried out in the same Falcon tube either for 2, 4 or 20 h. As described in section 4.2.2.1, either digestive enzymes were added or replaced by simulated fluids. After the respective time of the duodenal phase, the digesta was centrifuged at 3,000xg for 20 min (Centrifuge Megafuge 16 Heraeus, Thermo Fisher Scientific, US) and the supernatant separated from the pellet. The supernatant was either used for rheological analysis (n=3) as described in section 2.3.7 or for BA determination and BG extraction (n=4) as follows.

A 0.2 mL sample was taken from the supernatant for BA analysis as described in section 2.3.3.1. For the BG extracts, hydrated fibre material in the pellet was separated from insoluble fibre tissue by pressing it through a bolting cloth ("Spectra/Mesh woven filter" nylon, mesh size 53 μm) and dissolved in water for subsequent BG extraction. Precipitation of BG in this mixture as well as in the supernatant was done according to protocol code 'P3' with IPA (see 2.2.2.3). BG extracts from supernatant, hydrated pellet and the

insoluble residue were analysed for their BG content as described in section 2.3.12.

*Table 4.1 - BG in bran flour and total according to amount of flour used*

| Fibre material | BG (%w/w) | Weighed in for 0.4 g TDF (g) | BG total in simulated digestion (g) |
|---|---|---|---|
| Oat bran | 26.8 ± 0.4 | 0.79 | 0.21 |
| Barley bran | 22.2 ± 0.7 | 1.01 | 0.22 |

### 4.2.2.3 Static digestion using Cholyl-Lysyl-Fluorescein in the duodenal phase

The simulated digestion (Minekus *et al.* 2014) was downscaled by a factor of 8 to 250 mg food with 50 mg total dietary fibre start weight (99 mg oat bran, 126 mg barley bran, 54 mg oat hull fibre control) or 'no fibre control' (250 mg deionised water) with a 2 min oral phase (α-amylase replaced by SSF), 2 h gastric phase (pepsin activity 2000 U/mL) and 2 h duodenal phase (see below for Methods A-D) at 37°C. In the duodenal phase, a BA mix was used containing Cholyl-Lysyl-Fluorescein (CLF), a BA conjugated with fluorescein (Figure 4.2). Fluorescein is a common fluorescent molecule used in microscopy.
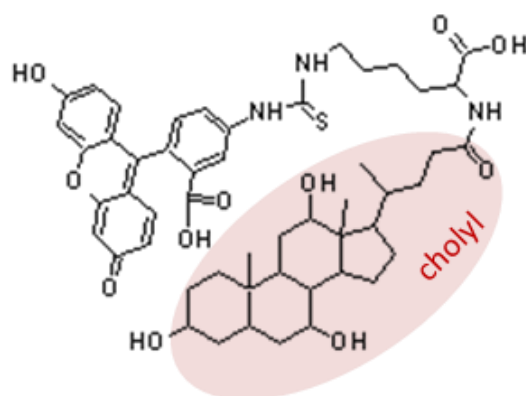
*Figure 4.2 – Structure of Cholyl-Lysyl-Fluorescein (CLF)*

*Table 4.2 - 160 mM BA mix stock containing CLF*

| Bile acids | CA | GCA | TCA | CDCA | DCA | CLF |
|---|---|---|---|---|---|---|
| % | 15 | 20 | 50 | 7.42 | 7.42 | 0.17 |
| mM | 24.0 | 32.0 | 80.0 | 11.87 | 11.87 | 0.27 |
| Notes | Abundance (%) according to bovine bile | | | Higher abundance than bovine bile | | Added |

The BA mix containing CLF used in the duodenal phase is outlined in Table 4.2. For the BA mix stock, CA, GCA TCA, CDCA and DCA were weighed in in the respective amounts and mixed with SIF. To solubilise the BAs, the mixture was placed in a sonicator (Sonicor, U.S.) for 10 minutes in total with a 2 minute break after 5 minutes. The mixture was transferred into a 5 mL centrifuge tube (black, light safe) and CLF added.

Due to interferences with other components in the digestion mixture (as further explained in section 4.3.6) the duodenal phase conditions varied, which are denoted Method A-D:

**A)** 2 h digestion with untreated pancreatin and BA mix containing CLF.

**B)** 2 h digestion with pancreatin which was centrifuged twice to remove interfering filaments as explained in section 4.3.6 (0.5 g/mL SIF centrifuged at 3,500xg for 10 minutes, supernatant was transferred into an Eppendorf tube and centrifuged at 15,000 rpm for 5 min, 125 µL of the resulting supernatant was used in the simulated digestion) and BA mix containing CLF.

**C)** 2 step duodenal digestion: 2 h digestion with pancreatic α-amylase (filtered through a 0.45 µm syringe filter) in absence of BAs to digest the starch before investigating the BA interaction as explained in section 4.3.6. After 2 h, digestion for 1 h with pancreatin (which was centrifuged twice: 1,325 rcf, 10 min at 4 °C, transfer of supernatant into an Eppendorf tube and centrifuged again at 15,000 rpm, 5 min at 4 °C, 125 µL of the resulting supernatant was used in the simulated digestion), and BA mix containing CLF.

**D)** 2 step duodenal digestion: The start weight was doubled for oral and gastric phase, followed by transfer of 250 mg digesta into a new tube for the duodenal phase. Duodenal phase included a 2 h digestion with pancreatin (which was centrifuged twice: 1325 rcf, 10 min at 4 °C, transfer of supernatant into an Eppendorf tube and centrifuged again at 15,000 rpm, 5 min at 4 °C, 125 µL of the resulting supernatant was used in the simulated

digestion) in absence of BAs, followed by 30 min digestion with BA mix including CLF.

After the duodenal phase, the digesta was centrifuged at 3,000xg for 20 min (Megafuge 16, Heraeus, Thermo Scientific, Germany) and the supernatant separated from the pellet. The BA concentration in supernatant was measured in duplicate using a fluorometer (FLUOstar OPTIMA, BMG Labtech, UK) at 450 nm excitation and 520 nm emission. Alongside the samples, BA mix stock standards of 0.5, 2.5, 5, 8 and 16 mM were measured in duplicate. BA concentration was calculated from the standard curve of the BA mix stock standards and the final results expressed as ratio to BA concentration of the control (in absence of fibre).

The pellet was imaged using a confocal microscope (Zeiss LSM 880 Airyscan confocal microscope) with and without calcofluor staining as described in section 2.3.6.

For a free fluorescein control experiment, fluorescein was added to the BA mix of CA, GCA TCA, CDCA and DCA instead of CLF in the same molarity. Simulated digestion protocol was conducted as described above using duodenal phase method A.

Another control experiment used the BA mix of CA, GCA TCA, CDCA and DCA without CLF. Simulated digestion protocol was conducted as described above using duodenal phase method A and samples taken from the digesta supernatant were analysed as using the total BA enzymatic colorimetric assay as described in section 2.3.3.1.

### 4.2.2.4 Rheology

The digesta (see section 4.2.2.1) was centrifuged at 3,000xg for 20 min (Megafuge 16, Heraeus, Thermo Scientific, Germany) to determine the viscosity of the supernatants as described in section 2.3.7.

### 4.2.2.5 Bile acid analysis

A colorimetric assay was used to determine total BA concentration as described in section 2.3.3.1. Individual species of BA were analysed using LC-MS/MS as described in section 2.3.3.2.

### 4.2.2.6 β-glucan determination assay

BG was quantified according to the AOAC Method 995.16 using a kit from Megazyme (Ireland) and modified as described in section 2.3.12.

### 4.2.2.7 β-glucan extractions

BG extraction protocol details are described in section 2.2.2.

### 4.2.2.8 Size-exclusion chromatography

SEC was used to determine size distributions of BG extracts from analytical extraction protocols (see section 2.2.2) as well as extracted from supernatant and hydrated pellet after simulated digestion (see section 4.2.2.2) as described in section 2.3.4.

### 4.2.2.9 Water-holding capacity

Dry weight of samples and Falcon tubes was noted. After simulated digestion as described section 4.2.2.2, the samples were centrifuged at 3000xg for 20 min. The supernatant was decanted, and the

volume measured using a volumetric cylinder and the hydrated pellet in Falcon tube weighed. Water-holding capacity was calculated as the fraction of retained water in relation to the dry weight of samples.

### 4.2.2.10 Data and statistical analysis

Statistical analyses were performed with R (version 4.0.2) (Team 2013) as described in section 2.4.2 with specifics as follows.

A first order kinetics model (see Equation 4.1) was fitted to the dialysis data in section 4.3.1 as described in section 2.4.1 to compare BA release rates and extent between the different fibres and control (without enzymes) (Naumann *et al.* 2018) using Dunnett's test comparing several treatments with a control. For comparison of two variables, t-test was used.

$$C_t = C_\infty \left(1 - e^{-k*t}\right)$$

*Equation 4.1 – BA release kinetics model: $C_t$ is the BA concentration at a given timepoint, $C_\infty$ extent of BA release at infinity, k is the apparent permeability rate and t is the timepoint (Naumann et al. 2018).*

## 4.3 Results

### 4.3.1 Physical entrapment leading to bile acid retention in some cereal fibres

The cereal fibres barley bran, oat bran, wheat bran and oat hull fibre as well as two concentrations of purified BG were tested for their potential to interact with BAs during simulated digestion with and without digestive enzymes using a dialysis model. As hydration was found to be of importance in pilot studies (see Appendix to Chapter 3), the fibres were hydrated during the process of the simulated digestion in an oral phase for 2 minutes, gastric phase for 2 hours followed by a duodenal phase performed during dialysis. Bovine bile extract was used as negative control (without fibre) for comparison. As shown in Figure 4.3, even in absence of fibre, not all BAs diffused through the dialysis membrane after 20 hours with only about 75% of the BAs recovered at the end of the experiment. The BA retention data was fitted to the model in Equation 4.1, to calculate an apparent permeability rate (k) and a final concentration ($C_\infty$) per treatment (see Table 4.3). A slower rate of diffusion of BAs through the dialysis membrane could be due to viscosity or adsorptive/binding effects, whereas a lower $C_\infty$ indicates long-term binding (Naumann *et al.* 2018).

Purified BG was tested as soluble fibre without a PCW matrix and resulted in BA diffusion at the same rate as the control and did not entrap BAs, irrespective of the presence of digestive enzymes (see Table 4.3). The rate of BA diffusion in the presence of oat hull fibre were comparable to the control (see Table 4.3). Oat hull fibre in absence of enzymes was the only condition with a significant difference in $C_\infty$ relative to the control (p=0.009, Dunnett's test comparing several treatments with a control, see Table 4.3).
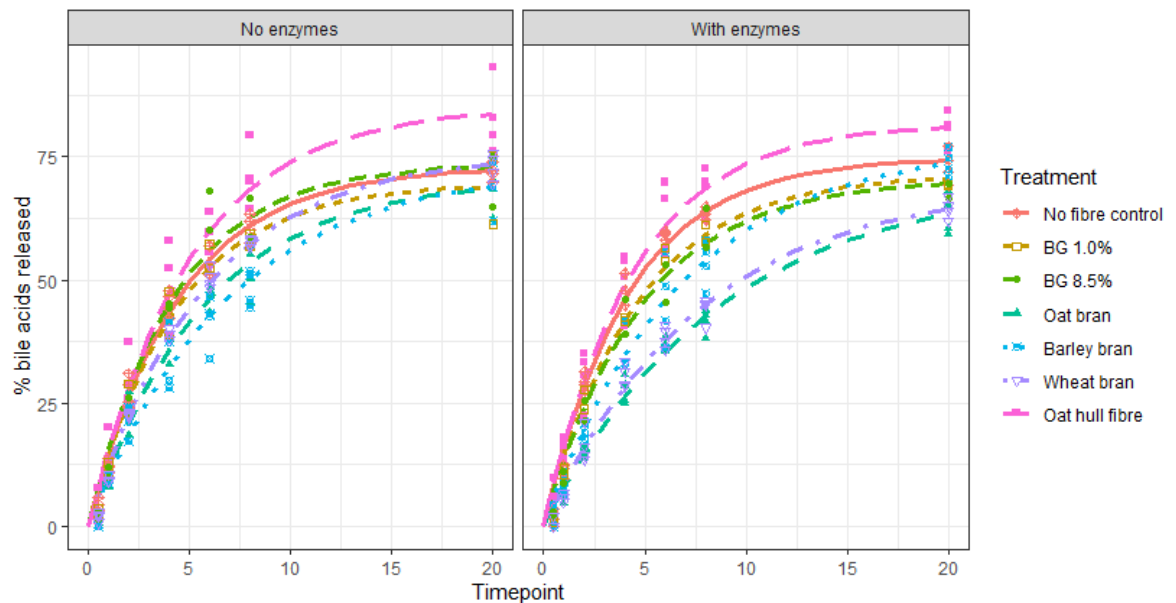


*Figure 4.3 – Percentage of bile acids released in an in vitro dialysis model after simulated digestion hydration (no enzymes) and simulated digestion (with enzymes) over time [h] for 20 hours with bovine bile extract only (no fibre control), 1 % β-glucan (BG 1.0%) and 8.5 % β-glucan (BG 8.5%), oat bran, barley bran, wheat bran and oat hull fibre. Lines represent the first order kinetic model fitted (Equation 4.1 ) and points in different shapes the samples taken at 0.5, 1, 2, 4, 6, 8 and 20 hours (n=2 for BG 1.0% + BG 8.5%, n=4 for all other treatments).*

*Table 4.3 – BA concentration at infinity ($C_\infty$) and apparent permeability rate (k) determined by fitting Equation 4.1: mean, lower 95% and upper 95% confidence interval, Dunnett's test p-value adjustment for comparing several treatments with a control, significance level: p≤0.05.*

| Treatment | Enzymes | $C_\infty$ mean [lower, upper 95% CI] | $C_\infty$ p-value | k mean [lower, upper 95% CI] | k p- value |
|---|---|---|---|---|---|
| No fibre control | No | 72.9 [68.0, 77.9] | n.a. | 0.227 [0.202, 0.252] | n.a. |
| BG 1.0% | No | 69.5 [62.6, 76.4] | 0.9616 | 0.234 [0.196, 0.272] | 0.9994 |
| BG 8.5% | No | 73.6 [66.7, 80.5] | 1.0000 | 0.238 [0.202, 0.275] | 0.9938 |
| Oat bran | No | 70.6 [65.3, 76.0] | 0.9856 | 0.176 [0.155, 0.198] | 0.0289 |
| Barley bran | No | 72.8 [67.0, 78.7] | 1.0000 | 0.146 [0.127, 0.165] | <.0001 |
| Wheat bran | No | 75.7 [70.3, 81.0] | 0.9707 | 0.176 [0.156, 0.196] | 0.0228 |
| Oat hull fibre | No | 85.2 [80.1, 90.3] | 0.009 | 0.202 [0.182, 0.221] | 0.6152 |
| No fibre control | Yes | 74.8 [69.9, 79.7] | 0.9929 | 0.242 [0.216, 0.267] | 0.9559 |
| BG 1.0% | Yes | 71.4 [64.4, 78.4] | 0.9988 | 0.221 [0.185, 0.256] | 0.9996 |
| BG 8.5% | Yes | 70.4 [63.3, 77.5] | 0.9899 | 0.212 [0.177, 0.247] | 0.9793 |
| Oat bran | Yes | 69.6 [62.9, 76.4] | 0.9634 | 0.119 [0.100, 0.138] | <.0001 |
| Barley bran | Yes | 77.4 [71.6, 83.1] | 0.8443 | 0.150 [0.132, 0.168] | <.0001 |
| Wheat bran | Yes | 69.3 [63.0, 75.6] | 0.936 | 0.132 [0.112, 0.151] | <.0001 |
| Oat hull fibre | Yes | 81.7 [76.8, 86.6] | 0.124 | 0.229 [0.207, 0.252] | 1.0000 |

Barley bran, oat bran and wheat bran did slow down the permeability rate with and without enzyme treatment in the following order starting with the lowest permeability rate: oat bran with enzymes < wheat bran with enzymes < barley bran without enzymes < barley bran with enzymes < oat bran / wheat bran without enzymes, which were all statistically significantly different from the control without enzymes (see Table 4.3). However, presence of wheat bran, oat bran and barley bran did not have an effect on $C_\infty$ which, if decreased, would have indicated prolonged binding of BAs (see Table 4.3).

Due to the observation that the presence of digestive enzymes slowed down the permeability rate further, the weight of the dialysis bags (dialysis membrane and digesta content) before and after the 20h dialysis was compared. This was done to determine if there could have been an osmotic effect due to the digestion of macronutrients like starch and the release of sugars. Without enzymes added, the dialysis bag weight increased by 1.0% (95% CI [-2.7, 4.7]), which was statistically significantly different (p=0.0078) from when enzymes were added and the weight increased by 8.2% (95% CI [4.6, 11.8]). The control with enzymes had a statistically significantly lower weight increase than oat bran (p=0.0016), barley bran (p=0.0025) and wheat bran (p=0.0198; pairwise comparison, Tukey correction) with added enzymes. Osmotic pressure may have added to the diffusion retention in digested oat bran, barley bran and wheat bran, but was not the only reason for the retarded release

as the undigested brans (in absence of enzymes) retained the BAs

as well, without a significant change in weight.

## 4.3.2 Retention of specific bile acid species

Bovine bile is a mix of several BA species with different adsorption–

desorption behaviours important in lipid digestion (Parker *et al.*

2014). Hence it was investigated if the cereal fibres interact with

certain BAs more than with others.

15 different BA species were detectable by LC-MS/MS in the bovine

bile extract stock solution, however, six of them, β-MCA, GLCA,

GUDCA, T-β-MCA, TLCA and UDCA, were close to the detection limit

and not included in the individual analyses of the samples taken

from the digesta dialysate. Not detectable were LCA, DHCA, MCA,

α-MCA, TDHCA, T-α-MCA, HDCA, GHDCA, GHCA, TUDCA, THDCA

and THCA. Figure 4.4 shows that the most abundant BA in the bile

stock solution was TCA which made up almost 50% of the total BA

content, followed by GCA with about 20% and CA with about 15%.

Among the secondary BAs, DCA, both conjugated and unconjugated

made the second largest group with a combined abundance of

approximately 12%, followed by CDCA with only 3% both

conjugated and unconjugated.
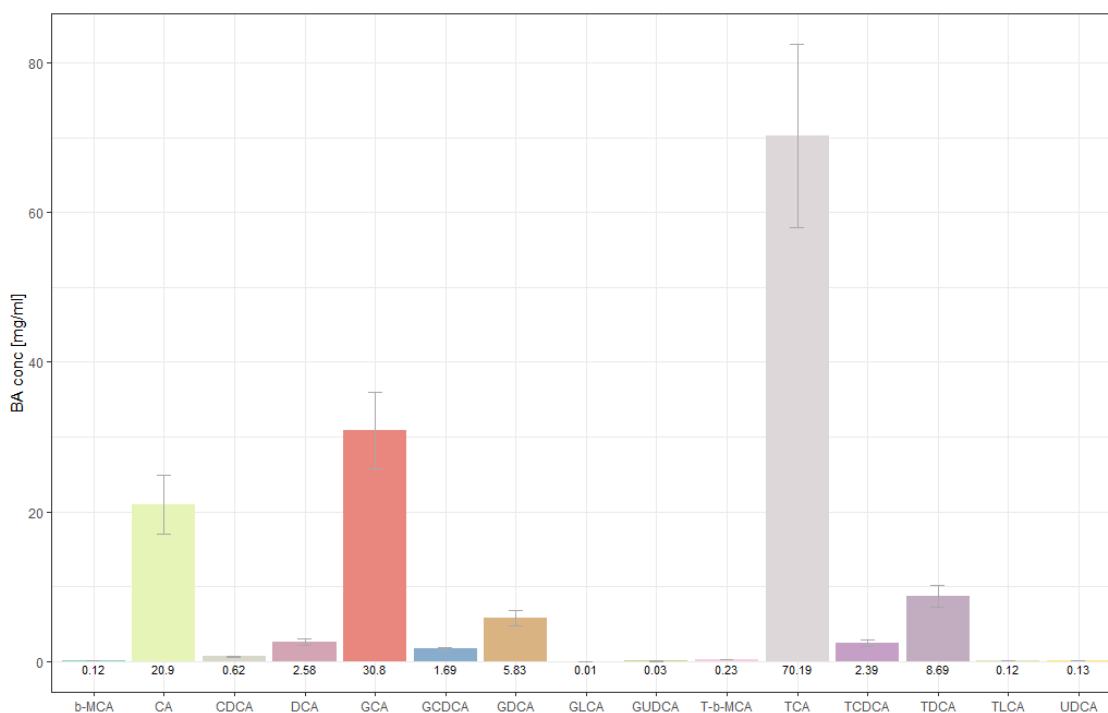
*Figure 4.4 – Abundance of individual BA species [mg/mL] in bovine bile extract stock solution, numbers are the respective concentrations per BA species, error bars are SDs, n = 2.*

Following on from the retarded total BA release with some cereal fibres, samples taken at 1, 2, 4 and 6 hours of duodenal dialysis in section 4.3.1 were chosen for further investigation of potential preferential retention of individual BA species. BA diffusion in this time window was linear for the total BA concentration (see Figure 4.5a) as well as for individual BA species CA, DCA, GCA, GCDCA, GDCA, TCA, TCDCA and TDCA with $R^2$ between 0.86 and 1, except for DCA in presence of oat hull fibre without enzymes which gave a $R^2$ of 0.75. The linear fit for CDCA release over time was good for the controls with and without digestive enzymes with an $R^2$ of 0.95 and 0.87, respectively. However, CDCA release of some of the cereal

fibres plateaued after 4 hours. Therefore, the linear fit was lower, especially for oat bran with an $R^2$ of 0.57 and 0.68 with and without enzymes, respectively (see Figure 4.5b). Overall, the results showed a reasonable linear fit so the release rate was based on the slope of the linear regression.

Negative control showed a differential retention of BA species depending on the abundance of the respective BAs determined in the bile stock. The release rates in presence and absence of enzymes of the control were 83 and 85 μg/mL per hour, respectively. The overall BA release rate was substantially slower in barley bran with and without enzymes (49 and 56 μg/mL per hour, respectively), oat bran with and without enzymes (58 and 39 μg/mL per hour, respectively) as well as wheat bran with enzymes (56 μg/mL per hour), but only slightly delayed in wheat bran without enzymes with 74 μg/mL per hour as compared to negative control. Therefore, the release rate of each BA per treatment with or without enzymes as well as the total BA release was compared to the negative control as shown in Figure 4.6. In presence of oat bran (with and without enzymes), barley bran with enzymes and oat hull fibre without enzymes, the release of the BA species DCA and CDCA was even further delayed than the total BA release rate in the presence of the respective fibre. This showed an additional BA interaction effect on top of the decreased overall diffusion rate. Also wheat bran seemed to preferentially retain DCA, GCDCA, GDCA, TCDCA and TDCA with

and without enzymes as well as in absence of enzymes additionally

CDCA (see Figure 4.6).
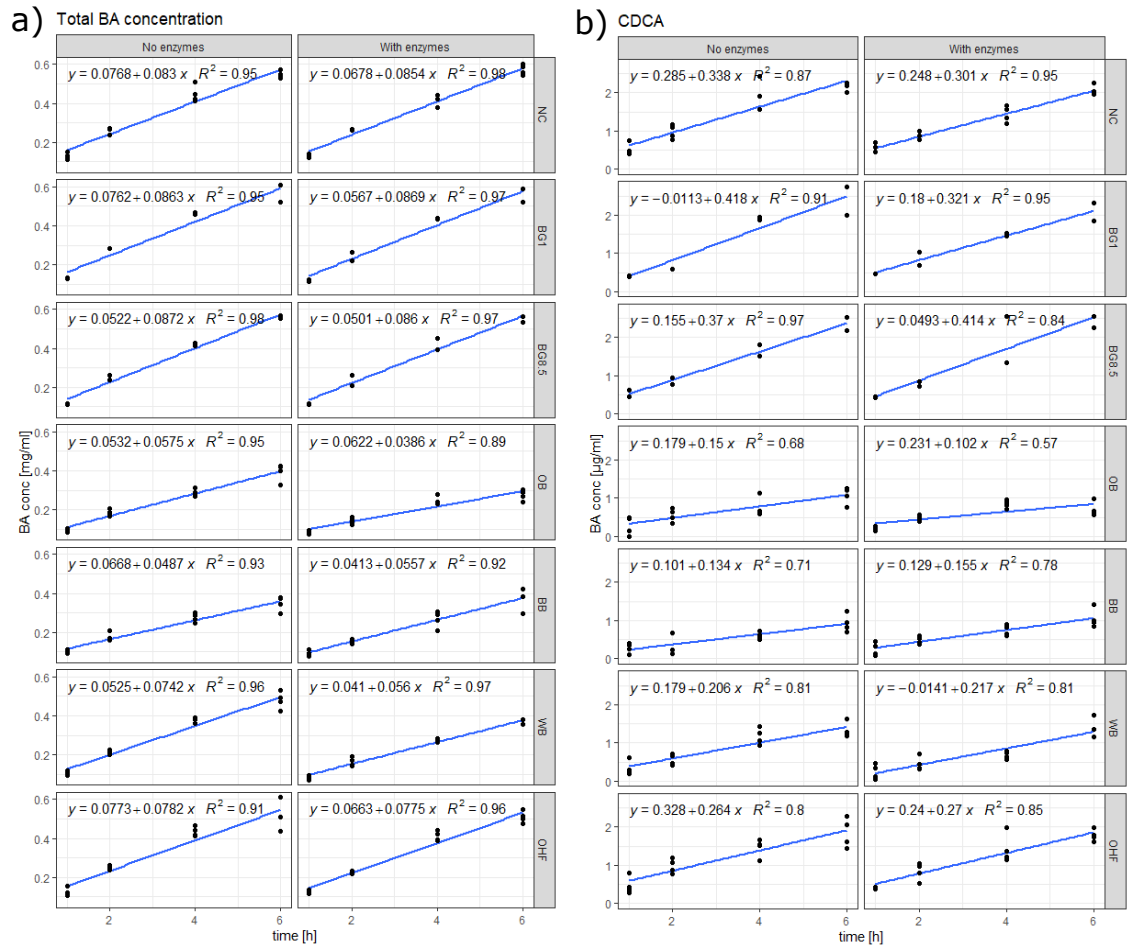


*Figure 4.5 – a) Total BA concentration and b) CDCA concentration at timepoints 1, 2, 4 and 6 hours taken from dialysate (outer volume) of digesta containing no fibre (NC), 1 % β-glucan (BG1), 8.5 % β-glucan, oat bran (OB), barley bran (BB), wheat bran (WB) and oat hull fibre (OHF) as determined with LC-MS/MS after simulated digestion hydration (no enzymes) and simulated digestion (with enzymes). Blue lines, equation and r² are fitted linear regressions (n=2 for BG1+BG8.5, n=4 for all other treatments).*
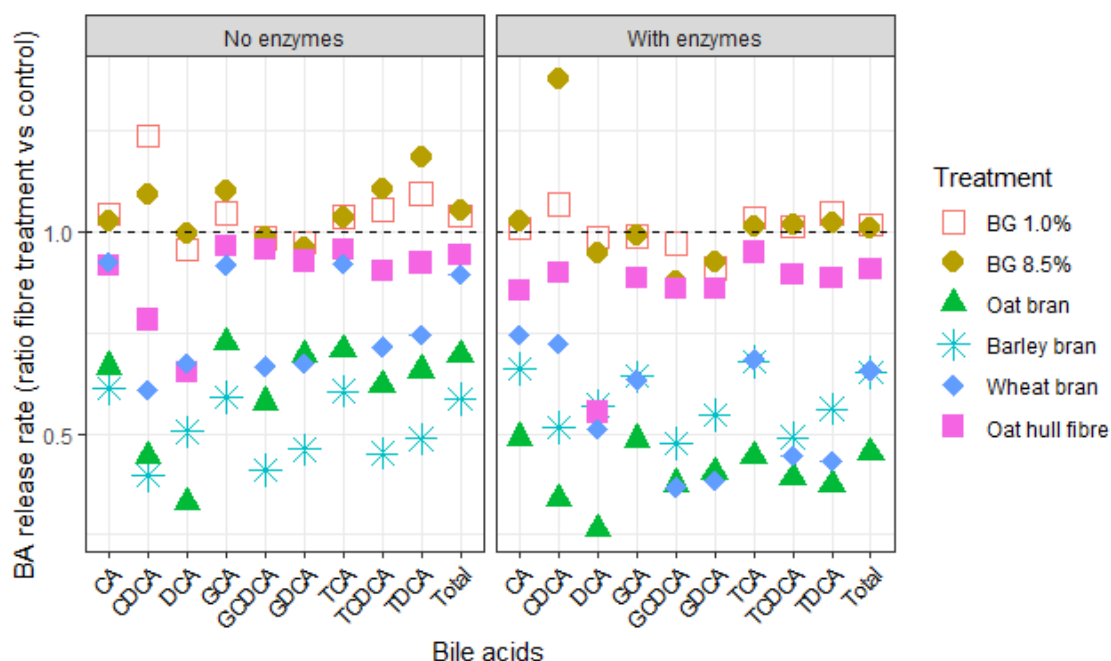
*Figure 4.6 – Ratio of release rate between 1 and 6h of CA, CDCA, DCA, GCA, GDCA, TCA, TCDCA, TDCA and total BAs of the treatments 1 % β-glucan (BG 1.0%) and 8.5 % β-glucan (BG 8.5%) starting concentration, oat bran, barley bran, wheat bran and oat hull fibre to bovine bile extract only (black dashed line represents no fibre control) as determined with LC-MS/MS from samples taken from an in vitro dialysis model after simulated digestion hydration (no enzymes) and simulated digestion (with enzymes) (n=2 for BG1+BG8.5, n=4 for all other treatments).*

## 4.3.3 Rheology of supernatant of digesta after 20h dialysis

The viscosity of the aqueous phase of digesta with or without added digestive enzymes in presence and absence of fibre and was measured after 20 h simulated digestion in a dialysis membrane. Only oat bran and barley bran had an increased viscous aqueous phase (see Figure 4.7). Both showed shear thinning behaviour. Oat bran had a much higher viscosity at the beginning of the shear ramp, but shear thinning was greater than for barley bran and therefore aligned with the viscosity of barley bran at the very high shear rates. When these two brans were digested with enzymes, they both had a lower viscosity than in absence of enzymes. All other fibre

materials – wheat bran, oat hull fibre and the purified BG samples –

did not lead to an increased viscosity and were comparable to water.

Although BG 1% and BG 8.5% started in the digestion model in

these concentrations, they were consequently diluted during the

simulated digestion process. The undiluted 1% BG solution had a

viscosity of about 0.013 Pa.s before the simulated digestion which

was lower than both oat bran and barley bran in the duodenal

digestion phase (Figure 4.8). Increasing the amount of BG to a 8.5%

BG solution at the start of the digestion led to aggregation of BG and

gel-like structures which did not dissolve and therefore did not

contribute to the overall viscosity of the supernatant.
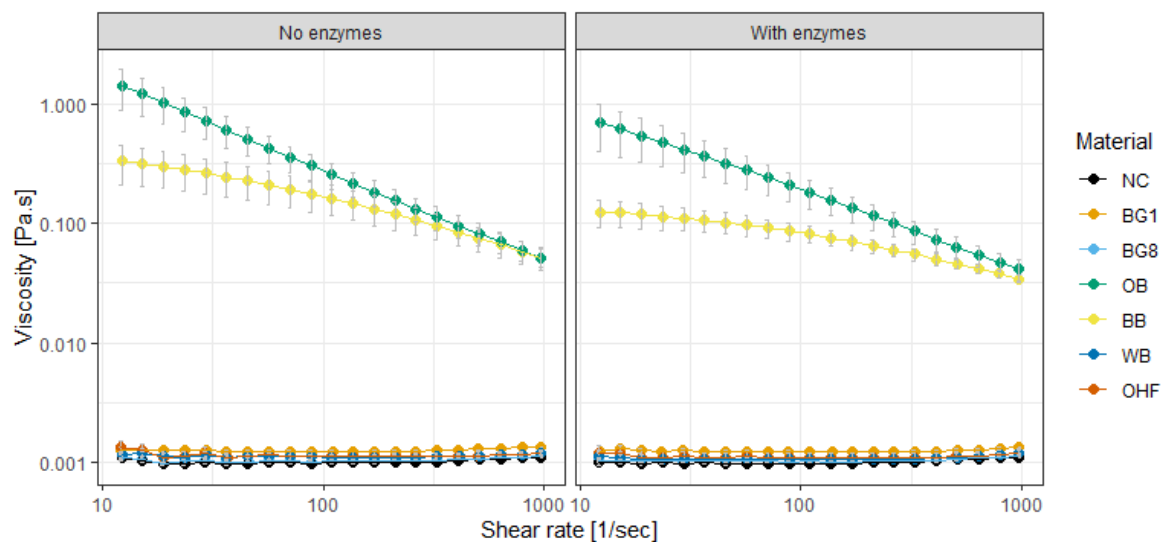


*Figure 4.7 – Apparent viscosity [Pa.s] on a log scale as a function of log shear rate [s⁻¹] of bovine bile extract (negative control, NC), 1 % β-glucan (BG1) and 8.5 % β-glucan starting concentration, oat bran (OB), barley bran (BB), wheat bran (WB) and oat hull fibre (OHF) measured from the aqueous phase of the digesta (with and without enzymes) after 20h in a dialysis membrane (n=2 for BG1+BG8.5, n=4 for all other treatments).*
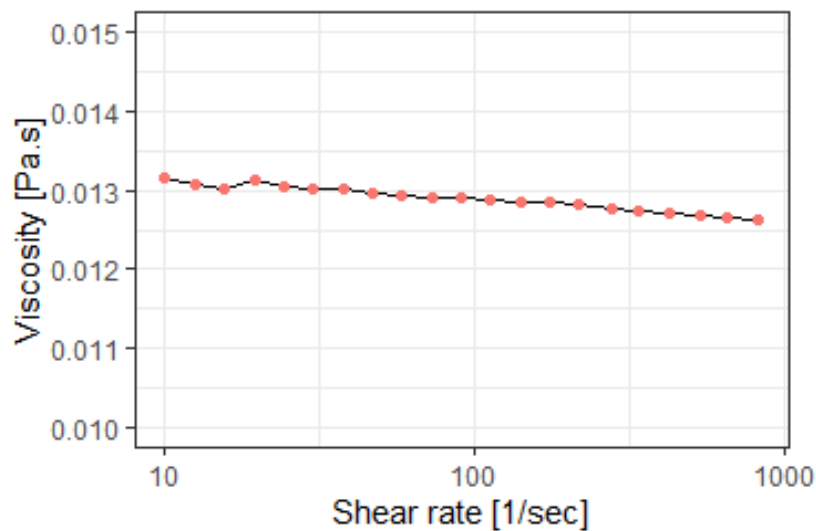
*Figure 4.8 – Apparent viscosity [Pa.s] on a log scale as a function of log shear rate [$s^{-1}$] of BG1% before simulated digestion.*

The difference in viscosities of *in vitro* digesta in presence and absence of enzymes in both barley and oat bran, was investigated further to explore potential dilution effects by the dialysate. Therefore, the simulated digestion was repeated for barley and oat bran in a static digestion model (closed system) and rheological measurements taken after 2, 4 and 20 hours duodenal phase. Results are shown in Figure 4.9 together with the viscosity measured after 20 hours dialysis.
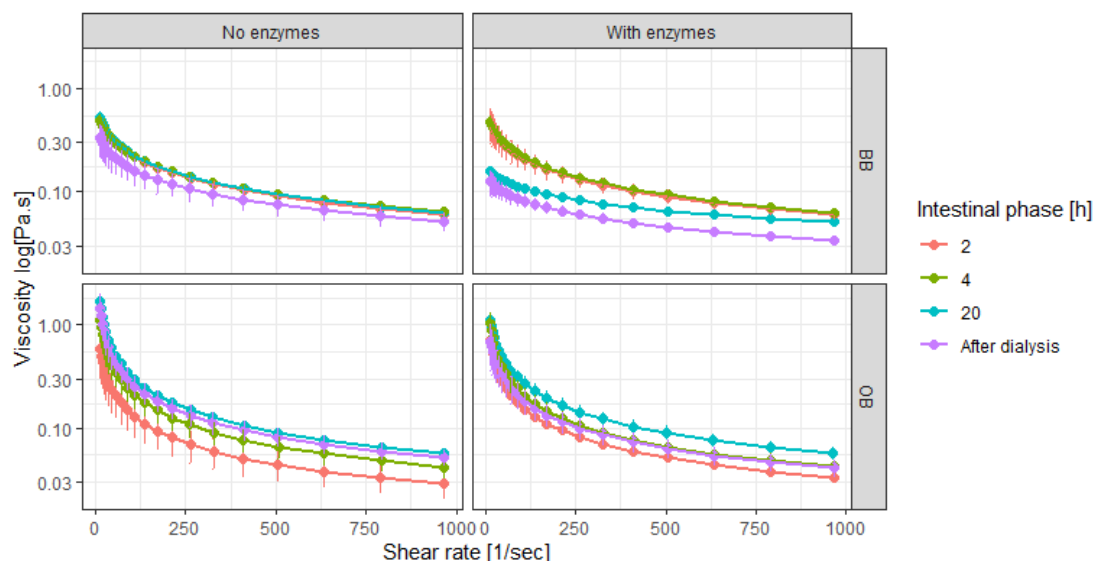
*Figure 4.9 – Apparent viscosity [Pa.s] on a log scale as a function of shear rate [s⁻¹] of barley bran (BB, 2 upper plots) or oat bran (OB, 2 lower plots) with or without enzymes after an intestinal phase of 2, 4 or 20 hours or 20 hours in a dialysis system.*

As shown in Figure 4.9, the viscosity of barley bran after dialysis was slightly lower which could be due to a dilution of the digesta in the dialysis bag. The viscosity of barley bran digesta after 2 and 4 hours of intestinal phase was the same irrespective of enzyme addition. Interestingly, the viscosity decreased after 20 hours duodenal digestion when barley bran was digested with enzymes. The same lower levels of viscosity were seen after dialysis.

The highest viscosity was produced when the duodenal phase of oat bran was extended to 20 hours without addition of enzymes. Under both conditions, with and without enzymes added, viscosity increased over time, indicating a slow oat BG release from oat bran over time. Comparing the 20h closed tube oat bran viscosity with

the results after dialysis showed a slightly lower viscosity after dialysis when no enzymes were present but a substantially lower viscosity of the aqueous phase of digested oat bran after dialysis. This could be due to a dilution effect due to osmotic pressure. However, both barley bran and oat bran, produced lower viscosities after digestion with enzymes.

Barley bran digesta supernatant had a lower viscosity than oat bran. However in barley bran, the viscosity did not change over time when no enzymes were added. As viscosity depends on the molecular size as well as the concentration of BG (Figure 1.7) (Wang and Ellis 2014), these two observations indicated that barley bran had a more rapid dissolution of BG but a lower Mw compared to oat bran.

### 4.3.4 BG release kinetics from barley and oat

The first objective of this set of experiments was to investigate the BG release kinetics from a bran matrix further and compare barley bran with oat bran. BG is expected to be the main contributor to the viscosity of digesta as presented in Figure 4.9 (Rieder *et al.* 2017). Barley bran and oat bran are both rich in BG with 22 and 27 %(w/w), respectively, but were normalised for total DF which led to a comparable BG content of 0.2 g in the simulated digestion (see Table 4.1). BG release is usually determined as dissolved BG in the supernatant after centrifugation (Rieder *et al.* 2017, Grundy *et al.* 2017a, Rosa-Sibakov *et al.* 2020, Tosh *et al.* 2010, Moriartey *et al.* 2010), however, as visible from the gel layer in Figure 4.10 and the

blue and fluorescent area stained with calcofluor in Figure 4.11, hydrated BG can also be found in the pellet. The hydrated BG leached out from the cell wall but may still be attached to the cereal tissue giving it different properties than the dissolved BG. This may be an important aspect of the BG release kinetics and contribute to the mechanistic effects seen with BG-rich food in comparison with added purified BG. Three BG hydration stages were determined and quantified in a simulated digestion of barley and oat bran: 1) solubilised BG in the aqueous phase (supernatant BG), 2) hydrated BG which remained with the insoluble fibre (pellet BG) and 3) insoluble BG (residual BG) in the plant tissue (see Figure 4.12).
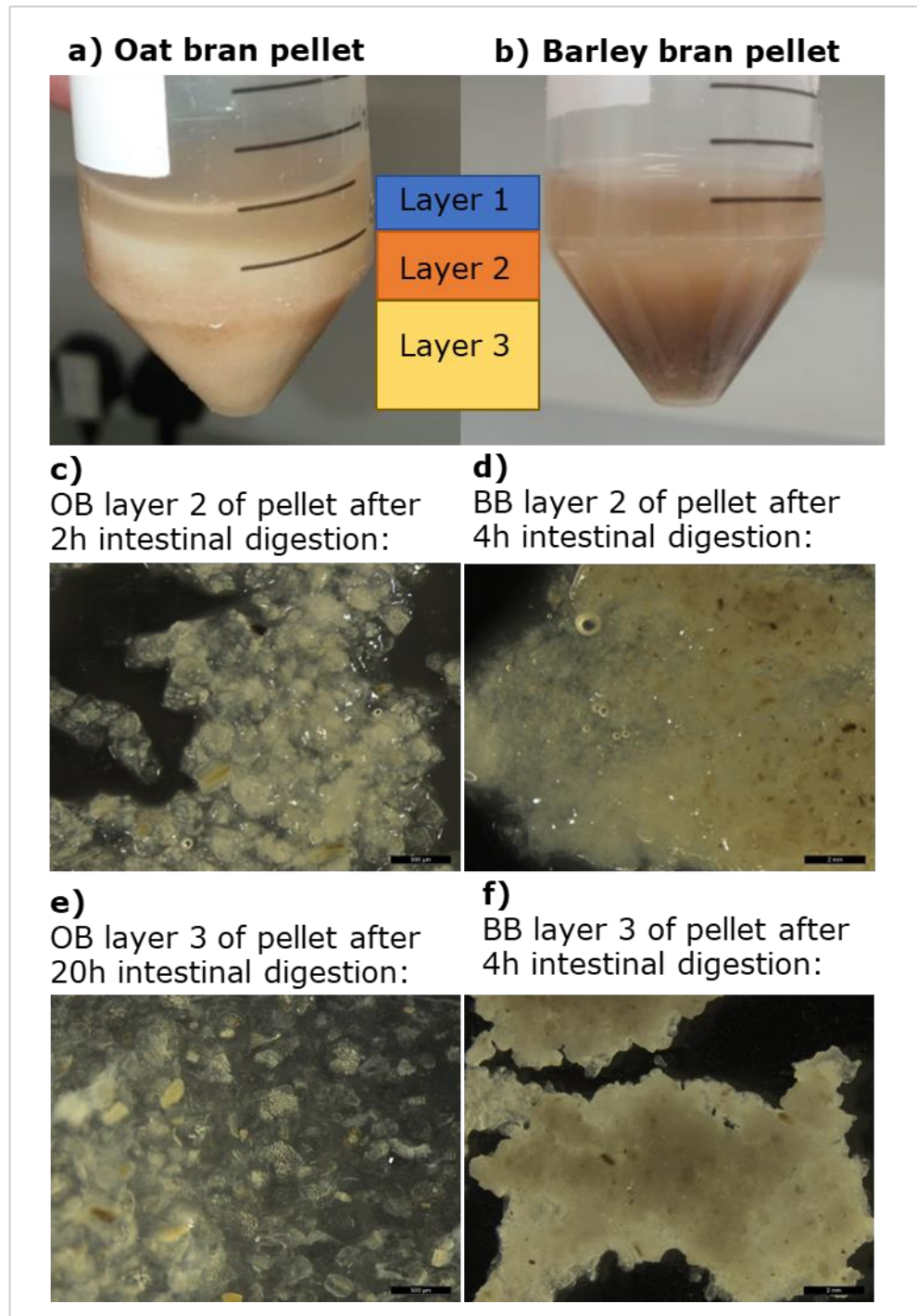
*Figure 4.10 – Pellet after centrifugation of digesta of oat bran (OB, left) or barley bran (BB, right) after simulated digestion, imaged with a regular camera (a + b) or Leica stereomicroscope (c, d, e, f)*
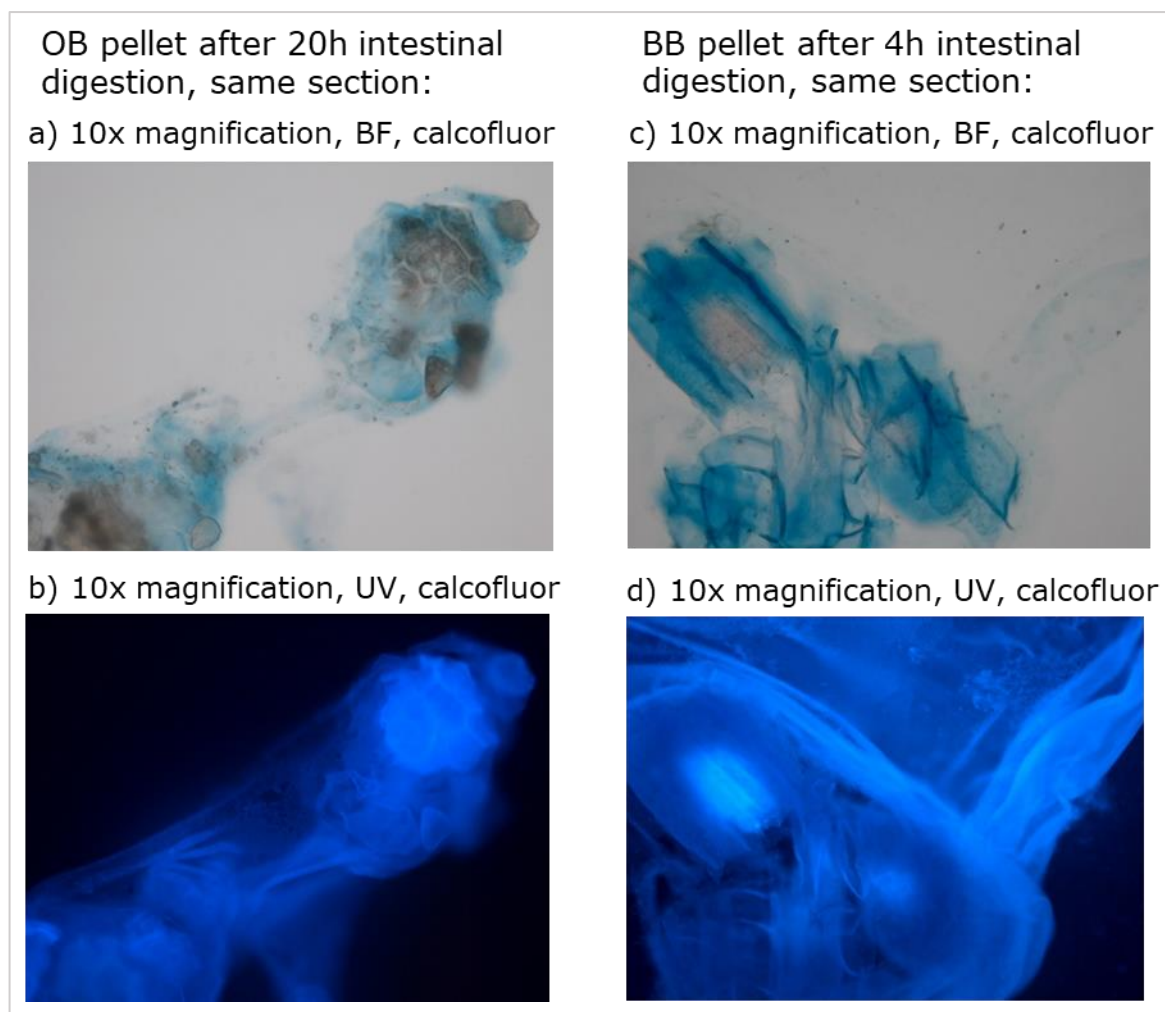
*Figure 4.11 - Pellet of (a) + (b) oat bran (OB) or c) + d) barley bran (BB) after simulated digestion, ß-glucan is stained with calcofluor (+ evans blue) and imaged with a BX60 wide-field microscope (Olympus, Germany) in a) + c) brightfield (BF) and (b) + (d) fluorescence (UV) mode.*

Figure 4.12 shows that compared to oat bran, barley bran had a quicker and overall higher BG dissolution with up to 40% BG solubilised in the supernatant after 4 hours. With digestive enzymes present, oat BG dissolution was slower and to a lesser extent. Oat bran showed only a significant increase to about 40% of the total BG after 20 hours since the hydrated BG found in the pellet seems to remain attached to the plant tissue. This hydrated pellet BG made up about 20% of the total oat BG, in an equal amount as solubilised

after 2 hours, which is usually regarded as insoluble fibre and, to the best of my knowledge, has not been quantified before. The insoluble BG content of the remaining residue decreased in barley bran until the 4h timepoint whereas with oat bran, the BG release continued till 20 hours and was overall less than barley bran. Both brans had a lot of insoluble BG still entrapped in the cell walls after simulated digestion. Taken all BG recovered from the three stages together, barley bran and oat bran had a total BG mean of 184 ± 19 mg and 142 ± 19 mg, respectively. In both, total BG this was less than expected with 18% less for barley bran and 33% for oat bran and presumably lost during processing or became unavailable for the lichenase treatment in the BG determination assay after processing.

Comparing the BG release differences in barley bran and oat bran (Figure 4.12) with their rheology data (Figure 4.9), demonstrates that the molecular size of the BG from the two sources must be different with barley bran releasing more BG but resulting in a lower viscosity as opposed to a lesser amount released from oat bran, which showed a higher viscosity. Therefore, the next step was to investigate, using SEC, whether differences in Mw of the BG released from the two bran samples would explain this.
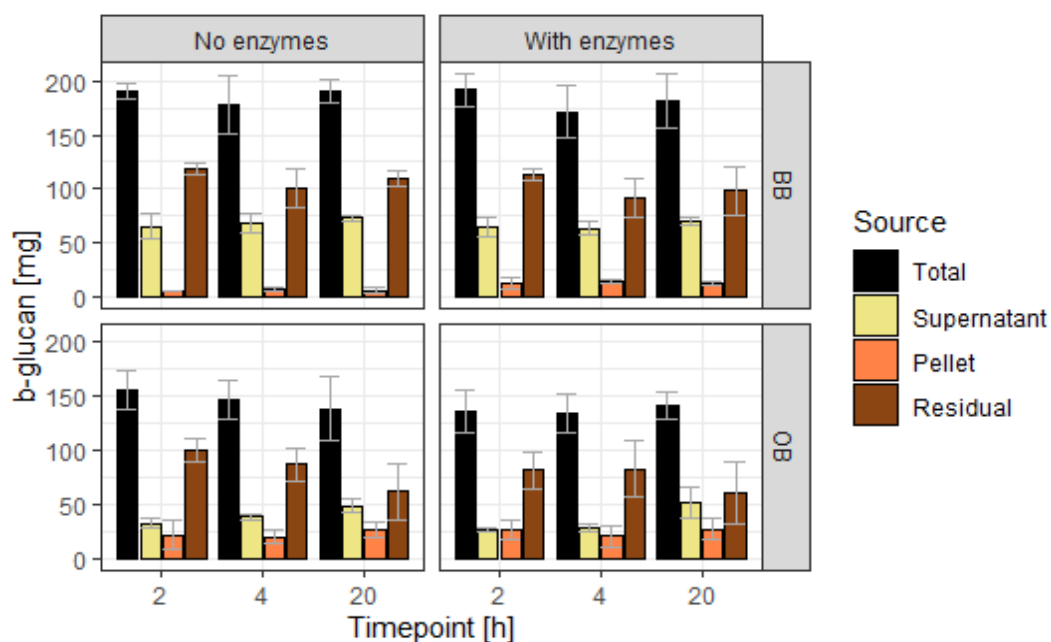
*Figure 4.12 – Solubilised BG in the aqueous phase (supernatant), hydrated BG which remained with the insoluble fibre (pellet) and insoluble BG in the plant tissue (residual) from barley bran (BB) and oat bran (OB) were measured after 2, 4 or 20 hours of intestinal simulated digestion with or without digestive enzymes. Total represents the sum of supernatant BG, pellet BG and residual BG. Error bars are SDs, n=4.*

Figure 4.13 shows the size distribution of hydrated BGs recovered from the pellet after a 2-, 4- or 20-hours intestinal digestion as well as of solubilised BGs from the supernatant after 4 hours. As elution times between pullulan standards and BG standards were found to differ significantly in respect to their Mw and the lack of Mark-Houwink parameters specifically for BG in DMSO+LiBr (see Appendix figure A4.4 and Appendix figure A4.5), the peak DP was largely qualitative but used as a surrogate to compare changes in BG size distribution among the various treatments.

As expected from literature (Tosh *et al.* 2010, Rieder *et al.* 2017), all extracted BGs had a high polydispersity. Figure 4.13 shows that BG extracted from the pellet or the supernatant of digesta containing barley bran was significantly lower (mean peak DP of 3,694 ± 1,203) than BG from oat bran (mean peak DP of 10,448 ± 1,617; p<0.0001, Student's t-test). The peak DP of dissolved oat BG from the supernatant (mean peak DP of 10,387 ± 277) was lower than the one recovered from the 2h- and 4h-pellet (mean peak DP of 12,025 ± 0; p=0.004, Student's t-test). The opposite was the case in barley bran digesta where the higher DP BG was dissolved in the supernatant (mean peak DP of 4,673 ± 54) and barley BG of lower size was found with the 2h- and 4h-pellet (mean peak DP of 3,209 ± 129; p=0.0003, Student's t-test). Both, in barley and oat, the Mw decreased after 20h digestion (Figure 4.13). This potential breakdown of BG might be due to endogenous β-glucanases present in the cereals (Rieder *et al.* 2017). Especially barley BG from the 20h-pellet had a small but substantial new peak appearing before 100 DP, demonstrating an increase in smaller BG molecules compared to the earlier timepoints. As the digestive enzymes used in the *in vitro* digestion are not able to digest DF, the breakdown of BG is unlikely due to the enzymes added to simulate digestion. This is also in line with the observation of lower viscosity at the 20h timepoint compared to the earlier timepoints (see Figure 4.9).
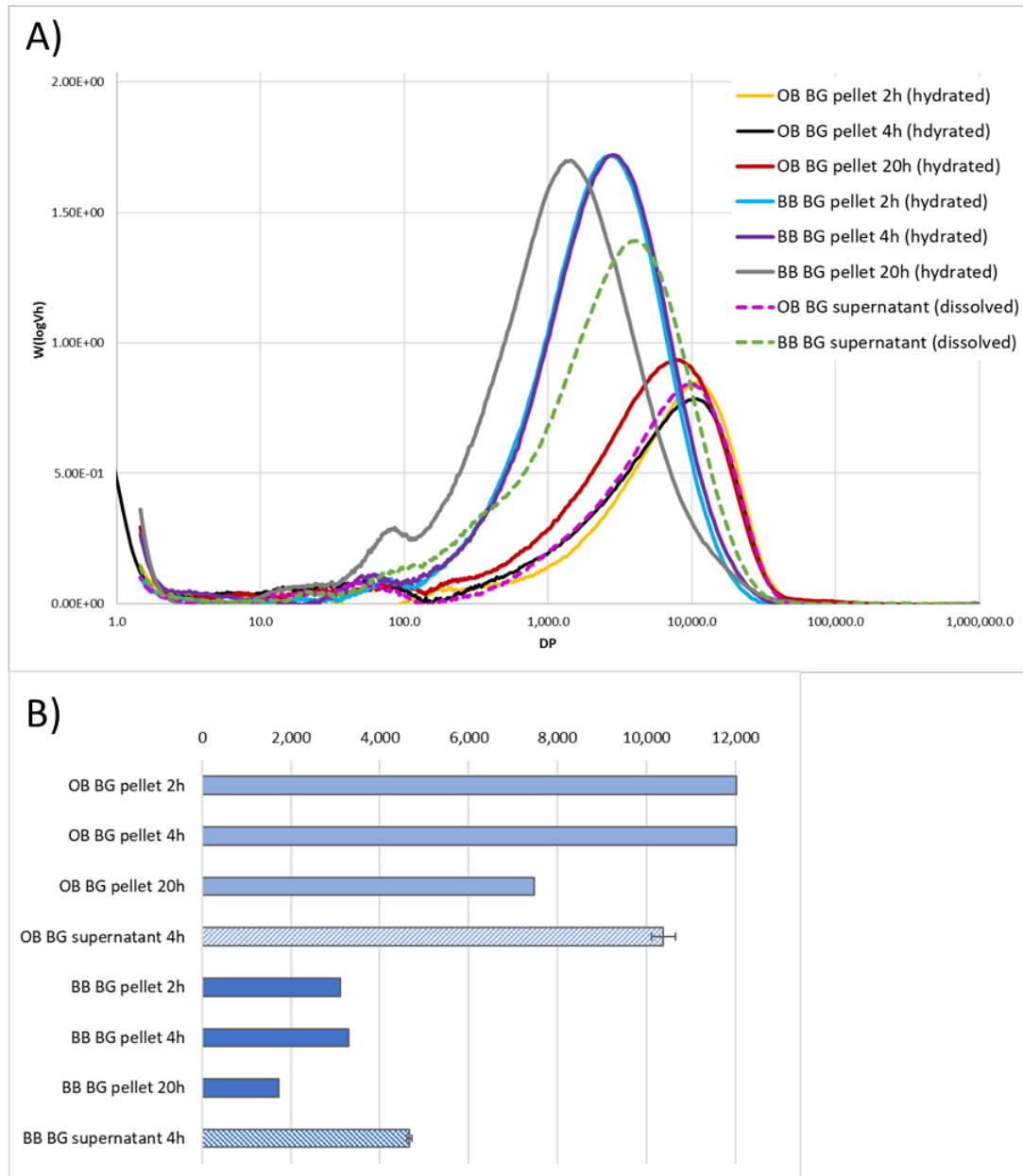
*Figure 4.13 – A) Size distribution in degree of polymerization (DP) and B) peak degree of polymerization (DP) of β-glucan (BG) extracts from supernatant (dissolved BG) after 4h (n=3) and pellet (hydrated BG) after 2, 4 and 20h (n=1) simulated digestion intestinal phase from oat bran (OB) and barley bran (BB).*

## 4.3.4.1  Analytical BG extraction from barley, oat and wheat bran and BG Mw distribution

To establish a baseline for the highest expected BG molecule size, different analytical extraction procedures were tested (see section 2.2.2). As shown in Figure 4.14, the size distribution and peak DP

of extracted BG depended on the analytical extraction procedure. Especially for barley bran, one extraction procedure resulted in a BG more than triple the peak DP size of all other extracted barley BGs. Overall, BG from barley bran (mean peak DP of 3,275 ± 2,780) was smaller in size than oat BG (mean peak DP of 10,861 ± 1,679; p=0.003, Student's t-test). Oat bran residue after the extraction procedure had still about 20% BG left whereas almost all of the BGs could be extracted from barley bran with only about 8% remaining. This could be due to lower Mw BGs being easier extractable than larger BG. All BG extracts had a BG content between 63 and 72% (see Appendix table A4.1).

Comparing the BG Mw results from the simulated digestion (Figure 4.13) with the Mw's of analytically extracted BGs (Figure 4.14), a similar peak DP of analytically extracted oat BGs and the extracted hydrated BGs from the pellet after digestion were found. With barley bran the highest peak DP value of almost 7,500 extracted analytically could neither be found in the supernatant nor in the hydrated pellet from barley bran digesta with a peak DP in the digesta supernatant of about 4,700 DP. Hence, analytical extraction can lead to different BG size distributions than BG solubilised or hydrated under simulated digestion conditions, both in barley bran and oat bran.
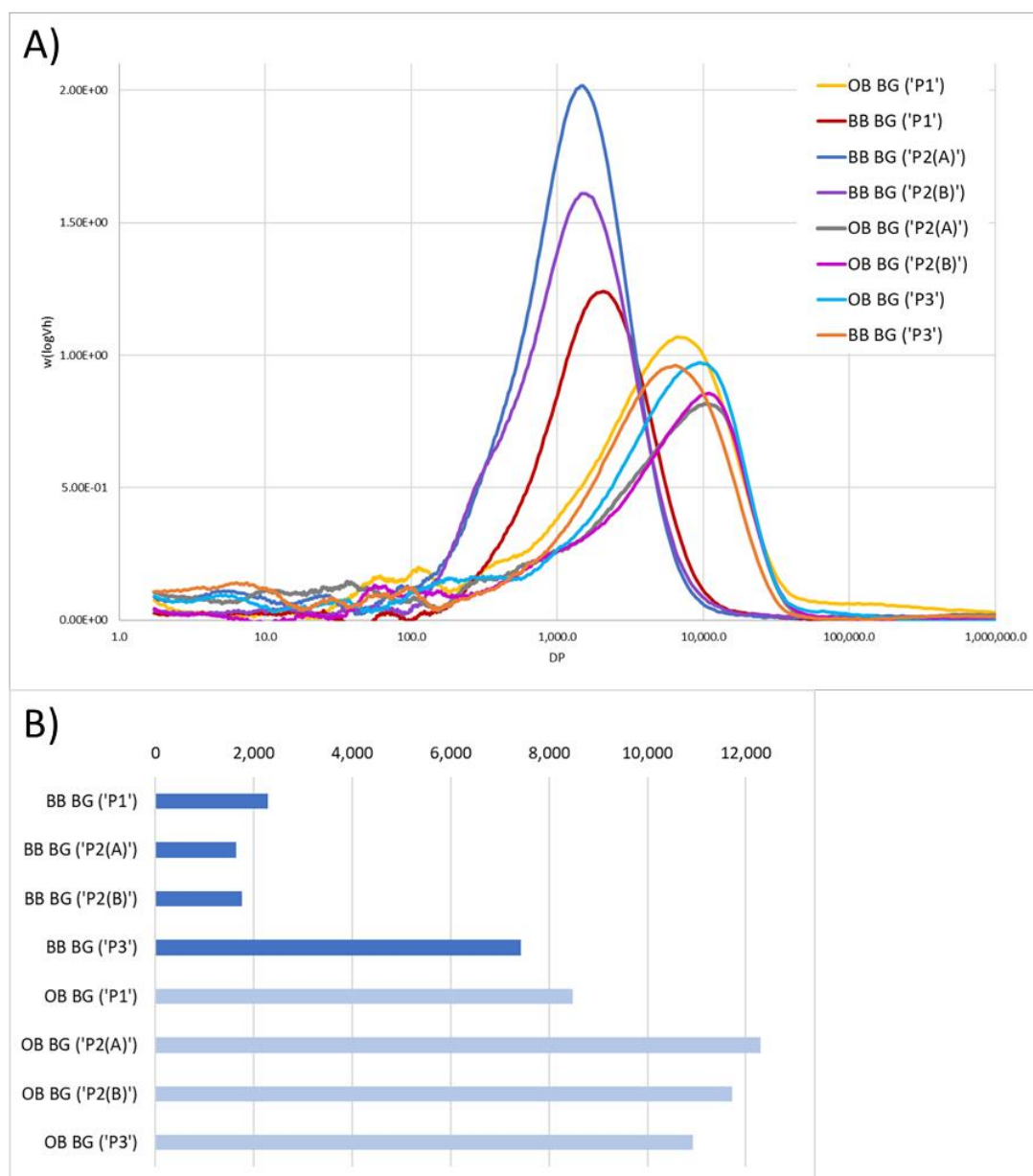
*Figure 4.14 – A) Size distribution based on degree of polymerization (DP) and B) peak degree of polymerization (DP) of ß-glucan (BG) extracts from oat bran (OB) and barley bran (BB) with 3 different extraction protocols indicated in brackets, all 4 mg/mL DMSO apart from OB BG 'P2(A)' + 'P2(B)' and OB BG 'P3' which were 2 mg/mL DMSO.*

### 4.3.5 Interaction of soluble, hydrated and insoluble cereal fibre with bile acids

The second objective of this set of experiments was to determine any correlation of the total BA concentration in the aqueous phase with the BG content in any of the three hydration stages of BG from barley or oat bran as both showed a delayed release of BAs through a dialysis membrane compared to control (see section 4.3.1). Using the centrifugation method, BA concentrations of the samples taken after 2, 4 and 20 hours of intestinal phase simulated digestion with and without enzymes were compared between barley or oat bran and negative control (Figure 4.15). Concentrations of BAs in the liquid phase of samples taken from barley or oat bran with and without enzymes were not different from control in any of the three timepoints ($p > 0.05$, Dunnett's test for 6 tests). The tendency for the higher BA concentration in digested oat bran supernatant compared to control could be due to different water-holding capacities of the bran samples (see Figure 4.15B) and the subsequent lower volume of the aqueous phase. If the different supernatant volume per sample was taken into account and the BAs calculated in absolute quantities as mMols, a significant reduction in BAs was found in all fibres and timepoints ($p \leq 0.05$, Dunnett's test for 6 tests) except for digested barley bran after 2 hours ($p = 0.1468$) compared to control (Figure 4.15C). This suggests that some BAs were entrapped in the pellet either by the hydrated BG or the insoluble fibre. However, this assumes that the centrifugation method to determine water-holding

capacity is precise in separating bound water from free water which is unlikely the case.

The amount of BG recovered from the three different hydration stages – solubilised, hydrated or insoluble BG content – did not correlate with the BA concentration [mM] determined in the liquid phase.
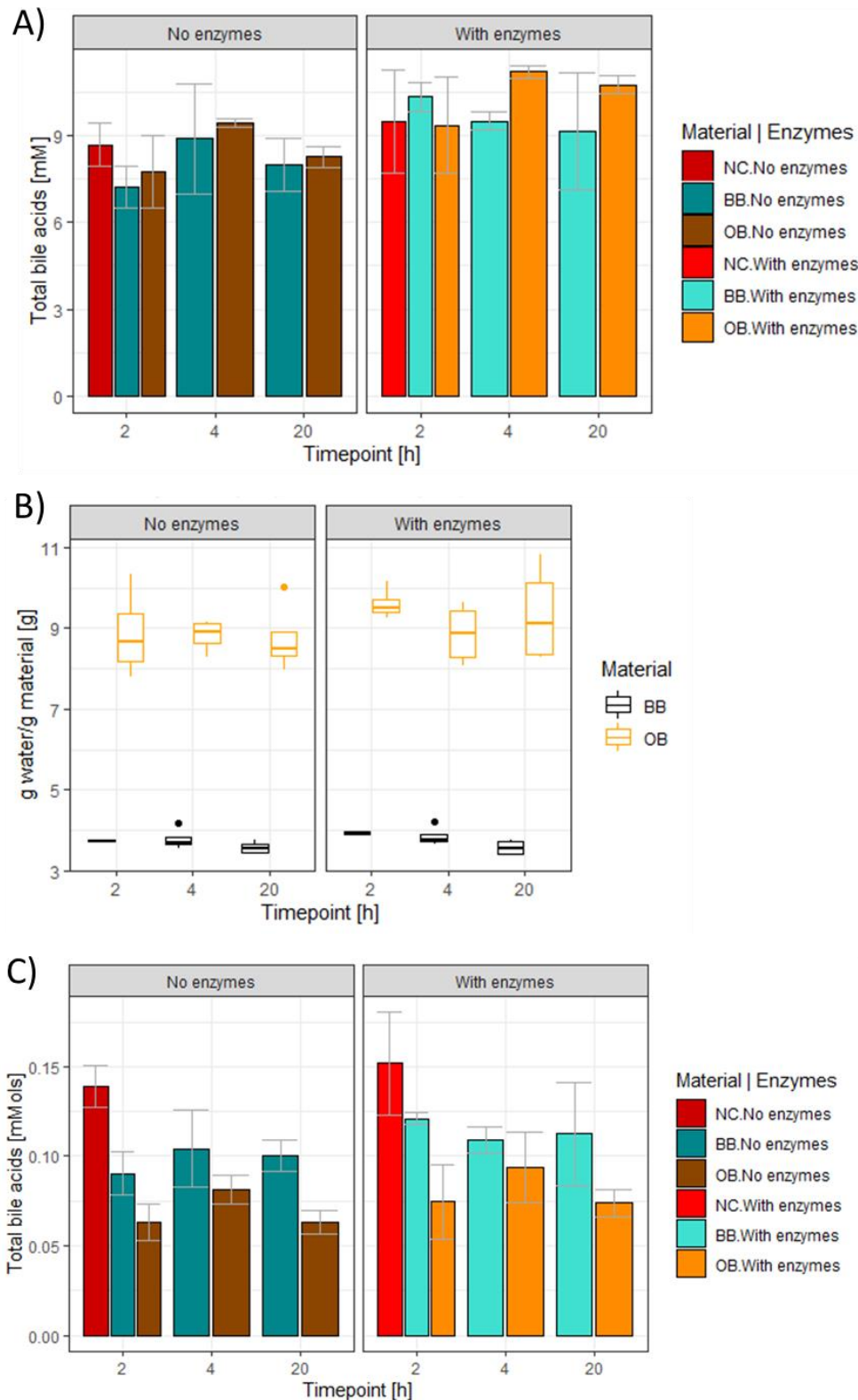
*Figure 4.15 – Barley bran (BB) and oat bran (OB) digesta measurements after 2, 4 and 20 hours intestinal digestion with or without digestive enzymes: A) Total bile acid concentration [mM] in digesta supernatant as determined in sample taken including no fibre control (NC) after 2 hours intestinal digestion, B) water-holding capacity in g water per g bran material, C) total bile acids [mMol] corrected for different supernatant volume as per water-holding capacity. Error bars in A) and C) are SD, n=4.*

### 4.3.6 Testing dietary fibre/bile acid interactions using a fluorescein labelled bile acid

To test fibre interaction with BAs by focusing on both the aqueous phase and the fibre matrix, a new method was developed using a fluorescein labelled BA (CLF). CLF was quantified in the supernatant and imaged in the pellet. During method development oat hull fibre was used as a control which did not show BA retention (see 4.3.1). A control experiment with free fluorescein confirmed that fluorescein did not bind to fibre material as it had the same concentration in oat bran, barley bran and oat hull fibre digesta supernatant as the control (Table 4.4).

Using CLF in a simulated digestion with pancreatin led to a reduction in CLF concentration in the supernatants of oat bran and barley bran whereas the result for oat hull fibre was the same as control. Initially, this was thought to be due to undigested starch as during method development a high affinity of CLF to starch in undigested bran was found (see Appendix figure A4.6). However, confocal microscopy showed that CLF bound to fibrous material in the pellet of oat bran and barley bran (Figure 4.16). These fibrous filaments were not stained by calcofluor which stains DF and could not be detected in oat hull fibre (Figure 4.16). The fibrous material was found attached to the cereal fibre tissue but also detached in both oat bran and barley bran pellets. To investigate this further, pancreatin on its own was incubated with CLF and the same fibrous filaments were found although it seemed that CLF did not bind as much as after the bran

digestion as the fluorescein signal was lower (see Appendix figure A4.7).

Twice centrifuged pancreatin was used henceforth. When the filament-free pancreatin solution was used in a 2 hour intestinal phase in presence of a bile mix containing CLF, CLF was only reduced in the aqueous phase of barley bran but not oat bran. However, confocal microscopy of the insoluble barley fibre showed that CLF bound to undigested starch (Figure 4.17). Therefore, a new approach was taken to digest the starch for 2 hours with ɑ-amylase and addition of the CLF bile mix together with pancreatin for 1 hour once starch has been digested. The supernatant of oat bran was more viscous than before (making it impossible to take a sample for the fluorometer with one of the two repeats). No binding of CLF to insoluble/hydrated fibre was detected when starch was digested before addition of CLF (Table 4.4, method C).

To test if fibre aggregates with hydrated BG formed during digestion (see section 4.3.4) would entrap CLF, the sample start weight was doubled for the oral and gastric phase and 250 mg bran digesta transferred to a new tube for intestinal digestion for 2 hours with pancreatin without the bile mix present which was added later. This approach also did not show any reduction in CLF in the aqueous phase compared to control (Table 4.4, method D).

In conclusion, no binding of fluorescein-labelled BA to insoluble or hydrated fibre was found using this newly developed method. A

limitation of this method was that the BA species CA was used instead of DCA or CDCA which both showed a delayed release in the dialysis model (see section 4.3.2). In addition, labelling the BA with fluorescein, which is a relatively big molecule in relation to the BA (see Figure 4.2), might have changed the BA's properties. The fluorescein having a high affinity to starch granules, which might not have been fully digested, might change how the BA behaves compared to an unlabelled BA. Another reason could be that the DF/BA interaction is due to a different mechanism other than binding to a specific component of the soluble, insoluble and/or hydrated fibre which cannot be picked up with this method.

*Table 4.4 – BA concentration in supernatant (SN) of digesta containing oat bran (OB), barley bran (BB) and oat hull fibre (OHF) as ratio to concentration measured in negative control (in absence of fibre), mean ± standard deviation (SD), n=2.*

| Protocol | CLF or free fluorescein concentration in SN ratio to negative control ± SD | | |
|---|---|---|---|
| | **OB** | **BB** | **OHF** |
| Free fluorescein control | 0.98 ± 0.07 | 0.96 ± 0.01 | 1.06 ± 0.05 |
| CLF method A | 0.82 ± 0.04 | 0.85 ± 0.04 | 1.03 ±0.02 |
| CLF method B | 1.06 ± 0.01 | 0.74 ± 0.05 | not tested |
| CLF method C | 1.28 ± NA | 0.97 ± 0.02 | not tested |
| CLF method D | 1.02 ±0.02 | 0.96 ± 0.02 | not tested |

(a)



(b)

(c)
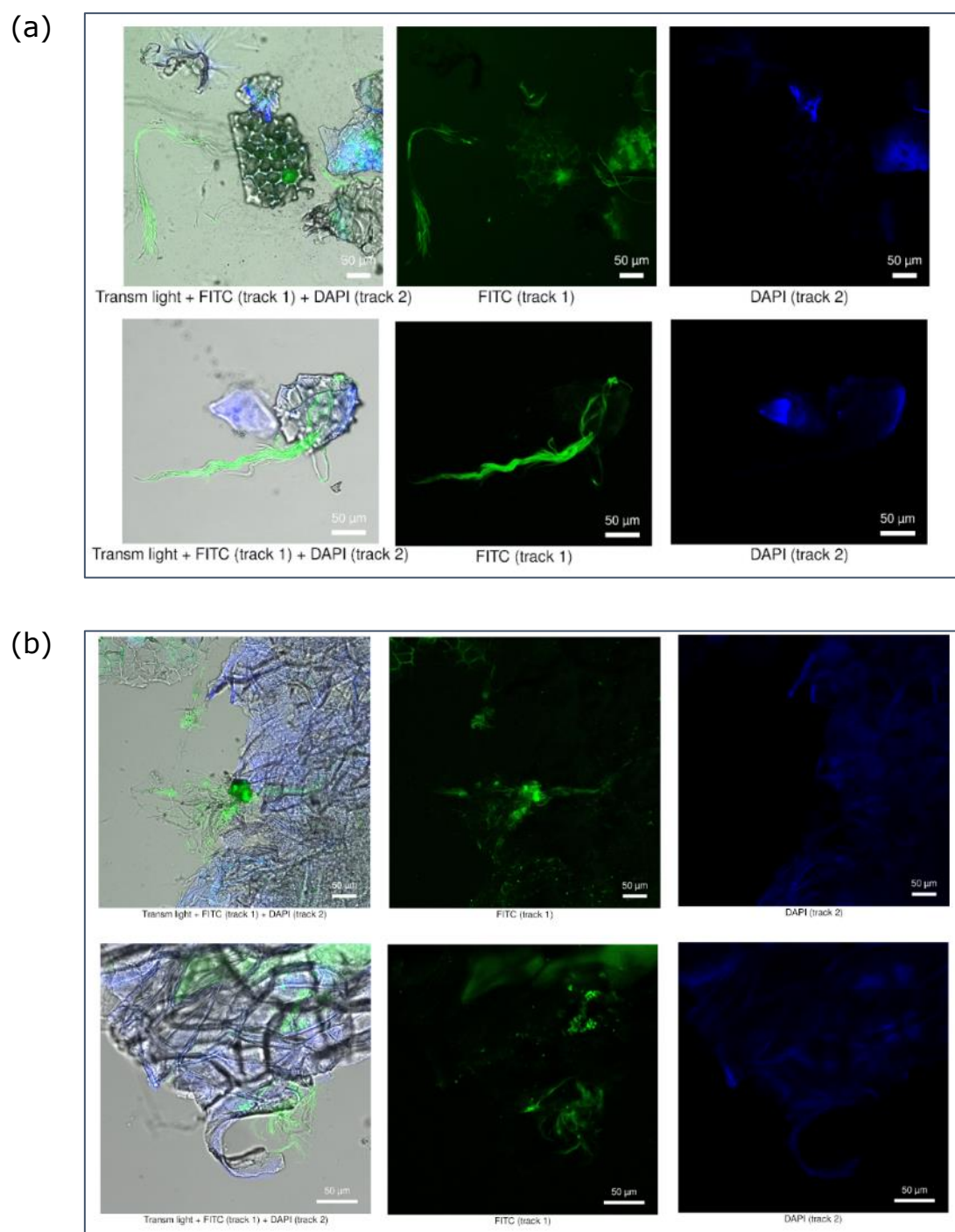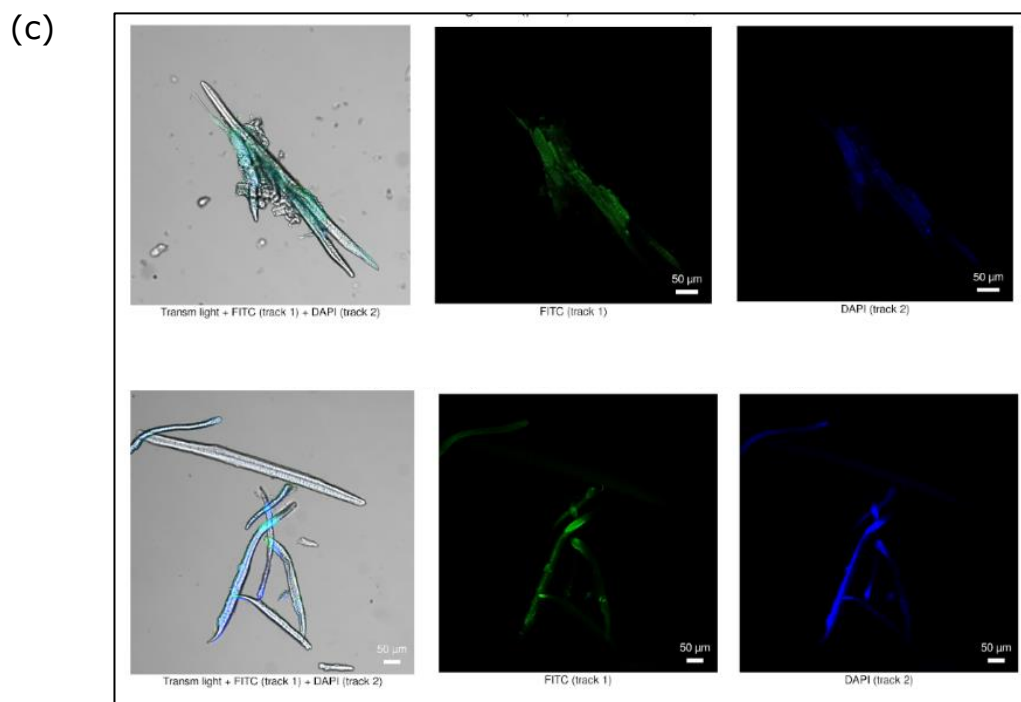


*Figure 4.16 – Confocal microscopy pictures of (a) oat bran, (b) barley bran or (c) oat hull fibre pellet after digestion protocol (A), stained with Calcofluor white: overlay of transmitted light, FITC and DAPI channel (left), FITC channel (middle) and DAPI channel (right).*

(a)                                                (b)
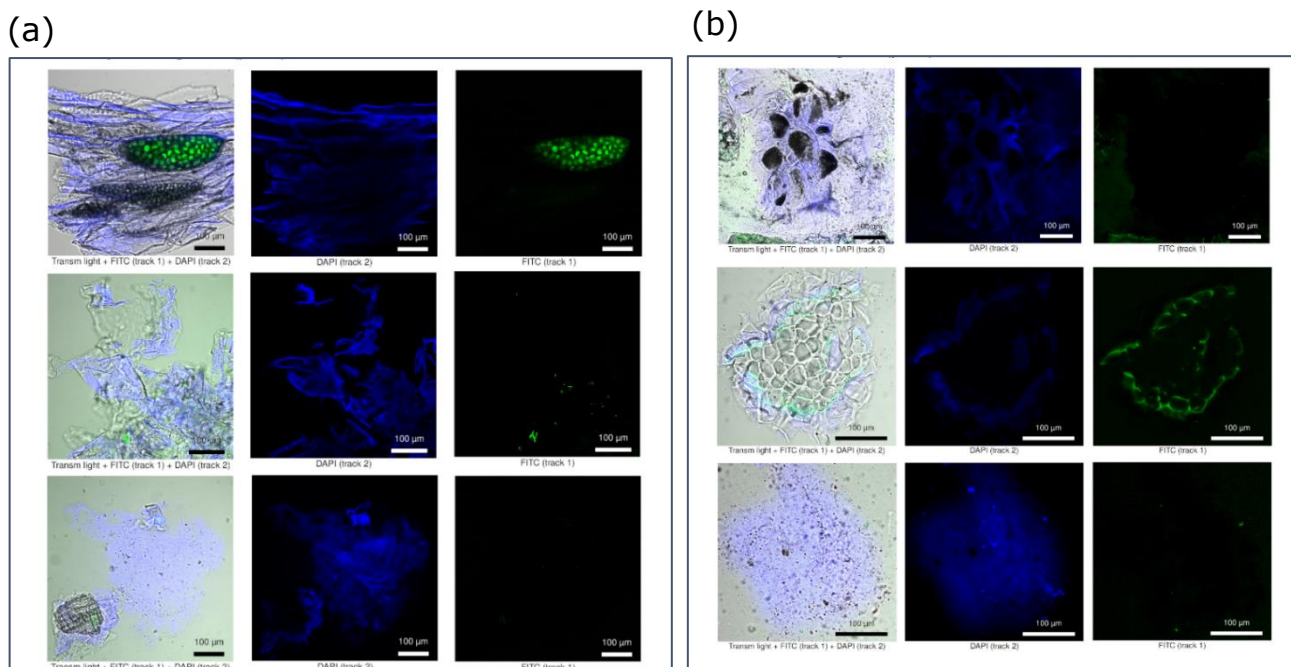


*Figure 4.17– Confocal microscopy pictures of (a) barley or (b) oat bran pellet after digestion protocol (B), stained with Calcofluor white: overlay of transmitted light, FITC and DAPI channel (left), FITC channel (middle) and DAPI channel (right).*

(a)
(b)
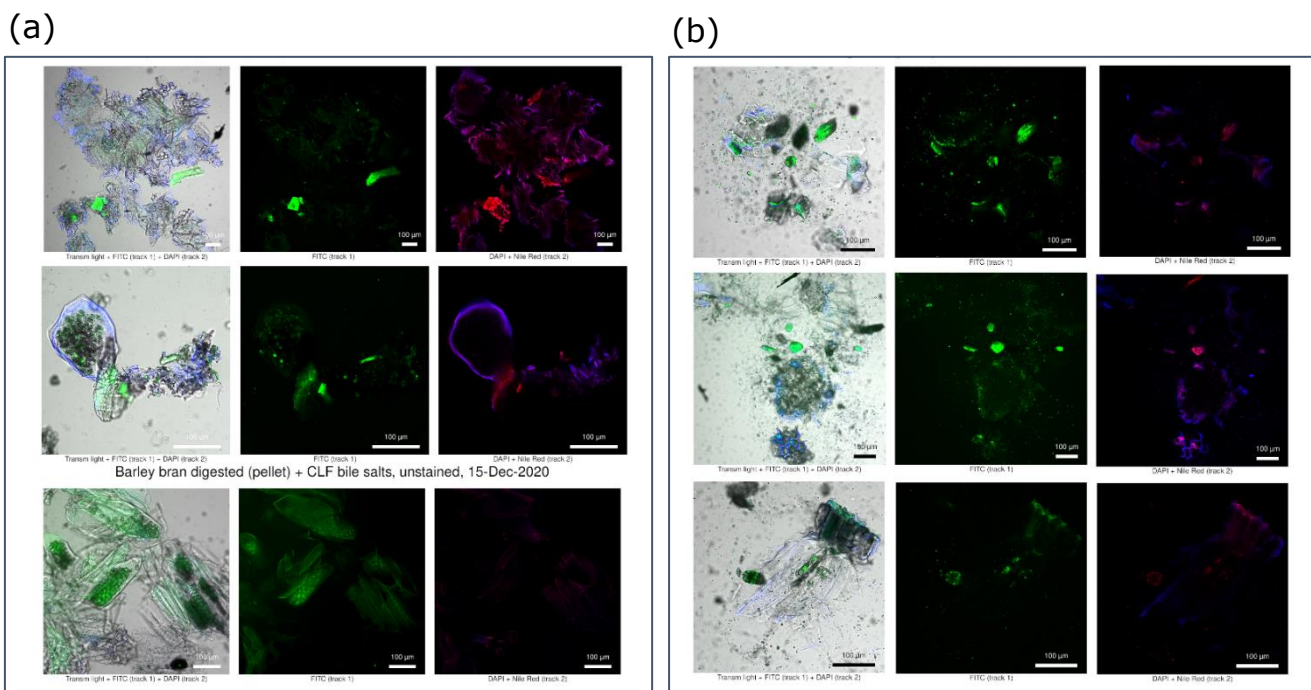


*Figure 4.18 – Confocal microscopy pictures of barley or oat bran pellet after digestion protocol (C) : overlay of transmitted light, FITC and DAPI channel (left), FITC channel (middle) and DAPI channel (right).*

## 4.4 Discussion

BA interactions with DF have been extensively studied, however it is not clear how the interaction is mediated. From the results as presented in this thesis it seems unlikely that BAs interact with a single component of the cereal fibres (see sections 4.3.5 and 4.3.6). Presence of a cell wall matrix seems to be an important factor with a potential synergistic effect of soluble and insoluble fibre. Purified BG was tested as merely soluble DF and oat hull fibre essentially being insoluble DF, but neither of the two showed BA retention. The latter is in accordance with literature as oat hull fibre contains mainly cellulose which is usually used as non-binding control in DF/BA centrifugation experiments (Sayar *et al.* 2005, Kahlon and Woodruff 2003). A dialysis study on a similar oat spelt product found a BA retention only with GCDCA out of six BAs tested (Naumann *et al.* 2019a). Total DF content does not explain the different BA retention effects seen in the presented study in this thesis as the cereal DFs tested were normalised according to their total DF content. This is in agreement with literature results on cereal brans (Kahlon and Woodruff 2003).

The DF's physico-chemical properties seem to be a better predictor for potential interaction mechanisms. Fibre properties which were found to lead to increased DF/BA interaction in the literature are anionic charge with chitosan (Chiappisi and Gradzielski 2015), hydrophobicity with chitosan (Chiappisi and Gradzielski 2015) but also hydroxypropyl methylcellulose (HPMC) (Pilosof 2017) and

smaller particle size, i.e. bigger surface area, with wheat bran (Kahlon *et al.* 2006). Rheological properties like higher bulk viscosity, i.e. resistance to flow across the entire sample overall, for fibre samples from citrus, lupin kernel, potato and cellulose (Naumann *et al.* 2018, Gunness *et al.* 2012), the ability to form polymer aggregates or local viscosity with barley BG and AX (Gunness *et al.* 2016) or higher Mw with oat BG (Rosa-Sibakov *et al.* 2020) all led to improved DF/BA binding. Contradictions in the optimum conditions for DF/BA interaction are reported as higher fibre solubility with oat BG increased BA binding (Kim and White 2010) but other studies found a correlation with higher IDF content in oat flours (Sayar *et al.* 2005) as well as in rice bran, oat bran, barley, and BG-enriched barley and higher DF/BA interaction (Kahlon and Woodruff 2003). Some literature also suggest other components like protein with cereal fibres (Kahlon and Woodruff 2003, Naumann *et al.* 2018) or phytosterol with oats (Wilde *et al.* 2019) to be important for BA interaction.

The *in vitro* method conditions can affect DF/BA interactions as for example no gastric protein digestion or no acidic pH pre-condition (Robertson *et al.* 1976, Colosimo *et al.* 2020a, Macierzanka *et al.* 2019) reduced the extent of BA binding. BA incubation time (Drzikova *et al.* 2005, Kahlon *et al.* 2006, Kahlon and Woodruff 2003, Li *et al.* 2017, Naumann *et al.* 2018) and the pH condition of the experiment (Drzikova *et al.* 2005) have been shown to change the

extent of BA interaction with DF. Conditions which have been proposed in published studies to impact the extent of DF/BA interaction are the use of individual BAs instead of bovine/porcine bile (Gunness *et al.* 2012) as well as concentrations below CMC (Maldonado-Valderrama *et al.* 2011) in contrast to an interaction with micelles (Gunness *et al.* 2016). Different *in vitro* methods test different interaction behaviours. A dialysis model can reveal physical entrapment in a viscous network whereas centrifugation experiments seem to detect molecular binding (Naumann *et al.* 2018). As presented in this thesis (see section 4.3.1), using the dialysis method, there was a viscous or entrapment effect leading to BA retention with barley, oat and wheat bran in line with Naumann *et al.* (Naumann *et al.* 2018). Whereas these potentially dynamic immobilisation interactions between DF and BAs (Gunness *et al.* 2016) could not be determined using the centrifugation method (see section 4.3.5) nor fluorescein labelled BA (see section 4.3.6).

## 4.4.1 Viscosity and BG solubilisation during digestion as underlying mechanism(s) of DF/BA interactions

Increased viscosity is the main proposed mechanism of DF/BA interactions in the present study. In the dialysis model, oat, barley and wheat bran retained BAs but did not seem to chemically bind BAs irreversibly as the final extent of BA release after 20 hours was not different from control. Purified BG did not interact with BAs but had a very low viscosity as opposed to oat bran and barley bran. This is in line with a study on oat bran showing viscosity being the

underlying mechanism (Rosa-Sibakov *et al.* 2020) as well as in another study on purified barley and oat BG, which were compared in a native state with a modified state to reduce the viscosity (Marasca *et al.* 2020). Naumann *et al.* found BA binding as opposed to a viscous effect with a barley fibre product in a dialysis model, although it had a lower fibre content (Naumann *et al.* 2018) than the barley bran tested in this thesis. This could be the reason for the contradicting results as the authors suggested a role of barley protein in the BA binding (Naumann *et al.* 2018). Similarly to a wheat fibre product reported in the literature (Naumann *et al.* 2019a), wheat bran did not increase the bulk viscosity (see section 4.3.3), but delayed BA release (see section 4.3.1). Naumann *et al.* did not find an interaction between BAs and wheat fibre. This could be due to a lower SDF content (Naumann *et al.* 2019a), which in wheat is usually AX (Izydorczyk 2009), and has been shown to immobilise BA micelles by formation of aggregates (Gunness *et al.* 2016, Gunness *et al.* 2010). In a different study, purified wheat AX delayed BA diffusion through a semi-permeable membrane in a dose-dependent manner (Gunness *et al.* 2012).

The main SDF in barley and oat bran is BG. Purified BG on its own did not interact with BAs, hence the cell wall matrix seems to play an important role in the interaction mechanism between barley bran or oat bran and BAs. Digesta containing barley bran or oat bran had higher viscosities than purified BG as BG was released from the

barley bran or oat bran cell wall matrix during the course of the *in vitro* digestion. Investigating the dissolution behaviour of BG from the bran matrices of barley and oat bran further, it was found that presence of digestive enzymes decreased BG dissolution. This is the opposite of what has been reported in a human study with flapjacks showing that proteolytic enzymes enhanced BG extractability (Robertson *et al.* 1997). The extent of BG release was similar to what was observed by Grundy *et al.* and Rieder *et al.*, however both studies only determined dissolved BG solubility in the supernatant after centrifugation (Grundy *et al.* 2017a, Rieder *et al.* 2017). As shown in this thesis (see section 4.3.5), hydrated BG which was still associated with the pellet/insoluble fibre formed a significant share of the overall BG content released from the cell wall matrix and should be differentiated from insoluble fibre. This might be the mechanism behind the suggestion from recent reviews that solubilisation of fibres and subsequent generation of viscosity needs to occur during digestion for observing an effect (Grundy *et al.* 2018a, Grundy *et al.* 2016, Holland *et al.* 2020, Henrion *et al.* 2019).

In line with literature (Rieder *et al.* 2017, Grundy *et al.* 2017a, Tosh *et al.* 2010, Rosa-Sibakov *et al.* 2020), under physiological conditions only a small share of BG was extractable from barley bran or oat bran whereas with an analytical method, more than 80% BG was extracted. The extraction conditions used in an analytical extraction have an impact on yield and Mw (Robertson *et al.* 1997,

Mäkelä *et al.* 2020). However, as opposed to Rieder *et al.* who found the BG's Mw to be similar between physiological and analytical extraction (Rieder *et al.* 2017), peak DP of BG depended on the method used as well as on the BG hydration status under physiological conditions (see section 4.3.4).

Not only the amount of BG, but also the Mw is very important for generating viscosity and exerting the physiological effects as C* depends on both, solubilised BG and its Mw (Rieder *et al.* 2017, Goudar *et al.* 2020). Barley bran had a quicker and higher release of dissolved BG than oat bran. The dissolved BG from oat bran had a lower peak DP than the one extracted as hydrated BG from oat bran. Hence, the higher Mw BG in oat bran stayed with the cell tissue. In contrast, in barley bran, the BG had a lower DP overall which may led to its quick dissolution. A Mw dependent dissolution rate or extent is also in line with literature (Tosh *et al.* 2010), though not entirely understood in the context of digestion (Rieder *et al.* 2017). Whereas dissolved BG is important for supernatant viscosity, the intermediate state of BG being hydrated but remaining with the cell particle can however also impact the digesta viscosity. Viscosity measured on whole digesta was higher (see Figure 3.9, Chapter 3 and Appendix figure A3.2) than the viscosity of digesta supernatant (see Figure 4.9). Fibre particles take up space in the volume fraction (Lentle and Janssen 2010) and interactions between particles occur (Genovese 2012).

It was investigated whether any BA interactions could be related to whether BG is dissolved, hydrated or insoluble but no correlation was found when BA concentrations were compared in the supernatant. Different water-holding capacities seemed to play an important role as the absolute BA content was significantly reduced (see 4.3.5). This is in line with a study by Rosa-Sibakov *et al.* using a similar method in oat bran to account for different water-holding capacities (Rosa-Sibakov *et al.* 2020).

The effective functional dose of fibre seems to depend on the hydration properties of BG, the Mw and the resulting viscosity, rather than an amount of BG per g food product as it is currently defined in health claims around cardiovascular health.

## 4.4.2 Preferential retention of specific BA species by cereal fibres

DCA and CDCA were retained preferentially by cereal brans, hence some form of molecular interaction between DF and these BAs delayed their release even further than the total BA release. An interaction with specific BAs is in line with a human cross-over study, which found a higher faecal BA excretion of DCA and CDCA after high Mw BG consumption compared to the low Mw BG in a meal (Hakkola *et al.* 2021). It is also in agreement with *in vitro* data by Naumann *et al.* who tested different fibre material from barley, lupin, oat and maize and found DF interactions with dihydroxy BAs (CDCA and DCA) and to some extent also with CA (Naumann *et al.* 2019a). An interaction with specific BA species can affect lipolysis kinetics as

different BA species contribute in different ways to lipolysis kinetics due to their different adsorption and desorption behaviour at the interface (Pabois *et al.* 2020, Parker *et al.* 2014).

Again, the bran matrix seemed to be important as there was no preferential retention with purified BG. A fractionation study of DF from lupin kernels found that fractions containing pectin-like fibres, as well as the cellulose-lignin fraction, showed a minimal decrease in BA diffusion rate and no adsorptive effects. However, when the whole cotyledon was used, a high adsorption capacity for CDCA was observed (Naumann *et al.* 2019b). Other compounds associated with the cell wall, such as protein, lignin and polyphenols, have been speculated in the past to enhance the BA adsorption effect (Naumann *et al.* 2019b, Naumann *et al.* 2018, Kahlon and Smith 2007). Another reason could be that there is a synergistic effect between the soluble fibres and the insoluble fibre matrix. BAs could be entrapped in the viscous network around the insoluble particles when BG or AX is partly solubilised and hydrated which could also explain the differences among the cereal brans due to different dissolution kinetics of the soluble fibre.

### 4.4.3   Conclusion

It seems unlikely that BAs interact with a single component of the fibre, while presence of a cell wall matrix seems to be important. A delayed release of BAs through a dialysis membrane in presence of barley bran and oat bran may be due to a viscous entrapment and

interaction between the fibre digesta and the BAs and not due to binding of BAs to insoluble fibre. However, increased viscosity does not explain the preferred retention of some BA species with barley bran or oat bran nor the BA retention of wheat bran which did not increase digesta viscosity. The cereal fibres potentially exert their BA retention effect via different mechanisms, depending on dissolution kinetics of their soluble DF. Barley and oat showed important differences in their BG hydration properties and release kinetics which can affect local as well as bulk viscosity. BG dissolving from a cell wall matrix is important in exerting functionality.

# Chapter 5 – Starch gelatinisation and digestion in presence of dietary fibre

## 5.1 Introduction

There is an established protective effect of DF consumption against type 2 diabetes (Reynolds *et al.* 2019, Davison and Temple 2018). A proposed underlying mechanism in the literature is reduced starch digestion in presence of DF (Dhital *et al.* 2015, Ramírez *et al.* 2015, Colosimo *et al.* 2020b, Slaughter *et al.* 2002) resulting in a slower insulin response (Stephen *et al.* 2017). Non-digested starch is fermented in the colon, which has positive health implications (Liu *et al.* 2020). Different DFs gave inconsistent effects on glycaemic response in randomized controlled trials (Davison and Temple 2018). However, different physico-chemical properties of DFs may lead to different health outcomes. A low moisture food system was used to study the effect of presence of certain DFs on starch gelatinisation and *in vitro* starch digestibility.

Starch gelatinisation is important for its bioavailability since uncooked (ungelatinized) starch is much slower metabolised than cooked starch (Fessas and Schiraldi 2000). During hydrothermal processing, starch undergoes a transformation from semicrystalline to an amorphous state which is called gelatinisation (Van der Sman and Mauer 2019, Pérez and Bertoft 2010). During the process of gelatinisation, water acts as a plasticiser by entering the starch granule, making the starch granule swell, and the molecular

architectural order becomes lost (BeMiller and Whistler 2009, Van der Sman and Mauer 2019). Heat is required for this process and the temperature at which it occurs is called the gelatinisation temperature. In excess water systems, between 65 and 70°C are required for this order-disorder phase transition to occur. If the mass of water is lower than the mass of starch, a double endothermic transition and a broadening of the gelatinisation temperature range towards higher temperatures is seen which is termed 'limiting water behaviour' (Donovan 1979, Donovan and Mapes 1980, Perry and Donald 2002). Addition of sugars and other polyols to starch-water systems elevates the starch gelatinisation temperature. However, this temperature increase is not equivalent to a starch gelatinisation temperature elevation under a limiting water regime (Perry and Donald 2002). Small molecules may act as plasticisers whereas high Mw DFs may compete for water (Woodbury *et al.* 2021, Lai *et al.* 2012, Ramírez *et al.* 2015, Hou *et al.* 2020). However, plasticization or 'antiplasticization' effects of these molecules depend on water or other diluent concentrations in the system. Interactions of water molecules with other food components have not been fully understood and remain a subject of great interest to food scientists, especially in low moisture food systems such as a biscuit (Seow *et al.* 1999, Roos 2003).

Therefore, the presence of DF in food can impact the food chemistry and DF's presence in the GI tract can interfere with macronutrient

digestion. The aim of this chapter was to investigate if physico-chemical properties of DF determine its impact on starch gelatinisation via acting as a plasticiser or water competitor in a food system. First, starch gelatinisation in a biscuit model system consisting of wheat starch, sucrose and different levels of water and DF was tested using DSC. Second, two inulin fibres with different physico-chemical properties were incorporated into a biscuit recipe to test whether there is a dose-dependent decrease in *in vitro* starch digestibility in the presence of the inulin and whether this is due to an effect on starch gelatinisation.

## 5.2 Materials and Methods

### 5.2.1 Materials

Wheat starch (cat# S5127) and sucrose (cat# S9378) were purchased from Merck (UK). Sucrose was sieved to a particle size smaller than 600 µm before use. DF materials were used as listed in Table 2.2.

Biscuit ingredients were wheat flour (medium soft North American biscuit flour) from Mondelez, Nonfat Dry Milk 'Alpine skimmed milk powder' from Omira (Germany); PDV salt and sodium bicarbonate from Kilo (UK); caster sugar from British sugar (UK); fat (palm oil) from Bunge (US).

All other materials are described in section 2.1.3.

### 5.2.2 Methods

#### 5.2.2.1 AACC 10-53 biscuit recipe and baking procedure

Method AACC 10-53 (macro method) (AACC 1999) is based on 13% flour moisture and eight biscuits per dough batch. The recipe was modified and tested for use as outlined in Table 5.1 to omit high fructose corn syrup as fructose affects starch gelatinisation (Allan *et al.* 2018).
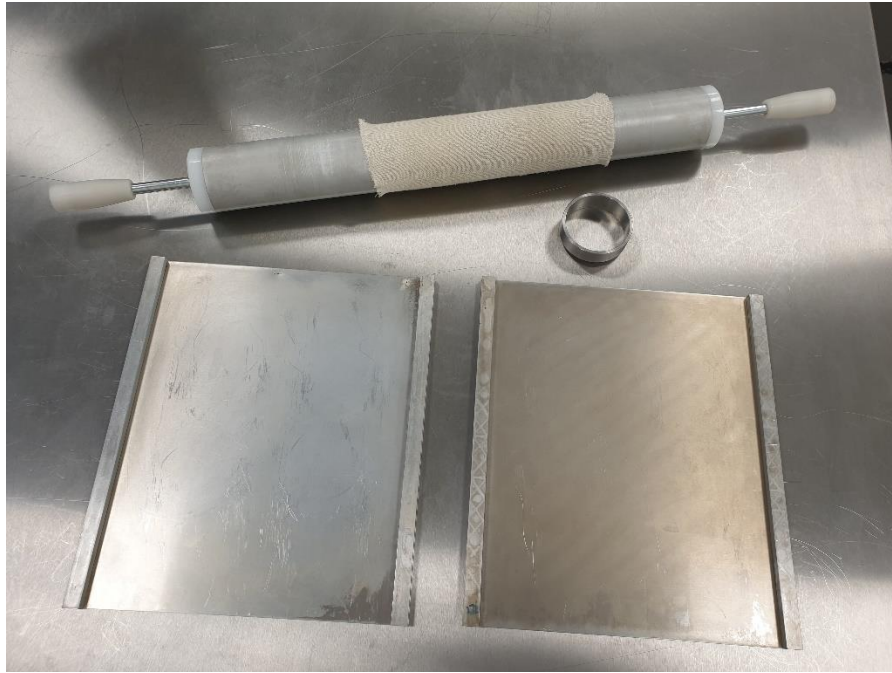
*Figure 5.1 – Roller pin with sleeve on, cookie cutter with a diameter of 6 cm and two baking trays with guiding edges for equal rolling thickness*

All ingredients were kept at 21°C, including palm oil, and weighed out according to Table 5.1. At stage 1, the creaming step, ingredients as listed under stage 1 (Table 5.1) were mixed using a Hobart mixer (Hobart N50-110, Peterborough, UK) for 3 min at speed 1. At stage 2, ammonium bicarbonate was dissolved in water, added to the cream and mixed for 1 min at speed 1 and for another minute at speed 2 with a Hobart mixer. At stage 3, a calculated amount of flour based on the flour's moisture content was added and mixed for 2 minutes in total at speed 1, stopped every 30 seconds to scrape the dough off from the side of the bowl using a spatula and bring it back into the middle of the bowl. Without resting time, the dough was divided into two parts, each divided again into 4 portions to bake four biscuits each on two baking trays. Baking

trays with guiding edges for consistent dough height of 7 mm when rolled (Figure 5.1) were weighed empty and weight noted. The dough was rolled on a baking tray with one forward stroke using a roller pin with a sleeve on to mark the direction of rolling and cut with a cookie cutter with an inner diameter of 6 cm, excess dough was discarded, and cutter removed. This was quickly repeated for all 8 biscuits. Baking trays with the cut raw dough were weighed again and weight noted to calculate the dough weight of 4 raw biscuits. The biscuits on both baking trays were baked immediately together at a measured temperature of 205°C for 11 minutes using an oven (Elettrodrago oven, Elektros 212 – Avant 212, Polin, Verona, Italy) with the settings 215°C (top 70/ bottom 30).

*Table 5.1 – AACC 10-53 method recipe in three stages, modified to omit high fructose corn syrup*

| Method | AACC 10-53 (modified) | |
|---|---|---|
| Number of biscuits | 8 | |
| Flour moisture | 13.0 | % |
| Ingredient/Stage | g | % |
| **Stage 1** | | |
| Nonfat Dry Milk | 2.25 | 0.48 |
| Salt | 2.81 | 0.60 |
| Sodium bicarbonate | 2.25 | 0.48 |
| Caster sugar | 94.50 | 20.22 |
| Fat (palm oil) | 90.00 | 19.25 |
| **Stage 2** | | |
| Ammonium Bicarbonate | 1.13 | 0.24 |
| High Fructose Corn Syrup | 0.00 | 0.00 |
| Water (distilled) | 49.50 | 10.59 |
| **Stage 3** | | |
| Flour | 225.00 | 48.13 |
| TOTAL BATCH | 467.44 | 100.0 |
| water from flour + added water | 78.75 | |
| Dough moisture (%) | | 16.85 |

## 5.2.2.2 AACC 10-53 (modified) with inulin

The AACC 10-53 recipe without fructose syrup was used as a basis to incorporate one of two different inulins (soluble or insoluble) into biscuits. Since sugar acts as a plasticiser on starch gelatinisation (Perry and Donald 2002), both flour and sugar were reduced equally and kept at a ratio of sugar:flour of 1:2.5 (+/-0.05) when inulin was added. Different levels of inulin were tested with a maximum of 30% inulin, which was more inulin than flour, however incorporation levels of 10 and 20% inulin were found to give consistent batches with similar dough moisture levels as the control. Addition of 20%

soluble inulin at stage 3 (pre-mixed together with flour) or 20% insoluble inulin at stage 2 (pre-mixed together with water) of the mixing procedure resulted in non-workable doughs.

*Table 5.2 – Biscuit recipes overview displaying the main components of the recipe (see Table 5.1 – control) to highlight the adjustments made to incorporate inulin*

| Recipe (Name) | Flour (g) | Inulin type | Stage | Inulin (g) | Sugar (g) | Dough mois-ture (%) |
|---|---|---|---|---|---|---|
| Control (C0) | 225.0 | None | 0 | 0 | 94.5 | 16.9 |
| 10% soluble inulin (S10) | 190.2 | Soluble | 3 | 46.8 (dw) | 77.9 | 16.9 |
| 10% insoluble inulin (I10) | 190.2 | Insoluble | 3 | 46.8 (dw) | 77.9 | 16.9 |
| 19% soluble inulin (S19) | 154.8 | Soluble | 3 | 93.5 (ww) | 62.0 | 17.6 |
| 19% insoluble inulin (I19) | 154.8 | Insoluble | 3 | 93.5 (ww) | 62.0 | 18.0 |
| 20% soluble inulin (S20) | 154.8 | Soluble | 2 | 93.5 (dw) | 62.0 | 16.9 |
| 20% insoluble inulin (I20) | 154.8 | Insoluble | 3 | 93.5 (dw) | 62.0 | 16.9 |

Seven different recipes (based on Table 5.1) with differences between them as outlined in Table 5.2 were baked in at least 3 batches according to the baking procedure described above. With some inulin recipes, there was a deviation from the procedure at stage 3 when the mixing time was shortened and stopped as soon as the dough was formed and consistent. Details of all recipes tested can be found in Appendix table A5.3.

### 5.2.2.3  Ingredient and biscuit measurements

The ingredient moisture of both inulins as well as flour was measured by heat treatment at 130°C of the exact weight of around 3 g powder to constant weight using a HG63 Halogen Moisture Analyser (Mettler Toledo, UK).

Water activity ($a_w$) was measured on the raw biscuit dough using an Aqualab 4TE water activity meter (Meter, US) which was calibrated on the day according to the instrument instructions using commercial salt solutions in the expected water activity range of the samples. Water activity is the measure of energy status of water in a system and is expressed as a ratio of the vapor pressure of water above the sample at a given temperature compared to the vapor pressure of pure water at the same temperature. The higher the water activity, the more energy is available for e.g. microbial growth, moisture migration as well as chemical and physical reactions. All measurements were taken on a small aliquot of the final dough at room temperature in triplicate.

After baking, the baking trays were taken out of the oven and left to rest for 5 minutes on the tray. They were transferred to a cooling rack and left to cool for at least 30 minutes before measurements were taken. Average stack height was measured using a calliper and stacking the four biscuits per tray on top of each other with one random change of order. The length of the four biscuits was

measured using a ruler by placing the biscuits next to each other and width by rotating each biscuit by 90°.

Biscuits were stored in air-tight plastic containers at room temperature. After at least seven days, one biscuit per tray was gently ground using a food processor and used to measure product moisture and water activity. Using a HG63 Halogen Moisture Analyser (Mettler Toledo, UK), 5 g of ground biscuit was heat treated at 105°C until no difference in weight was detected by the instrument. Water activity was measured on the ground biscuit using an Aqualab 4TE water activity meter (Meter, US) as described above.

### 5.2.2.4 DSC analysis of a biscuit model system

A biscuit model system was analysed using DSC as described in section 2.3.9, consisting of 125 mg of wheat starch, 100 mg sucrose and either no fibre, called 'no fibre control' or increasing amounts of four fibres: BG, cellulose, insoluble inulin or soluble inulin, details are listed in Appendix table A5.1 and Appendix table A5.2.

For samples called 'crystalline', ingredients were weighed in and mixed with water only at the start of the measurement to resemble a biscuit system. The respective amount of degassed, deionised water was calculated as a percentage of the total mass and mixed gently with a spatula and hermetically sealed. Samples were scanned from 10–150 °C, with a heating rate of $1\,°C\,min^{-1}$. For samples called 'solubilised', sucrose and fibre were weighed in into the cells and mixed with degassed, deionised water, hermetically

sealed, and heated from 10–150 °C, with a heating rate of 2 °C min$^{-1}$. The cells were cooled to room temperature, opened and 125 mg starch was added and scanned from 10–150 °C, with a heating rate of 1 °C min$^{-1}$.

The slow heating rate was chosen to ensure that gelatinisation occurred under pseudo-equilibrium conditions (Bogracheva *et al.* 2002). The thermograms were analysed using TA instruments NanoAnalyze software, establishing the onset, peak and end temperature and the overall enthalpy of each thermal transition based on the amount of wheat starch weighed in. Cells were weighed before and after the measurement to ensure constant weight of sample through the measurement. All scans were done at least in triplicate and all obtained results are presented as means. Overlay graphs were made using the TA Universal Analysis software package.

### 5.2.2.5  DSC on dough and biscuits

Dough and biscuit samples were analysed as described in section 5.2.2.4 with the following differences: Samples were weighed in on a 300 mg solids basis and deionised, degassed water added for a final water content of 70%. The thermograms were analysed using the TA instruments Universal Analysis software on a total starch basis as determined using the total starch assay (section 2.3.13). Control doughs and biscuits were measured on two biscuit batches in triplicate, all other samples were measured on one batch in triplicate.

### 5.2.2.6 Powder X-ray diffraction

Biscuit crumbs of the core (see above) of a particle size between 600 and 500 μm were washed three times with 80 % ethanol to remove the sugar: 850 mg biscuit sample was mixed with 50 mL 80% ethanol and centrifuged at 4000 rpm for 8 min and the supernatant discarded, which was repeated three times. The washed biscuit particles were moisture equilibrated in a hygrostat using saturated NaCl under vacuum for four days.

XRD measurements were performed as described in section 2.3.10, using a Rigaku Smartlab SE instrument with a Cu X-ray tube and Kα radiation, 40kV – 50mA, from 3 to 50 degrees, step 0.02 degrees at a speed of 4 degrees/min on ground biscuit core samples. The diffractograms were plotted using Microsoft Excel and signal intensity was analysed using Peakfit version 4.12. Due to the heterogeneity of the biscuit matrix, diffraction signals originated from several ingredients. Raw biscuit flour as well as raw soluble and insoluble inulin were measured separately to identify relevant peaks. The XRD data between 13° and 26° were selected for peak deconvolution of all seven recipes (3 batches per recipe), a linear baseline was fitted and peaks added with varying widths and heights to achieve an overall fit of $R^2>0.86$ (see Appendix figure A5.1 for an example). The relevant starch crystallinity peaks were identified from raw biscuit flour between 15° and 15.25° (starch peak 1), between 17° and 17.3° (starch peak 2) and between 22.8° and 23°

(starch peak 3). The area under the curve (AUC, Gauss Area) of these three starch peaks was compared across the seven recipes.

### 5.2.2.7  Moisture content determination

AACC International method 44-15.02 as described in section 2.3.11 was used to determine moisture content.

### 5.2.2.8  Total starch assay

Total starch was determined using method AOAC Official Method 996.11 as described in section 2.3.13.

### 5.2.2.9  Simulated mastication and particle size distribution analysis using standardised sieves

The core of the biscuit was cut out using a sterilin tube with a diameter of 2.3 cm in the centre of the biscuit and pressed through a garlic press (Lakeland, UK) to simulate mastication. After undergoing simulated mastication, biscuit crumbs were cooled in the fridge (4°C) for at least 30 minutes to avoid aggregation before they were analysed for their particle size distribution using sieves with apertures of 1.0 mm, 600 μm, 500 μm, 400 μm and 250 μm by hand shaking for 3 min and vortex vibration set to speed 5 for 1 min. Each fraction was weighed and presented as percentage of total weight. This was repeated once per batch for three biscuit batches per recipe.

### 5.2.2.10 Digestive enzyme activities

Digestive enzyme activities were determined as described in section 2.3.2.

## 5.2.2.11 Static gastric digestion followed by a duodenal starch digestion assay

Simulated gastric digestion of biscuits was based on Minekus *et al*. (Minekus *et al.* 2014) followed by a duodenal starch digestion assay according to Edwards *et al.* (Edwards *et al.* 2019), modified as follows. The core of the biscuits was cut out with a diameter of 2.3 cm in the centre of the biscuit. Both core and edge were ground separately to a particle size of <500>250 μm. Ground biscuits containing 120 mg starch based on total starch content (for a final starch content of 10 mg/mL in the duodenal phase) were weighed per biscuit recipe batch in duplicate (= 2x2 samples per biscuit recipe) and made up to 1.5 mL with water. A simulated oral phase (2 min, salivary α-amylase replaced by SSF) and gastric phase (pH 3, 2 hours, 37°C) either containing pepsin (at an activity of 2000 U/mL) or replacing pepsin with SGF. For the duodenal phase, the digesta was diluted 1:1 in total by addition of SIF, the pH adjusted to 7 with 1 M NaOH, as well as $CaCl_2$ and water added to made up 12 mL in total. The starch digestion assay was started by taking a 200 μL timepoint 0 sample and addition of 200 μL α-amylase solution (α-amylase from porcine pancreas) to reach an enzyme activity of 4 U/mL in the digestion mixture containing 10 mg/mL starch. The tubes were incubated at 37°C on a rotary mixer with samples of 100 μL taken at 2.5, 5, 10, 15, 30, 60, 90 and 120 minutes, which were mixed immediately with an equal amount of stop solution. 0.3 M $Na_2CO_3$, referred to as 'stop solution', inactivates

the α-amylase activity in the aliquots and is used to promptly stop the amylolysis at each timepoint (Edwards *et al.* 2019). The samples were centrifuged at 15,000xg for 5 minutes and the supernatant was used for reducing sugar analysis (see section 2.3.14).

Core biscuit comparisons across all seven biscuit recipes (4 biscuit cores per batch ground together which were digested in duplicate per batch, 3 batches per recipe) were done according to the same protocol with addition of pepsin but ground to a particle size of <600>500 µm.

### 5.2.2.12 Reducing sugar analysis (PAHBAH assay)

Samples taken from simulated digestions of biscuits (section 5.2.2.11) were analysed using PAHBAH assay as described in section 2.3.14). Concentrations of maltose in the sample were calculated from the maltose standard curve and corrected by subtracting timepoint 0 to account for endogenous reducing sugars. Percentage of digested starch was calculated based on the assumption that all amylolysis of starch yields maltose using Equation 5.1, with the limitation that this approach does not precisely account for minor products of starch amylolysis (glucose, α-limit dextrins and maltodextrins) which could lead to an underestimation of total starch amylolysis (Edwards *et al.* 2019).

$$\% \, digested \, starch = \frac{[\text{Maltose}]_t}{[\text{Maltose}]_{substrate}} \, x \, 100$$

*Equation 5.1 – Calculation of digested starch from measured Maltose concentration at timepoint t and assumed maltose concentration of substrate based on total starch weight.*

### 5.2.2.13 High-performance anion-exchange chromatography

Soluble and insoluble inulin were analysed as described in section 2.3.5 after three different treatments, each in triplicate per inulin. To analyse native inulin, 300 mg inulin was mixed with 3 mL 70% ethanol and heated treated in a 50°C water bath for 10 minutes, 5 mL deionised water added and heat treated in a 80°C water bath with regular vortex mixing for 15 minutes. To resemble dry heat treatment under baking conditions, 300 mg inulin was heat treated in the oven at 250°C for 11 minutes and underwent the same extraction procedure as native inulin using 70% ethanol at 50°C after which deionised water was added incubated at 80°C. To test hydrothermal stability in excess water, 100 mg inulin was weighed into DSC pans, 1 mL deionised, degassed water added and heat treated on a temperature ramp up to 150°C in a DSC instrument (see section 5.2.2.4). Samples were freeze-dried prior to analysis.

### 5.2.2.14 Data and statistical analysis

Statistical analyses were performed with R (version 4.0.2) (Team 2013) as described in section 2.4.2 with specifics as follows.

Starch digestion kinetics data were fitted to Equation 5.2 as described in section 2.4.1. Coefficients of core vs edge experiments

were compared pairwise with Tukey correction. Coefficients of biscuit recipes containing fibre were compared against the control containing no fibre using Dunnett's test comparing several treatments with a control.

For comparison of two variables, t-test was used and for three or more variables, ANOVA with a pairwise comparison and Tukey adjustment was used. Figures were made using Microsoft Excel or R.

$$C_t = C_\infty \left(1 - e^{-k*t}\right)$$

*Equation 5.2 – Starch digestion kinetics model: $C_t$ is the digested starch (%) at a given timepoint, $C_\infty$ extent digested starch at infinity (%), k is the starch digestion rate and t is the timepoint (Edwards et al. 2019).*

## 5.3 Results

### 5.3.1 Impact of DF on starch gelatinisation in a biscuit model system

Wheat starch alone in excess water had a gelatinisation enthalpy of 9.6 ± 0.1 J/g starch, and an onset, peak and end temperature of 45.9°C ± 0.8, 60.2°C ± 0.1 and 78.4°C ± 2.2, respectively. Starch gelatinisation enthalpies between 9.8 J/g (Warren *et al.* 2011) and slightly higher values of 12.5 J/g (Kumar and Khatkar 2017) and 13.6 J/g (Warren *et al.* 2016) are described in the literature for wheat starch. Wheat starch in the presence of sucrose and different levels of water were measured as no fibre controls. Figure 5.2 shows decreased starch gelatinisation, i.e. enthalpy per g starch, from high to low water conditions as expected for a 'limited water behaviour' (Donovan 1979, Donovan and Mapes 1980, Perry and Donald 2002). Between 7.5 and 22.5% water, starch gelatinisation is greatly reduced in the tested temperature range of up to 150°C. With decreasing water levels, higher temperatures are required for starch gelatinisation as seen in onset, peak and end temperatures in line with literature (Perry and Donald 2002, Ahmad and Williams 1999).

Addition of 2.5 and 5% oat BG to the biscuit model system had no effect on the gelatinisation enthalpy or temperatures compared to no fibre control ($p > 0.05$, pairwise comparison, Tukey correction). Figure 5.3A shows that the thermograms presented a normal starch gelatinisation peak which was reproducible. From 7.5% BG upwards, thermograms had broad and unusual peak shapes, which were not

reproducible and difficult to integrate which may be an indication of a 'limiting water behaviour'. Overall, there was a reduced gelatinisation enthalpy ($p<0.0001$) in presence of BG and a shift of the gelatinisation onset towards higher temperatures ($p=0.0137$), but no difference in peak ($p=0.491$) nor end temperature ($p=0.122$) compared to no fibre control (crystalline sucrose).

Addition of cellulose led overall to a higher onset ($p=0.049$) and lower peak temperature ($p=0.0209$) with no effect on end temperature ($p=0.947$) compared to no fibre control (Figure 5.2). From 30% cellulose (47.5% water) upwards, peak shapes varied and became less reproducible (Figure 5.3D), which could be due to 'limiting water behaviour'. There seemed to be a trend for decreased gelatinisation enthalpy between 7.5% cellulose (70% water) and 20% cellulose (57.5% water) however this was not statistically significant ($p>0.05$, pairwise comparison, Tukey correction).
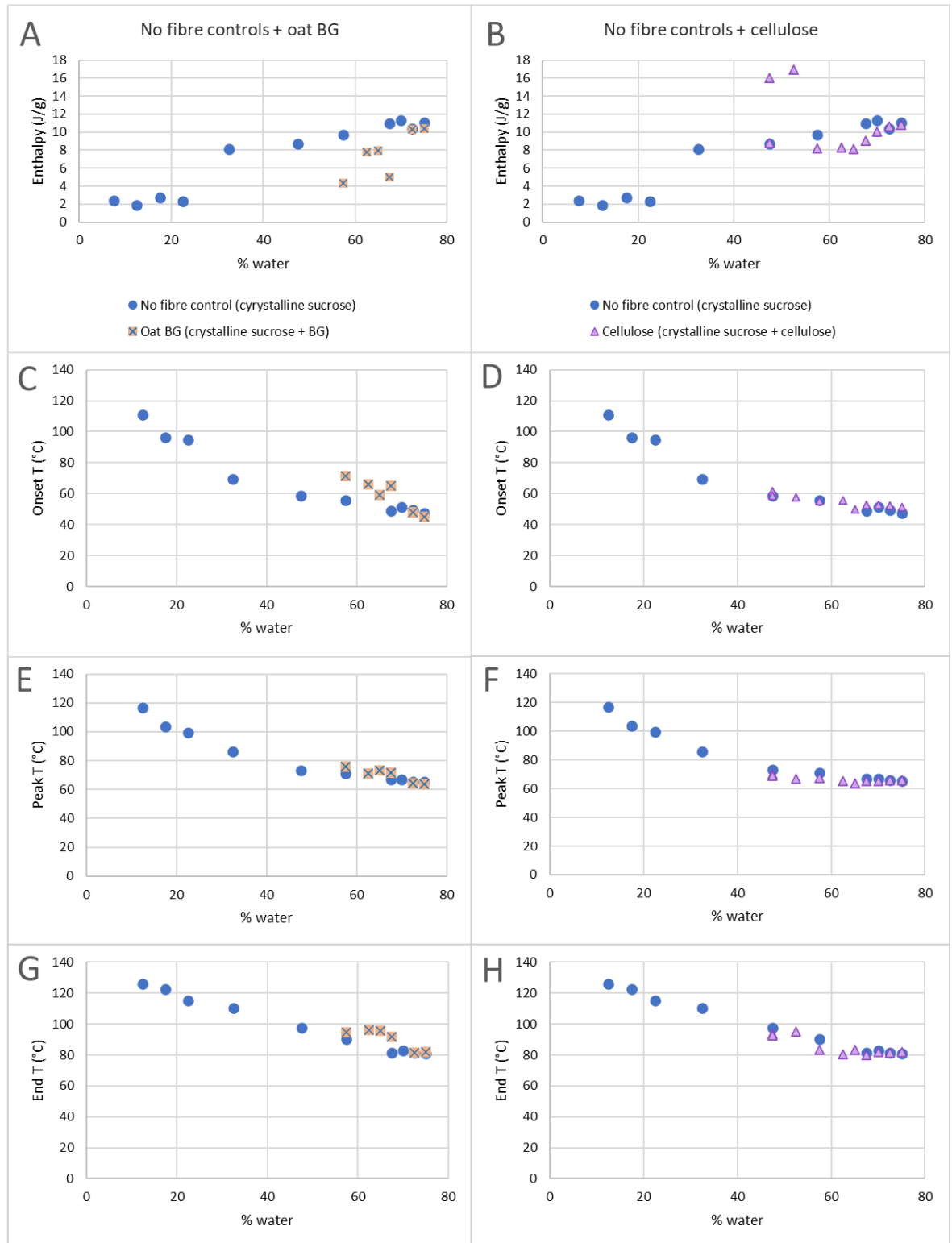
*Figure 5.2 – Starch gelatinisation (A+B) enthalpy (J/g starch), (C+D) onset, (E+F) peak and (G+H) end temperature (°C) of no fibre control (biscuit model system of wheat starch, sucrose and water) without pre-solubilisation of sucrose (crystalline sucrose) or biscuit model system in presence of (A, C, E, G) oat BG or (B, D, F, H) cellulose as a function of percentage of water (%); points, squares and triangles represent the mean of 3 technical replicates.*
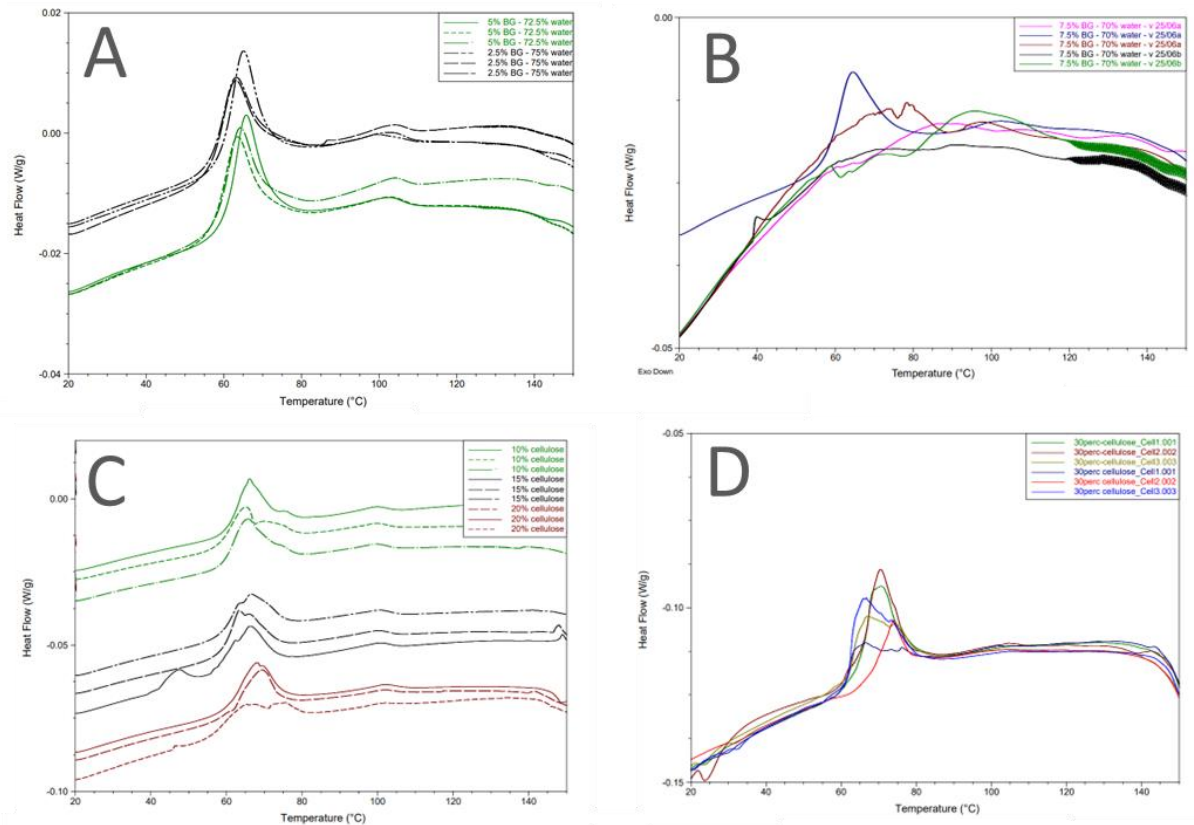
*Figure 5.3 – Examples of thermograms of biscuit model systems containing (A) 2.5% BG (75% water) in black and 5% BG (72.5% water) in green; (B) 7.5% BG (70% water) in different colours representing individual replicates; (C) 10% cellulose (67.5% water) in green, 15% cellulose (62.5% water) in black and 20% cellulose (57.5% water) in brown; (D) 30% cellulose (47.5% water) in different colours representing individual replicates.*

Insoluble inulin added to the biscuit model system resulted in an additional peak which was attributed to inulin solubilisation with an onset temperature overlapping with the starch gelatinisation peak, which resulted in a double peak in the thermogram (Figure 5.4A). A similar interference is suspected with soluble inulin, although not obvious on the thermogram (Figure 5.4B), as integrating the peak resulted in an enthalpy of 17.3 ± 1.6 J/g starch, although wheat starch in excess water only had an endothermic peak area of 9.6 ± 0.1 J/g starch. Both inulin's were tested pre-solubilised in the

respective amount of water under heat in a boiling water bath before addition to sucrose and starch. As shown in blue in Figure 5.4A, this only resulted in a better distinction of the starch and insoluble inulin peak but not a separation or removal of the insoluble inulin peak. The same solubilisation procedure applied to soluble inulin resulted in an enthalpy of 10.6 ± 1.1 J/g starch, comparable to no fibre control ($p=0.3244$) (Figure 5.4C). Also, the gelatinisation start and end temperature were not statistically significantly different from the no fibre control, although by 5.3°C ($p=0.1718$) and 2.2°C ($p=0.3424$) higher, respectively. However, the peak temperature was elevated by 6.9°C ($p<0.0001$) compared to the no fibre control at the same water level. The solubilisation procedure was changed to solubilise sucrose and either soluble or insoluble inulin in the respective amount of water using a heat treatment up to 150°C in a DSC pan and addition of starch after cooling down. This led in both, insoluble inulin (Figure 5.4B) and soluble inulin (Figure 5.4D), to reproducible starch gelatinisation peaks without interference of any other signals.
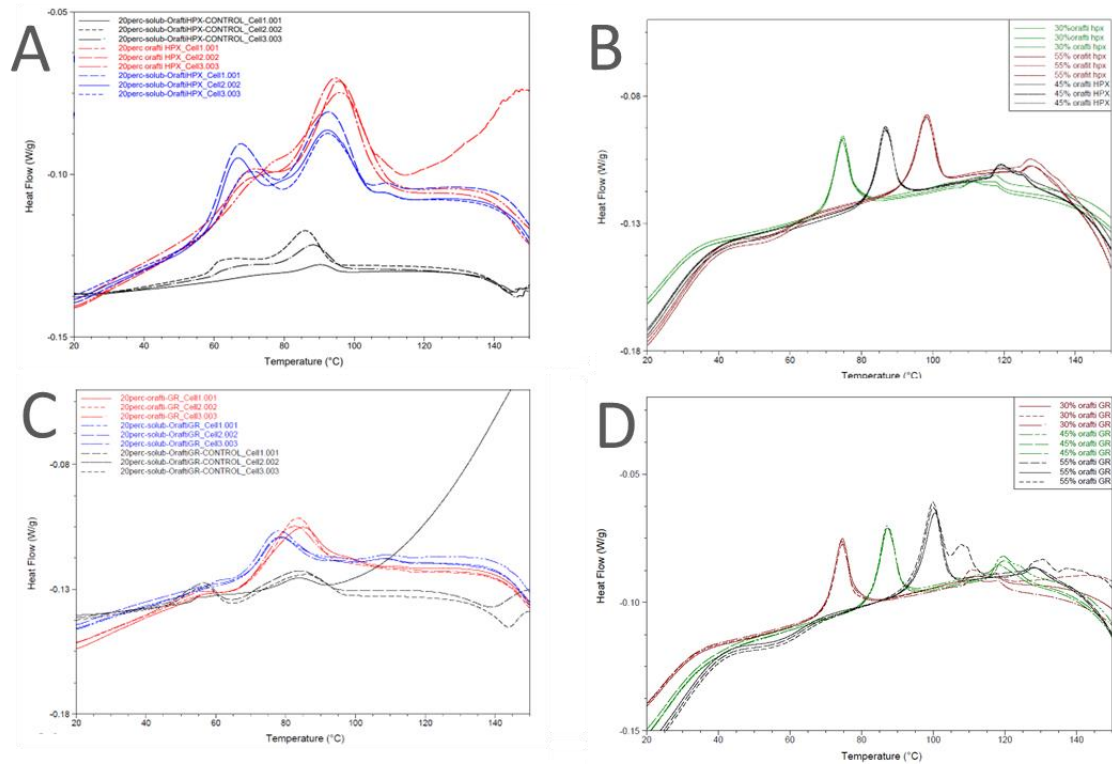
*Figure 5.4 – Examples of thermograms of (A) 20% insoluble inulin in a biscuit model system without pre-solubilisation in red, insoluble inulin solubilised in the respective amount of water in a boiling water bath before addition to sucrose and starch in blue or insoluble inulin in water in absence of starch and sucrose in black; (B) solubilised sucrose and insoluble inulin in a biscuit model system with different insoluble inulin levels: 30% in green, 45% in black and 55% in brown; (C) 20% soluble inulin in a biscuit model system without pre-solubilisation in red, soluble inulin solubilised in the respective amount of water in a boiling water bath before addition to sucrose and starch in blue or soluble inulin in water in absence of starch and sucrose in black; (D) solubilised sucrose and soluble inulin in a biscuit model system with different soluble inulin levels: 30% in brown, 45% in green and 55% in black; all in triplicate.*
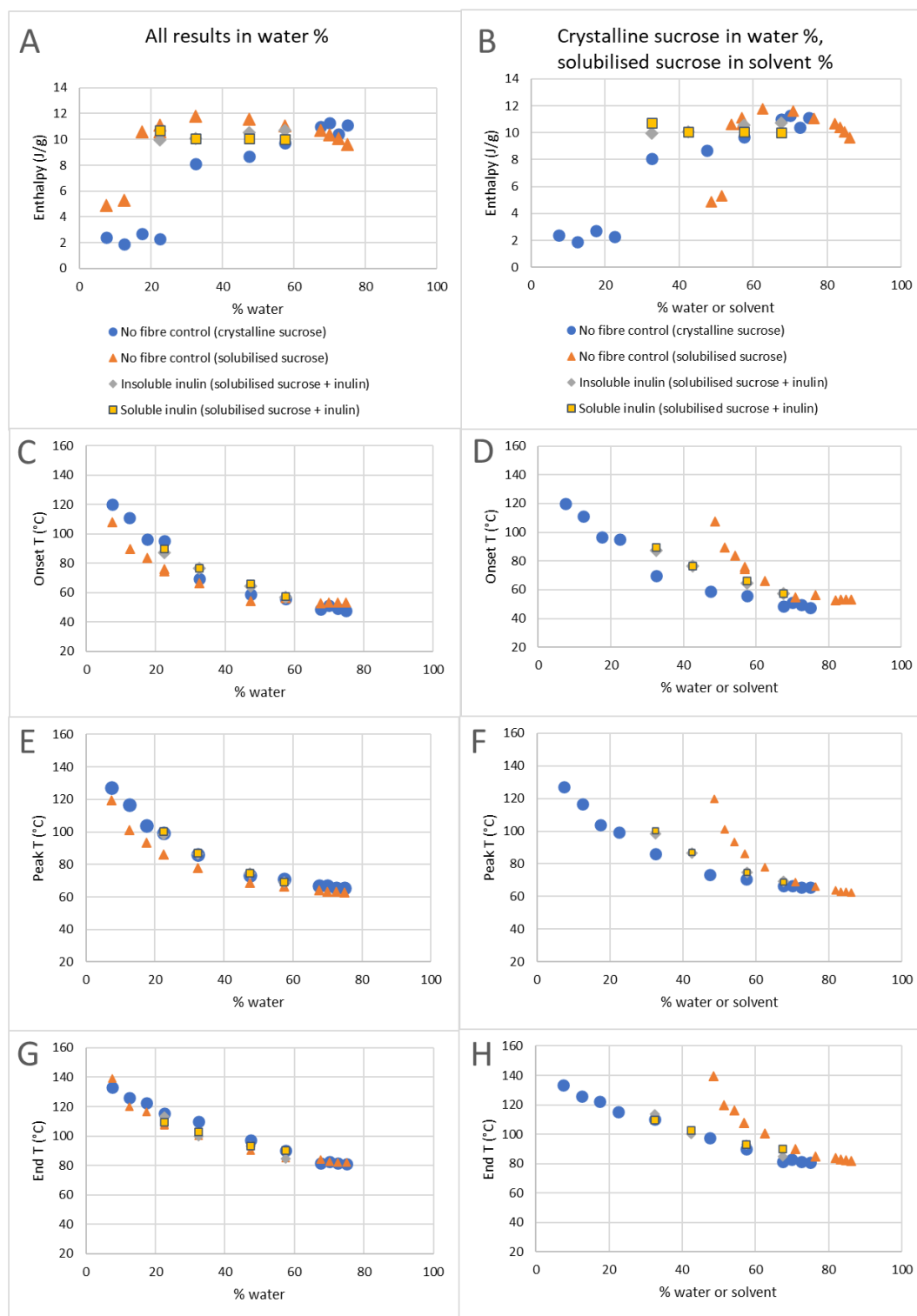
*Figure 5.5 – Starch gelatinisation (A+B) enthalpy (J/g starch), (C+D) onset, (E+F) peak and (G+H) end temperature (°C) of biscuit model system in the absence of fibre (no fibre control) without pre-solubilisation of sucrose (crystalline sucrose) or solubilisation of sucrose in water before addition of starch (solubilised sucrose) or in presence of soluble inulin or insoluble inulin, same data plotted either (A,C,E,G) all as a function of percentage of water (%) or (B,D,F,H) no fibre control containing crystalline sucrose as a function of % water and no fibre control containing solubilised sucrose as well as samples containing inulins as a function of % solvent [(mass of water + sucrose)/mass total]; points, triangles, diamonds and squares represent the mean of 3 technical replicates.*

The series of no fibre controls was repeated at the same water levels to investigate starch gelatinisation behaviour in presence of solubilised sucrose. As shown by Perry & Donald, solubilised sucrose acts as a plasticiser and together with water as one plasticising solvent (Perry and Donald 2002). Figure 5.5A shows that between 75.0 and 67.5 % water, the enthalpy change associated with starch gelatinisation increased from 9.6 to 10.7 J/g but was not significantly different ($p>0.05$, pairwise comparison, Tukey correction). Enthalpy significantly increased further with reducing water content [to 11.05 J/g starch at 57.5% water ($p=0.0365$), 11.59 J/g at 47.5% water ($p=0.0015$), 11.8 J/g at 32.5% water ($p=0.0004$, pairwise comparison, Tukey correction)]. Starch gelatinisation enthalpy declined at 22.5% water to 10.8 J/g, which was still higher than 75% water ($p=0.0396$) and was with 10.6 J/g at 17.5% water comparable to the highest water level ($p=0.3340$, pairwise comparison, Tukey correction). At low water levels of 12.5 and 7.5 %, starch gelatinisation was very reduced to 5.3 and 4.9 J/g, respectively ($p\leq0.05$, pairwise comparison, Tukey correction). Starch gelatinisation enthalpy was defined by available percentage of solvent rather than water (Figure 5.5A) and different from no fibre controls with crystalline sucrose ($p=0.0012$, ANOVA), whereas gelatinisation temperatures increased as a function of decreasing water levels (Figure 5.5B-D) and were not different from the no fibre controls with crystalline sucrose ($p>0.05$, ANOVA). The same applied for solubilised inulins together with sucrose and both inulins

had a comparable effect on gelatinisation. However, there was a big difference between sucrose and inulins in the onset of 'limiting water behaviour'. The full extent of gelatinisation was still observed at very high inulin levels of 30 and 45% (the equivalent of 32.5 and 22.5% sucrose/water solvent, respectively), whereas the no fibre control (solubilised sucrose) showed a very reduced gelatinisation enthalpy already from 51.4% sucrose/water solvent. Therefore, both inulins seem to act as more effective plasticisers than sucrose. Under this assumption, inulin may act together with sucrose and water as one plasticising solvent and its mass would be added, which makes a solvent share of 87.5% for all tested inulin samples. This would explain why the starch gelatinisation enthalpies did not differ from each other ($p > 0.05$, pairwise comparison, Tukey correction), irrespective of the level of water added and were comparable to the no fibre control (solubilised sucrose) enthalpies with 86 and 85% sucrose/water solvent ($p > 0.05$, pairwise comparison, Tukey correction).

Soluble and insoluble inulin were selected for further investigation of the presence of DFs on starch gelatinisation in biscuits. Cellulose and BG however were not investigated further due to inconsistent results in the model system.

### 5.3.2 Incorporation of two different inulin fibres into biscuits

Figure 5.6 shows images of the baked biscuits. No fibre control biscuits had a wide, round spread during baking, which led to a

higher biscuit diameter compared to all other recipes (p<0.0001, pairwise comparison, Tukey correction) as shown in Figure 5.7. Biscuits with soluble inulin spread oval in the direction of rolling. Incorporating 19% soluble inulin at stage 3 of the recipe led to a dome-shaped cross-section whereas 20% soluble inulin at stage 2 resulted in a more even spread. The biscuits containing 19% or 20% insoluble inulin had the least spread (p<0.0001, pairwise comparison, Tukey correction) with a final diameter of 6.47 cm and 6.33 cm, respectively, hence also the highest stack heights (p≤0.05, pairwise comparison, Tukey correction) (Figure 5.7). Only 10% soluble inulin biscuits had a lower stack height than control (p<0.001, pairwise comparison, Tukey correction) and only 20 % soluble inulin had the same as control (p=0.7919) (Figure 5.7).
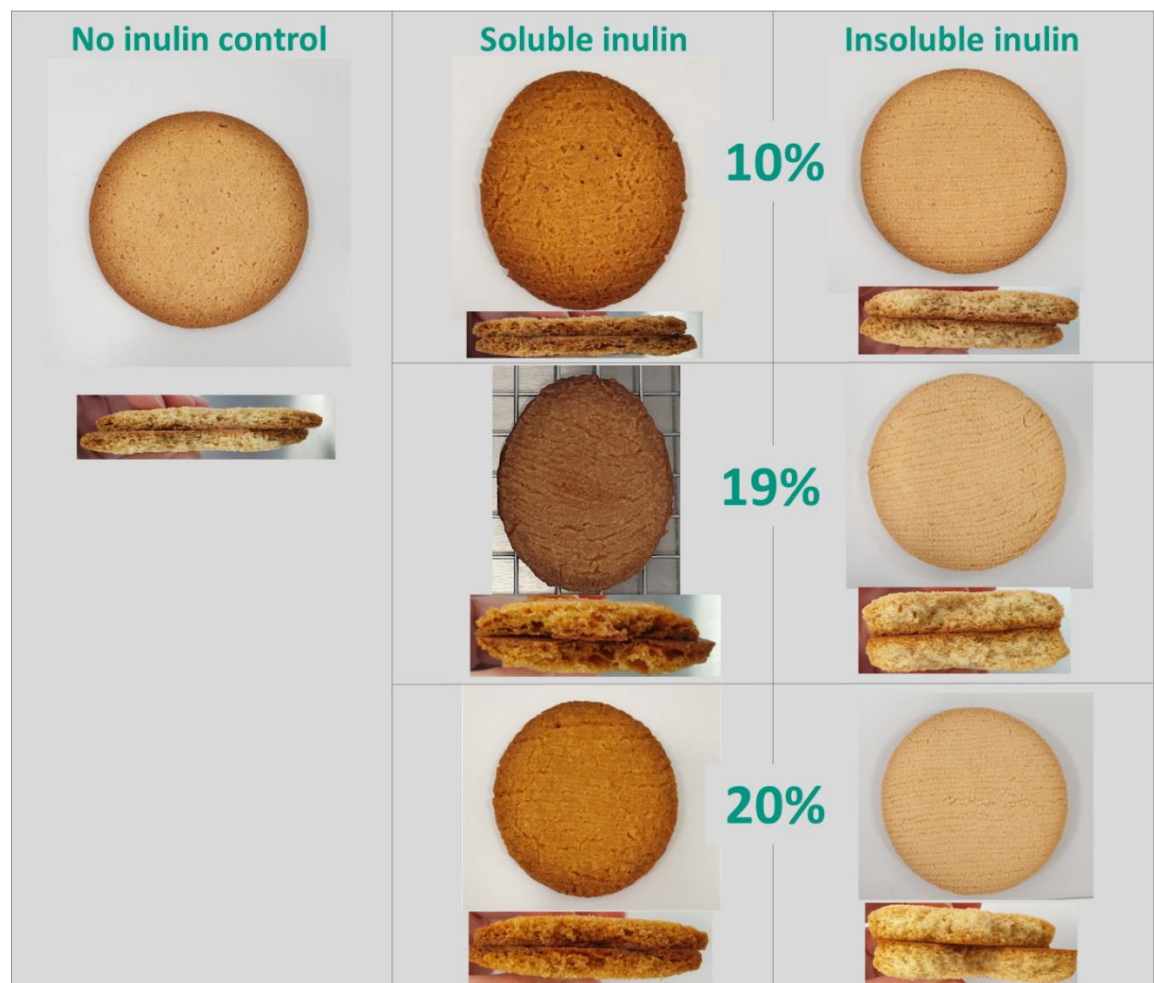
*Figure 5.6 - Baking results comparison of seven biscuit recipes containing either no inulin (control), 10%, 19% or 20% soluble or insoluble inulin. Photos taken in overhead angle of an intact biscuit and a cross-section of both sides of a biscuit stacked after broken in two halves.*
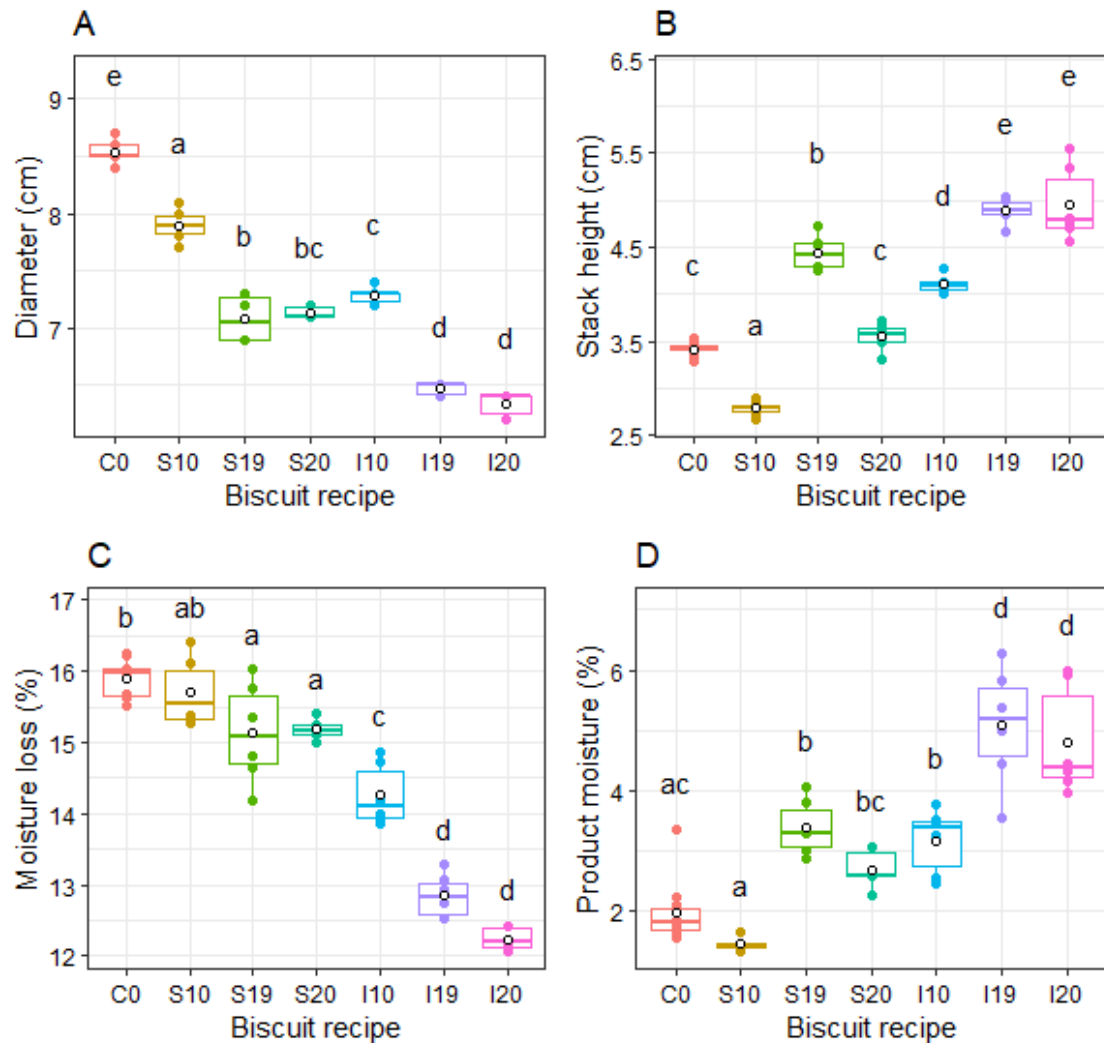
*Figure 5.7 – (A) Spread as biscuit diameter (cm) of one biscuit as an average across four biscuits, (B) stack height (cm) of four biscuits, (C) moisture loss (%) per biscuit averaged over four biscuits per baking tray, (D) product moisture (%) of one biscuit per tray one week after baking for seven different recipes containing no inulin (C0) or 10 % (S10), 19 % (S19) or 20 % (S20) soluble inulin, or 10 % (I10), 19% (I19) or 20% insoluble inulin (I20). Boxplots are two trays of four biscuits per dough batch, n = 3 batches for inulin biscuits, 5 batches for control, coloured dots represent respective individual results, mean results are black circles, different letters indicate significant differences on a p ≤ 0.05 level basis, pairwise comparison, Tukey correction.*

The differences in spread may be a cause for different moisture losses during baking. 10% soluble inulin biscuits had the same moisture loss as control (15.7 vs 15.9%, p=0.9470, pairwise comparison, Tukey correction). All other biscuit recipes had a

statistically significantly lower moisture loss than control (p≤0.05, pairwise comparison, Tukey correction). 19% as well as 20% insoluble inulin biscuits had the lowest moisture loss with 12.8% and 12.2%, respectively (p<0.0001, pairwise comparison, Tukey correction). These two biscuit recipes also had the highest product moisture one week after baking (p≤0.05, pairwise comparison, Tukey correction). Product moisture correlated with moisture loss during baking (Figure 5.8). Biscuit spread measured as diameter of the baked biscuit correlated with stack height (Figure 5.9) as well as moisture loss (Figure 5.10).
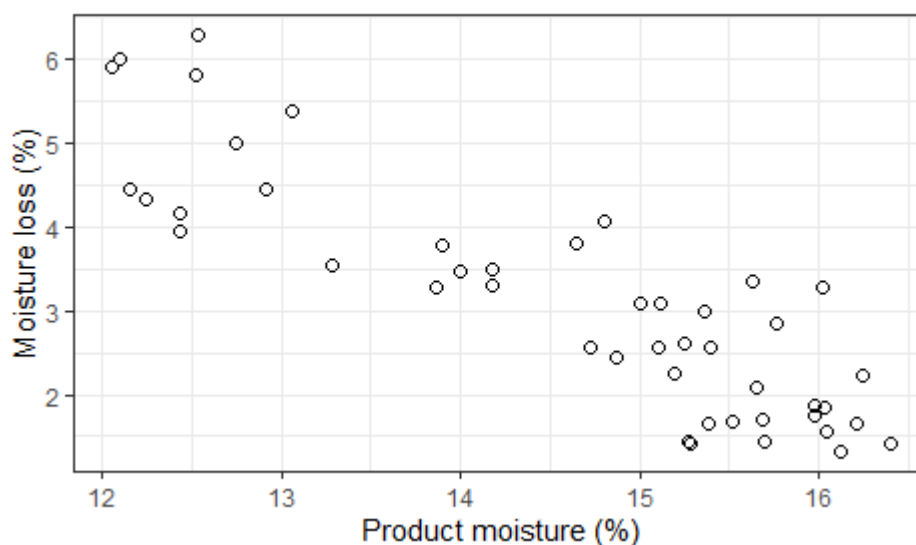


*Figure 5.8 – Relationship between moisture loss during baking (%) and product moisture (%) one week after baking*
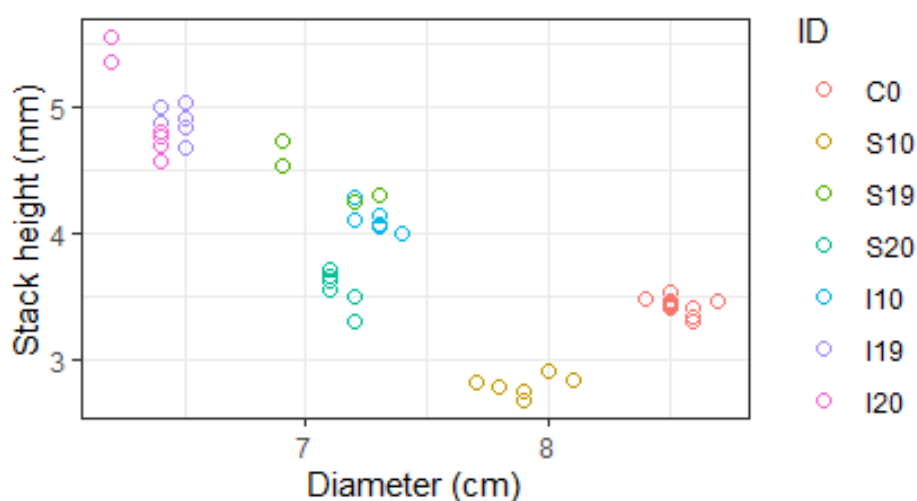
*Figure 5.9 – Relationship between stack height of 4 biscuits (mm) and spread as biscuit diameter (cm)*
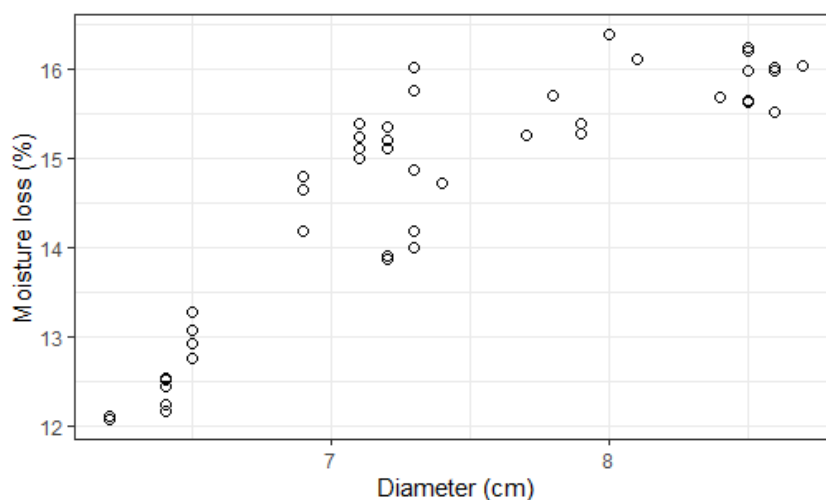


*Figure 5.10 – Relationship between moisture loss during baking (%) and spread as biscuit diameter (cm)*

Figure 5.11 shows the dough weight for 4 biscuits which was the same as control for all recipes except for insoluble inulin biscuits containing 19% (p=0.0001, pairwise comparison, Tukey correction) and 20% inulin (p=0.0320, pairwise comparison, Tukey correction)

which had a statistically significantly lower dough weight than the control. After baking, only 19% insoluble inulin biscuits had a 1.5 g lower biscuit weight than the control (p=0.0135, pairwise comparison, Tukey) (Figure 5.11). Compared to control, 19% (p=0.0004, pairwise comparison, Tukey correction) and 20% insoluble inulin biscuits (p=0.0132, pairwise comparison, Tukey correction) had a higher water activity. Figure 5.11 shows that 19% insoluble inulin biscuit dough which had a higher dough moisture according to the recipe had also a significantly higher water activity than 19% soluble inulin (p=0.0010, pairwise comparison, Tukey correction) and 20% soluble inulin dough (p=0.0317, pairwise comparison, Tukey correction). The water activity of the baked biscuits was statistically significantly higher in presence of both inulin types and all three levels of inulin compared to control for all recipes (p≤0.05) except 10% soluble inulin (p=0.9231) (Figure 5.11).
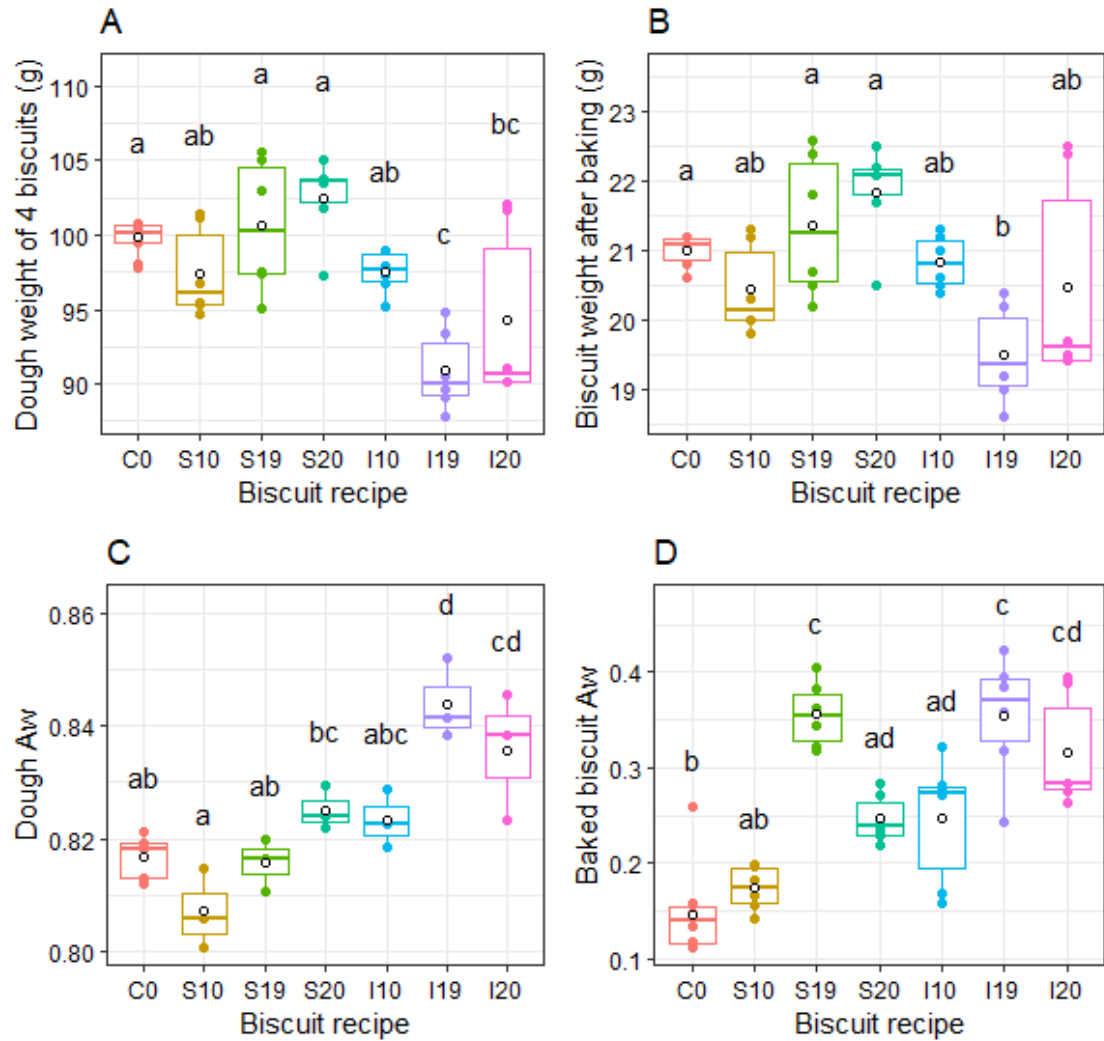
*Figure 5.11 – (A) Dough weight (g) of four biscuits before baking, (B) biscuit weight (g) after baking per biscuit, (C) water activity (Aw) of raw dough, (D) water activity (Aw) of one baked biscuit per tray one week after baking for seven different recipes containing no inulin (C0) or 10 % (S10), 19 % (S19) or 20 % (S20) soluble inulin, or 10 % (I10), 19% (I19) or 20% insoluble inulin (I20). Boxplots are two trays of four biscuits per dough batch, n = 3 batches for inulin biscuits, 5 batches for control, coloured dots represent respective individual results, mean results are black circles, different letters indicate significant differences on a p ≤ 0.05 level basis, pairwise comparison, Tukey correction.*

### 5.3.3 Clear difference in starch digestion kinetics between core and edge of biscuits

Control biscuits were used to test whether the edge and core of the biscuit digest differently and whether a simulated gastric digestion using pepsin has an effect on starch digestion. Due to the differences

in biscuit spread (diameter and stack height) between the different recipes, it could be more consistent to digest only the core of the biscuit rather than an average sample over the entire biscuit. The starch content was 38.9% (dw) for the core and 39.1% (dw) for the edge which was not statistically significantly different (p=0.7257, Student's t-test, 2-tailed, paired), but the core had a higher moisture content of 2.95 ± 0.53% compared to the edge with 2.85 ± 0.55% (p=0.0220, Student's t-test, 2-tailed, paired). Figure 5.12 shows that the edge of the biscuit had a lower starch digestion extent than the core over the course of the 2 hour duodenal digestion (see Table 5.3). Comparing the digestion kinetic parameters within the same sampling origin of core or edge with regards to necessity of a gastric phase did not show a statistically significant difference. The digestion rate was only lower when the edge of the biscuit also underwent gastric protein digestion compared to the core in absence of pepsin (p=0.0211, pairwise comparison, Tukey correction). Therefore, to reach maximum digestibility and to maintain consistency between samples, all other biscuit recipes were compared using the core of the biscuits with addition of pepsin in a gastric phase.
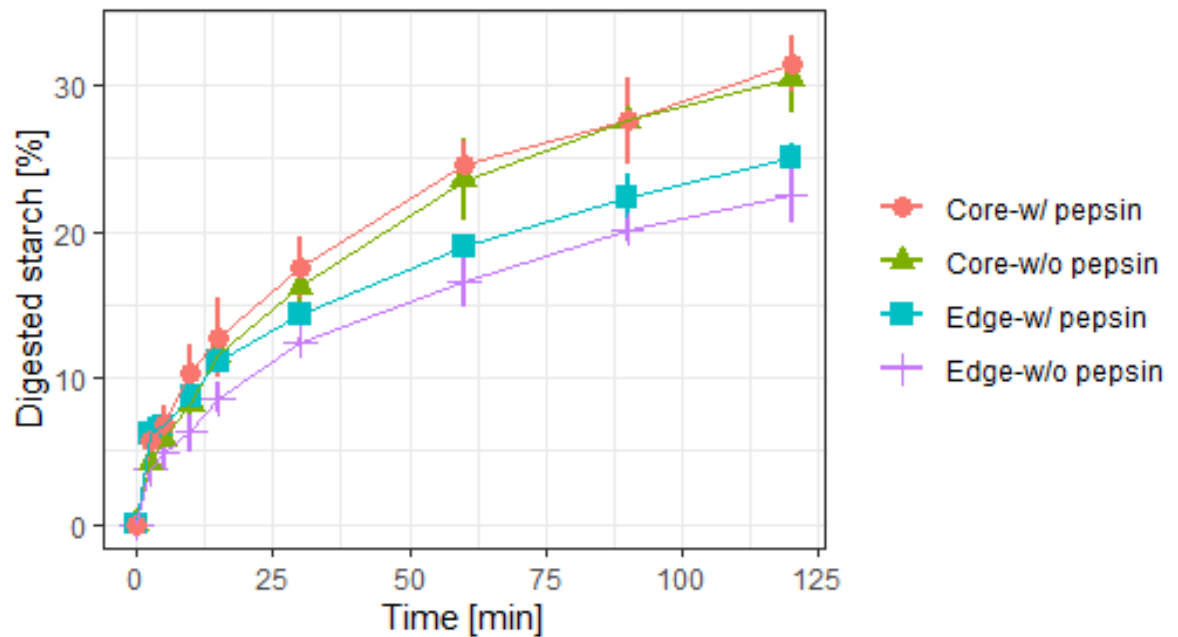
*Figure 5.12 – Biscuit core or edge digested starch [%] over 2 hours duodenal phase with pancreatic α-amylase after a 2 hour gastric phase with pepsin (w/ pepsin) or pepsin replaced by simulated gastric fluid (w/o pepsin). Samples were taken before adding α-amylase and after 2.5, 5, 10,15, 30, 60, 90 and 120 min and analysed for reducing sugars. n = 3 replicates per 2 biscuit batches.*

*Table 5.3 – Starch digestion kinetics rate (k) and extent ($C_\infty$ ) calculated from fitting Equation 5.2 to digestion results of control biscuit cores or edges with (w/) or without (w/o) gastric protein digestion using pepsin, mean [lower and upper 95% confidence interval] of n = 4 (2 control biscuit batches, each in duplicate), different letters indicate significant differences on a p≤0.05 level basis, pairwise comparison, Tukey correction.*

| Name | k [95% CI] | $C_\infty$ [95% CI] |
|---|---|---|
| Edge w/o pepsin | 3.5 [3.2, 3.7][a] | 21.7 [19.8, 23.5][a] |
| Core w/o pepsin | 3.6 [3.4, 3.7][ab] | 30.1 [28.2, 32.1][b] |
| Edge w/ pepsin | 3.2 [3.0, 3.4][ac] | 22.9 [21.5, 24.4][a] |
| Core w/ pepsin | 3.3 [3.2, 3.5][a] | 29.7 [28.0, 31.3][b] |

### 5.3.4  Lower starch digestibility with soluble inulin

As expected, due to the reduction of flour content to incorporate the different levels of inulin, the biscuit cores of inulin biscuits had a lower starch content depending on the level of inulin incorporated

(p≤0.05), except 10% soluble inulin which was not statistically significantly different from control (p=0.1978, pairwise comparison, Tukey correction). Therefore, the starting weight of the biscuit cores was normalised for their starch content at the start of the digestion assay.
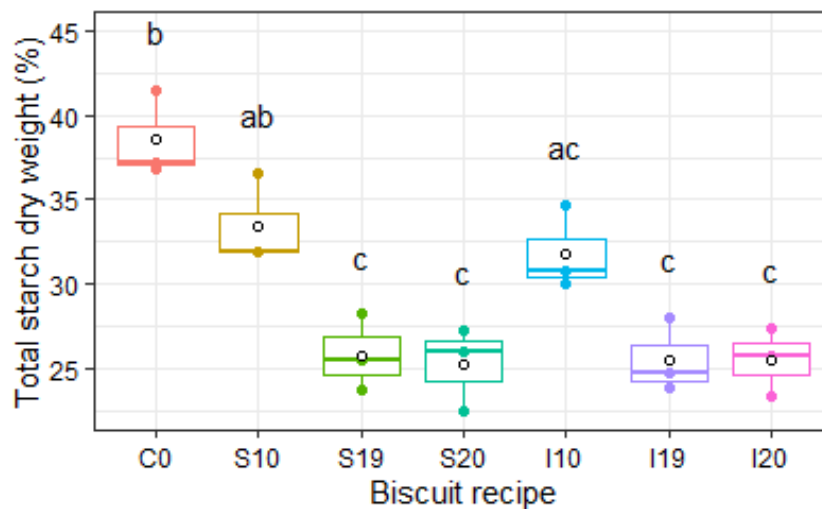


*Figure 5.13 – Total starch content (%) as per dry weight per biscuit recipe, boxplots of individual measurements, black circles represent the mean, different letters indicate significant differences on a p ≤ 0.05 level basis, pairwise comparison, Tukey correction (n = 3 batches each).*

Particle size distribution data following simulated mastication showed that the type of inulin used had a big effect on breakup (Figure 5.14). Biscuits containing insoluble inulin disintegrated to smaller particles similar to the control. The soluble inulin led to cohesion and hardness in the biscuits, so they were more difficult to break up in the simulated mastication, leading to bigger crumb particles. As particle size could lead to different starch digestion kinetics, particles between <600>500 μm were selected for the starch digestion assay.
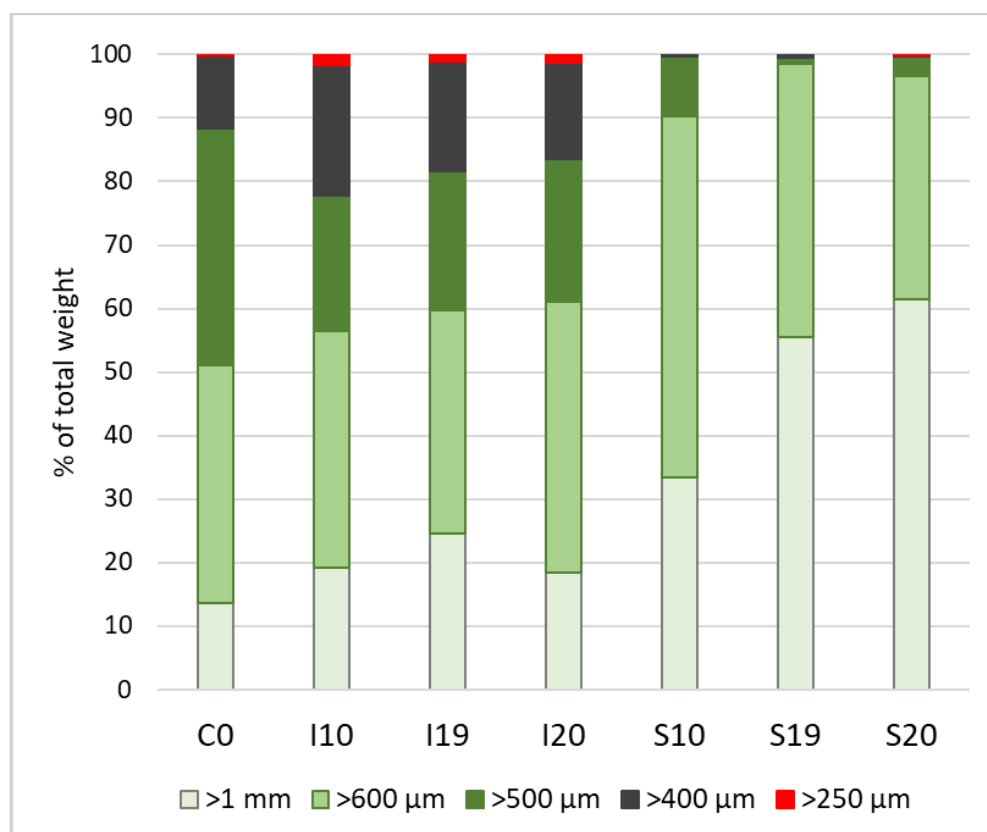
*Figure 5.14 – Particle size distribution after simulated mastication of biscuit cores (n=3).*

Table 5.4 and Figure 5.15 show the starch digestion results of the seven biscuit recipes (model fits are shown in Appendix figure A5.2). All inulin biscuits had the same starch digestion rate as the control (p>0.05, Dunnett's test). However, biscuits containing any level of soluble inulin had a lower starch digestion extent than the control (all <0.0001, Dunnett's test), whereas 10% and 20% insoluble inulin biscuits were not different from control. 19% insoluble inulin biscuits, which had a slightly higher dough moisture content than the control dough, had a statistically significantly higher digestion extent than control (p=0.0009, Dunnett's test).
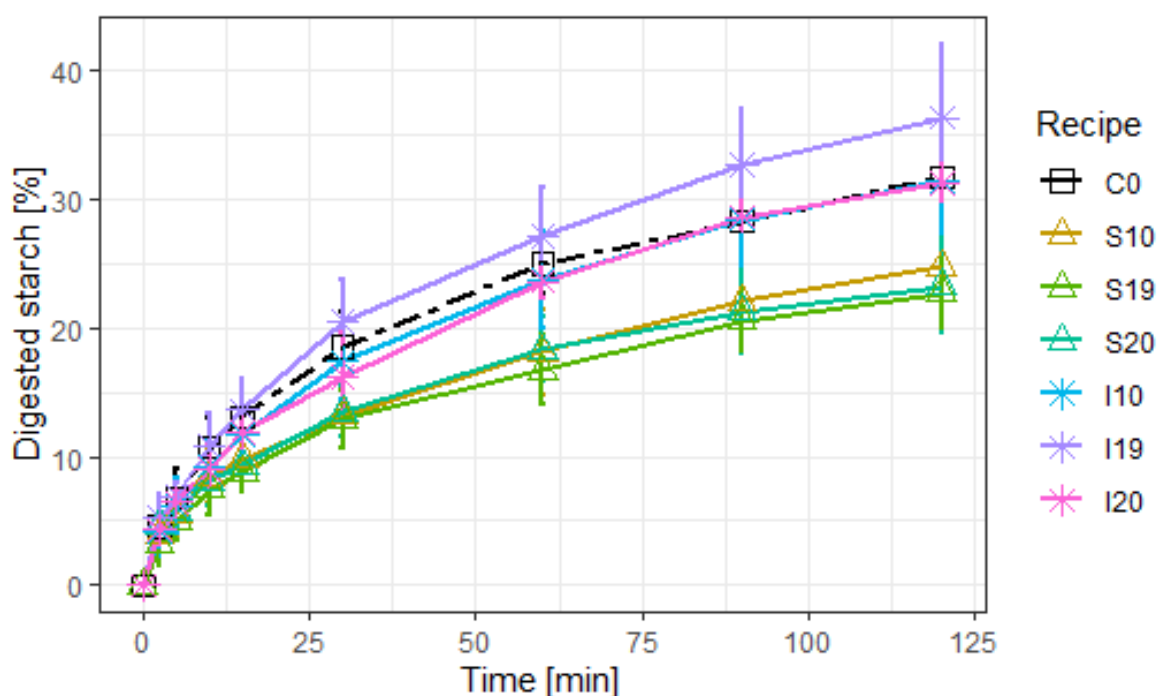
*Figure 5.15 – Digested starch [%] over 2 hours duodenal starch digestion (4 U alpha-amylase activity/mL, 10 mg starch/mL)  after 2 hour gastric digestion with samples taken at timepoint 0, 2.5 and 120 minutes, [7 different recipes, n = 6 (3 batches per recipe, each in duplicate)]*

*Table 5.4 – Starch digestion kinetics rate (k) and extent ($C_\infty$ ) calculated from fitting Equation 5.2 to digestion results of biscuit cores with seven different recipes, mean [lower and upper 95% confidence interval] of n = 6 (3 batches per recipe, each in duplicate), p-values indicate statistical difference comparted to control, Dunnett's test.*

| Name | k [95% CI] | p-value | $C_\infty$ [95% CI] | p-value |
|------|------------|---------|---------------------|---------|
| Control-0 | 3.3 [3.1, 3.5] | n.a. | 30.0 [28.3, 31.8] | n.a. |
| Soluble-10 | 3.4 [3.2, 3.6] | 0.9283 | 23.4 [21.5, 25.2] | <0.0001 |
| Soluble-19 | 3.4 [3.2, 3.6] | 0.9419 | 21.7 [19.8, 23.5] | <0.0001 |
| Soluble-20 | 3.3 [3.1, 3.5] | 0.9972 | 22.1 [20.4, 23.8] | <0.0001 |
| Insoluble-10 | 3.5 [3.3, 3.7] | 0.4603 | 30.7 [28.6, 32.7] | 0.9703 |
| Insoluble-19 | 3.5 [3.3, 3.6] | 0.5055 | 35.2 [33.2, 37.2] | 0.0009 |
| Insoluble-20 | 3.6 [3.4, 3.7] | 0.2321 | 31.0 [28.8, 33.1] | 0.9270 |

## 5.3.5 Extent of starch gelatinisation and remaining starch crystallinity as underlying mechanism

To test the hypothesis that the lower starch digestion in biscuits containing soluble inulin was due to a lower extent of starch gelatinisation, starch gelatinisation parameters of biscuit dough samples were compared with baked biscuit samples using DSC (Figure 5.16). The wheat starch peak was identified between 62 and 83°C based on results from the biscuit model system (see 5.3.1). Comparing the starch gelatinisation parameters of the raw control dough with the control biscuits showed no difference in the area under the curve with 10.8 and 11.1 J/g starch (p=0.1459), respectively, as well as in the end temperature with 82.2 and 82.0°C (p=0.8068), respectively. However, there was a difference in the start temperature with 65.1 and 64.2°C (p=0.0019) as well as in the peak temperature with 70.3 and 69.6°C (p=0.0008) for control dough and biscuit samples, respectively. Determination of the starch gelatinisation parameters in dough containing insoluble inulin resulted in a peak from insoluble inulin interfering with the starch gelatinisation peak from about 80°C (Figure 5.16B). A pilot test of comparing the dough containing 10 or 20% soluble inulin with the control dough showed a statistically significantly lower enthalpy with 9.8 J/g starch for 10% inulin (p=0.0082, pairwise comparison, Tukey correction) as well with 9.7 J/g starch for 20% inulin (p=0.0056, pairwise comparison, Tukey correction). The start temperature was 1.2°C higher for 20% soluble inulin dough

compared to control (p=0.0067, pairwise comparison, Tukey correction) as well as the end temperature by 2.9°C (p=0.0037, pairwise comparison, Tukey correction). Peak temperatures increased with increasing levels of soluble inulin incorporation with 70.3°C for control, 71.4°C for 10% and 72.2°C for 20% soluble inulin (p≤0.05, pairwise comparison, Tukey correction).
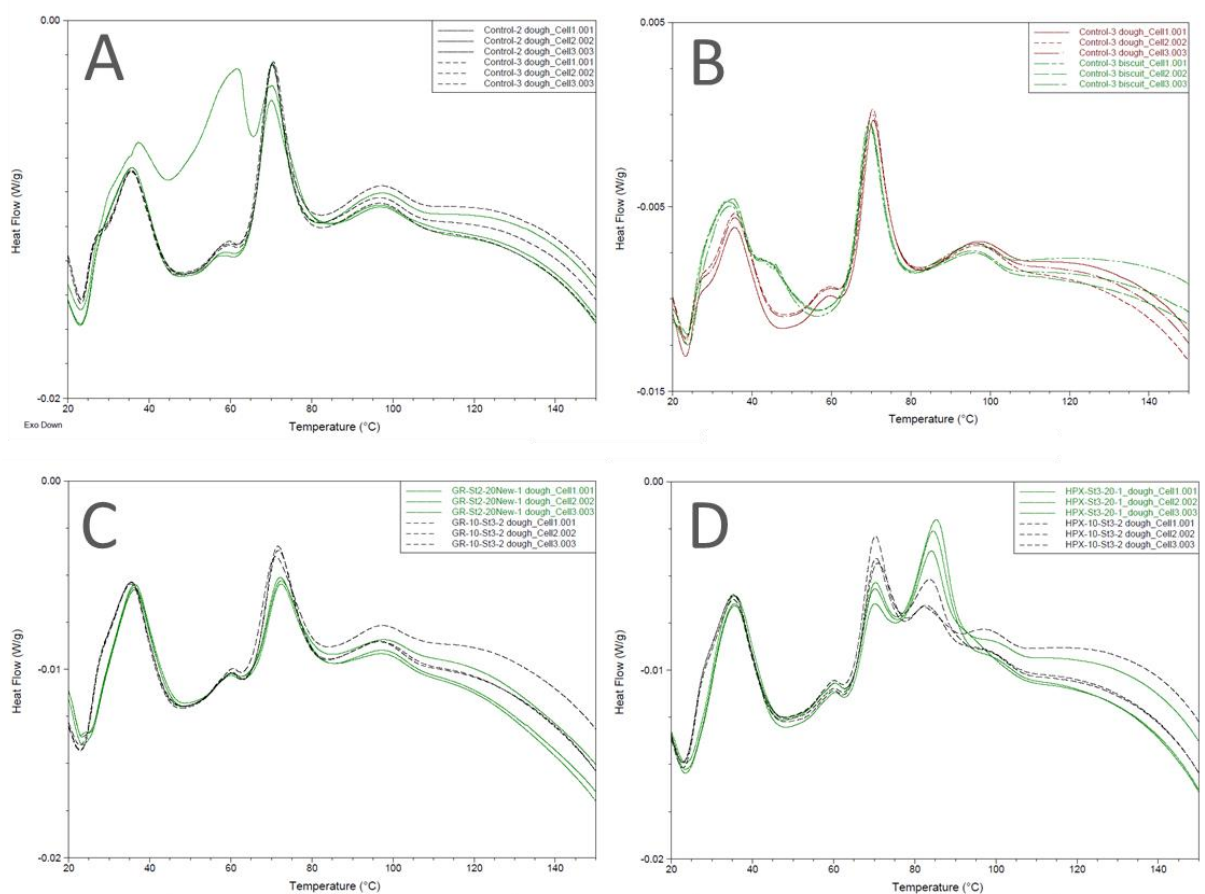


*Figure 5.16 – DSC thermogram examples of biscuit samples based on 300 mg total solids (A) 2 batches control dough each in triplicate; (B) control dough in brown vs control biscuit after baking in green of the same batch, each in triplicate; (C) 20% (green solid line) or 10% (black dashed line) soluble inulin biscuit dough, each in triplicate; (D) 19% (green solid line) or 10% (black dashed line) insoluble inulin biscuit dough, each in triplicate.*
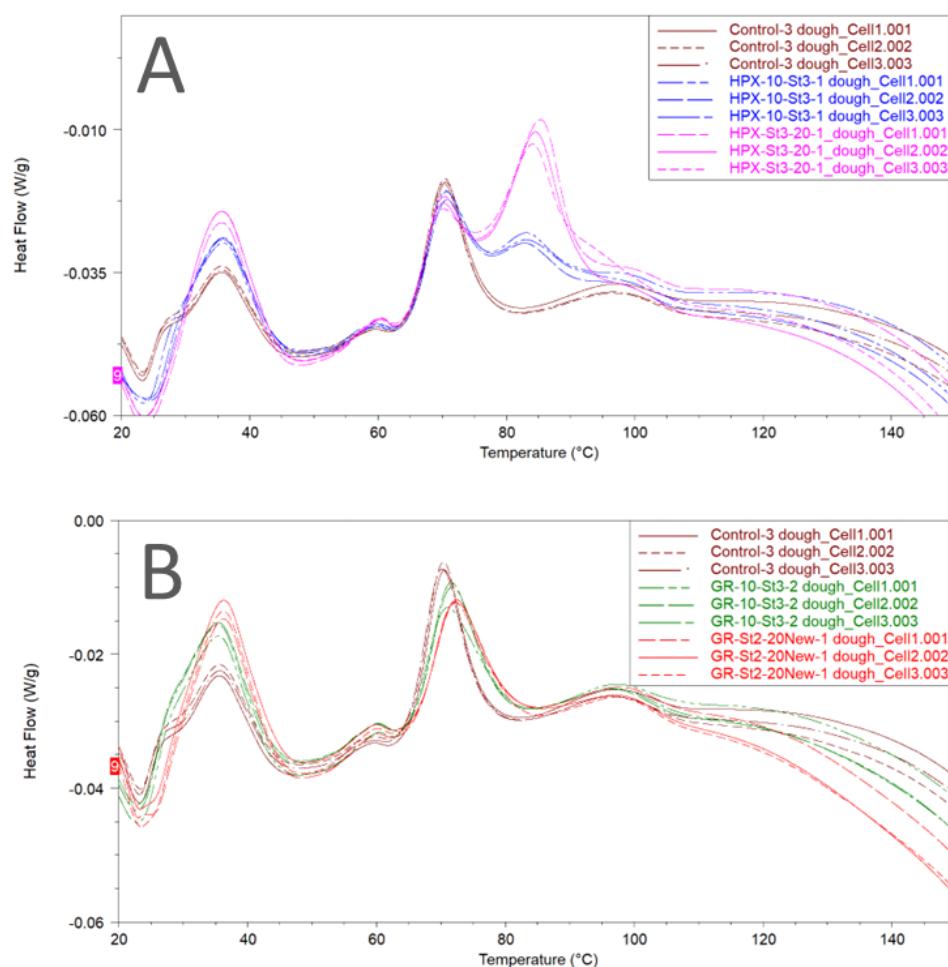
*Figure 5.17 – DSC thermogram examples of biscuit dough samples based on their respective total starch content with control dough in brown on each plot and (A) 10%(in blue) and 19% (in pink) insoluble inulin dough; (B) 10%(in green) and 19% (in red) soluble inulin dough, all in triplicate.*
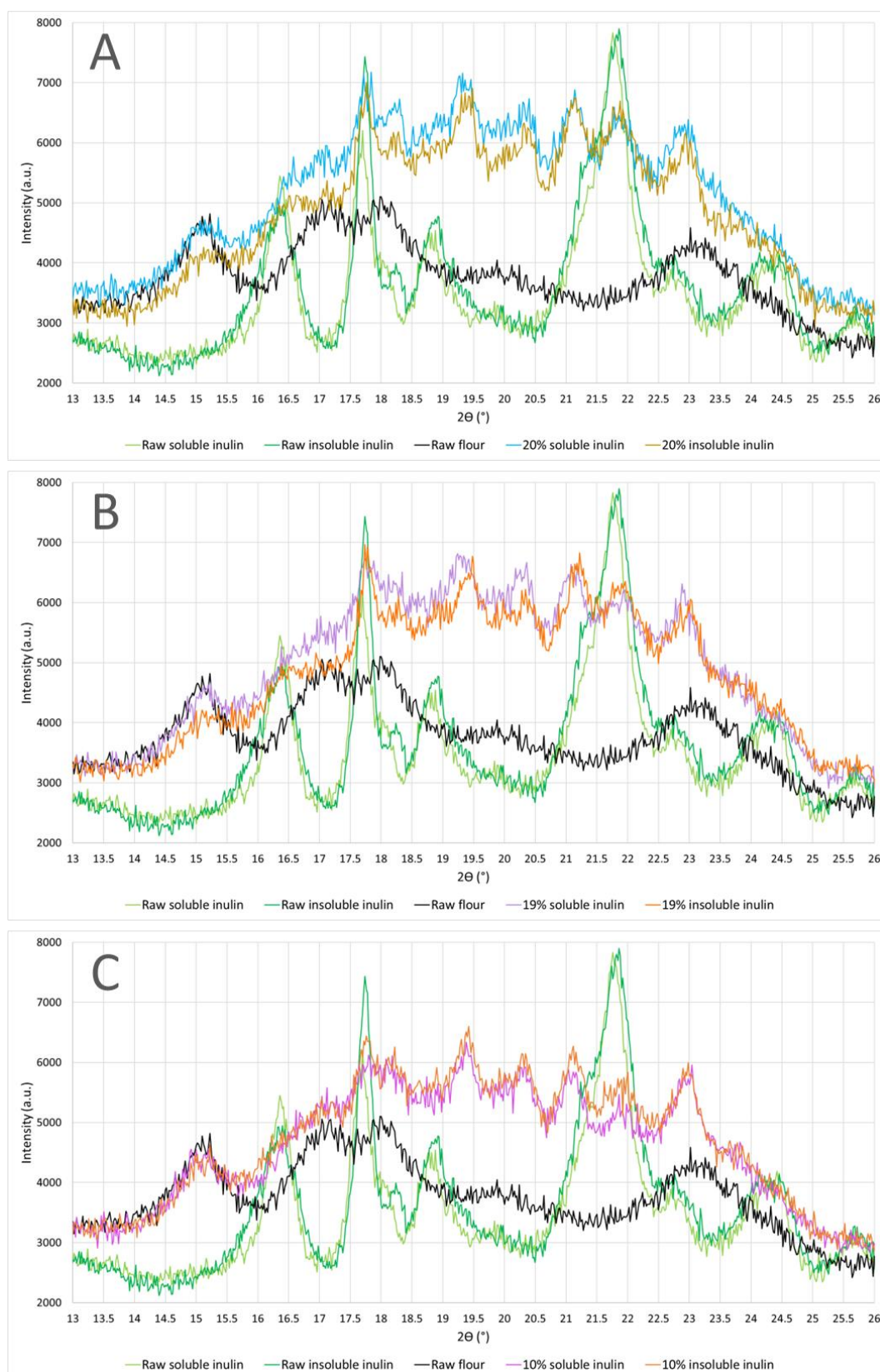
*Figure 5.18 – XRD diffractogram examples of biscuits containing (A) 20%, (B) 19%, (C) 10% soluble or insoluble inulin with diffractograms of raw soluble inulin, raw insoluble inulin and raw biscuit wheat flour on each plot.*
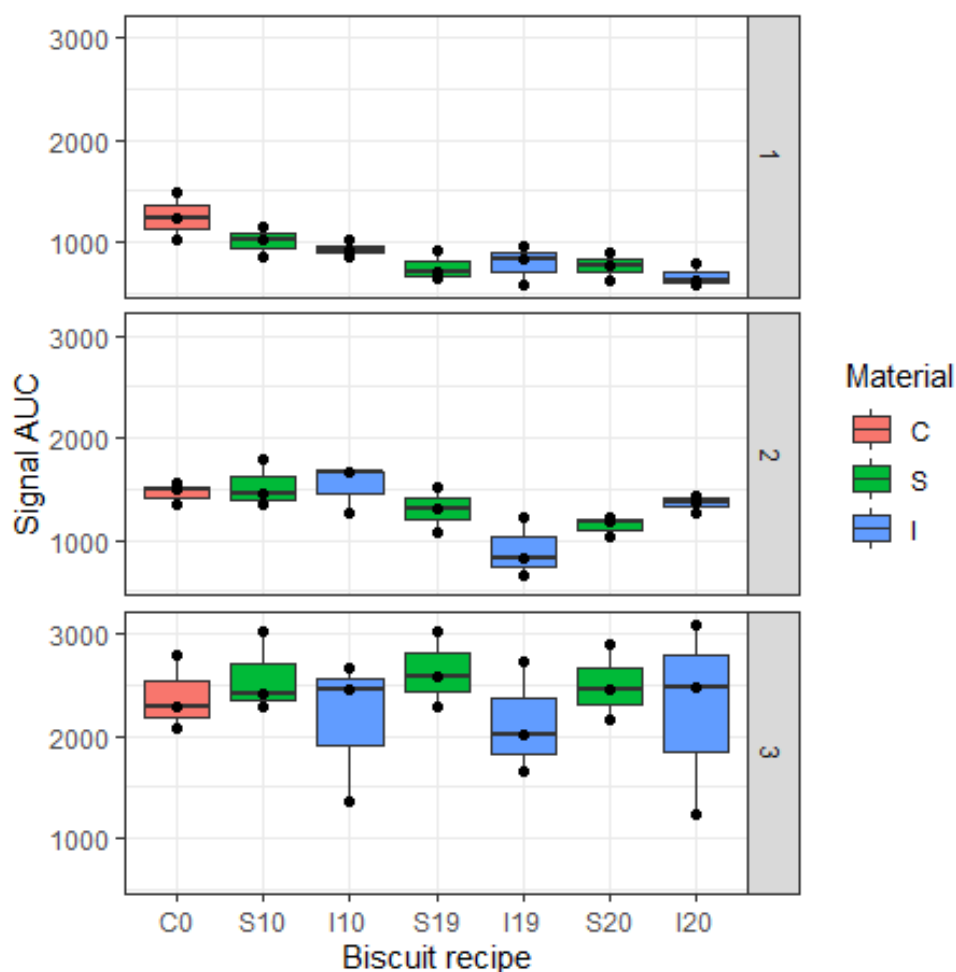
*Figure 5.19 – XRD signal intensity area under the curve (AUC) (determined using Peakfit, see Appendix figure A5.1 for an example) of seven different biscuit recipes of the relevant starch crystallinity peak between 1) 15.0° and 15.25°, 2) 17.0° and 17.3°and 3) 22.8° and 23.0°, n=3 batches per recipe.*

As a biscuit is a heterogenous complex matrix with several ingredients, a complementary technique was used to investigate the impact of biscuit baking on starch further. Using XRD, starch crystallinity was measured in baked biscuit across all seven recipes and compared relevant raw ingredients. Raw biscuit flour had a diffractogram similar to examples of wheat flour and wheat starch diffractograms in the literature (Lopez-Rubio *et al.* 2008, Leblanc *et*

*al.* 2008). Diffractograms of both raw inulins were very similar, i.e. had a comparable crystallinity. By overlaying the diffractograms of raw biscuit wheat flour and the raw inulin samples, three relevant peaks originating from crystalline starch were identified between 15.0° and 15.25°, 17.0° and 17.3° as well as between 22.8° and 23.0° (Figure 5.18), in regions where peaks were not observed in the inulin samples. Comparing diffractions in these three areas between soluble and insoluble inulin biscuits showed a higher signal, i.e. crystallinity, in soluble inulin biscuits with 20% (Figure 5.18A) and 19% (Figure 5.18B) compared to their respective insoluble inulin recipe counterparts, especially in the first (15.0°) and second (17.0°) starch peak. Signal intensity (AUC) of these relevant starch peaks were significantly lower than control in S19 ($p=0.0242$, pairwise comparison, Tukey correction), I19 ($p=0.0404$, pairwise comparison, Tukey correction), S20 ($p=0.0274$, pairwise comparison, Tukey correction) and I20 ($p=0.0067$, pairwise comparison, Tukey correction) for the first starch peak and I19 ($p=0.0486$, pairwise comparison, Tukey correction) for the second starch peak (see Figure 5.19).

### 5.3.6 Inulin size distribution differences and thermostability

Qualitative comparison of chromatograms shows that soluble inulin (Figure 5.20A) had a diffuse range of chain lengths including mono- and disaccharides whereas insoluble inulin (Figure 5.20B) had a

much narrower (focused) range of longer DP as they eluted at a later time. After heating the inulins in excess water to temperatures up to 150°C, both of them broke down (Figure 5.20C+D), however the insoluble inulin to a lesser extent as a few longer chains are still detected and the fructose peak (largest peak on chromatogram) is smaller (Figure 5.20D) than the one of soluble inulin (Figure 5.20C). Neither of the inulins were thermostable when exposed to dry heat, which led to similarities in the chromatogram for both inulins (Figure 5.20E+F).
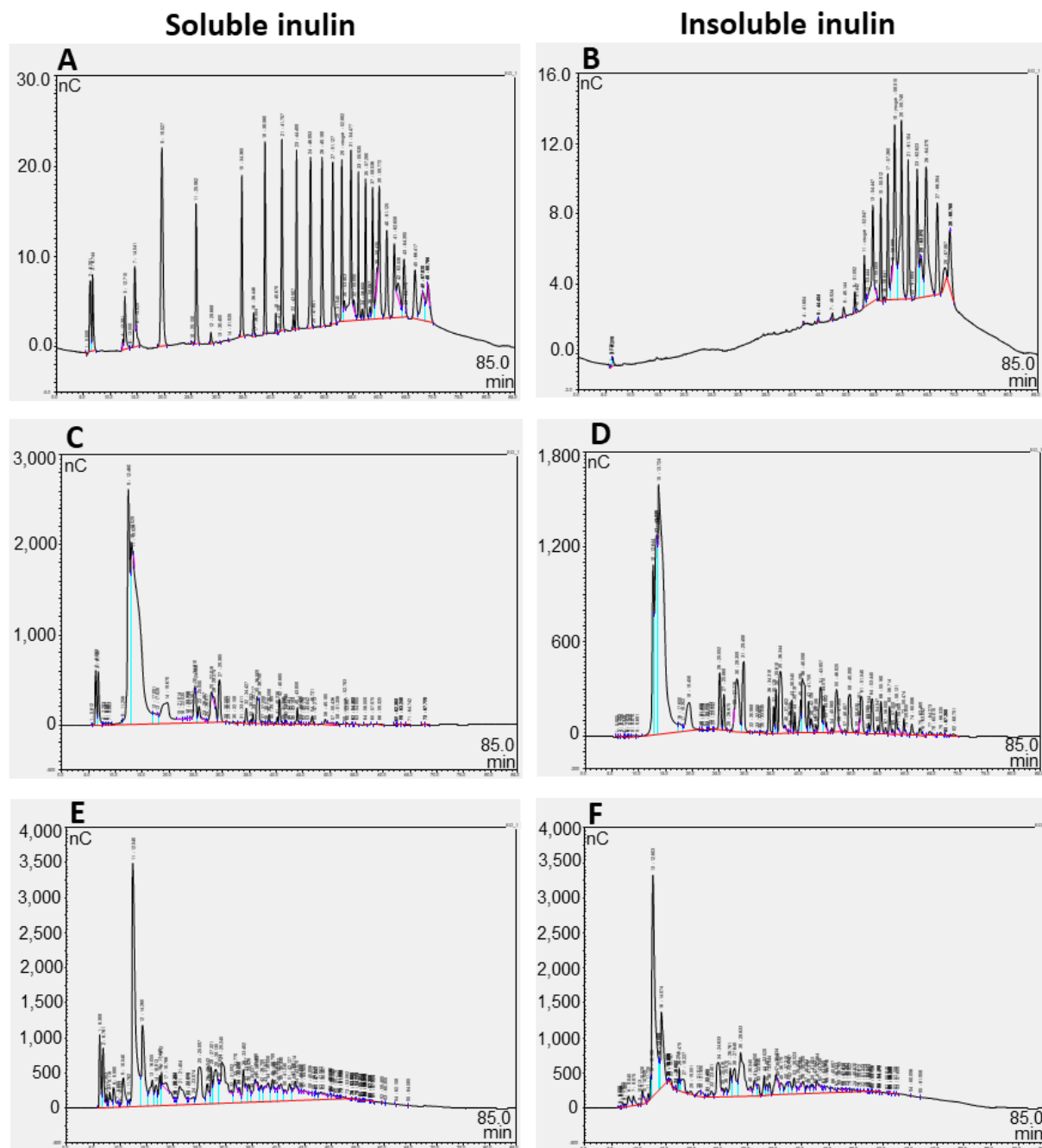
*Figure 5.20 – Chromatograms of soluble inulin (left side numbered A, C, E) and insoluble inulin (right side numbered B, D, F) under different processing conditions: uncooked (A, B), heated to 150°C in excess water (C, D) and baked at 205°C (dry heat) for 11 min (E, F).*

## 5.4 Discussion

### 5.4.1 Lower starch digestibility due to limited water availability in presence of soluble inulin

Soluble inulin incorporated into biscuits reduced starch digestibility, whereas insoluble inulin did not. A mechanism behind it could be limiting the amount of available water for starch to absorb which reduces the extent of starch gelatinisation. In such low water systems, higher temperatures are required to gelatinise starch (Perry and Donald 2002). Adding an ingredient, which competes for water and increases the gelatinisation onset temperature can be a good strategy to decrease the extent of starch gelatinisation with the aim to reduce starch digestibility in a processed food. However, the relationship between extent of starch gelatinisation and enzymatic degradation is complex (Wang *et al.* 2017a, Wang *et al.* 2020). Solely the amount of starch is not a good predictor for postprandial glycaemic response. Edwards *et al.* have shown that starch digestibility ($C_\infty$) in an *in vitro* simulated digestion correlates with glycaemic index from human studies (Edwards *et al.* 2019), which was the method used to compare starch digestibility among the seven biscuit recipes in this thesis. Mechanisms of a reduced starch gelatinisation can be due to competition for available water, i.e. differences in water sorption capacities as well as due to differences in moisture loss during baking which correlated with biscuit spread. Insoluble inulin biscuits had a lower spread and lower moisture loss leaving more water for starch gelatinisation. Also

different levels of digestibility between the core of control biscuits and their edge indicated a relationship between moisture loss and starch digestibility. The core retained more moisture during baking and digested to a higher extent than the edge of control biscuits. A nonsignificant lower spread and decreased reducing sugar release from inulin-enriched biscuits was also found by Brennan & Samyue. In the same study, they reported a lower viscosity with increasing levels of inulin incorporation which was attributed either to the lower starch level overall or to inhibition of starch gelatinisation (Brennan and Samyue 2004). Lower pasting after addition of different fibres was attributed to lower amounts of starch granules and available water in a study investigating biscuit doughs. Inulin had the biggest effect due to its ability to form a gel and microcrystals in solution, which trapped water and therefore reduced starch hydration (Blanco Canalis *et al.* 2019). In the competition for the limited amount of dough moisture with sucrose and flour, inulin has a high affinity for water. Low DP inulin especially showed a higher hydrostatic packing and interaction with water (Franck 2002, Handa *et al.* 2012, Mensink *et al.* 2015, de Gennaro *et al.* 2000, Tsatsaragkou *et al.* 2021, Schaller-Povolny *et al.* 2000), which is comparable in chain length to the soluble inulin tested in this thesis. Biscuit doughs containing 19 and 20% insoluble inulin, which had a higher DP, had higher water activity levels than control and soluble inulin doughs, which further correlated with moisture loss.

Hence in conclusion, soluble inulin in biscuits limited the amount of water available for starch gelatinisation in two ways. Firstly, the lower DP soluble inulin was superior in competing for water in the biscuit dough and secondly, biscuits had a higher moisture loss during baking due to the greater spread.

## 5.4.2 Starch not gelatinised during biscuit baking but structural modifications occur

If starch gelatinisation is defined as full, irreversible disintegration of the ordered structure of a starch granule (Cooke and Gidley 1992, Zobel 1984), starch does not gelatinise during biscuit baking as control biscuits had the same enthalpy as the dough which is in line with other studies (Kulp *et al.* 1991, Zhang *et al.* 2021b). Enthalpy changes in DSC measurements primarily reflect the disruption of the double helices in starch, i.e. the short-range ordered structures, rather than the changes in crystalline order of the granule, i.e. long-range ordered structures (Zhang *et al.* 2021b, Cooke and Gidley 1992). Zhang *et al.* found that biscuit baking decreased the average amylose chain length as well as the average molecular size of whole starch molecules, amylopectin and amylose molecules. However, baking had no effect on the degree of branching, i.e. the amylose content, or relative crystallinity measured with XRD. Attenuated Total Reflection-Fourier Transform Infrared (ATR-FTIR) and DSC measurements suggested that biscuit baking made the starch granules only slightly gelatinized but decreased ordered structures in the starch external region (Zhang *et al.* 2021b). These structural

changes are important determinants for starch digestibility in terms of enzyme binding as α-amylase binds to starch granules quicker if the surface is less crystalline (Warren *et al.* 2013, Roder *et al.* 2009). XRD measurements of the different biscuit recipes indicated that the starch in biscuits containing soluble inulin was more crystalline than the one containing insoluble inulin, which is suggested by Wang *et al.* as the rate-limiting step for starch digestion. The disruption of the outer layer of the wheat starch determined access/binding of α-amylase to the starch rather than the overall degree of gelatinisation and once the enzymes had access, hydrolysis rates were comparable (Wang *et al.* 2017a). This is in line with the digestion kinetics results of soluble inulin biscuits, which had more crystalline starch. The extent of starch digestion was lower but the rate was not different from control, which, according to Wang *et al.* indicates that the enzyme access was impeded (Wang *et al.* 2017a).

### 5.4.3 The role of the biscuit matrix

The differences in starch digestibility between control, soluble and insoluble inulin biscuits could be due to less starch gelatinisation as discussed above, but could also be influenced by to physical barriers in the biscuit matrix, i.e. hardness and particle breakdown. The two inulins with different chain lengths led to differences in biscuit shape, colour and particle disintegration, in line with differences in baking outcomes in cakes (Tsatsaragkou *et al.* 2021). Therefore, a physical barrier could be another reason for differences in starch digestibility. Although the particle size was standardised to <600>500 μm in line

with mastication data from human studies (Hoebler *et al.* 1998, Jiffry 1981, Peyron *et al.* 2004, Flynn 2012), biscuits containing soluble inulin were harder and disintegrated less than control or insoluble inulin biscuits. It has been shown previously that particle size affects starch digestibility (Cañas *et al.* 2020, Edwards *et al.* 2018, Petropoulou *et al.* 2020) and differences in particle sizes after mastication was suggested as cause for interindividual glycaemic variability (Ranawana *et al.* 2010). A difference in access to starch granules among the different biscuit recipes is suggested to be tested in the future, e.g. by using FITC-labelled amylase confocal microscopy (Colosimo *et al.* 2020b, Dhital *et al.* 2014b).

### 5.4.4 Solubilised inulins act as more effective plasticisers than sucrose

Sucrose is difficult to replace in a food product due to its functionality, one of which is increasing the starch gelatinisation temperature (Perry and Donald 2002, Allan *et al.* 2018). The effect of sucrose and sugar replacements on gelatinisation enthalpy on the other hand is inconsistent in the literature from no change (Perry and Donald 2002) to slightly higher enthalpies than in water (Allan *et al.* 2018). Ahmad & Williams found that gelatinisation enthalpy increased with increasing sucrose concentration until a plateau was reached at about 30% sucrose (Ahmad and Williams 1999), whereas Eliasson found that enthalpy changes were defined by water to starch ratios in the same manner as in the absence of sucrose (Eliasson 1992).

Added sucrose behaved differently in the model biscuit system depending on whether it was in a crystalline form or pre-solubilised. Crystalline sucrose is the form found in a biscuit after baking (Kulp *et al.* 1991). Perry and Donald demonstrated that mixtures of water and sugars act as a single plasticizing solvent, but sugars are less effective plasticisers than pure water, hence more energy is needed to gelatinise starch, reflected in higher gelatinisation temperatures (Perry and Donald 2002). We found the same increase in gelatinisation temperatures as a result of sucrose addition in crystalline and solubilised biscuit model systems, as a function of decreasing water levels. Sucrose elevates the starch gelatinisation temperature more than many other sugars (Allan *et al.* 2018, Spies and Hoseney 1982, Van der Sman and Mauer 2019), but the polymer-based sugar replacements Benefibre and Miralax increased the gelatinisation temperature to a higher extent than sucrose, which the authors called an 'antiplasticising' effect on water (Woodbury *et al.* 2021). BG and cellulose only increased the onset temperature compared to the no fibre control at low levels, but resulted in starch gelatinisation behaviour similar to that observed under limiting water conditions at higher levels of inclusion.

Comparing no fibre controls containing crystalline with solubilised sucrose, the biggest difference in starch gelatinisation extent was in the area where starch showed 'limited water behaviour', which is the area relevant for biscuits as it is a low moisture product with an

average dough moisture of 17%. In presence of crystalline sucrose, a sharp drop in starch gelatinisation extent occurs at 22.5% water, whereas complete gelatinisation was still observed at this water level when sucrose was solubilised. Even at very low water levels of 12.5 and 7.5%, more than half of the starch was still gelatinised in presence of solubilised sucrose. Hence use of crystalline sugar as opposed to syrup may impact starch gelatinisation in biscuits.

Also for inulin, a crystalline as opposed to a solubilised state changed the impact on starch gelatinisation in the biscuit model system, in a similar manner as sucrose. In a solubilised state, both inulins acted as one plasticising solvent together with sucrose and water, more efficiently than solubilised sucrose in absence of inulin. However as neither of the two inulins were thermostable during the applied solubilisation procedure, the plasticising solvent more likely contained fructose and oligosaccharides rather than the native inulin. This was surprising as thermal degradation of inulin was reported when heated above 200-225°C (Mensink *et al.* 2015, Dan *et al.* 2009, Heyer *et al.* 1998, Ronkart *et al.* 2010). Soluble inulin in a crystalline state led to increased gelatinisation temperatures, both in the biscuit model system as well as in dough containing soluble inulin. Hence more energy in the form of heat was needed for gelatinisation which can impact the extent of gelatinisation (Perry and Donald 2002).

### 5.4.5    Conclusion

Incorporation of soluble inulin into biscuits by reducing sucrose and flour may be a good strategy for a lower glycaemic load as they contained less sugar and starch overall. More importantly the starch that was present in these biscuits was less digestible which further reduces the glycaemic load. The thermal stability of inulin should be investigated further as the biscuit matrix may protect the inulin from being broken down. So far, inulin incorporated biscuits have only been tested in an *in vitro* digestion. A human study would be needed to confirm the results. Additionally, sensory testing by trained panellists are suggested to assess the biscuit's taste and likeability.

# Chapter 6 – Discussion: Mechanisms and functionalities underpinning health benefits of dietary fibres

## 6.1 Specifics of water interactions underpin fibre functionality

An important physical property of DF is its ability to bind and interact with water in foods or digesta that results in viscosity changes (Poutanen *et al.* 2018, Vuksan *et al.* 2011, Wanders *et al.* 2013, Wanders *et al.* 2011, Wanders *et al.* 2014, Jensen *et al.* 2012, Wang *et al.* 2017b, Anderson *et al.* 2000, Brouns *et al.* 2011, Jenkins *et al.* 1979). However, foods and digesta are heterogenous systems which makes studying their rheology much more complex than that of homogenous fluids or suspensions of monodisperse, solid spheres (Moelants *et al.* 2014). Digesta containing DF and other food components are suspensions, which can be defined as "a biphasic system, where a continuous and a discrete phase coexist in a given volume" (Genovese 2012), see Figure 6.1. DF can be found as plant-tissue based particles constituting the discrete phase or as dissolved polymers in a continuous aqueous phase (Moelants *et al.* 2014), see Figure 6.2. Studies presented in this thesis have shown some underpinning mechanisms of how DF in the continuous phase (as discussed in section 6.1.1), particulate DF in the discrete phase (as discussed in section 6.1.2) of digesta as well as DF in a food matrix (as discussed in section 6.1.3) impact digestive processes which can lead to observed health benefits.

**DIGESTA**

Overall viscosity depends on both phases and interaction between phases

**CONTINUOUS PHASE**

Contains solubilised fibre, digestion products, bile acids

$H_2O$

Viscosity depends on
- Concentration
- Mw
- Conformation (e.g. random coil)
- Ionic strength
- Solvent
- pH (for charged polymers)
- Temperature
- Shear

**DISCRETE PHASE**

Contains insoluble fibre particles, swollen hydrated fibre particles, macronutrients before digestion, enzymes, micelles

Viscosity depends on
- Concentration
- Particle size and size distribution
- Particle deformability
- Particle morphology
- Aggregation/attraction forces
- Temperature
- Shear

*Figure 6.1 – Viscosity relationship of digesta as suspension of a discrete phase in a continuous phase [modified from (Moelants et al. 2014) and (Rao 2007)]*



C Solubilised fibre

A Insoluble fibre particle

B Swollen, hydrated fibre particle

D Aggregated swollen, hydrated fibre particles
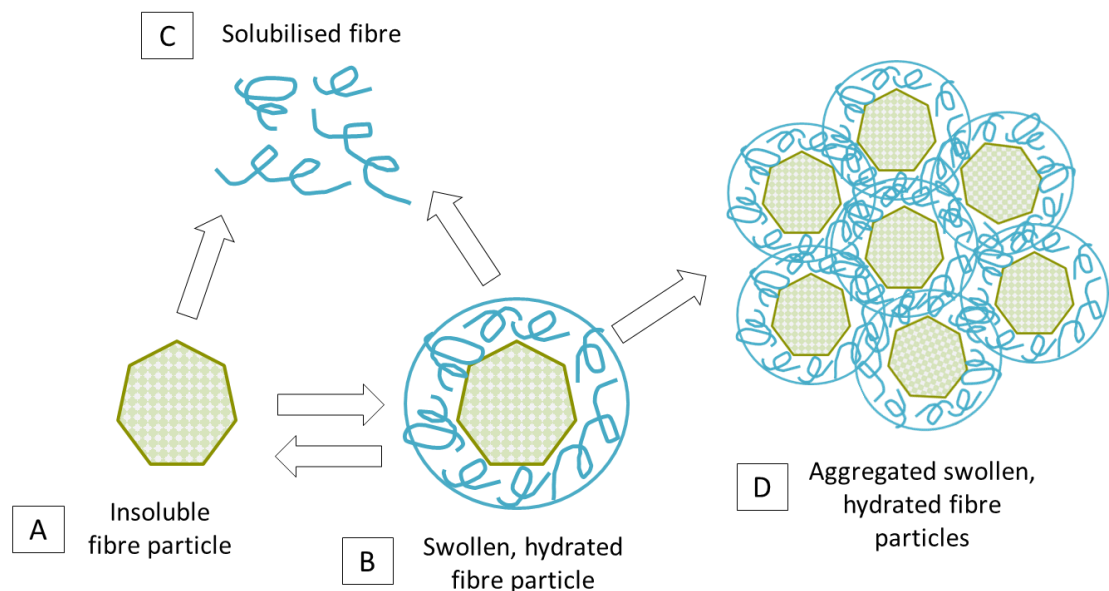
*Figure 6.2 – Diagram of proposed BG dissolution kinetics from barley vs oat bran particles: A) insoluble fibre particle with intact cell wall structure, B) swollen, hydrated fibre particle with soluble fibre leached from cell wall matrix but still attached, C) solubilised fibre in the aqueous phase, D) aggregates of swollen, hydrated fibre particles.*

## 6.1.1 Increased viscosity of the continuous phase impacts digestion

In this thesis, viscous entrapment of BA by some DFs was shown to reduce BA diffusion rates (section 4.3.1). This is likely to impact lipid digestion by reducing the BA's ability to facilitate the stages of lipid digestion in line with the experimental finding of a reduced lipolysis rate (section 3.3.1 and 3.3.2). The importance of mixing was shown in simulated lipid digestion experiments in this thesis (section 3.3.3 and 3.3.4). Hence increased digesta viscosity as a result of viscous DF can impact digestive processes in two ways, by reduced mixing of digesta which decreases the likelihood of substrate/enzyme contact as well as by physical entrapment and reduced diffusion of BA. These mechanisms enable cereal fibre to impact lipid metabolism and the enterohepatic circulation of BAs leading to lower plasma cholesterol levels and prevention of CV-related diseases.

In more detail, the continuous phase of digesta contains soluble DFs (Figure 6.1) which have the ability to form molecular solutions when dispersed in the aqueous phase. Their dissolution is governed by their hydration properties which depend on Mw, final solution concentration and the surface area exposed to water, usually defined by particle size, and can take several days to be fully hydrated (Wang *et al.* 2008). The effective concentration of hydrated polymer, the polymer's intrinsic viscosity (molecular structure, e.g. branching, Mw and conformation) and environmental conditions including shear rate and temperature determine the apparent viscosity of

'entanglement solutions' beyond the C* (see section 1.5.2, Figure 1.7) (Wang and Ellis 2014, Wang *et al.* 2008). The continuous phases of digesta containing barley or oat BG showed a dramatic shear thinning behaviour (section 4.3.3), typical for concentrated polymer solutions at C* (Morris *et al.* 1981, Rieder *et al.* 2017). Although the concentration of dissolved BG was higher in barley, the continuous phase had a lower viscosity compared to oat due to the lower Mw of barley BG (section 4.3.4). Beneficial effects of BG in human studies can be predicted from whether C* is achieved by BG solubilisation during digestion. Simply the amount of TDF or BG in a food does not determine whether the fibre impacts digestion as shown in this thesis (section 3.3.2 and 4.3.1) in line with Rieder *et al.* comparing human studies (Rieder *et al.* 2017). Two aspects of BG have to be known for predicting health outcomes by determination of C*: amount of BG effectively solubilised under physiological conditions as well as the Mw of the BG (Rieder *et al.* 2017). However, concentrations needed might be lower than expected due to associations between the fibre molecules occurring under simulated small intestinal conditions (Repin *et al.* 2018). There might also be an upper limit where 'hyperentanglement' can occur at very high polysaccharide concentrations and high Mw. Depending on the structure, BG can form microgels, micron-sized aggregates, in aqueous solutions following hyperentanglement (Shelat *et al.* 2011, Zielke *et al.* 2019, Lazaridou *et al.* 2004, Lazaridou and Biliaderis 2007). These aggregates will have

important implications on diffusion rates as they lead to the creation of 'microvoids', localised regions with a lower microviscosity which would not be obvious from a bulk viscosity measurement averaging across the whole sample. Studies investigating diffusion rates in BG as well as AX solutions found that samples with higher viscosities could indeed have a faster enzyme diffusion rate due to microvoids big enough for enzyme diffusion. The entanglements and aggregate formation depend on the structure of the soluble fibre, hence the relation between bulk viscosity and diffusion are not simple (Shelat *et al.* 2010, Shelat *et al.* 2011). Similarly it was shown with a carboxymethyl cellulose that lower Mw polymers build denser networks, which led to the lowest glucose diffusion, despite all tested samples had concentrations above C*. However, flow behaviours changed when stirring was used which negated the superior effect (Miehle *et al.* 2021) in line with Dhital *et al.* (Dhital *et al.* 2014a). Hence it is debated in the literature, whether these diffusion and digestion reductions detected *in vitro* (Ramírez *et al.* 2015, Hou *et al.* 2020, Shelat *et al.* 2010, Shelat *et al.* 2011, Miehle *et al.* 2021) are relevant *in vivo* (Goff *et al.* 2018, Dhital *et al.* 2014a, Rieder *et al.* 2017). The results appear to depend on whether glucose is tested (Dhital *et al.* 2014a, Miehle *et al.* 2021) which is a small molecule, dissolved in the continuous phase and capable of diffusing through a microgel network, or an enzyme (Shelat *et al.* 2010, Shelat *et al.* 2011) which is a much bigger molecule that may

be retained in the discrete phase, which can include swollen, hydrated fibre particles (Figure 6.2 and section 6.1.2).

Digestive processes are not governed by diffusion only but rely on digesta mixing (Mackie 2019). Due to the complex shear thinning behaviour of digesta, relevant conditions reflecting the human digestive tract are needed but are still unclear (Poutanen *et al.* 2018). Physiological shear rates reported vary between $0.1\ \text{s}^{-1}$ and $10\ \text{s}^{-1}$ (Hardacre *et al.* 2016), $15\ \text{s}^{-1}$ (Naumann *et al.* 2018, Gunness *et al.* 2012) $30\ \text{s}^{-1}$ (Tosh *et al.* 2010) or $10\ \text{s}^{-1}$ and $50\ \text{s}^{-1}$ (Poutanen *et al.* 2018). Hardacre *et al.* suggested that mixing impairment under physiological conditions can be expected from a threshold of 0.1 Pa.s apparent viscosity if the physiological shear rate is $10\ \text{s}^{-1}$ (Hardacre *et al.* 2016), based on a shear stress developed by the gut of up to 1.2 Pa (Hardacre *et al.* 2016, Jeffrey *et al.* 2003). Barley bran and oat bran have been shown in this thesis (section 3.3.3 and 4.3.3) to reach this apparent viscosity threshold at shear rate $10\ \text{s}^{-1}$ at certain concentrations and hence may impair digesta mixing. Similarly, Wood suggested an *in vivo* glucose lowering effect at an *in vitro* viscosity of at least 0.02 Pa.s at a shear rate of $30\ \text{s}^{-1}$ , with no further reductions seen beyond 2 Pa.s (Wang and Ellis 2014, Wood 2011). There were differences in the shear thinning behaviour between barley and oat (section 3.3.3 and 4.3.3), which may influence their ability to affect mixing, depending on the shear rates encountered in the gut as relevant human *in vivo* data are missing.

Other differences around BG dissolution kinetics depending on the botanical origin were investigated further as part of this thesis as natural BG-rich ingredients add more complexity due to a high polydispersity in molecular size of solubilised fibre (section 4.3.4), not all BG being solubilised during digestion (section 4.3.4) and other components including insoluble fibre particles present in the digesta which form the discrete phase.

## 6.1.2 Differences in solubility and hydration properties explain differences in digestion behaviour between barley and oat bran

Review papers suggest that solubilisation of BG needs to occur during the digestive process for an optimal health effect *in vivo* (Henrion *et al.* 2019, Khossousi *et al.* 2008, Grundy *et al.* 2016, Holland *et al.* 2020, Grundy *et al.* 2018a), but the reason behind it is unclear. Findings from this thesis showed that BG in a bran matrix undergoing a simulated digestion can be found in three different hydration stages: either as insoluble BG remaining part of the cell wall matrix (see A in Figure 6.2), as hydrated BG released from the cell wall, but is still associated with the plant tissue (see B in Figure 6.2) or BG which has been released and is fully dispersed in the aqueous phase (see C in Figure 6.2). Jarvis argues that the majority of non-cellulosic polysaccharides in primary cell walls are to some degree soluble. Hence once they are solubilised, only the insoluble cell wall structure remains (Jarvis 2011). However, *in vitro* digestions presented in this thesis showed that only 20-35% of BG

are solubilised from a bran matrix (section 4.3.4) in line with previous studies (Rieder *et al.* 2017, Tosh *et al.* 2010, Grundy *et al.* 2017a) and the extent and kinetics varied by botanical origin. A substantial amount of BG from oat bran was hydrated rather than fully solubilised (section 4.3.4). Hydrated BG was also found in barley bran but to a much lower extent. Since this was found to be a time-dependent process, it could be a matter of being a quicker process in barley bran while exerting all three stages. However, it could also be due to structural differences in BG depending on botanical origin. Barley and oat bran BG had very different Mw distributions with oat BG being much larger. A higher Mw BG could be the reason that oat fibre was found in a state of swollen hydrated fibre particles to a greater extent compared to barley. This also impacts BG extractability, i.e. the amount of BG solubilised in the continuous phase with Mw dependence also suggested by previous studies on different DFs including barley and oat (Robertson *et al.* 1997, Comino *et al.* 2013, Tosh *et al.* 2010, Goudar *et al.* 2020), which is however not supported by Rieder *et al.* (Rieder *et al.* 2017). Literature suggests that BGs have differences in cellotriosyl (DP3) and cellotetraosyl (DP4) units depending on their botanic origin with oat BG having a DP3:DP4 ratio of approximately 2:1 and barley BG of 3;1, which is suggested to affect solubility (Lazaridou *et al.* 2004, Lazaridou and Biliaderis 2007).

Insoluble fibre particles and any aggregates formed, increase the overall digesta viscosity as solid particles can act as active fillers, strengthening the interactions in the network (Genovese 2012). This was demonstrated in this thesis when supernatant viscosity was compared with whole digesta viscosity (Appendix figure A3.2). However, aggregates might decrease the overall viscosity by disrupting networks between polymers in the continuous phase. The difference in behaviour between oat and barley bran both in terms of impact on lipid digestion and on digesta viscosity seem therefore be due to their BG dissolution kinetics and/or interaction of the solubilised or swollen, hydrated fibre particle with other components in the digestion mixture.

Findings from the lipolysis study supported the functional importance of the BG dissolution kinetics concept (Figure 6.2). It was concluded that barley acts primarily as solubilised fibre as the lipolysis rate was delayed in the presence of barley BG irrespective of the presence of IDF. Oat fibres on the other hand, needed the presence of IDF, either as intact bran or added, to reduce lipolysis rate (section 3.3.2). The functionality in oat therefore seems to depend on its ability to form swollen, hydrated fibre particles or aggregates (see also Appendix figure A6.1). The concentrated layer of hydrated BG around the particles could entrap or retard digestion components on a local level which has the potential to slow down lipid digestion.

Studies using purified soluble DFs are easier to interpret as there are no other components present, like protein, lipids, particles etc., potentially affecting the results. Testing purified BG posed the challenge of polymer aggregation when not pre-hydrated or extensive hydration times of over 2 days to pre-solubilise the polymer (section 3.3.1) in line with other studies (Grundy *et al.* 2017b, Wang *et al.* 2008). Lipid digestion results indicated that the hydration status of extracted BG both from barley and oat influenced the effect (section 3.3.2). Grundy *et al.* reported the challenges to replicate *in vitro* the dynamic aspect of dissolution of the soluble fibre potentially happening *in vivo* and argued that pre-solubilisation may change the functionality (Grundy *et al.* 2017b). An important missing piece of information though is what dissolution kinetics and behaviours do purified DFs and heterogenous DF matrices exert during digestion *in vivo* as natural BG-rich wholefoods can be more efficient in reducing plasma cholesterol than purified BG, despite less consistent results (Grundy *et al.* 2018a), which are likely due to lack of C* (Rieder *et al.* 2017). Human feeding studies which take samples directly from the small intestine are needed to answer questions like: To what extent does a purified BG supplement sprinkled on a porridge hydrate during the course of a digestion? Can the three different hydration stages of oat and barley bran proposed in Figure 6.2 be found in digesta *in vivo*? Do the aggregates (see D in Figure 6.2) stay intact during the course of digestion?

Soluble DF dissolution kinetics from a bran matrix could also impact the cell wall integrity. There is a substantial amount of research under way to find ingredient processing conditions which keep the PCW intact so that the intracellular macronutrients can only come into contact with digestive enzymes if the pore size of the PCW is large enough (Capuano *et al.* 2018, Edwards *et al.* 2021, Pälchen *et al.* 2022, Holland *et al.* 2020, Ellis *et al.* 2004, Grundy *et al.* 2015). The porosity of a cell wall is determined by its composition and organisation of its components depending substantially on botanical origin and processing (Holland *et al.* 2020). Cell wall porosity may change over the course of digestion. Fibre solubilisation could make the PCW more porous in fibre matrices with rapid dissolution kinetics (see A and C in Figure 6.2). However, if the PCW turns into a swollen, hydrated particle (see B in Figure 6.2), the hydrated soluble fibre layer could further protect the intracellular macronutrients from digestion.

This implies that it is not just about the composition of the food or digesta but how the different components are organised around and interact with each other as well as with the solvent. This complexity will therefore help determine the physiological function of DF *in vivo*. Human digesta is not homogenous; it contains particles, aggregates and/or coagula. The results from this thesis suggest that the heterogeneity in the system is important for DF functionality.

### 6.1.3 Competition for water in a food matrix determines inulin functionality

In contrast to the systems in excess water discussed above, a biscuit dough is a low water food matrix and at the solid-like (elastic) end of the rheological spectrum. A polymer's rheological properties as part of this complex food matrix and how it interacts with water could impact on processes which require access to water, such as starch gelatinisation. Similar to BG, inulin also forms networks which trap and immobilise water (Franck 2002).

As presented in this thesis, DF can reduce starch gelatinisation and digestibility of starch, however, relevant hydration properties are more than just the solubility in an aqueous solution (section 5.3.4). Seven biscuit recipes were compared which had major differences in the recipes like the level of inulin incorporation or differences like slightly higher dough moisture or order of ingredient addition. Starch gelatinisation as well as starch digestibility was reduced in soluble inulin biscuits as the lower DP inulin outcompetes starch for the available water. The higher DP insoluble inulin on the other hand did not seem to be able to compete with starch for water as effectively and led to the same starch digestibility as control or, at higher dough moisture levels, to an even higher starch digestibility (section 5.3.4).

Inulin solubility in this case was indicative of the competition for water functionality (section 5.3.5), however does not reveal how it interacts with other components. Rheology may only be informative

under relevant conditions as investigated in a study by Tsatsaragkou *et al.* on sugar replacement with two different inulins. The higher DP inulin resulted in a higher cake batter viscosity at 25°C than the lower DP inulin. However, water retention functionalities were only visible when the cake batter's rheological properties were measured on a heat ramp to simulate baking temperatures. Interactions with water, assessed by the thermal setting temperature were significantly higher in presence of low DP inulin compared to high DP inulin (Tsatsaragkou *et al.* 2021). In this thesis, there was no dose-dependent reduction in starch digestibility in biscuits containing soluble inulin (section 5.3.4). Also the order of addition of ingredients did not lead to different digestibility results. With one of the recipes, soluble inulin was added together with the water, hence in a solubilised state. However, this recipe reduced the biscuit starch digestibility to the same extent as soluble inulin added together with the flour. Hence inulin's functionality appears to be largely due to how it interacts with water. Measuring the water activity of the raw dough was more informative with regards to water interaction (section 5.3.2) as opposed to differentiating the inulins based on their solubility.

### 6.1.4 Conclusions on fibre interactions with water

The digestion of macronutrients is impacted by the ability of DFs to absorb water as well as how DFs interact with water. Solubilised fibre can increase the viscosity of the continuous phase, whereas

insoluble fibre particles and swollen, hydrated fibre particles impact the overall digesta viscosity.

It is concluded that there is not a single, unique parameter which could be measured to reflect the manifold interaction behaviours of DFs with water which are relevant for revealing the underlying digestion interaction mechanisms. DF categorisation on the basis of a dichotomous solubility parameter has limited links to functionality. It does not represent the full spectrum of solubilities either. The extent of solubilisation of fibre and the respective dissolution kinetics under simulated digestion conditions inform predictions of physiological benefits. Rheological properties of the continuous phase under physiological conditions together with information on the fibre structure (molecular size, branching, conformation in a physiological solvent) are indicative for reduced diffusion prediction. Impaired mixing is defined by the properties of the continuous phase together with the particle fibre's hydration state in the discrete phase. With regards to water competition mechanisms, water activity measurements seem most informative for prediction of the functionality in a complex food matrix.

## 6.2 BA binding properties and its implications for lipid digestion and health

Binding properties of DF may be exerted in different forms, either as physical entrapment as discussed before or as direct molecular interactions leading to immobilisation. Evidence for both forms was

found as presented in this thesis, non-specific physical entrapment of BA based on total bovine bile (section 4.3.1 and 4.3.5) as well as molecular preference for specific BAs of barley, oat and wheat bran (section 4.3.2). The exact form of interaction is still to be elucidated, but there is an indication that BG and AX bind or complex BA by H-bonds and/or van der Waals forces with interactions being of dynamic nature (Gunness *et al.* 2016). The interactions were either with whole GCDC micelles or down to a change in the internal micelle organisation (Gunness *et al.* 2010, Gunness *et al.* 2016). The effect was much smaller with whole porcine bile (Gunness *et al.* 2016) which might be an indication that the interaction occurs with specific BA (micelles) only, in line with the findings in this thesis (section 4.3.2). BA micelles and mixed micelles are larger structures than individual BAs, hence more likely to be entrapped in polymeric network structures as suggested by some *in vivo* studies (Takagaki *et al.* 2018, Ellegard and Andersson 2007, Lia *et al.* 1997). However, BA micelles are very transient and therefore difficult to study in isolation hence there are limited publications available.

In this thesis, evidence for binding of BAs by certain cereal DFs was provided (section 4.3.2), which can be one of the mechanisms contributing to reduced lipid digestion (section 3.3.2) and may also increase BA excretion which reduces blood cholesterol levels (Grundy *et al.* 2018a). Different BAs contribute in different ways to lipid digestion, i.e. may be more or less efficient in solubilisation of

FFAs (Pabois *et al.* 2020, Parker *et al.* 2014). Both barley bran and oat bran reduced lipid digestion (section 3.3.2) and showed BA binding properties (section 4.3.2) as contributing mechanisms. Reduced lipase activity was also seen in the absence of BAs, so other mechanisms like viscosity related effects and/or lipase binding may have also contributed to the overall reduction in lipid digestion. Interactions of DF with BAs and digestive enzymes have been reported in the literature (Dhital *et al.* 2015, Colosimo *et al.* 2020b, Colosimo *et al.* 2020a, Naumann *et al.* 2018, Naumann *et al.* 2019a, Slaughter *et al.* 2002, Takagaki *et al.* 2018, Drzikova *et al.* 2005, Kahlon *et al.* 2006, Kahlon and Woodruff 2003, Gunness *et al.* 2012), with binding properties depending on the molecular structure of the DF (Gidley and Yakubov 2019). For BG this is suggested to depend on the amount of cellulose-like fragments in the structure (Lazaridou *et al.* 2004, Iaccarino *et al.* 2020). However, based on findings presented in this thesis, presence of a PCW matrix was essential for BA binding properties (section 4.3.1), which is in line with a review by Grundy *et al.* (Grundy *et al.* 2018a). BA binding properties of DF rich in BG seems to be the underlying mechanism for maintenance/reduction of blood cholesterol levels following consumption of BG.

# Chapter 7 – Conclusions and future directions

## 7.1   Functional categorisation of DF conclusion

Results presented in this thesis have shown clearly that physiological effects and health benefits are not determined purely by DF composition, nor an amount of DF, but by the DF's physico-chemical properties and behaviour during digestion. As these are governed by specific structural properties, even DFs with similar chemical compositions can have very different implications for digestion or the food matrix. Hence it is essential that studies investigating the impact of DF on health report detailed structural information, processing and preparation methods including the name and supplier to facilitate bringing together all available information to enable accurate structure-function relationships to be established. Specific recommendations were suggested by Poutanen *et al.* (Poutanen *et al.* 2018). However, there is still a gap in harmonisation of relevant methods for measurable DF properties *in vitro* which link them with their functionality underpinning their health benefits *in vivo* observed in epidemiological studies (Gidley and Yakubov 2019). Two aspects are important to acknowledge on our way forward: a) DF is not an inert material but undergoes structural and/or chemical changes during processing (section 5.3.6) as well as during digestion (section 4.3.4), and interacts on different length scales with other components in the matrix (sections 3.3.4, 4.3.2 and 5.3.5), and b) these properties determined under physiologically

relevant conditions should be regarded as a physical continuum rather than dichotomous (sections 3.3.3, 4.3.3, 4.3.4, 5.3.1 and 5.3.5). For example, BG solubility can be an informative measure if the underlying hypothesis of the putative benefit of BG from a barley bran matrix is thought to depend on physical entrapment in solubilised BG (section 6.1.1). In contrast, despite being a source of BG, BG in fungi is mostly insoluble and therefore need to have a different underpinning property than solubility underpinning their health benefits (Colosimo *et al.* 2021). Hence how DF and matrix are characterised as well as which parameters are relevant will be specific to the functionality investigated. The matrix structure must be considered together with the actual functional DF component thought to underpin the effect. As shown in this thesis (sections 3.3.2 and 4.3.1), how this functional DF is delivered, in an intact bran matrix or extracted, can impact the outcome. Similarly in human studies how BG was consumed, whether the food matrices were liquid, solid or semi-solid, as well as their level of processing played important roles in the resulting functionality of BG (Grundy *et al.* 2018a).

A key structural feature of BG and inulin is their molecular size, i.e. chain length as they are both unbranched linear chains. BG's health benefit is associated with achieving C*, which requires a certain Mw and effectively solubilised concentration *in vivo*. From the results presented in this thesis (section 4.3.4), high Mw BG seems to be

released slowly but eventually results in higher digesta viscosities (sections 3.4.2 and 4.3.3). However, very high Mw BG can form aggregates which are potentially unfavourable due to the creation of regions of lower microviscosity. It seems that there is an optimum, medium sized range for BG's Mw in terms of quick dissolution kinetics, solubility, viscosity and avoidance of aggregates. In a similar manner, also inulin might have an optimum range of Mw in terms of functionality as the long chain inulin did not have the capacity for efficient water binding and retention as opposed to the shorter chain inulin (sections 5.3.2, 5.3.4 and 5.3.5). Hence the highest Mw is not always the most favourable, neither for BG nor inulin.

DF's physico-chemical properties including rheology and water interaction as well as binding properties underpin the interference mechanisms during small intestinal duodenal digestion of lipids and starch as well as interactions with BA. This influence and reduction of macronutrient digestion and increased BA excretion can lead to health benefits such as reduced risk of diabetes and CV diseases as found in epidemiological studies among high fibre consumers (Stephen *et al.* 2017, Reynolds *et al.* 2019, Larrosa *et al.* 2020). Incorporation of DF into foods under controlled processing conditions to achieve the most effective matrix structure and physico-chemical behaviour during digestion seems to be a good

way to produce healthier foods designed to tackle a range of problems associated with obesity and poor health.

## 7.2  Future work

This thesis together with the current literature has proposed potential mechanisms underpinning the health benefits of DF. Further research into these possible mechanisms is required to help develop practical solutions and strategies that could be used in the development of healthier foods. Suggestions of future work were made throughout in the discussion sections including:

- Follow lipid droplet properties in *in vitro* lipid digestions in presence of oat and barley bran to test for flocculation

- Test different concentrations of barley or oat fibre at the same mixing speed, use lipase + colipase instead of pancreatin and less lipase overall, determine viscosity

- Investigate rheological properties and flow behaviour further including impact of fibre particles on viscous network properties (microviscosity vs bulk viscosity)

- Develop a DF lipase binding assay based on the solution depletion method

- Study impact of solubilisation of fibres on cell wall porosity for digestive enzymes

- Determine if oat bran particles can be found in the as hydrated, swollen fibre particles following digestion in a human study

- Investigate and define *in vitro* rheology conditions relevant *in vivo*

- Test long-term binding of specific BA species to barley, oat and wheat bran

- Determine inulin thermostability in biscuits

- Test with FITC-labelled amylase if there is a physical barrier mechanism adding to the lower starch digestibility results seen in soluble inulin biscuits

- Human glycaemic index study with inulin biscuits

- Sensory testing of inulin biscuits

## 7.3   Research impact and applications

Although DF intake recommendations exist, targeted intake advice towards a putative health benefit is limited as there is still a knowledge gap on DF structure-function relationships. This thesis has added knowledge on some of the causal mechanisms leading to beneficial health effects of DF. This can be used by government bodies to inform dietary recommendations as well as by food manufacturers to help develop healthier foods. This thesis also raises important questions around DF and shows gaps of knowledge to inform future research on DF.

# References

AACC 1999. 10-53.01 Baking Quality of Cookie Flour—Macro Wire-Cut Formulation. AACC International Methods.

AACC, A. A. O. C. C. 2001. The Definition of Dietary Fiber. *Cereal Foods World,* 46**,** 112-126.

ABUMWEIS, S. S., JEW, S. & AMES, N. P. 2010. beta-glucan from barley and its lipid-lowering capacity: a meta-analysis of randomized, controlled trials. *Eur J Clin Nutr,* 64**,** 1472-80.

AGUILAR, M.-I. 2004. Reversed-Phase High-Performance Liquid Chromatography. *In:* AGUILAR, M.-I. (ed.) *HPLC of Peptides and Proteins: Methods and Protocols.* Totowa, NJ: Springer New York.

AGUILERA, J. M. 2019. The food matrix: Implications in processing, nutrition and health. *Critical Reviews in Food Science and Nutrition,* 59**,** 3612-3629.

AGUILERA, J. M. & STANLEY, D. W. 1999. *Microstructural principles of food processing and engineering*, Springer Science & Business Media.

AHMAD, F. B. & WILLIAMS, P. A. 1999. Effect of sugars on the thermal and rheological properties of sago starch. *Biopolymers,* 50**,** 401-412.

AHMADI, S., YU, C., ZAEIM, D., WU, D., HU, X., YE, X. & CHEN, S. 2022. Increasing RG-I content and lipase inhibitory activity of pectic polysaccharides extracted from goji berry and raspberry by high-pressure processing. *Food Hydrocolloids,* 126**,** 107477.

ALLAN, M. C., RAJWA, B. & MAUER, L. J. 2018. Effects of sugars and sugar alcohols on the gelatinization temperature of wheat starch. *Food Hydrocolloids,* 84**,** 593-607.

ANDERSON, J. W., ALLGOOD, L. D., LAWRENCE, A., ALTRINGER, L. A., JERDACK, G. R., HENGEHOLD, D. A. & MOREL, J. G. 2000. Cholesterol-lowering effects of psyllium intake adjunctive to diet therapy in men and women with hypercholesterolemia: meta-analysis of 8 controlled trials. *The American Journal of Clinical Nutrition,* 71**,** 472-479.

ANDERSSON, A. A. M., ANDERSSON, R., JONSALL, A., ANDERSSON, J. & FREDRIKSSON, H. 2017. Effect of Different Extrusion Parameters on Dietary Fiber in Wheat Bran and Rye Bran. *J Food Sci,* 82**,** 1344-1350.

ANDERSSON, R., ELIASSON, C., SELENARE, M., KAMAL-ELDIN, A. & AMAN, P. 2003. Effect of endo-xylanase-containing enzyme preparations and laccase on the solubility of rye bran arabinoxylan. *Journal of the Science of Food and Agriculture,* 83**,** 617-623.

AUGUSTIN, L. S. A., AAS, A.-M., ASTRUP, A., ATKINSON, F. S., BAER-SINNOTT, S., BARCLAY, A. W., BRAND-MILLER, J. C., BRIGHENTI, F., BULLO, M., BUYKEN, A. E., CERIELLO, A., ELLIS, P. R., HA, M.-A., HENRY, J. C., KENDALL, C. W. C., LA VECCHIA, C., LIU, S., LIVESEY, G., POLI, A., SALAS-SALVADÓ, J., RICCARDI, G., RISERUS, U., RIZKALLA, S. W., SIEVENPIPER, J. L., TRICHOPOULOU, A., USIC, K., WOLEVER, T. M. S., WILLETT, W. C. & JENKINS, D. J. A. 2020. Dietary Fibre Consensus from the International Carbohydrate Quality Consortium (ICQC). *Nutrients,* 12**,** 2553.

BABIKER, R., MERGHANI, T. H., ELMUSHARAF, K., BADI, R. M., LANG, F. & SAEED, A. M. 2012. Effects of gum Arabic ingestion on body mass index and body fat percentage in healthy adult females: two-arm

randomized, placebo controlled, double-blind trial. *Nutrition Journal,* 11**,** 111.

BAJKA, B. H., PINTO, A. M., AHN-JARVIS, J., RYDEN, P., PEREZ-MORAL, N., VAN DER SCHOOT, A., STOCCHI, C., BLAND, C., BERRY, S. E., ELLIS, P. R. & EDWARDS, C. H. 2021. The impact of replacing wheat flour with cellular legume powder on starch bioaccessibility, glycaemic response and bread roll quality: A double-blind randomised controlled trial in healthy participants. *Food Hydrocolloids,* 114**,** 106565.

BALLANCE, S., LU, Y., ZOBEL, H., RIEDER, A., KNUTSEN, S. H., DINU, V. T., CHRISTENSEN, B. E., ULSET, A.-S., SCHMID, M., MAINA, N., POTTHAST, A., SCHIEHSER, S., ELLIS, P. R. & HARDING, S. E. 2022. Inter-laboratory analysis of cereal beta-glucan extracts of nutritional importance: An evaluation of different methods for determining weight-average molecular weight and molecular weight distribution. *Food Hydrocolloids,* 127**,** 107510.

BECKMAN COULTER. Accessed 02/07/2022. Available: https://www.beckman.com/resources/technologies/laser-diffraction [Accessed].

BELLESI, F. A., MARTINEZ, M. J., PIZONES RUIZ-HENESTROSA, V. M. & PILOSOF, A. M. R. 2016. Comparative behavior of protein or polysaccharide stabilized emulsion under in vitro gastrointestinal conditions. *Food Hydrocolloids,* 52**,** 47-56.

BEMILLER, J. N. & WHISTLER, R. L. 2009. *Starch: chemistry and technology*, Academic Press.

BHATTY, R. S. 1993. PHYSICOCHEMICAL PROPERTIES OF ROLLER-MILLED BARLEY BRAN AND FLOUR. *Cereal Chemistry,* 70**,** 397-402.

BIORKLUND, M., VAN REES, A., MENSINK, R. P. & ONNING, G. 2005. Changes in serum lipids and postprandial glucose and insulin concentrations after consumption of beverages with beta-glucans from oats or barley: a randomised dose-controlled trial. *Eur J Clin Nutr,* 59**,** 1272-81.

BLACKMAN, L. M., CULLERNE, D. P. & HARDHAM, A. R. 2014. Bioinformatic characterisation of genes encoding cell wall degrading enzymes in the Phytophthora parasitica genome. *Bmc Genomics,* 15.

BLANCO CANALIS, M. S., LEÓN, A. E. & RIBOTTA, P. D. 2019. Incorporation of dietary fiber on the cookie dough. Effects on thermal properties and water availability. *Food Chemistry,* 271**,** 309-317.

BOGRACHEVA, T., WANG, Y., WANG, T. & HEDLEY, C. 2002. Structural studies of starches with different water contents. *Biopolymers: Original Research on Biomolecules,* 64**,** 268-281.

BRENNAN, C. & SAMYUE, E. 2004. Evaluation of starch degradation and textural characteristics of dietary fiber enriched biscuits. *International Journal of Food Properties,* 7**,** 647-657.

BRODKORB, A., EGGER, L., ALMINGER, M., ALVITO, P., ASSUNÇÃO, R., BALLANCE, S., BOHN, T., BOURLIEU-LACANAL, C., BOUTROU, R., CARRIÈRE, F., CLEMENTE, A., CORREDIG, M., DUPONT, D., DUFOUR, C., EDWARDS, C., GOLDING, M., KARAKAYA, S., KIRKHUS, B., LE FEUNTEUN, S., LESMES, U., MACIERZANKA, A., MACKIE, A. R., MARTINS, C., MARZE, S., MCCLEMENTS, D. J., MÉNARD, O., MINEKUS, M., PORTMANN, R., SANTOS, C. N., SOUCHON, I., SINGH, R. P., VEGARUD, G. E., WICKHAM, M. S. J., WEITSCHIES, W. &

RECIO, I. 2019. INFOGEST static in vitro simulation of gastrointestinal food digestion. *Nature Protocols,* 14**,** 991-1014.

BROUNS, F., THEUWISSEN, E., ADAM, A., BELL, M., BERGER, A. & MENSINK, R. P. 2011. Cholesterol-lowering properties of different pectin types in mildly hyper-cholesterolemic men and women. *European Journal Of Clinical Nutrition,* 66**,** 591.

BRUMMER, Y., DUSS, R., WOLEVER, T. M. S. & TOSH, S. M. 2012. Glycemic Response to Extruded Oat Bran Cereals Processed to Vary in Molecular Weight. *Cereal Chemistry,* 89**,** 255-261.

BURKITT, D. P., WALKER, A. R. & PAINTER, N. S. 1972. Effect of dietary fibre on stools and the transit-times, and its role in the causation of disease. *Lancet,* 2**,** 1408-12.

BYRNE, C. S., BLUNT, D., BURN, J., CHAMBERS, E., DAGBASI, A., FRANCO BECKER, G., GIBSON, G., MENDOZA, L., MURPHY, K., POVEDA, C., RAMGULAM, A., TASHKOVA, M., WALTON, G., WASHIRASAKSIRI, C. & FROST, G. 2019. A study protocol for a randomised crossover study evaluating the effect of diets differing in carbohydrate quality on ileal content and appetite regulation in healthy humans. *F1000Res,* 8**,** 258.

CAÑAS, S., PEREZ-MORAL, N. & EDWARDS, C. H. 2020. Effect of cooking, 24 h cold storage, microwave reheating, and particle size on in vitro starch digestibility of dry and fresh pasta. *Food & function,* 11**,** 6265-6272.

CAPUANO, E. 2017. The behavior of dietary fiber in the gastrointestinal tract determines its physiological effect. *Crit Rev Food Sci Nutr,* 57**,** 3543-3564.

CAPUANO, E., OLIVIERO, T., FOGLIANO, V. & PELLEGRINI, N. 2018. Role of the food matrix and digestion on calculation of the actual energy content of food. *Nutr Rev,* 76**,** 274-289.

CARA, L., BOREL, P., ARMAND, M., LAFONT, H., LESGARDS, G. & LAIRON, D. 1992. Milling and processing of wheat and other cereals affect their capacity to inhibit pancreatic lipase in vitro. *Journal of food science,* 57**,** 466-469.

CAVE, R. A., SEABROOK, S. A., GIDLEY, M. J. & GILBERT, R. G. 2009. Characterization of Starch by Size-Exclusion Chromatography: The Limitations Imposed by Shear Scission. *Biomacromolecules,* 10**,** 2245-2253.

CERVANTES-PAZ, B., ORNELAS-PAZ, J. J., RUIZ-CRUZ, S., RIOS-VELASCO, C., IBARRA-JUNQUERA, V., YAHIA, E. M. & GARDEA-BEJAR, A. A. 2017. Effects of pectin on lipid digestion and possible implications for carotenoid bioavailability during pre-absorptive stages: A review. *Food Res Int,* 99**,** 917-927.

CHAMBERS, E. S., MORRISON, D. J. & FROST, G. 2015. Control of appetite and energy intake by SCFA: what are the potential underlying mechanisms? *Proceedings of the Nutrition Society,* 74**,** 328-336.

CHAWLA, R. & PATIL, G. R. 2010. Soluble Dietary Fiber. *Comprehensive Reviews in Food Science and Food Safety,* 9**,** 178-196.

CHIAPPISI, L. & GRADZIELSKI, M. 2015. Co-assembly in chitosan–surfactant mixtures: thermodynamics, structures, interfacial properties and applications. *Advances in Colloid and Interface Science,* 220**,** 92-107.

CODEX ALIMENTARIUS COMMISSION, C. 2009. Report of the 30th session of the Codex Commitee on Nutrition and Foods for Special Dietary Uses. *In:* PROGRAMME, J. F. W. F. S. (ed.).

COLOSIMO, R., MULET-CABERO, A.-I., CROSS, K. L., HAIDER, K., EDWARDS, C. H., WARREN, F. J., FINNIGAN, T. J. A. & WILDE, P. J. 2021. β-glucan release from fungal and plant cell walls after simulated gastrointestinal digestion. *Journal of Functional Foods,* 83, 104543.

COLOSIMO, R., MULET-CABERO, A.-I., WARREN, F. J., EDWARDS, C. H., FINNIGAN, T. J. & WILDE, P. J. 2020a. Mycoprotein ingredient structure reduces lipolysis and binds bile salts during simulated gastrointestinal digestion. *Food & function,* 11, 10896-10906.

COLOSIMO, R., WARREN, F. J., EDWARDS, C. H., FINNIGAN, T. J. A. & WILDE, P. J. 2020b. The interaction of α-amylase with mycoprotein: Diffusion through the fungal cell wall, enzyme entrapment, and potential physiological implications. *Food Hydrocolloids,* 108, 106018.

COMINO, P., SHELAT, K., COLLINS, H., LAHNSTEIN, J. & GIDLEY, M. J. 2013. Separation and purification of soluble polymers and cell wall fractions from wheat, rye and hull less barley endosperm flours for structure-nutrition studies. *J Agric Food Chem,* 61, 12111-22.

COOKE, D. & GIDLEY, M. J. 1992. Loss of crystalline and molecular order during starch gelatinisation: origin of the enthalpic transition. *Carbohydrate research,* 227, 103-112.

CORSTENS, M. N., BERTON-CARABIN, C. C., DE VRIES, R., TROOST, F. J., MASCLEE, A. A. & SCHROËN, K. 2017. Food-grade micro-encapsulation systems that may induce satiety via delayed lipolysis: a review. *Critical Reviews in Food Science and Nutrition,* 57, 2218-2244.

COURTIN, C. M. & DELCOUR, J. A. 2002. Arabinoxylans and Endoxylanases in Wheat Flour Bread-making. *Journal of Cereal Science,* 35, 225-243.

CRAIG, D. Q., ROYALL, P. G., KETT, V. L. & HOPTON, M. L. 1999. The relevance of the amorphous state to pharmaceutical dosage forms: glassy drugs and freeze dried systems. *International journal of pharmaceutics,* 179, 179-207.

DAN, A., GHOSH, S. & MOULIK, S. P. 2009. Physicochemical studies on the biopolymer inulin: A critical evaluation of its self-aggregation, aggregate-morphology, interaction with water, and thermal stability. *Biopolymers: Original Research on Biomolecules,* 91, 687-699.

DAVISON, K. M. & TEMPLE, N. J. 2018. Cereal fiber, fruit fiber, and type 2 diabetes: Explaining the paradox. *J Diabetes Complications,* 32, 240-245.

DE GENNARO, S., BIRCH, G. G., PARKE, S. A. & STANCHER, B. 2000. Studies on the physicochemical properties of inulin and inulin oligomers. *Food Chemistry,* 68, 179-183.

DE GRAAF, C. 2012. Texture and satiation: the role of oro-sensory exposure time. *Physiol Behav,* 107, 496-501.

DHINGRA, D., MICHAEL, M., RAJPUT, H. & PATIL, R. T. 2012. Dietary fibre in foods: a review. *J Food Sci Technol,* 49, 255-66.

DHITAL, S., DOLAN, G., STOKES, J. R. & GIDLEY, M. J. 2014a. Enzymatic hydrolysis of starch in the presence of cereal soluble fibre polysaccharides. *Food & Function,* 5, 579-586.

DHITAL, S., GIDLEY, M. J. & WARREN, F. J. 2015. Inhibition of α-amylase activity by cellulose: Kinetic analysis and nutritional implications. *Carbohydrate Polymers,* 123**,** 305-312.

DHITAL, S., WARREN, F. J., ZHANG, B. & GIDLEY, M. J. 2014b. Amylase binding to starch granules under hydrolysing and non-hydrolysing conditions. *Carbohydrate Polymers,* 113**,** 97-107.

DIAS, C. B., ZHU, X., THOMPSON, A. K., SINGH, H. & GARG, M. L. 2019. Effect of the food form and structure on lipid digestion and postprandial lipaemic response. *Food Funct,* 10**,** 112-124.

DONOVAN, J. & MAPES, C. 1980. Multiple phase transitions of starches and Nägeli amylodextrins. *Starch‐Stärke,* 32**,** 190-193.

DONOVAN, J. W. 1979. Phase transitions of the starch–water system. *Biopolymers: Original Research on Biomolecules,* 18**,** 263-275.

DORNEZ, E., GEBRUERS, K., JOYE, I. J., DE KETELAERE, B., LENARTZ, J., MASSAUX, C., BODSON, B., DELCOUR, J. A. & COURTIN, C. M. 2008. Effects of genotype, harvest year and genotype-by-harvest year interactions on arabinoxylan, endoxylanase activity and endoxylanase inhibitor levels in wheat kernels. *Journal of Cereal Science,* 47**,** 180-189.

DRESSMAN, J. B. 1986. Comparison of canine and human gastrointestinal physiology. *Pharmaceutical Research,* 3**,** 123-131.

DRZIKOVA, B., DONGOWSKI, G., GEBHARDT, E. & HABEL, A. 2005. The composition of dietary fibre-rich extrudates from oat affects bile acid binding and fermentation in vitro. *Food Chemistry,* 90**,** 181-192.

DUTTA, S. K. & HLASKO, J. 1985. Dietary fiber in pancreatic disease: Effect of high fiber diet on fat malabsorption in pancreatic insufficiency and in vitro study of the interaction of dietary fiber with pancreatic enzymes. *The American Journal of Clinical Nutrition,* 41**,** 517-525.

EASTWOOD, M. A. & MORRIS, E. R. 1992. Physical properties of dietary fiber that influence physiological function: a model for polymers along the gastrointestinal tract. *Am J Clin Nutr,* 55**,** 436-42.

EDWARDS, C. H., COCHETEL, N., SETTERFIELD, L., PEREZ-MORAL, N. & WARREN, F. J. 2019. A single-enzyme system for starch digestibility screening and its relevance to understanding and predicting the glycaemic index of food products. *Food & function,* 10**,** 4751-4760.

EDWARDS, C. H., MAILLOT, M., PARKER, R. & WARREN, F. J. 2018. A comparison of the kinetics of in vitro starch digestion in smooth and wrinkled peas by porcine pancreatic alpha-amylase. *Food Chemistry,* 244**,** 386-393.

EDWARDS, C. H., RYDEN, P., MANDALARI, G., BUTTERWORTH, P. J. & ELLIS, P. R. 2021. Structure–function studies of chickpea and durum wheat uncover mechanisms by which cell wall properties influence starch bioaccessibility. *Nature Food,* 2**,** 118-126.

EDWARDS, C. H. & WARREN, F. J. 2019. Starchy Foods: Human Nutrition and Public Health. *In:* GOUSETI, O., BORNHORST, G. M., BAKALIS, S. & MACKIE, A. (eds.) *Interdisciplinary Approaches to Food Digestion.* Cham: Springer International Publishing.

EFSA PANEL ON DIETETIC PRODUCTS, N. & ALLERGIES 2009. Scientific Opinion on the substantiation of health claims related to beta glucans and maintenance of normal blood cholesterol concentrations (ID 754, 755, 757, 801, 1465, 2934) and maintenance or achievement of a normal body weight (ID 820, 823)

pursuant to Article 13(1) of Regulation (EC) No 1924/2006. *EFSA Journal,* 7**,** 1254.

EFSA PANEL ON DIETETIC PRODUCTS, N. & ALLERGIES 2010a. Scientific Opinion on the substantiation of a health claim related to oat beta glucan and lowering blood cholesterol and reduced risk of (coronary) heart disease pursuant to Article 14 of Regulation (EC) No 1924/2006. *EFSA Journal,* 8**,** 1885.

EFSA PANEL ON DIETETIC PRODUCTS, N. & ALLERGIES 2010b. Scientific Opinion on the substantiation of health claims related to beta glucans and maintenance or achievement of normal blood glucose concentrations (ID 756, 802, 2935) pursuant to Article 13(1) of Regulation (EC) No 1924/2006. *EFSA Journal,* 8**,** 1482.

EFSA PANEL ON DIETETIC PRODUCTS, N. & ALLERGIES 2011a. Scientific Opinion on the substantiation of a health claim related to barley beta-glucans and lowering of blood cholesterol and reduced risk of (coronary) heart disease pursuant to Article 14 of Regulation (EC) No 1924/2006. *EFSA Journal,* 9**,** 2470.

EFSA PANEL ON DIETETIC PRODUCTS, N. & ALLERGIES 2011b. Scientific Opinion on the substantiation of health claims related to beta-glucans from oats and barley and maintenance of normal blood LDL-cholesterol concentrations (ID 1236, 1299), increase in satiety leading to a reduction in energy intake (ID 851, 852), reduction of post-prandial glycaemic responses (ID 821, 824), and "digestive function" (ID 850) pursuant to Article 13(1) of Regulation (EC) No 1924/2006. *EFSA Journal,* 9**,** 2207.

ELIASSON, A. C. 1992. A calorimetric investigation of the influence of sucrose on the gelatinization of starch. *Carbohydrate Polymers,* 18**,** 131-138.

ELLEGARD, L. & ANDERSSON, H. 2007. Oat bran rapidly increases bile acid excretion and bile acid synthesis: an ileostomy study. *Eur J Clin Nutr,* 61**,** 938-45.

ELLIS, P. R., KENDALL, C. W. C., REN, Y., PARKER, C., PACY, J. F., WALDRON, K. W. & JENKINS, D. J. A. 2004. Role of cell walls in the bioaccessibility of lipids in almond seeds. *The American Journal of Clinical Nutrition,* 80**,** 604-613.

ENGLAND, P. H. 2017. Nutrient analysis of fruits and vegetables 2015.

EPP, J. 2016. 4 - X-ray diffraction (XRD) techniques for materials characterization. *In:* HÜBSCHEN, G., ALTPETER, I., TSCHUNCKY, R. & HERRMANN, H.-G. (eds.) *Materials Characterization Using Nondestructive Evaluation (NDE) Methods.* Woodhead Publishing.

ESFANDI, R., SEIDU, I., WILLMORE, W. & TSOPMO, A. 2022. Antioxidant, pancreatic lipase, and α-amylase inhibitory properties of oat bran hydrolyzed proteins and peptides. *Journal of Food Biochemistry,* 46**,** e13762.

EUSTON, S. R., BAIRD, W. G., CAMPBELL, L. & KUHNS, M. 2013. Competitive adsorption of dihydroxy and trihydroxy bile salts with whey protein and casein in oil-in-water emulsions. *Biomacromolecules,* 14**,** 1850-1858.

FAAS, H., STEINGOETTER, A., FEINLE, C., RADES, T., LENGSFELD, H., BOESIGER, P., FRIED, M. & SCHWIZER, W. 2002. Effects of meal consistency and ingested fluid volume on the intragastric distribution of a drug model in humans—a magnetic resonance

imaging study. *Alimentary pharmacology & therapeutics,* 16**,** 217-224.

FESSAS, D. & SCHIRALDI, A. 2000. Starch Gelatinization Kinetics in Bread Dough. DSC investigations on'simulated'baking processes. *Journal of Thermal Analysis and Calorimetry,* 61**,** 411-423.

FLYNN, C. S. 2012. *The particle size distribution of solid foods after human mastication.* PhD, Massey University, Aukland, New Zealand.

FRANCK, A. 2002. Technological functionality of inulin and oligofructose. *British journal of Nutrition,* 87**,** S287-S291.

GALANTINI, L., DI GREGORIO, M. C., GUBITOSI, M., TRAVAGLINI, L., TATO, J. V., JOVER, A., MEIJIDE, F., TELLINI, V. H. S. & PAVEL, N. V. 2015. Bile salts and derivatives: Rigid unconventional amphiphiles as dispersants, carriers and superstructure building blocks. *Current Opinion in Colloid & Interface Science,* 20**,** 170-182.

GEMEN, R., DE VRIES, J. F. & SLAVIN, J. L. 2011. Relationship between molecular structure of cereal dietary fiber and health effects: focus on glucose/insulin response and gut health. *Nutr Rev,* 69**,** 22-33.

GENOVESE, D. B. 2012. Shear rheology of hard-sphere, dispersed, and aggregated suspensions, and filler-matrix composites. *Advances in Colloid and Interface Science,* 171-172**,** 1-16.

GENTILCORE, D., CHAIKOMIN, R., JONES, K. L., RUSSO, A., FEINLE-BISSET, C., WISHART, J. M., RAYNER, C. K. & HOROWITZ, M. 2006. Effects of fat on gastric emptying of and the glycemic, insulin, and incretin responses to a carbohydrate meal in type 2 diabetes. *The Journal of Clinical Endocrinology & Metabolism,* 91**,** 2062-2067.

GIDLEY, M. J. & YAKUBOV, G. E. 2019. Functional categorisation of dietary fibre in foods: Beyond 'soluble' vs 'insoluble'. *Trends in Food Science & Technology,* 86**,** 563-568.

GOFF, H. D., REPIN, N., FABEK, H., EL KHOURY, D. & GIDLEY, M. J. 2018. Dietary fibre for glycaemia control: Towards a mechanistic understanding. *Bioactive Carbohydrates and Dietary Fibre,* 14**,** 39-53.

GOLDING, M. & WOOSTER, T. J. 2010. The influence of emulsion structure and stability on lipid digestion. *Current Opinion in Colloid & Interface Science,* 15**,** 90-101.

GOUDAR, G., SHARMA, P., JANGHU, S. & LONGVAH, T. 2020. Effect of processing on barley β-glucan content, its molecular weight and extractability. *International Journal of Biological Macromolecules,* 162**,** 1204-1216.

GRANTHAM, N. J., WURMAN-RODRICH, J., TERRETT, O. M., LYCZAKOWSKI, J. J., STOTT, K., IUGA, D., SIMMONS, T. J., DURAND-TARDIF, M., BROWN, S. P., DUPREE, R., BUSSE-WICHER, M. & DUPREE, P. 2017. An even pattern of xylan substitution is critical for interaction with cellulose in plant cell walls. *Nature Plants,* 3**,** 859-865.

GRIBBLE, F. M. & REIMANN, F. 2022. Nutrient sensing in the gut and the regulation of appetite. *Current Opinion in Endocrine and Metabolic Research,* 23**,** 100318.

GRUNDY, M. M., EDWARDS, C. H., MACKIE, A. R., GIDLEY, M. J., BUTTERWORTH, P. J. & ELLIS, P. R. 2016. Re-evaluation of the mechanisms of dietary fibre and implications for macronutrient bioaccessibility, digestion and postprandial metabolism. *Br J Nutr,* 116**,** 816-33.

GRUNDY, M. M., FARDET, A., TOSH, S. M., RICH, G. T. & WILDE, P. J. 2018a. Processing of oat: the impact on oat's cholesterol lowering effect. *Food Funct,* 9**,** 1328-1343.

GRUNDY, M. M., QUINT, J., RIEDER, A., BALLANCE, S., DREISS, C. A., BUTTERWORTH, P. J. & ELLIS, P. R. 2017a. Impact of hydrothermal and mechanical processing on dissolution kinetics and rheology of oat beta-glucan. *Carbohydr Polym,* 166**,** 387-397.

GRUNDY, M. M., WILDE, P. J., BUTTERWORTH, P. J., GRAY, R. & ELLIS, P. R. 2015. Impact of cell wall encapsulation of almonds on in vitro duodenal lipolysis. *Food Chem,* 185**,** 405-12.

GRUNDY, M. M. L., MCCLEMENTS, D. J., BALLANCE, S. & WILDE, P. J. 2018b. Influence of oat components on lipid digestion using an in vitro model: Impact of viscosity and depletion flocculation mechanism. *Food Hydrocoll,* 83**,** 253-264.

GRUNDY, M. M. L., QUINT, J., RIEDER, A., BALLANCE, S., DREISS, C. A., CROSS, K. L., GRAY, R., BAJKA, B. H., BUTTERWORTH, P. J., ELLIS, P. R. & WILDE, P. J. 2017b. The impact of oat structure and beta-glucan on in vitro lipid digestion. *J Funct Foods,* 38**,** 378-388.

GUERRA, A., ETIENNE-MESMIN, L., LIVRELLI, V., DENIS, S., BLANQUET-DIOT, S. & ALRIC, M. 2012. Relevance and challenges in modeling human gastric and small intestinal digestion. *Trends in Biotechnology,* 30**,** 591-600.

GUILLON, F. & CHAMP, M. 2000. Structural and physical properties of dietary fibres, and consequences of processing on human physiology. *Food Research International,* 33**,** 233-245.

GUILLON, F. & CHAMP, M. M. 2002. Carbohydrate fractions of legumes: uses in human nutrition and potential for health. *Br J Nutr,* 88 Suppl 3**,** S293-306.

GUNNESS, P., FLANAGAN, B. M. & GIDLEY, M. J. 2010. Molecular interactions between cereal soluble dietary fibre polymers and a model bile salt deduced from 13C NMR titration. *Journal of Cereal Science,* 52**,** 444-449.

GUNNESS, P., FLANAGAN, B. M., MATA, J. P., GILBERT, E. P. & GIDLEY, M. J. 2016. Molecular interactions of a model bile salt and porcine bile with (1,3:1,4)-beta-glucans and arabinoxylans probed by (13)C NMR and SAXS. *Food Chem,* 197**,** 676-85.

GUNNESS, P., FLANAGAN, B. M., SHELAT, K., GILBERT, R. G. & GIDLEY, M. J. 2012. Kinetic analysis of bile salt passage across a dialysis membrane in the presence of cereal soluble dietary fibre polymers. *Food Chem,* 134**,** 2007-13.

GUNNESS, P. & GIDLEY, M. J. 2010. Mechanisms underlying the cholesterol-lowering properties of soluble dietary fibre polysaccharides. *Food Funct,* 1**,** 149-55.

GUO, H., LIN, S., LU, M., GONG, J. D. B., WANG, L., ZHANG, Q., LIN, D.-R., QIN, W. & WU, D.-T. 2018. Characterization, in vitro binding properties, and inhibitory activity on pancreatic lipase of β-glucans from different Qingke (Tibetan hulless barley) cultivars. *International journal of biological macromolecules,* 120**,** 2517-2522.

GUO, Q., BELLISSIMO, N. & ROUSSEAU, D. 2017. Role of gel structure in controlling in vitro intestinal lipid digestion in whey protein emulsion gels. *Food Hydrocolloids,* 69**,** 264-272.

HAIDER, K. & WILDE, P. 2020. Digestion and metabolism of pectin. *Pectin: Technological and Physiological Properties.* Springer.

HAKKOLA, S., NYLUND, L., ROSA-SIBAKOV, N., YANG, B., NORDLUND, E., PAHIKKALA, T., KALLIOMÄKI, M., AURA, A.-M. & LINDERBORG, K. M. 2021. Effect of oat β-glucan of different molecular weights on fecal bile acids, urine metabolites and pressure in the digestive tract – A human cross over trial. *Food Chemistry,* 342**,** 128219.

HAN, J., LIU, Y., WANG, R., YANG, J., LING, V. & BORCHERS, C. H. 2015. Metabolic profiling of bile acids in human and mouse blood by LC–MS/MS in combination with phospholipid-depletion solid-phase extraction. *Analytical chemistry,* 87**,** 1127-1136.

HANDA, C., GOOMER, S. & SIDDHU, A. 2012. Physicochemical properties and sensory evaluation of fructoligosaccharide enriched cookies. *Journal of food science and technology,* 49**,** 192-199.

HARDACRE, A. K., LENTLE, R. G., YAP, S.-Y. & MONRO, J. A. 2016. Does viscosity or structure govern the rate at which starch granules are digested? *Carbohydrate Polymers,* 136**,** 667-675.

HASJIM, J., AI, Y. & JANE, J.-L. 2013. Novel Applications of Amylose-Lipid Complex as Resistant Starch Type 5. *Resistant Starch.*

HELLSTRÖM, P. M., GRYBÄCK, P. & JACOBSSON, H. 2006. The physiology of gastric emptying. *Best Practice & Research Clinical Anaesthesiology,* 20**,** 397-407.

HENRION, M., FRANCEY, C., LE, K. A. & LAMOTHE, L. 2019. Cereal B-Glucans: The Impact of Processing and How It Affects Physiological Responses. *Nutrients,* 11.

HEYER, A., SCHROEER, B., RADOSTA, S., WOLFF, D., CZAPLA, S. & SPRINGER, J. 1998. Structure of the enzymatically synthesized fructan inulin. *Carbohydrate research,* 313**,** 165-174.

HOEBLER, C., KARINTHI, A., DEVAUX, M.-F., GUILLON, F., GALLANT, D., BOUCHET, B., MELEGARI, C. & BARRY, J.-L. 1998. Physical and chemical transformations of cereal food during oral digestion in human subjects. *British Journal of Nutrition,* 80**,** 429-436.

HOLLAND, C., RYDEN, P., EDWARDS, C. H. & GRUNDY, M. M.-L. 2020. Plant Cell Walls: Impact on Nutrient Bioaccessibility and Digestibility. *Foods,* 9**,** 201.

HOLMA, R., HONGISTO, S. M., SAXELIN, M. & KORPELA, R. 2010. Constipation is relieved more by rye bread than wheat bread or laxatives without increased adverse gastrointestinal effects. *J Nutr,* 140**,** 534-41.

HOU, C., ZHAO, X., TIAN, M., ZHOU, Y., YANG, R., GU, Z. & WANG, P. 2020. Impact of water extractable arabinoxylan with different molecular weight on the gelatinization and retrogradation behavior of wheat starch. *Food chemistry,* 318**,** 126477.

HOUSTON, K., TUCKER, M. R., CHOWDHURY, J., SHIRLEY, N. & LITTLE, A. 2016. The Plant Cell Wall: A Complex and Dynamic Structure As Revealed by the Responses of Genes under Stress Conditions. *Frontiers in Plant Science,* 7.

HUR, S. J., LIM, B. O., DECKER, E. A. & MCCLEMENTS, D. J. 2011. In vitro human digestion models for food applications. *Food chemistry,* 125**,** 1-12.

IACCARINO, N., KHAKIMOV, B., MIKKELSEN, M. S., NIELSEN, T. S., JENSEN, M. G., RANDAZZO, A. & ENGELSEN, S. B. 2020. Structurally different mixed linkage β-glucan supplements differentially increase secondary bile acid excretion in hypercholesterolaemic rat faeces. *Food & Function,* 11**,** 514-523.

IZYDORCZYK, M. S. 2009. Arabinoxylans. *Handbook of Hydrocolloids.*

JARVIS, M. C. 2011. Plant cell walls: Supramolecular assemblies. *Food Hydrocolloids,* 25**,** 257-262.

JEFFREY, B., UDAYKUMAR, H. S. & SCHULZE, K. S. 2003. Flow fields generated by peristaltic reflex in isolated guinea pig ileum: impact of contraction depth and shoulders. *American Journal of Physiology-Gastrointestinal and Liver Physiology,* 285**,** G907-G918.

JENKINS, D. J. A., LEEDS, A. R., SLAVIN, B., MANN, J. & JEPSON, E. M. 1979. Dietary fiber and blood lipids: reduction of serum cholesterol in type II hyperlipidemia by guar gum. *The American Journal of Clinical Nutrition,* 32**,** 16-18.

JENSEN, M. G., KNUDSEN, J. C., VIERECK, N., KRISTENSEN, M. & ASTRUP, A. 2012. Functionality of alginate based supplements for application in human appetite regulation. *Food Chemistry,* 132**,** 823-829.

JIFFRY, M. T. M. 1981. Analysis of particles produced at the end of mastication in subjects with normal dentition. *Journal of Oral Rehabilitation,* 8**,** 113-119.

JOVANOVSKI, E., MAZHAR, N., KOMISHON, A., KHAYYAT, R., LI, D., BLANCO MEJIA, S., KHAN, T., A, L. J., SMIRCIC-DUVNJAK, L., J, L. S. & VUKSAN, V. 2020. Can dietary viscous fiber affect body weight independently of an energy-restrictive diet? A systematic review and meta-analysis of randomized controlled trials. *Am J Clin Nutr,* 111**,** 471-485.

KAHLON, T. S., BERRIOS, J. D., SMITH, G. E. & PAN, J. L. 2006. In vitro bile acid binding capacity of wheat bran extruded at five specific mechanical energy levels. *Cereal Chemistry,* 83**,** 157-160.

KAHLON, T. S. & SMITH, G. E. 2007. In vitro binding of bile acids by bananas, peaches, pineapple, grapes, pears, apricots and nectarines. *Food Chemistry,* 101**,** 1046-1051.

KAHLON, T. S. & WOODRUFF, C. L. 2003. In vitro binding of bile acids by rice bran, oat bran, barley and beta-glucan enriched barley. *Cereal Chemistry,* 80**,** 260-263.

KAMAL-ELDIN, A., LAERKE, H. N., KNUDSEN, K. E., LAMPI, A. M., PIIRONEN, V., ADLERCREUTZ, H., KATINA, K., POUTANEN, K. & MAN, P. 2009. Physical, microscopic and chemical characterisation of industrial rye and wheat brans from the Nordic countries. *Food Nutr Res,* 53.

KANG, J.-S. 2012. Principles and applications of LC-MS/MS for the quantitative bioanalysis of analytes in various biological samples. *Tandem Mass Spectrometry–Applications and Principles***,** 441-492.

KHOSSOUSI, A., BINNS, C. W., DHALIWAL, S. S. & PAL, S. 2008. The acute effects of psyllium on postprandial lipaemia and thermogenesis in overweight and obese men. *Br J Nutr,* 99**,** 1068-75.

KIM, H. J. & WHITE, P. J. 2010. In Vitro Bile-Acid Binding and Fermentation of High, Medium, and Low Molecular Weight β-Glucan. *Journal of Agricultural and Food Chemistry,* 58**,** 628-634.

KIMURA, H., FUTAMI, Y., TARUI, S.-I. & SHINOMIYA, T. 1982. Activation of human pancreatic lipase activity by calcium and bile salts. *The Journal of Biochemistry,* 92**,** 243-251.

KONG, F. & SINGH, R. P. 2008. Disintegration of solid foods in human stomach. *Journal of food science,* 73**,** R67-R80.

KRISTENSEN, M. & JENSEN, M. G. 2011. Dietary fibres in the regulation of appetite and food intake. Importance of viscosity. *Appetite,* 56**,** 65-70.

KULP, K., OLEWNIK, M., LORENZ, K. & COLLINS, F. 1991. Starch Functionality in Cookie Systems. *Starch - Stärke,* 43**,** 53-57.

KUMAR, R. & KHATKAR, B. S. 2017. Thermal, pasting and morphological properties of starch granules of wheat (Triticum aestivum L.) varieties. *J Food Sci Technol,* 54**,** 2403-2410.

LAI, P., SHIAU, C. J. & WANG, C. C. 2012. Effects of oligosaccharides on phase transition temperatures and rheological characteristics of waxy rice starch dispersion. *Journal of the Science of Food and Agriculture,* 92**,** 1389-1394.

LAIRON, D., PLAY, B. & JOURDHEUIL-RAHMANI, D. 2007. Digestible and indigestible carbohydrates: interactions with postprandial lipid metabolism. *The Journal of Nutritional Biochemistry,* 18**,** 217-227.

LAMBO, A. M., OSTE, R. & NYMAN, M. 2005. Dietary fibre in fermented oat and barley beta-glucan rich concentrates. *Food Chemistry,* 89**,** 283-293.

LARROSA, S., LUQUE, V., GROTE, V., CLOSA-MONASTEROLO, R., FERRÉ, N., KOLETZKO, B., VERDUCI, E., GRUSZFELD, D., XHONNEUX, A. & ESCRIBANO, J. 2020. Fibre intake is associated with cardiovascular health in european children. *Nutrients,* 13**,** 12.

LATTIMER, J. M. & HAUB, M. D. 2010. Effects of dietary fiber and its components on metabolic health. *Nutrients,* 2**,** 1266-89.

LAZARIDOU, A. & BILIADERIS, C. G. 2007. Molecular aspects of cereal β-glucan functionality: Physical properties, technological applications and physiological effects. *Journal of Cereal Science,* 46**,** 101-118.

LAZARIDOU, A., BILIADERIS, C. G., MICHA-SCRETTAS, M. & STEELE, B. R. 2004. A comparative study on structure–function relations of mixed-linkage (1→3), (1→4) linear β-d-glucans. *Food Hydrocolloids,* 18**,** 837-855.

LEBLANC, N., SAIAH, R., BEUCHER, E., GATTIN, R., CASTANDET, M. & SAITER, J.-M. 2008. Structural investigation and thermal stability of new extruded wheat flour based polymeric materials. *Carbohydrate Polymers,* 73**,** 548-557.

LECLERE, L., VAN CUTSEM, P. & MICHIELS, C. 2013. Anti-cancer activities of pH- or heat-modified pectin. *Frontiers in Pharmacology,* 4.

LENTH, R. 2020. *emmeans: Estimated Marginal Means, aka Least-Squares Means* [Online]. Available: https://CRAN.R-project.org/package=emmeans [Accessed].

LENTLE, R. G. & JANSSEN, P. W. 2010. Manipulating digestion with foods designed to change the physical characteristics of digesta. *Crit Rev Food Sci Nutr,* 50**,** 130-45.

LEVER, M. 1972. A new reaction for colorimetric determination of carbohydrates. *Analytical biochemistry,* 47**,** 273-279.

LI, C.-Y., MENSE, A. L., BREWER, L. R., LAU, C. & SHI, Y.-C. 2017. In Vitro Bile Acid Binding Capacity of Wheat Bran with Different Particle Sizes. *Cereal Chemistry Journal,* 94**,** 654-658.

LI, Y., HU, M. & MCCLEMENTS, D. J. 2011. Factors affecting lipase digestibility of emulsified lipids using an in vitro digestion model: Proposal for a standardised pH-stat method. *Food Chemistry,* 126**,** 498-505.

LI, Y. & MCCLEMENTS, D. J. 2010. New Mathematical Model for Interpreting pH-Stat Digestion Profiles: Impact of Lipid Droplet Characteristics on in Vitro Digestibility. *Journal of Agricultural and Food Chemistry,* 58**,** 8085-8092.

LIA, A., ANDERSSON, H., MEKKI, N., JUHEL, C., SENFT, M. & LAIRON, D. 1997. Postprandial lipemia in relation to sterol and fat excretion in ileostomy subjects given oat-bran and wheat test meals. *Am J Clin Nutr,* 66**,** 357-65.

LIN, X. & WRIGHT, A. J. 2018. Pectin and gastric pH interactively affect DHA-rich emulsion in vitro digestion microstructure, digestibility and bioaccessibility. *Food hydrocolloids,* 76**,** 49-59.

LIU, H., ZHANG, M., MA, Q., TIAN, B., NIE, C., CHEN, Z. & LI, J. 2020. Health beneficial effects of resistant starch on diabetes and obesity via regulation of gut microbiota: a review. *Food & Function,* 11**,** 5749-5767.

LOPEZ-RUBIO, A., FLANAGAN, B. M., GILBERT, E. P. & GIDLEY, M. J. 2008. A novel approach for calculating starch crystallinity and its correlation with double helix content: A combined XRD and NMR study. *Biopolymers: Original Research on Biomolecules,* 89**,** 761-768.

LOVEGROVE, A., EDWARDS, C. H., DE NONI, I., PATEL, H., EL, S. N., GRASSBY, T., ZIELKE, C., ULMIUS, M., NILSSON, L., BUTTERWORTH, P. J., ELLIS, P. R. & SHEWRY, P. R. 2017. Role of polysaccharides in food, digestion, and health. *Crit Rev Food Sci Nutr,* 57**,** 237-253.

LUHALOO, M., MARTENSSON, A. C., ANDERSSON, R. & AMAN, P. 1998. Compositional analysis and viscosity measurements of commercial oat brans. *Journal of the Science of Food and Agriculture,* 76**,** 142-148.

MACIERZANKA, A., TORCELLO-GÓMEZ, A., JUNGNICKEL, C. & MALDONADO-VALDERRAMA, J. 2019. Bile salts in digestion and transport of lipids. *Advances in Colloid and Interface Science,* 274**,** 102045.

MACKIE, A. 2019. The Digestive Tract: A Complex System. *In:* GOUSETI, O., BORNHORST, G. M., BAKALIS, S. & MACKIE, A. (eds.) *Interdisciplinary Approaches to Food Digestion.* Cham: Springer International Publishing.

MADENCI, D. & EGELHAAF, S. U. 2010. Self-assembly in aqueous bile salt solutions. *Current Opinion in Colloid & Interface Science,* 15**,** 109-115.

MÄKELÄ, N., BRINCK, O. & SONTAG-STROHM, T. 2020. Viscosity of β-glucan from oat products at the intestinal phase of the gastrointestinal model. *Food Hydrocolloids,* 100**,** 105422.

MAKKI, K., DEEHAN, E. C., WALTER, J. & BACKHED, F. 2018. The Impact of Dietary Fiber on Gut Microbiota in Host Health and Disease. *Cell Host Microbe,* 23**,** 705-715.

MALDONADO-VALDERRAMA, J., MUROS-COBOS, J., HOLGADO-TERRIZA, J. & CABRERIZO-VÍLCHEZ, M. 2014. Bile salts at the air–water interface: adsorption and desorption. *Colloids and Surfaces B: Biointerfaces,* 120**,** 176-183.

MALDONADO-VALDERRAMA, J., WILDE, P., MACIERZANKA, A. & MACKIE, A. 2011. The role of bile salts in digestion. *Adv Colloid Interface Sci,* 165**,** 36-46.

MARASCA, E., BOULOS, S. & NYSTRÖM, L. 2020. Bile acid-retention by native and modified oat and barley β-glucan. *Carbohydrate Polymers,* 236**,** 116034.

MARCIANI, L., GOWLAND, P. A., SPILLER, R. C., MANOJ, P., MOORE, R. J., YOUNG, P., AL-SAHAB, S., BUSH, D., WRIGHT, J. & FILLERY-TRAVIS, A. J. 2000. Gastric response to increased meal viscosity assessed by echo-planar magnetic resonance imaging in humans. *The journal of nutrition,* 130**,** 122-127.

MARCIANI, L., GOWLAND, P. A., SPILLER, R. C., MANOJ, P., MOORE, R. J., YOUNG, P. & FILLERY-TRAVIS, A. J. 2001. Effect of meal viscosity and nutrients on satiety, intragastric dilution, and emptying assessed by MRI. *American Journal of Physiology-Gastrointestinal and Liver Physiology,* 280**,** G1227-G1233.

MARTÍNEZ, M., MOTILVA, M.-J., LÓPEZ DE LAS HAZAS, M.-C., ROMERO, M.-P., VACULOVA, K. & LUDWIG, I. A. 2018. Phytochemical composition and β-glucan content of barley genotypes from two different geographic origins for human health food production. *Food Chemistry,* 245**,** 61-70.

MAT, D. J. L., LE FEUNTEUN, S., MICHON, C. & SOUCHON, I. 2016. In vitro digestion of foods using pH-stat and the INFOGEST protocol: Impact of matrix structure on digestion kinetics of macronutrients, proteins and lipids. *Food Research International,* 88**,** 226-233.

MCCLEARY, B. V., DEVRIES, J. W., RADER, J. I., COHEN, G., PROSKY, L., MUGFORD, D. C., CHAMP, M. & OKUMA, K. 2010. Determination of total dietary fiber (CODEX definition) by enzymatic-gravimetric method and liquid chromatography: collaborative study. *J AOAC Int,* 93**,** 221-33.

MCCLEMENTS, D. J. 2000. Comments on viscosity enhancement and depletion flocculation by polysaccharides. *Food Hydrocolloids,* 14**,** 173-177.

MCDOUGALL, G. J., MORRISON, I. M., STEWART, D. & HILLMAN, J. R. 1996. Plant cell walls as dietary fibre: Range, structure, processing and function. *Journal of the Science of Food and Agriculture,* 70**,** 133-150.

MCRORIE, J. W. & CHEY, W. D. 2016. Fermented Fiber Supplements Are No Better Than Placebo for a Laxative Effect. *Dig Dis Sci,* 61**,** 3140-3146.

MCRORIE, J. W., JR. & MCKEOWN, N. M. 2017. Understanding the Physics of Functional Fibers in the Gastrointestinal Tract: An Evidence-Based Approach to Resolving Enduring Misconceptions about Insoluble and Soluble Fiber. *J Acad Nutr Diet,* 117**,** 251-264.

MENSINK, M. A., FRIJLINK, H. W., VAN DER VOORT MAARSCHALK, K. & HINRICHS, W. L. J. 2015. Inulin, a flexible oligosaccharide I: Review of its physicochemical characteristics. *Carbohydrate Polymers,* 130**,** 405-419.

MERTENS, K. L., KALSBEEK, A., SOETERS, M. R. & EGGINK, H. M. 2017. Bile Acid Signaling Pathways from the Enterohepatic Circulation to the Central Nervous System. *Front Neurosci,* 11**,** 617.

MEYER, J. H. & DOTY, J. 1988. GI transit and absorption of solid food: multiple effects of guar. *The American journal of clinical nutrition,* 48**,** 267-273.

MIEHLE, E., BADER-MITTERMAIER, S., SCHWEIGGERT-WEISZ, U., HAUNER, H. & EISNER, P. 2021. Effect of Physicochemical Properties of

Carboxymethyl Cellulose on Diffusion of Glucose. *Nutrients,* 13**,** 1398.

MINEKUS, M., ALMINGER, M., ALVITO, P., BALLANCE, S., BOHN, T., BOURLIEU, C., CARRIERE, F., BOUTROU, R., CORREDIG, M., DUPONT, D., DUFOUR, C., EGGER, L., GOLDING, M., KARAKAYA, S., KIRKHUS, B., LE FEUNTEUN, S., LESMES, U., MACIERZANKA, A., MACKIE, A., MARZE, S., MCCLEMENTS, D. J., MENARD, O., RECIO, I., SANTOS, C. N., SINGH, R. P., VEGARUD, G. E., WICKHAM, M. S., WEITSCHIES, W. & BRODKORB, A. 2014. A standardised static in vitro digestion method suitable for food - an international consensus. *Food Funct,* 5**,** 1113-24.

MOELANTS, K. R. N., CARDINAELS, R., VAN BUGGENHOUT, S., VAN LOEY, A. M., MOLDENAERS, P. & HENDRICKX, M. E. 2014. A Review on the Relationships between Processing, Food Structure, and Rheological Properties of Plant-Tissue-Based Food Suspensions. *Comprehensive Reviews in Food Science and Food Safety,* 13**,** 241-260.

MORGAN, L. M., TREDGER, J. A., SHAVILA, Y., TRAVIS, J. S. & WRIGHT, J. 1993. The effect of non-starch polysaccharide supplementation on circulating bile acids, hormone and metabolite levels following a fat meal in human subjects. *British Journal of Nutrition,* 70**,** 491-501.

MORIARTEY, S., TEMELLI, F. & VASANTHAN, T. 2010. Effect of Formulation and Processing Treatments on Viscosity and Solubility of Extractable Barley β-Glucan in Bread Dough Evaluated Under In Vitro Conditions. *Cereal Chemistry,* 87**,** 65-72.

MORRIS, E. R., CUTLER, A., ROSS-MURPHY, S., REES, D. & PRICE, J. 1981. Concentration and shear rate dependence of viscosity in random coil polysaccharide solutions. *Carbohydrate polymers,* 1**,** 5-21.

MULET-CABERO, A.-I., MACKIE, A. R., WILDE, P. J., FENELON, M. A. & BRODKORB, A. 2019. Structural mechanism and kinetics of in vitro gastric digestion are affected by process-induced changes in bovine milk. *Food Hydrocolloids,* 86**,** 172-183.

MULET-CABERO, A.-I., RIGBY, N. M., BRODKORB, A. & MACKIE, A. R. 2017. Dairy food structures influence the rates of nutrient digestion through different in vitro gastric behaviour. *Food Hydrocolloids,* 67**,** 63-73.

NAUMANN, S., SCHWEIGGERT-WEISZ, U., BADER-MITTERMAIER, S., HALLER, D. & EISNER, P. 2018. Differentiation of Adsorptive and Viscous Effects of Dietary Fibres on Bile Acid Release by Means of In Vitro Digestion and Dialysis. *Int J Mol Sci,* 19.

NAUMANN, S., SCHWEIGGERT-WEISZ, U., EGLMEIER, J., HALLER, D. & EISNER, P. 2019a. In Vitro Interactions of Dietary Fibre Enriched Food Ingredients with Primary and Secondary Bile Acids. *Nutrients,* 11.

NAUMANN, S., SCHWEIGGERT-WEISZ, U., HALLER, D. & EISNER, P. 2019b. Retention of Primary Bile Acids by Lupin Cell Wall Polysaccharides Under In Vitro Digestion Conditions. *Nutrients,* 11.

NILSSON, M., AMAN, P., HARKONEN, H., HALLMANS, G., KNUDSEN, K. E. B., MAZUR, W. & ADLERCREUTZ, H. 1997. Content of nutrients and lignans in roller milled fractions of rye. *Journal of the Science of Food and Agriculture,* 73**,** 143-148.

O'KEEFE, S. J. D. 2017. Can a change in diet change your cancer risk [abstract]. *Cancer Research,* 77(13 Suppl):Abstract nr SY17-03.

PABOIS, O., ANTOINE-MICHARD, A., ZHAO, X., OMAR, J., AHMED, F., ALEXIS, F., HARVEY, R. D., GRILLO, I., GERELLI, Y., GRUNDY, M. M., BAJKA, B., WILDE, P. J. & DREISS, C. A. 2020. Interactions of bile salts with a dietary fibre, methylcellulose, and impact on lipolysis. *Carbohydr Polym,* 231**,** 115741.

PÄLCHEN, K., VAN DEN WOUWER, B., DUIJSENS, D., HENDRICKX, M. E., VAN LOEY, A. & GRAUWET, T. 2022. Utilizing Hydrothermal Processing to Align Structure and In Vitro Digestion Kinetics between Three Different Pulse Types. *Foods,* 11**,** 206.

PARKER, M. L., NG, A. & WALDRON, K. W. 2005. The phenolic acid and polysaccharide composition of cell walls of bran layers of mature wheat (Triticum aestivum L. cv. Avalon) grains. *Journal of the Science of Food and Agriculture,* 85**,** 2539-2547.

PARKER, R., RIGBY, N. M., RIDOUT, M. J., GUNNING, A. P. & WILDE, P. J. 2014. The adsorption-desorption behaviour and structure function relationships of bile salts. *Soft Matter,* 10**,** 6457-66.

PASQUIER, B., ARMAND, M., GUILLON, F., CASTELAIN, C., BOREL, P., BARRY, J.-L., PLERONI, G. & LAIRON, D. 1996. Viscous soluble dietary fibers alter emulsification and lipolysis of triacylglycerols in duodenal medium in vitro. *The Journal of Nutritional Biochemistry,* 7**,** 293-302.

PEDERSEN, A., BARDOW, A., JENSEN, S. B. & NAUNTOFTE, B. 2002. Saliva and gastrointestinal functions of taste, mastication, swallowing and digestion. *Oral Diseases,* 8**,** 117-129.

PEREZ-MORAL, N., PLANKEELE, J.-M., DOMONEY, C. & WARREN, F. J. 2018. Ultra-high performance liquid chromatography-size exclusion chromatography (UPLC-SEC) as an efficient tool for the rapid and highly informative characterisation of biopolymers. *Carbohydrate Polymers,* 196**,** 422-426.

PÉREZ, S. & BERTOFT, E. 2010. The molecular structures of starch components and their contribution to the architecture of starch granules: A comprehensive review. *Starch‐Stärke,* 62**,** 389-420.

PERRY, P. & DONALD, A. 2002. The effect of sugars on the gelatinisation of starch. *Carbohydrate Polymers,* 49**,** 155-165.

PETROPOULOU, K., SALT, L. J., EDWARDS, C. H., WARREN, F. J., GARCIA-PEREZ, I., CHAMBERS, E. S., ALSHAALAN, R., KHATIB, M., PEREZ-MORAL, N., CROSS, K. L., KELLINGRAY, L., STANLEY, R., KOEV, T., KHIMYAK, Y. Z., NARBAD, A., PENNEY, N., SERRANO-CONTRERAS, J. I., CHARALAMBIDES, M. N., MIGUENS BLANCO, J., CASTRO SEOANE, R., MCDONALD, J. A. K., MARCHESI, J. R., HOLMES, E., GODSLAND, I. F., MORRISON, D. J., PRESTON, T., DOMONEY, C., WILDE, P. J. & FROST, G. S. 2020. A natural mutation in Pisum sativum L. (pea) alters starch assembly and improves glucose homeostasis in humans. *Nature Food,* 1**,** 693-704.

PEYRON, M.-A., MISHELLANY, A. & WODA, A. 2004. Particle Size Distribution of Food Boluses after Mastication of Six Natural Foods. *Journal of Dental Research,* 83**,** 578-582.

PICOUT, D. R. & ROSS-MURPHY, S. B. 2003. Rheology of biopolymer solutions and gels. *TheScientificWorldJOURNAL,* 3**,** 105-121.

PILOSOF, A. M. R. 2017. Potential impact of interfacial composition of proteins and polysaccharides stabilized emulsions on the modulation of lipolysis. The role of bile salts. *Food Hydrocolloids,* 68**,** 178-185.

PINHEIRO, J., BATES, D., DEBROY, S., SARKAR, D., HEISTERKAMP, S., VAN WILLIGEN, B. & MAINTAINER, R. 2017. Package 'nlme'. *Linear and nonlinear mixed effects models, version,* 3.

POUTANEN, K. S., FISZMAN, S., MARSAUX, C. F. M., PENTIKAINEN, S. P., STEINERT, R. E. & MELA, D. J. 2018. Recommendations for characterization and reporting of dietary fibers in nutrition research. *Am J Clin Nutr*.

QUEENAN, K. M., STEWART, M. L., SMITH, K. N., THOMAS, W., FULCHER, R. G. & SLAVIN, J. L. 2007. Concentrated oat β-glucan, a fermentable fiber, lowers serum cholesterol in hypercholesterolemic adults in a randomized controlled trial. *Nutrition Journal,* 6**,** 6.

RAKHA, A., AMAN, P. & ANDERSSON, R. 2011. How does the preparation of rye porridge affect molecular weight distribution of extractable dietary fibers? *Int J Mol Sci,* 12**,** 3381-93.

RAMÍREZ, C., MILLON, C., NUNEZ, H., PINTO, M., VALENCIA, P., ACEVEDO, C. & SIMPSON, R. 2015. Study of effect of sodium alginate on potato starch digestibility during in vitro digestion. *Food Hydrocolloids,* 44**,** 328-332.

RANAWANA, V., MONRO, J. A., MISHRA, S. & HENRY, C. J. K. 2010. Degree of particle size breakdown during mastication may be a possible cause of interindividual glycemic variability. *Nutrition Research,* 30**,** 246-254.

RAO, M. A. 2007. Introduction: Food Rheology and Structure. *In:* RAO, M. A. (ed.) *Rheology of Fluid and Semisolid Foods: Principles and Applications.* Boston, MA: Springer US.

RAYNER, M., ÖSTBRING, K. & PURHAGEN, J. 2016. Application of Natural Polymers in Food. *Natural Polymers.*

REPIN, N., CUI, S. W. & GOFF, H. D. 2018. Rheological behavior of dietary fibre in simulated small intestinal conditions. *Food Hydrocolloids,* 76**,** 216-225.

REPIN, N., KAY, B. A., CUI, S. W., WRIGHT, A. J., DUNCAN, A. M. & DOUGLAS GOFF, H. 2017. Investigation of mechanisms involved in postprandial glycemia and insulinemia attenuation with dietary fibre consumption. *Food Funct,* 8**,** 2142-2154.

REYNOLDS, A., MANN, J., CUMMINGS, J., WINTER, N., METE, E. & TE MORENGA, L. 2019. Carbohydrate quality and human health: a series of systematic reviews and meta-analyses. *The Lancet,* 393**,** 434-445.

RIEDER, A., KNUTSEN, S. H. & BALLANCE, S. 2017. In vitro digestion of beta-glucan rich cereal products results in extracts with physicochemical and rheological behavior like pure beta-glucan solutions – A basis for increased understanding of in vivo effects. *Food Hydrocolloids,* 67**,** 74-84.

RIGAUD, D., PAYCHA, F., MEULEMANS, A., MERROUCHE, M. & MIGNON, M. 1998. Effect of psyllium on gastric emptying, hunger feeling and food intake in normal volunteers: a double blind study. *European Journal of Clinical Nutrition,* 52**,** 239-245.

ROBERTSON, J., EASTWOOD, M. A., ANDERSON, R., MITCHELL, W. D. & POCOCK, S. 1976. A Method to Measure the Adsorption of Bile Salts to Vegetable Fiber of Differing Water Holding Capacity. *The Journal of Nutrition,* 106**,** 1429-1432.

ROBERTSON, J., MAJSAK-NEWMAN, G., RING, S. & SELVENDRAN, R. 1997. Solubilisation of mixed linkage (1→ 3),(1→ 4) β-D-glucans from

barley: Effects of cooking and digestion. *Journal of Cereal Science,* 25**,** 275-283.

ROBERTSON, J. A., DE MONREDON, F. D., DYSSELER, P., GUILLON, F., AMADO, R. & THIBAULT, J.-F. 2000. Hydration Properties of Dietary Fibre and Resistant Starch: a European Collaborative Study. *LWT - Food Science and Technology,* 33**,** 72-79.

RODER, N., GERARD, C., VEREL, A., BOGRACHEVA, T. Y., HEDLEY, C. L., ELLIS, P. R. & BUTTERWORTH, P. J. 2009. Factors affecting the action of α-amylase on wheat starch: Effects of water availability. An enzymic and structural study. *Food Chemistry,* 113**,** 471-478.

ROHRER, J. S. 2021. Chapter 4 - High-performance anion-exchange chromatography with pulsed amperometric detection for carbohydrate and glycoconjugate analyses. *In:* EL RASSI, Z. (ed.) *Carbohydrate Analysis by Modern Liquid Phase Separation Techniques (Second Edition).* Amsterdam: Elsevier.

RONKART, S. N., DEROANNE, C., PAQUOT, M., FOUGNIES, C. & BLECKER, C. S. 2010. Impact of the crystallisation pathway of inulin on its mono-hydrate to hemi-hydrate thermal transition. *Food Chemistry,* 119**,** 317-322.

ROOS, Y. 2003. Thermal analysis, state transitions and food quality. *Journal of Thermal Analysis and Calorimetry,* 71**,** 197-203.

ROSA-SIBAKOV, N., MÄKELÄ, N., AURA, A.-M., SONTAG-STROHM, T. & NORDLUND, E. 2020. In vitro study for investigating the impact of decreasing the molecular weight of oat bran dietary fibre components on the behaviour in small and large intestine. *Food & function,* 11**,** 6680-6691.

SAITO, D., NAKAJI, S., FUKUDA, S., SHIMOYAMA, T., SAKAMOTO, J. & SUGAWARA, K. 2005. Comparison of the amount of pectin in the human terminal ileum with the amount of orally administered pectin. *Nutrition,* 21**,** 914-919.

SÁNCHEZ, A., MACEIRAS, R., CANCELA, A. & RODRÍGUEZ, M. 2012. Influence of n-hexane on in situ transesterification of marine macroalgae. *Energies,* 5**,** 243-257.

SANDBERG, A.-S., AHDERINNE, R., ANDERSSON, H., HALLGREN, B. & HULTÉN, L. 1983. The effect of citrus pectin on the absorption of nutrients in the small intestine. *Human nutrition. Clinical nutrition,* 37**,** 171-183.

SARKAR, A., YE, A. & SINGH, H. 2016. On the role of bile salts in the digestion of emulsified lipids. *Food Hydrocolloids,* 60**,** 77-84.

SAYAR, S., JANNINK, J.-L. & WHITE, P. J. 2005. In Vitro Bile Acid Binding of Flours from Oat Lines Varying in Percentage and Molecular Weight Distribution of β-Glucan. *Journal of Agricultural and Food Chemistry,* 53**,** 8797-8803.

SCHALLER-POVOLNY, L. A., SMITH, D. E. & LABUZA, T. P. 2000. Effect of water content and molecular weight on the moisture isotherms and glass transition properties of inulin. *International Journal of Food Properties,* 3**,** 173-192.

SELVENDRAN, R. R. & ROBERTSON, J. A. 1990. *THE CHEMISTRY OF DIETARY FIBER - AN HOLISTIC VIEW OF THE CELL-WALL MATRIX*.

SEOW, C., CHEAH, P. & CHANG, Y. 1999. Antiplasticization by water in reduced-moisture food systems. *Journal of food science,* 64**,** 576-581.

SHELAT, K. J., VILAPLANA, F., NICHOLSON, T. M., GIDLEY, M. J. & GILBERT, R. G. 2011. Diffusion and rheology characteristics of barley mixed linkage β-glucan and possible implications for digestion. *Carbohydrate Polymers,* 86**,** 1732-1738.

SHELAT, K. J., VILAPLANA, F., NICHOLSON, T. M., WONG, K. H., GIDLEY, M. J. & GILBERT, R. G. 2010. Diffusion and viscosity in arabinoxylan solutions: Implications for nutrition. *Carbohydrate Polymers,* 82**,** 46-53.

SLAUGHTER, S. L., ELLIS, P. R., JACKSON, E. C. & BUTTERWORTH, P. J. 2002. The effect of guar galactomannan and water availability during hydrothermal processing on the hydrolysis of starch catalysed by pancreatic alpha-amylase. *Biochimica Et Biophysica Acta-General Subjects,* 1571**,** 55-63.

SLAVIN, J. 2013. Fiber and prebiotics: mechanisms and health benefits. *Nutrients,* 5**,** 1417-35.

SPIES, R. & HOSENEY, R. 1982. Effect of sugars on starch gelatinization.

STEPHEN, A. M., CHAMP, M. M., CLORAN, S. J., FLEITH, M., VAN LIESHOUT, L., MEJBORN, H. & BURLEY, V. J. 2017. Dietary fibre in Europe: current state of knowledge on definitions, sources, recommendations, intakes and relationships to health. *Nutr Res Rev,* 30**,** 149-190.

STRIEGEL, A. M. 2017. Chapter 10 - Size-exclusion chromatography. *In:* FANALI, S., HADDAD, P. R., POOLE, C. F. & RIEKKOLA, M.-L. (eds.) *Liquid Chromatography (Second Edition).* Elsevier.

TAKAGAKI, R., ISHIDA, Y., SADAKIYO, T., TANIGUCHI, Y., SAKURAI, T., MITSUZUMI, H., WATANABE, H., FUKUDA, S. & USHIO, S. 2018. Effects of isomaltodextrin in postprandial lipid kinetics: Rat study and human randomized crossover study. *PLoS One,* 13**,** e0196802.

TEAM, R. C. 2013. R: A language and environment for statistical computing.

TERRETT, O. M. & DUPREE, P. 2019. Covalent interactions between lignin and hemicelluloses in plant secondary cell walls. *Current Opinion in Biotechnology,* 56**,** 97-104.

TIMM, D., WILLIS, H., THOMAS, W., SANDERS, L., BOILEAU, T. & SLAVIN, J. 2011. The use of a wireless motility device (SmartPill®) for the measurement of gastrointestinal transit time after a dietary fibre intervention. *British Journal of Nutrition,* 105**,** 1337-1342.

TORCELLO-GÓMEZ, A. & FOSTER, T. J. 2016. Influence of interfacial and bulk properties of cellulose ethers on lipolysis of oil-in-water emulsions. *Carbohydrate Polymers,* 144**,** 495-503.

TOSH, S. M., BRUMMER, Y., MILLER, S. S., REGAND, A., DEFELICE, C., DUSS, R., WOLEVER, T. M. S. & WOOD, P. J. 2010. Processing Affects the Physicochemical Properties of β-Glucan in Oat Bran Cereal. *Journal of Agricultural and Food Chemistry,* 58**,** 7723-7730.

TOSH, S. M. & YADA, S. 2010. Dietary fibres in pulse seeds and fractions: Characterization, functional attributes, and applications. *Food Research International,* 43**,** 450-460.

TSATSARAGKOU, K., METHVEN, L., CHATZIFRAGKOU, A. & RODRIGUEZ-GARCIA, J. 2021. The Functionality of Inulin as a Sugar Replacer in Cakes and Biscuits; Highlighting the Influence of Differences in Degree of Polymerisation on the Properties of Cake Batter and Product. *Foods,* 10**,** 951.

TUNCEL, A., CORBIN, K. R., AHN-JARVIS, J., HARRIS, S., HAWKINS, E., SMEDLEY, M. A., HARWOOD, W., WARREN, F. J., PATRON, N. J. &

SMITH, A. M. 2019. Cas9-mediated mutagenesis of potato starch-branching enzymes generates a range of tuber starch phenotypes. *Plant Biotechnology Journal,* 17**,** 2259-2271.

TUNGLAND, B. C. & MEYER, D. 2002. Nondigestible Oligo- and Polysaccharides (Dietary Fiber): Their Physiology and Role in Human Health and Food. *Comprehensive Reviews in Food Science and Food Safety,* 3**,** 90-109.

U.S. FOOD AND DRUG ADMINISTRATION, F. 2018. Review of the Scientific Evidence on the Physiological Effects of Certain Non-Digestible Carbohydrates. *In:* U.S. DEPARTMENT OF HEALTH AND HUMAN SERVICES, O. O. N. A. F. L., CENTER FOR FOOD SAFETY AND APPLIED NUTRITION (ed.).

U.S. FOOD AND DRUG ADMINISTRATION, F. 2021. *Questions and Answers on Dietary Fiber* [Online]. Available: https://www.fda.gov/food/food-labeling-nutrition/questions-and-answers-dietary-fiber [Accessed 24 July 2022 2022].

URDANETA, V. & CASADESÚS, J. 2017. Interactions between bacteria and bile salts in the gastrointestinal and hepatobiliary tracts. *Frontiers in medicine,* 4**,** 163.

VAN DER SMAN, R. & MAUER, L. J. 2019. Starch gelatinization temperature in sugar and polyol solutions explained by hydrogen bond density. *Food hydrocolloids,* 94**,** 371-380.

VUKSAN, V., JENKINS, A. L., ROGOVIK, A. L., FAIRGRIEVE, C. D., JOVANOVSKI, E. & LEITER, L. A. 2011. Viscosity rather than quantity of dietary fibre predicts cholesterol-lowering effect in healthy individuals. *Br J Nutr,* 106**,** 1349-52.

WALDRON, K. W., PARKER, M. L. & SMITH, A. C. 2003. Plant Cell Walls and Food Quality. *Comprehensive Reviews in Food Science and Food Safety,* 2**,** 128-146.

WALKER, A. R. 1961. Crude fibre, bowel motility, and pattern of diet. *South African medical journal = Suid-Afrikaanse tydskrif vir geneeskunde,* 35**,** 114-5.

WANDERS, A. J., FESKENS, E. J., JONATHAN, M. C., SCHOLS, H. A., DE GRAAF, C. & MARS, M. 2014. Pectin is not pectin: a randomized trial on the effect of different physicochemical properties of dietary fiber on appetite and energy intake. *Physiol Behav,* 128**,** 212-9.

WANDERS, A. J., JONATHAN, M. C., VAN DEN BORNE, J. J., MARS, M., SCHOLS, H. A., FESKENS, E. J. & DE GRAAF, C. 2013. The effects of bulking, viscous and gel-forming dietary fibres on satiation. *Br J Nutr,* 109**,** 1330-7.

WANDERS, A. J., VAN DEN BORNE, J. J., DE GRAAF, C., HULSHOF, T., JONATHAN, M. C., KRISTENSEN, M., MARS, M., SCHOLS, H. A. & FESKENS, E. J. 2011. Effects of dietary fibre on subjective appetite, energy intake and body weight: a systematic review of randomized controlled trials. *Obes Rev,* 12**,** 724-39.

WANG, J., WANG, Y., WANG, X., ZHANG, D., WU, S. & ZHANG, G. 2016. Enhanced thermal stability of lichenase from Bacillus subtilis 168 by SpyTag/SpyCatcher-mediated spontaneous cyclization. *Biotechnology for biofuels,* 9**,** 1-9.

WANG, Q. & ELLIS, P. R. 2014. Oat beta-glucan: physico-chemical characteristics in relation to its blood-glucose and cholesterol-lowering properties. *Br J Nutr,* 112 Suppl 2**,** S4-S13.

WANG, Q., ELLIS, P. R. & ROSS-MURPHY, S. B. 2008. Dissolution kinetics of water-soluble polymers: The guar gum paradigm. *Carbohydrate Polymers,* 74**,** 519-526.

WANG, S., CHAO, C., HUANG, S. & YU, J. 2020. Phase Transitions of Starch and Molecular Mechanisms. *In:* WANG, S. (ed.) *Starch Structure, Functionality and Application in Foods.* Singapore: Springer Singapore.

WANG, S., WANG, S., LIU, L., WANG, S. & COPELAND, L. 2017a. Structural orders of wheat starch do not determine the in vitro enzymatic digestibility. *Journal of Agricultural and Food Chemistry,* 65**,** 1697-1706.

WANG, Y., HARDING, S. V., THANDAPILLY, S. J., TOSH, S. M., JONES, P. J. H. & AMES, N. P. 2017b. Barley beta-glucan reduces blood cholesterol levels via interrupting bile acid metabolism. *Br J Nutr,* 118**,** 822-829.

WARREN, F. J., BUTTERWORTH, P. J. & ELLIS, P. R. 2013. The surface structure of a complex substrate revealed by enzyme kinetics and Freundlich constants for α-amylase interaction with the surface of starch. *Biochimica et Biophysica Acta (BBA) - General Subjects,* 1830**,** 3095-3101.

WARREN, F. J., GIDLEY, M. J. & FLANAGAN, B. M. 2016. Infrared spectroscopy as a tool to characterise starch ordered structure—a joint FTIR–ATR, NMR, XRD and DSC study. *Carbohydrate Polymers,* 139**,** 35-42.

WARREN, F. J., ROYALL, P. G., GAISFORD, S., BUTTERWORTH, P. J. & ELLIS, P. R. 2011. Binding interactions of α-amylase with starch granules: The influence of supramolecular structure and surface area. *Carbohydrate Polymers,* 86**,** 1038-1047.

WEITKUNAT, K., STUHLMANN, C., POSTEL, A., RUMBERGER, S., FANKHANEL, M., WOTING, A., PETZKE, K. J., GOHLKE, S., SCHULZ, T. J., BLAUT, M., KLAUS, S. & SCHUMANN, S. 2017. Short-chain fatty acids and inulin, but not guar gum, prevent diet-induced obesity and insulin resistance through differential mechanisms in mice. *Sci Rep,* 7**,** 6109.

WHELAN, W. 1960. The Action Patterns of α-Amylases. *Starch-Stärke,* 12**,** 358-364.

WICKHAM, H., CHANG, W. & WICKHAM, M. H. 2016. Package 'ggplot2'. *Create elegant data visualisations using the grammar of graphics. Version,* 2**,** 1-189.

WILDE, P. J., GARCIA-LLATAS, G., LAGARDA, M. J., HASLAM, R. P. & GRUNDY, M. M. L. 2019. Oat and lipolysis: Food matrix effect. *Food Chemistry,* 278**,** 683-691.

WILLIAMS, B. A., GRANT, L. J., GIDLEY, M. J. & MIKKELSEN, D. 2017. Gut Fermentation of Dietary Fibres: Physico-Chemistry of Plant Cell Walls and Implications for Health. *Int J Mol Sci,* 18.

WOOD, P. J. 2011. Oat beta-glucan: properties and function. *Oats: Chemistry and Technology.* 2nd ed.: AACC.

WOOD, P. J., WEISZ, J., FEDEC, P. & BURROWS, V. D. 1989. Large-scale preparation and properties of oat fractions enriched in (1-3)(1-4)-β-D-glucan. *Cereal Chemistry,* 66**,** 97-103.

WOODBURY, T. J., LUST, A. L. & MAUER, L. J. 2021. The effects of commercially available sweeteners (sucrose and sucrose replacers)

on wheat starch gelatinization and pasting, and cookie baking. *Journal of Food Science,* 86**,** 687-698.

XIE, C., JONES, K. L., RAYNER, C. K. & WU, T. 2020. Enteroendocrine hormone secretion and metabolic control: importance of the region of the gut stimulation. *Pharmaceutics,* 12**,** 790.

YE, Z., CAO, C., LIU, Y., CAO, P. & LI, Q. 2018. Digestion fates of different edible oils vary with their composition specificities and interactions with bile salts. *Food Research International,* 111**,** 281-290.

ZACHERL, C., EISNER, P. & ENGEL, K.-H. 2011. In vitro model to correlate viscosity and bile acid-binding capacity of digested water-soluble and insoluble dietary fibres. *Food Chemistry,* 126**,** 423-428.

ZANGENBERG, N. H., MÜLLERTZ, A., KRISTENSEN, H. G. & HOVGAARD, L. 2001. A dynamic in vitro lipolysis model: I. Controlling the rate of lipolysis by continuous addition of calcium. *European Journal of Pharmaceutical Sciences,* 14**,** 115-122.

ZHAI, H., GUNNESS, P. & GIDLEY, M. J. 2016. Effects of cereal soluble dietary fibres on hydrolysis of p-nitrophenyl laurate by pancreatin. *Food & function,* 7**,** 3382-3389.

ZHAI, H., GUNNESS, P. & GIDLEY, M. J. 2020. Barley β-glucan effects on emulsification and in vitro lipolysis of canola oil are modulated by molecular size, mixing method, and emulsifier type. *Food Hydrocolloids,* 103.

ZHAI, H., GUNNESS, P. & GIDLEY, M. J. 2021. Depletion and bridging flocculation of oil droplets in the presence of β-glucan, arabinoxylan and pectin polymers: Effects on lipolysis. *Carbohydrate Polymers,* 255**,** 117491.

ZHANG, J. X., HALLMANS, G., ANDERSSON, H., BOSAEUS, I., AMAN, P., TIDEHAG, P., STENLING, R., LUNDIN, E. & DAHLGREN, S. 1992. EFFECT OF OAT BRAN ON PLASMA-CHOLESTEROL AND BILE-ACID EXCRETION IN 9 SUBJECTS WITH ILEOSTOMIES. *American Journal of Clinical Nutrition,* 56**,** 99-105.

ZHANG, Y., YU, J., WANG, X., DURACHKO, D. M., ZHANG, S. & COSGROVE, D. J. 2021a. Molecular insights into the complex mechanics of plant epidermal cell walls. *Science,* 372**,** 706-711.

ZHANG, Z., FAN, X., MA, H., LI, C., LI, E. & GILBERT, R. G. 2021b. Characterization of the baking-induced changes in starch molecular and crystalline structures in sugar-snap cookies. *Carbohydrate Polymers,* 256**,** 117518.

ZIEGLER, J. U., STEINER, D., LONGIN, C. F. H., WÜRSCHUM, T., SCHWEIGGERT, R. M. & CARLE, R. 2016. Wheat and the irritable bowel syndrome – FODMAP levels of modern and ancient species and their retention during bread making. *Journal of Functional Foods,* 25**,** 257-266.

ZIELKE, C., LU, Y. & NILSSON, L. 2019. Aggregation and microstructure of cereal β-glucan and its association with other biomolecules. *Colloids and Surfaces A: Physicochemical and Engineering Aspects,* 560**,** 402-409.

ZOBEL, H. F. 1984. Gelatinization of starch and mechanical properties of starch pastes. *Starch: chemistry and technology.* Elsevier.

# Appendices

# Appendix to Chapter 3

### A3.1 Pilot study: DF interference with lipolysis using pH-stat and rheology

A pilot study to test the conditions of a 6% O/W emulsion digested together with bran samples containing 200 mg BG using the pH-stat technique as described in section 3.2.2.3. In the presence of oat bran, lipid digestions were slower over the course of one hour compared to barley bran (Appendix figure A3.1). The mixing rate used in the reaction vessel was adjusted per sample to ensure digesta mixing despite differences in viscosity.
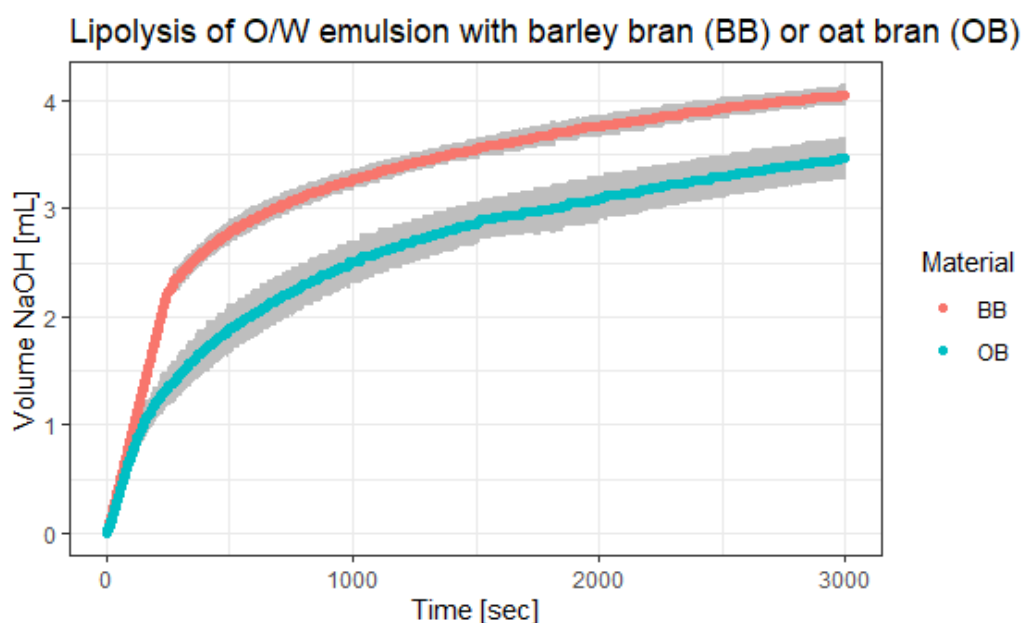


*Appendix figure A3.1 – Lipid digestion of a 6 % O/W emulsion in presence of barley (BB) or oat bran (OB) with 200 mg BG content over 1 hour -pilot study (n=3).*

## A3.1.1. Whole digesta vs supernatant rheology

As the mixing rate would affect the enzyme and substrate dispersion but sufficient mixing is needed with the pH-stat technique to ensure pH measurement across the digesta, an attempt was made to adjust the fibre quantity to align the viscosity between oat and barley. The whole digesta viscosity varied more between replicates, whereas the supernatant viscosity was very consistent with less shear thinning than the whole digesta viscosity (Appendix figure A3.2). Both, whole digesta and supernatant viscosity were higher in oat bran. It was decided to normalise the bran starting weight of the two different cereal brans for BG content as aiming for the same viscosity would be shear dependent.
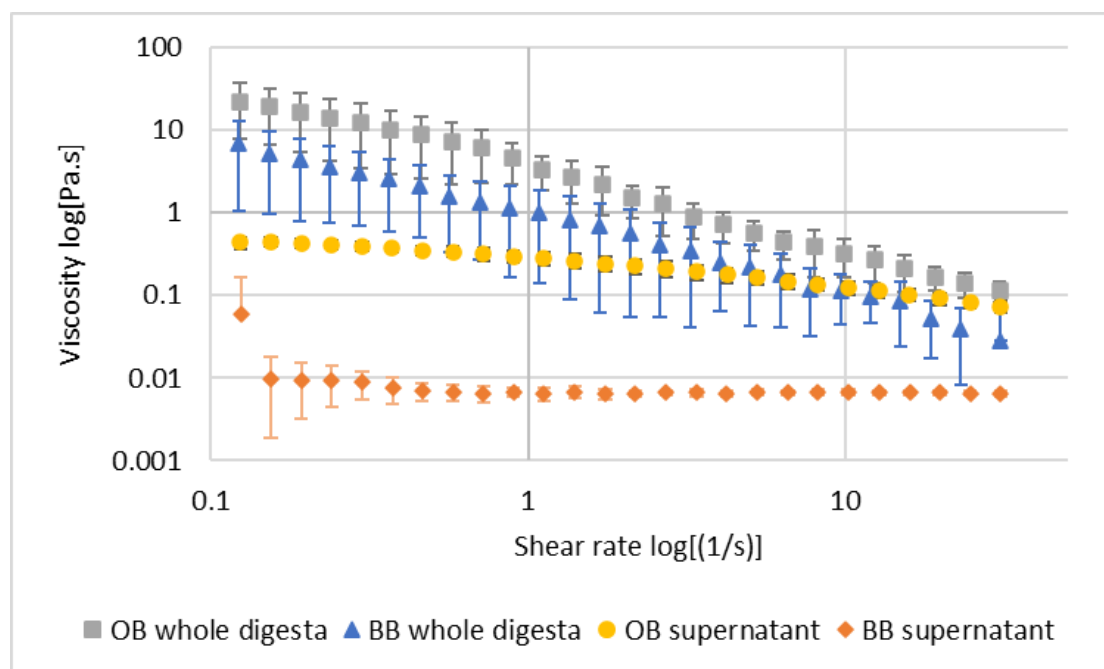


*Appendix figure A3.2 – Apparent viscosity (log[Pa.s]) over a shear rate ramp from 0.1 to 31 [log(s⁻¹)] of digested barley (BB) and oat bran (OB) comparing viscosities of same sample whole digesta vs supernatant.*

## A3.2    FFA release of emulsion controls

Different amounts of emulsion controls in the absence of DF had a final FFA release after 2 hours between 65 and 80% (Appendix figure A3.3) which is in line with the literature for a canola oil emulsion stabilised with WPI after 2 hours lipid digestion (Zhai *et al.* 2020, Zhai *et al.* 2021). Only the emulsion control containing 30 mg lipid had >100% FFA release, which may be due to a specific enzyme to substrate ratio, similarly to the highest concentration of lipase in a study by Li *et al.* which led to a 120% digestion (Li *et al.* 2011).
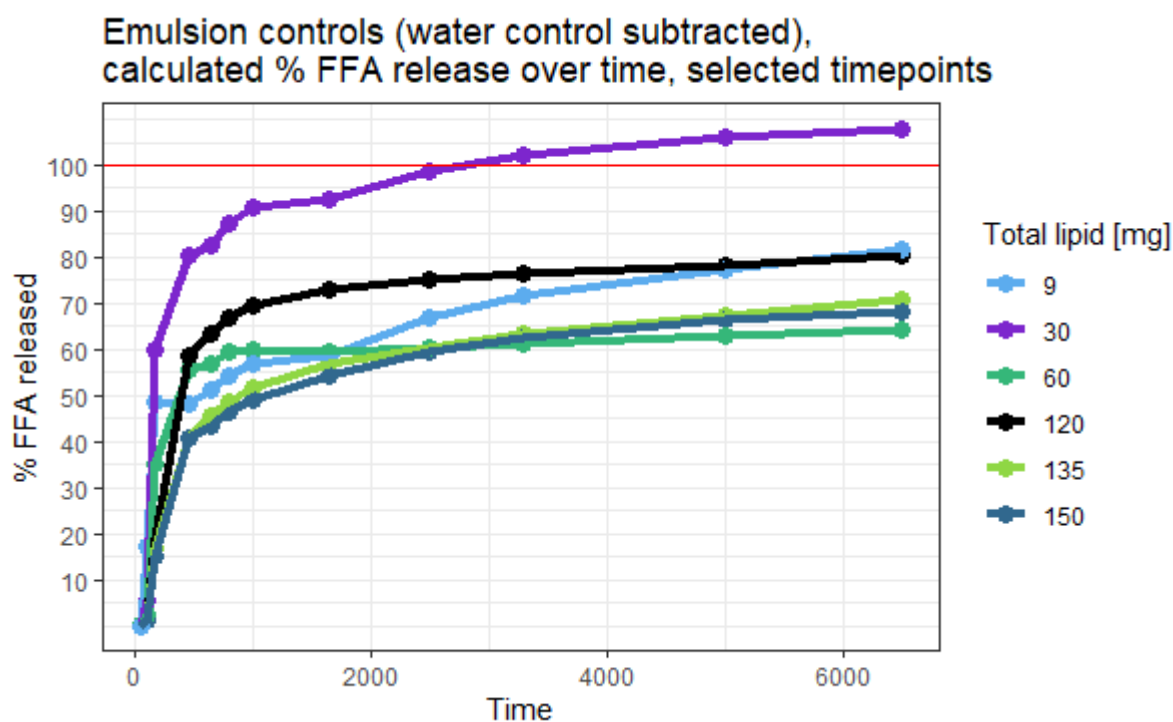


*Appendix figure A3.3 – FFA release (%) over time (sec) of emulsion controls calculated using Equation 3.3 per timepoint (mean of n = 3).*

## A3.3 Lipase activity in presence of bile acids at different mixing regimes

Lipase activity in the absence of fibre but with added bile acids (see method description in section 2.3.2.4) increased linearly with increasing mixing rate and started to plateau at the highest mixing speeds (Appendix figure A3.4, Appendix table A3.1).

*Appendix table A3.1 – Lipase activity of pancreatic lipase in presence of bile acids and absence of fibre, values are mean and standard deviations.*

| Material | BG content (mg) | Mixing (RPM) | Bile acids present | Lipase activity (U/mg pancreatin) | Standard deviation |
|---|---|---|---|---|---|
| Lipase activity assay solution | 0 | 200 | Yes | 36.75 | 5.98 |
| Lipase activity assay solution | 0 | 350 | Yes | 56.00 | 6.50 |
| Lipase activity assay solution | 0 | 520 | Yes | 72.63 | 6.33 |
| Lipase activity assay solution | 0 | 700 | Yes | 78.33 | 0.58 |
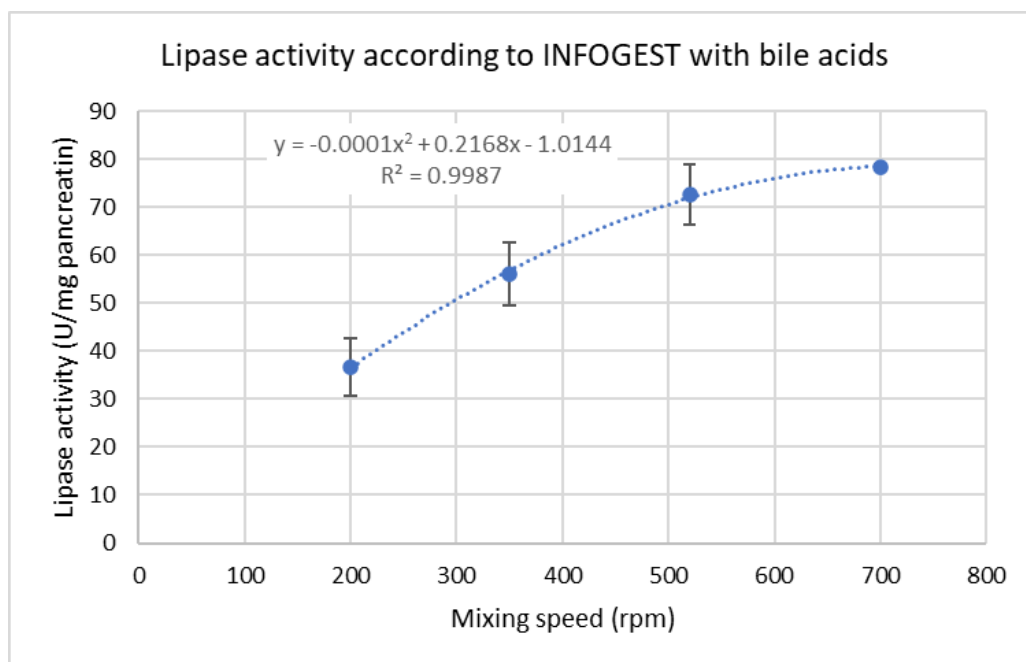
*Appendix figure A3.4 – Lipase activity of pancreatic lipase (U/mg pancreatin) assay according to INFOGEST protocol with bile acids at different mixing speeds of 200, 350, 520 and 700 RMP, mean +/- SD, n=at least 3.*

# Appendix to Chapter 4

## A4.1 Pilot studies dialysis model: method development

### A4.1.1 Fibre materials

Initial experiments were conducted on fibres materials different from the ones used in the main thesis. Wheat bran flakes (Neil's Yard Wholefoods, Holland & Barrett International Ltd., UK) and oat bran flakes (medium cut and fine cut; White's Speedicook Ltd., UK) were obtained locally from a grocery store. Oat flakes (whole oat flakes) were from the Belinda variety, BG90 (90% purified oat BG), both described earlier (Grundy *et al.* 2017b). Barley bran flakes from hulled barley, variety Tipple, was a gift from NIAB in Cambridge.

### A4.1.2 Results

Pilot studies showed that hydration of samples and the presence of the soluble phase together with the insoluble fibre component were important for a bile acid/fibre interaction. Hence fibre materials were hydrated overnight and then the hydrated fibres together with the hydration solution were mixed with a bovine bile solution. As shown in Appendix figure A4.1, compared to control in absence of fibre, BAs were released slower through the dialysis membrane in presence of the different hydrated cereal fibres. The difference between the DF sample and the negative control was statistically significant at 2 h for oat bran, at 6 h for oat bran and wheat bran, at 8 h for oat bran, wheat bran and oat flakes and at 24 h for oat bran and wheat bran. None of the timepoints for barley bran showed

statistically significant results versus negative control. Cholestyramine, used as positive control, is a resin which strongly binds BAs, hence very effectively retained BAs from diffusing through the dialysis membrane, which was significantly different from the negative control at all timepoints except at 0.5 h.

To see what role the insoluble and the soluble part of fibre play in BA retention, oat flakes were hydrated overnight, centrifuged and the pellet and supernatant tested separately in the dialysis model (Appendix figure A4.2). As displayed in Appendix figure A4.2, no BA retention was found. The pellet seemed to retain BAs in the dialysis bag slightly after 8 hours but the difference was not statistically significant compared to the negative control. Purified BG (called BG90) in a 1% solution had the same BA release as negative control. The supernatant of the oat flake overnight hydration did not retain BAs either, in line with purified BG (BG90).
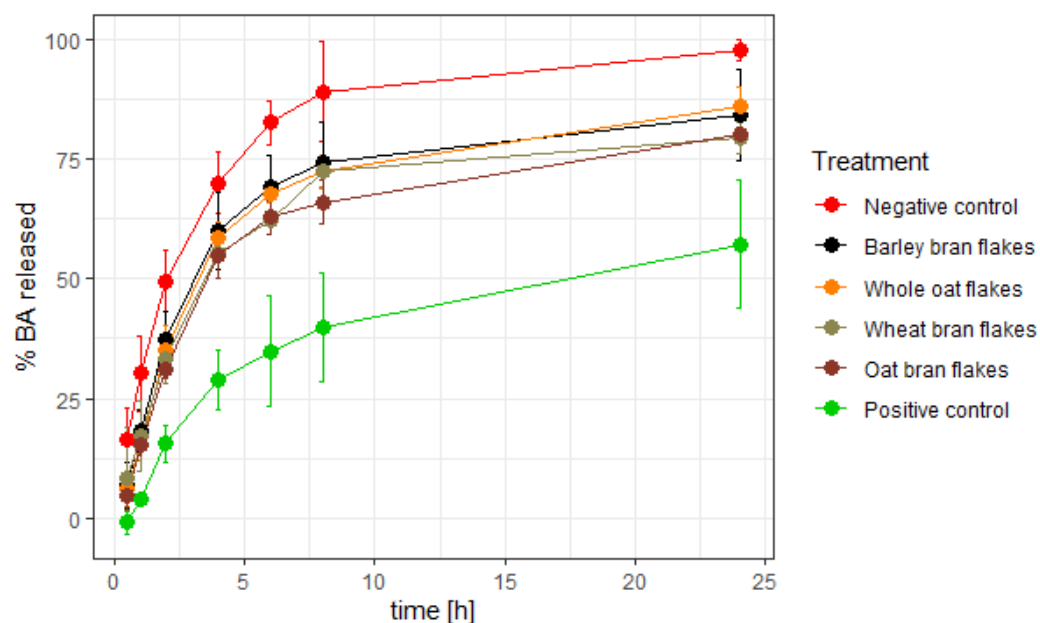
*Appendix figure A4.1 – Bile acid released (%) over time in presence of the treatments: Whole oat flakes, oat bran flakes, wheat bran flakes, barley bran flakes = 10 % hydrated samples with hydration solution kept, 1 % cholestyramine (positive control) or no treatment (10 mM bile acid only, negative control); dialysis started after 1 h incubation with bile (n=3).*
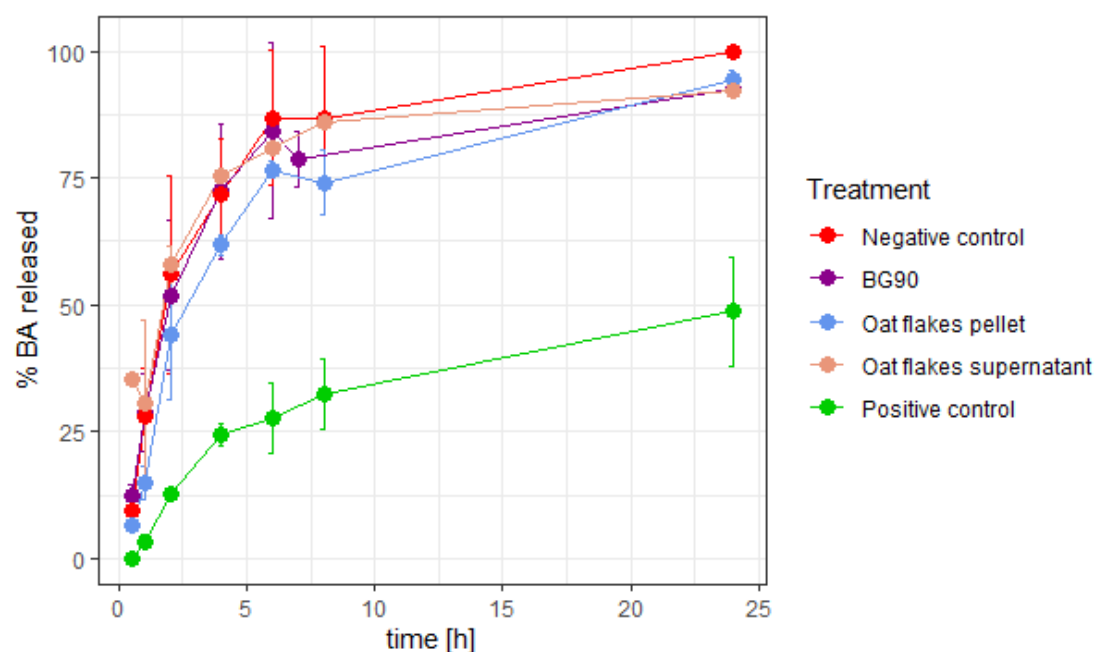


*Appendix figure A4.2 – Bile acid released (%) over time in presence of 10 % hydrated whole oat flakes pellet without hydration solution and whole oat flakes hydration solution (supernatant), 1 % cholestyramine (positive control) or no treatment (10 mM bile acid only, negative control); dialysis started after 1 h incubation with bile (n=2).*

An *in vitro* digestion protocol like the INFOGEST consortium (Minekus *et al.* 2014) follows a rigorous dilution and timed steps through the different phases of oral, gastric and intestinal digestion and was seen as a good standardised way of hydration. Appendix figure A4.3 shows that digested oat bran flakes decreased the BA release over time, whereas hydrated oat bran flakes without enzymes retained BAs only slightly from 8 hours onwards with 23 to 25 % of the BAs still entrapped after 20h inside the dialysis membrane. In absence of fibre (negative control) all BAs were released after 20 h. Interestingly, bovine bile extract with enzymes did show the same extent of retention as hydrated oat bran flakes after 20 hours with 23% of BAs still entrapped as OBC (Appendix figure A4.3). Cholestyramine (positive control) very effectively retained BAs from diffusing through a dialysis membrane, irrespective of whether digestive enzymes were present or not.

The pilot tests showed the importance of hydration and solubilisation of dietary fibre and highlighted a potential synergistic effect of soluble and insoluble dietary fibre.
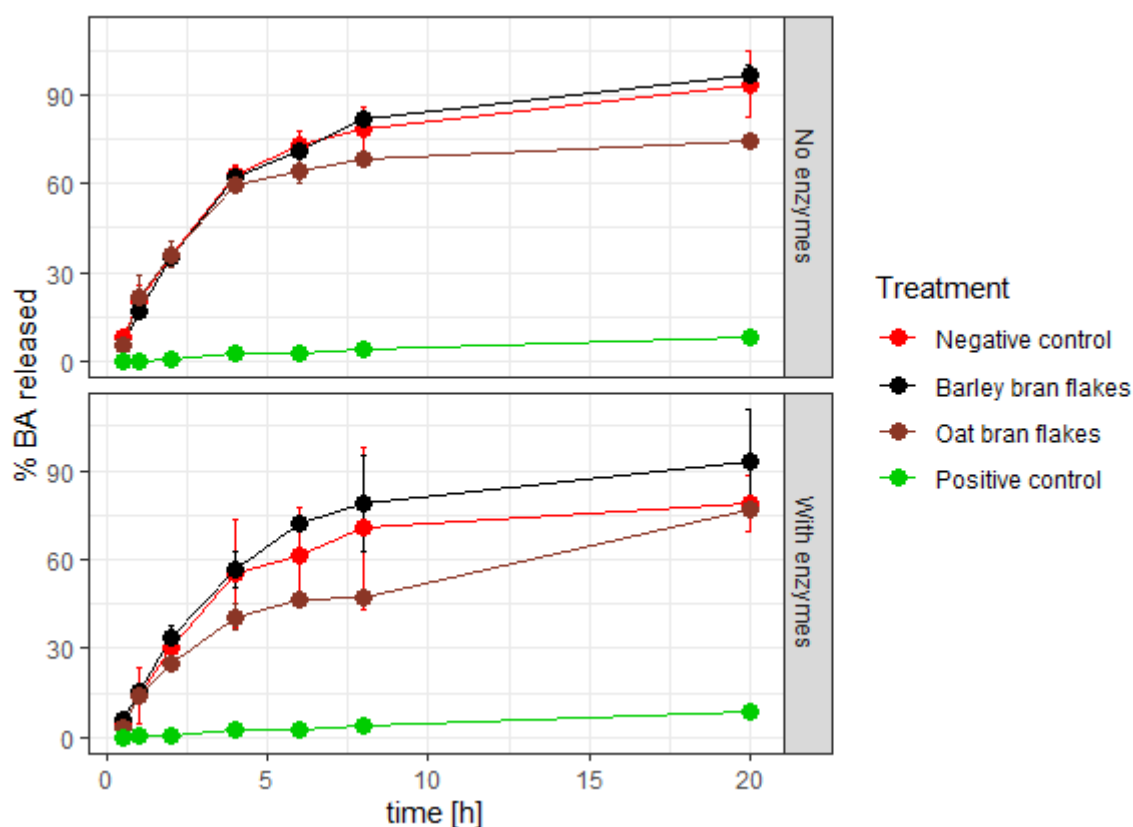
*Appendix figure A4.3 – Bile acid released (%) over time in an in vitro dialysis model after simulated digestion hydration (no enzymes) and simulated digestion (with enzymes) over time with bovine bile extract only (negative control), oat bran flakes and barley bran flakes and cholestyramine (positive control). Samples were taken at 0.5, 1, 2, 4, 6, 8 and 20 hours (n=2 for oat bran flakes, n=3 for all other treatments).*

## A4.2 Analytical BG extracts purity

Analytical extracts from barley bran and oat bran (see section 2.2.2) were analysed for their BG content as described in section 2.3.12 with results as listed in Appendix table A4.1.

*Appendix table A4.1 – β-glucan (BG) content of extracts from oat bran (OB) and barley bran (BB) with 3 different extraction protocols (protocol codes in brackets), mean of n = 2, standard deviation (SD).*

| Analytical extracts | BG (%w/w) | SD |
|---|---|---|
| Oat bran (OB) BG extract ('P1') | 67.03 | 0.04 |
| Barley bran (BB) BG extract ('P1') | 72.01 | 7.50 |
| Oat bran (OB) BG extract ('P2(B)') | 62.91 | 0.46 |
| Barley bran (BB) BG extract ('P2(B)') | 69.35 | 5.77 |
| Oat bran (OB) BG extract ('P3') | 64.28 | 2.12 |
| Barley bran (BB) BG extract ('P3') | 66.47 | 3.29 |

## A4.3    BG size distribution using SEC

The smallest BG standard (Mw 36500 Da) eluted at the same time (45 min) (Appendix figure A4.4) as the smallest Pullulan standard (maltose, Mw 356 Da) (Appendix figure A4.5). The differences in elution time get closer at the high Mw standards. BG standard with a Mw of 650K Da elutes off at 31 min close to the Pullulan standard with a Mw of 700K Da at 25 min. The calibration was based on the Mark-Houwink relation (see section 2.3.4) using the Mark-Houwink parameters of pullulan in DMSO at 90 °C (K = 0.0002427 dL g$^{-1}$ and α = 0.6804) because the corresponding parameters for BG in DMSO were not known. Mark-Houwink parameter of BG in an aqueous system were reported as 0.6 for α and 0.178 dL g$^{-1}$ for K with random coil conformation (Ballance *et al.* 2022). Therefore, SEC size distribution results were used to make qualitative comparison between samples.
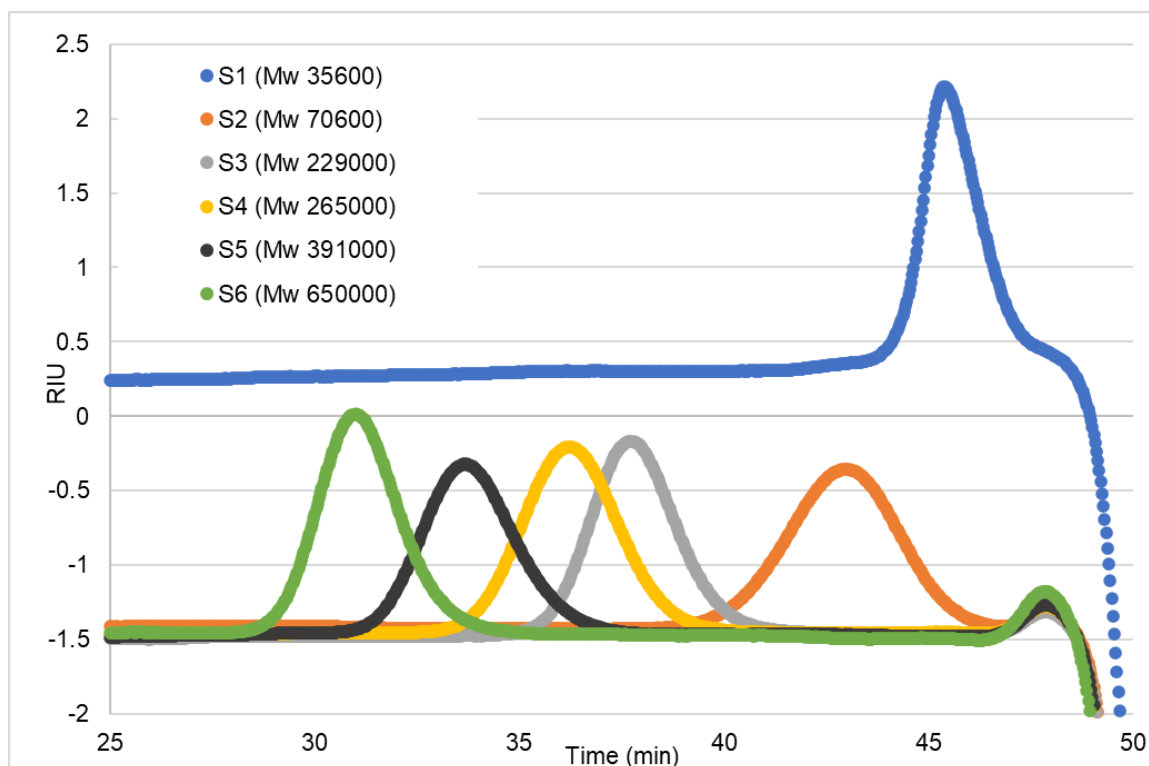
*Appendix figure A4.4 – BG Mw standards RI elution profiles with weight average molecular weight (as reported in the data sheet of P-MWBGS, Megazyme, 06/19) indicated per standard (S).*
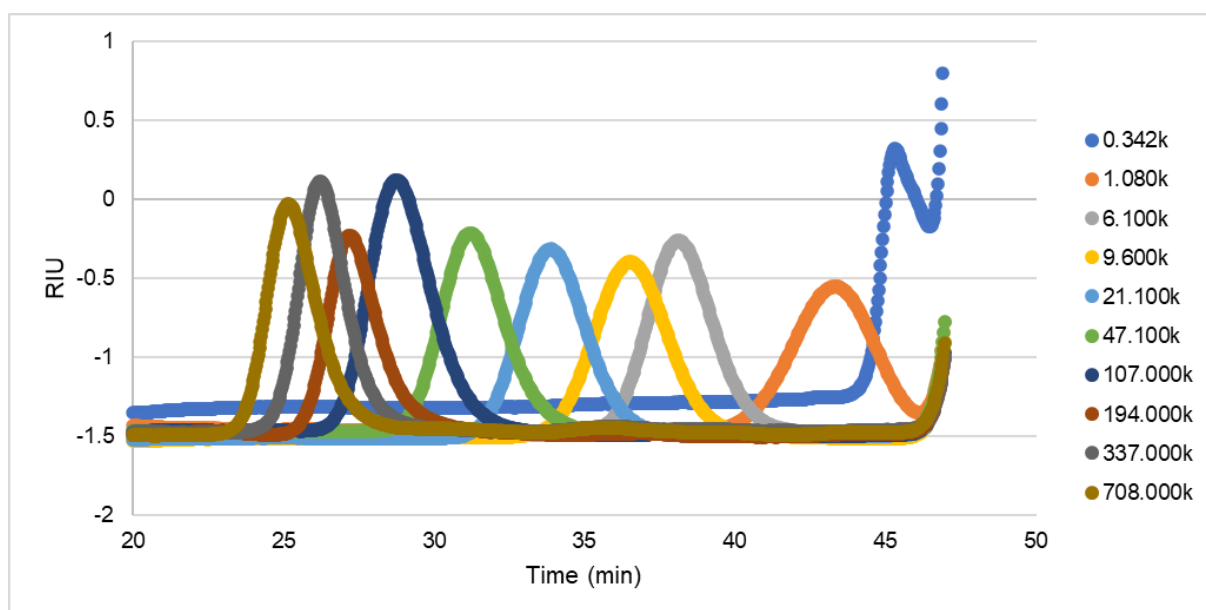


*Appendix figure A4.5 – Pullulan Mw standards RI elution profiles with weight average molecular weight (as reported by manufacturer) indicated in the legend.*

## A4.4 Cholyl-Lysyl-Fluorescein confocal microscopy
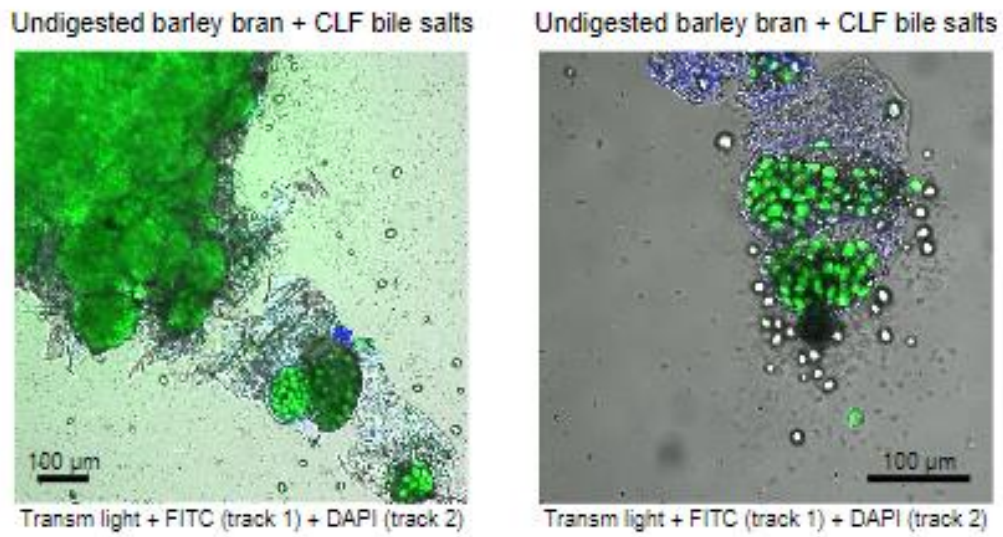


*Appendix figure A4.6 – Undigested barley bran showing a high affinity of CLF to starch (confocal microscopy overlay of transmitted light and FITC channel (track 1) and DAPI channel (track2).*
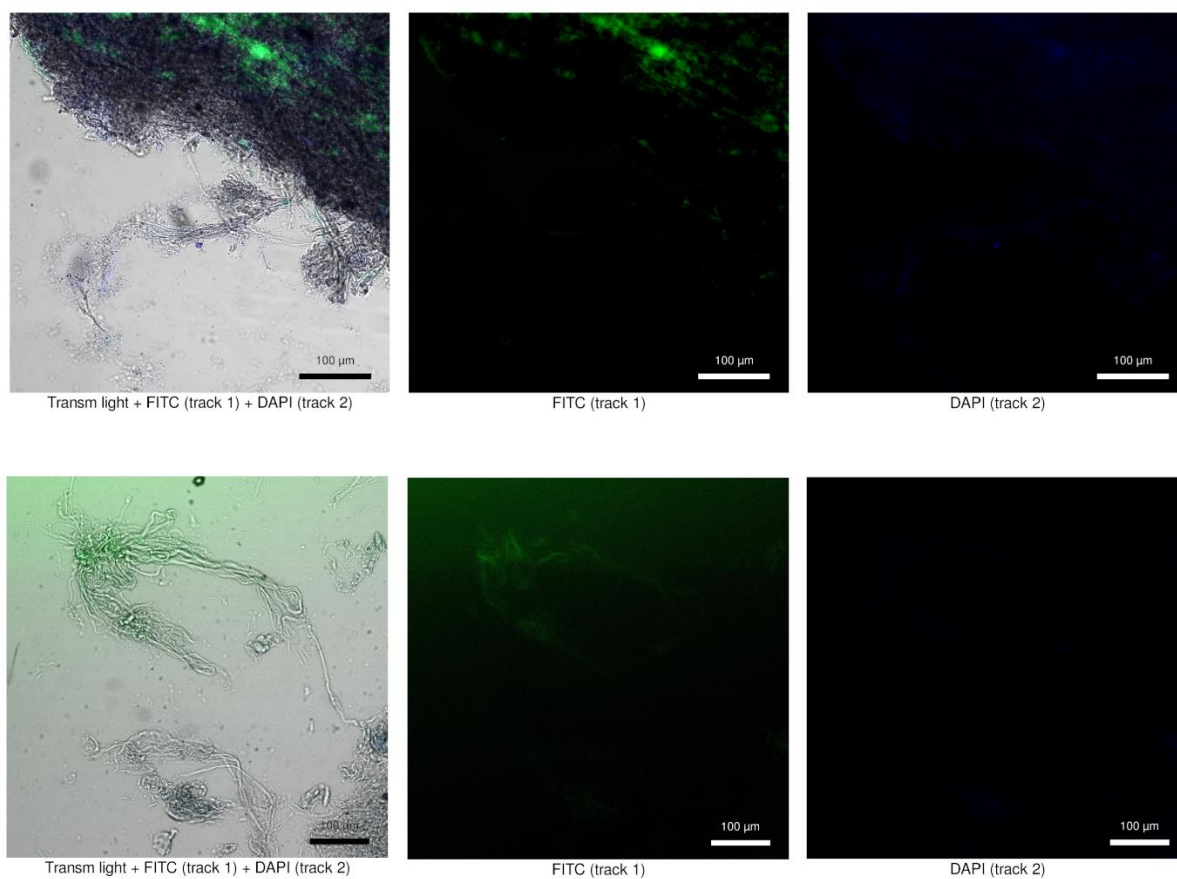
Appendix figure A4.7 – Pancreatin incubated with CLF and imaged using confocal microscopy, left: overlay of transmitted light and FITC channel (track 1) and DAPI channel (track2), middle: FITC (track 1), right: DAPI (track2).

# Appendix to Chapter 5

*Appendix table A5.1 – Sample overview of biscuit model systems containing fibre analysed using DSC*

| Water % | Fibre % | Starch (mg) | Su-crose (mg) | Water (µl) | Fibre (mg) | Tested fibres sample names |
|---|---|---|---|---|---|---|
| 75.0 | 2.5 | 125 | 100 | 750 | 25 | BG, Cellulose, Insoluble inulin (crystalline), Soluble inulin (crystalline) |
| 72.5 | 5.0 | 125 | 100 | 725 | 50 | BG, Cellulose, Insoluble inulin (crystalline), Soluble inulin (crystalline) |
| 70.0 | 7.5 | 125 | 100 | 700 | 75 | Cellulose, Insoluble inulin (crystalline), Soluble inulin (crystalline) |
| 67.5 | 10.0 | 125 | 100 | 675 | 100 | BG, Cellulose, Insoluble inulin (crystalline), Soluble inulin (crystalline) |
| 65.0 | 12.5 | 125 | 100 | 650 | 125 | BG, Cellulose, Insoluble inulin (crystalline), Soluble inulin (crystalline) |
| 62.5 | 15.0 | 125 | 100 | 625 | 150 | BG, Cellulose, Insoluble inulin (crystalline), Soluble inulin (crystalline) |
| 57.5 | 20.0 | 125 | 100 | 575 | 200 | BG, Cellulose, Insoluble inulin (crystalline), Soluble inulin (crystalline) |
| 52.5 | 25.0 | 125 | 100 | 525 | 250 | Cellulose |
| 47.5 | 30.0 | 125 | 100 | 475 | 300 | Cellulose, Insoluble inulin (crystalline), Insoluble inulin (solubilised), Soluble inulin (solubilised), Soluble inulin (crystalline) |
| 32.5 | 45.0 | 125 | 100 | 325 | 450 | Insoluble inulin (solubilised), Soluble inulin (solubilised) |
| 22.5 | 55.0 | 125 | 100 | 225 | 550 | Insoluble inulin (solubilised), Soluble inulin (solubilised) |

*Appendix table A5.2 – Sample overview of biscuit model system in absence of fibre ('no fibre control') analysed using DSC*

| Water % | Wheat starch (mg) | Su- crose (mg) | Water (µl) | Fibre (mg) | Sample names |
|---|---|---|---|---|---|
| 75.0 | 125 | 100 | 675 | 0 | No fibre control (crystalline sucrose), No fibre control (solubilised sucrose) |
| 72.5 | 125 | 100 | 593 | 0 | No fibre control (crystalline sucrose), No fibre control (solubilised sucrose) |
| 70.0 | 125 | 100 | 525 | 0 | No fibre control (crystalline sucrose), No fibre control (solubilised sucrose) |
| 67.5 | 125 | 100 | 468 | 0 | No fibre control (crystalline sucrose), No fibre control (solubilised sucrose) |
| 57.5 | 125 | 100 | 304 | 0 | No fibre control (crystalline sucrose), No fibre control (solubilised sucrose) |
| 47.5 | 125 | 100 | 204 | 0 | No fibre control (crystalline sucrose), No fibre control (solubilised sucrose) |
| 32.5 | 125 | 100 | 108 | 0 | No fibre control (crystalline sucrose), No fibre control (solubilised sucrose) |
| 22.5 | 125 | 100 | 65 | 0 | No fibre control (crystalline sucrose), No fibre control (solubilised sucrose) |
| 17.5 | 125 | 100 | 48 | 0 | No fibre control (crystalline sucrose), No fibre control (solubilised sucrose) |
| 12.5 | 125 | 100 | 32 | 0 | No fibre control (crystalline sucrose), No fibre control (solubilised sucrose) |
| 7.5 | 125 | 100 | 18 | 0 | No fibre control (crystalline sucrose), No fibre control (solubilised sucrose) |

*Appendix table A5.3 – Inulin biscuit recipes*

| Method: AACC 10-53 modified with | 10% inulin in stage 3 (inulin moisture adjusted, inulin = dw) | | 19% inulin in stage 3 (not adjusted to inulin moisture, inulin = ww) | | 20% inulin in stage 3 (inulin moisture adjusted, inulin = dw) | | 20% inulin in stage 2 (inulin moisture adjusted, inulin = dw) | |
|---|---|---|---|---|---|---|---|---|
| Number of biscuits | 8 | | 8 | | 8 | | 8 | |
| Flour moisture | 13.00 | | 13.00 | | 13.00 | | 13.00 | |
| Inulin moisture | 5.00 | | 5.00 | | 5.00 | | 5.00 | |
| **Ingredient/Stage** | | | | | | | | |
| **Stage 1** | **g** | **%** | **g** | **%** | **g** | **%** | **g** | **%** |
| Nonfat Dry Milk | 2.25 | 0.48 | 2.25 | 0.48 | 2.25 | 0.48 | 2.25 | 0.48 |
| Salt | 2.81 | 0.60 | 2.81 | 0.60 | 2.81 | 0.60 | 2.81 | 0.60 |
| Sodium bicarbonate | 2.25 | 0.48 | 2.25 | 0.48 | 2.25 | 0.48 | 2.25 | 0.48 |
| Caster sugar | 77.90 | 16.67 | 62.00 | 13.26 | 62.00 | 13.26 | 62.00 | 13.26 |
| Fat (palm oil) | 90.00 | 19.25 | 90.00 | 19.25 | 90.00 | 19.25 | 90.00 | 19.25 |
| INULIN | 0.00 | 0.00 | 0.00 | 0.00 | 0.00 | 0.00 | 0.00 | 0.00 |
| **Stage 2** | | | | | | | | |
| Ammonium Bicarbonate | 1.13 | 0.24 | 1.13 | 0.24 | 1.13 | 0.24 | 1.13 | 0.24 |
| Water (distilled) | 49.50 | 10.59 | 49.50 | 10.59 | 49.50 | 10.59 | 49.50 | 10.59 |
| additional water (distilled) | 2.14 | 0.46 | 9.20 | 1.97 | 4.28 | 0.92 | 4.28 | 0.92 |
| INULIN | 0.00 | 0.00 | 0.00 | 0.00 | 0.00 | 0.00 | 98.42 | 21.06 |
| **Stage 3** | | | | | | | | |
| Flour | 190.20 | 40.69 | 154.80 | 33.12 | 154.80 | 33.12 | 154.80 | 33.12 |
| INULIN | 49.26 | 10.54 | 93.50 | 20.00 | 98.42 | 21.06 | 0.00 | 0.00 |
| TOTAL BATCH | 467.44 | 100.0 | 467.44 | 100.0 | 467.44 | 100.0 | 467.44 | 100.0 |
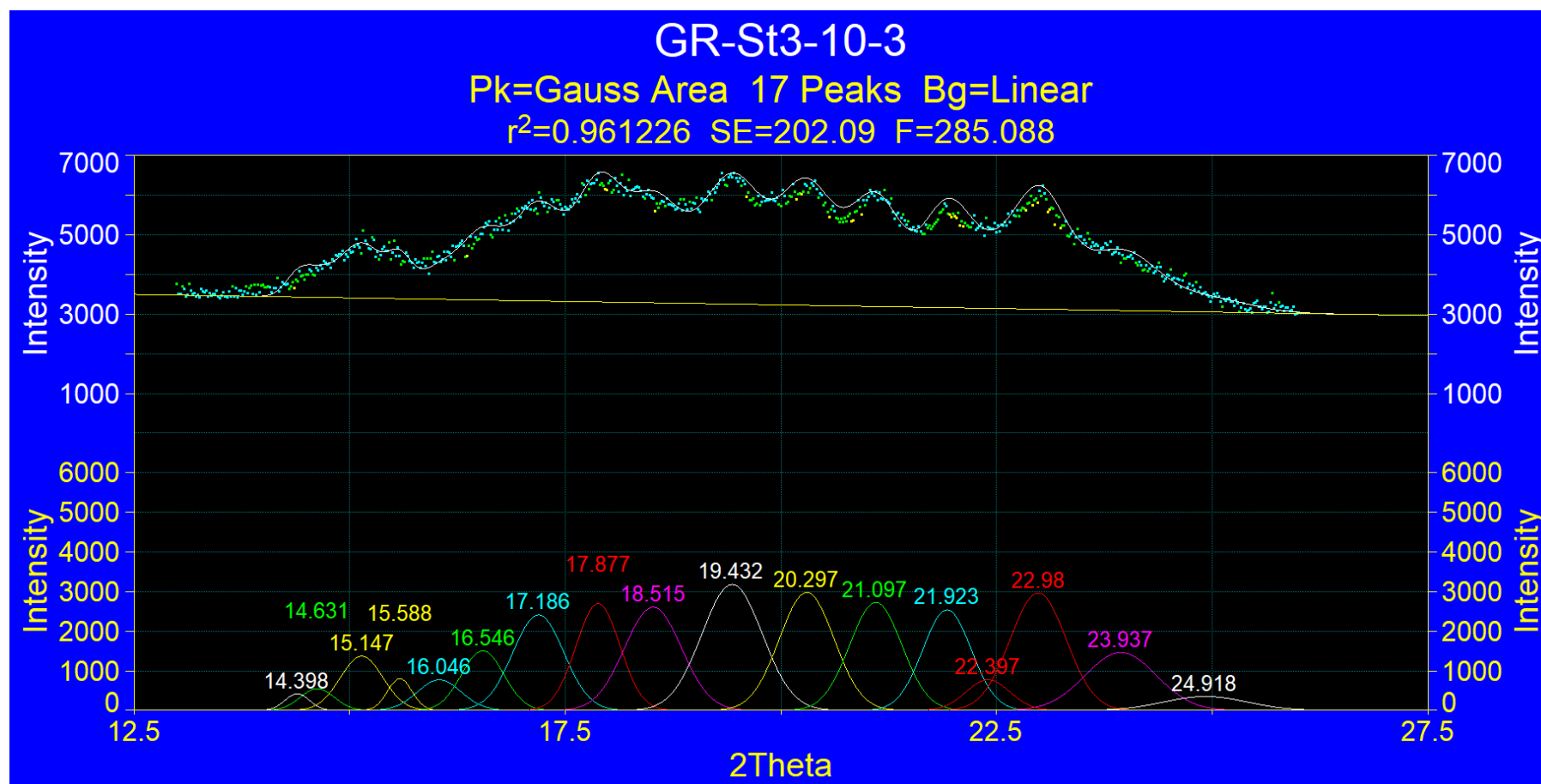
*Appendix figure A5.1 – Diffractogram peak deconvolution using Peakfit on the example of 10% soluble inulin biscuit, batch number 3. Starch crystallinity peaks (as identified from raw biscuit flour) selected were between 15° and 15.25° (starch peak 1), between 17° and 17.3° (starch peak 2) and between 22.8° and 23° (starch peak 3).*
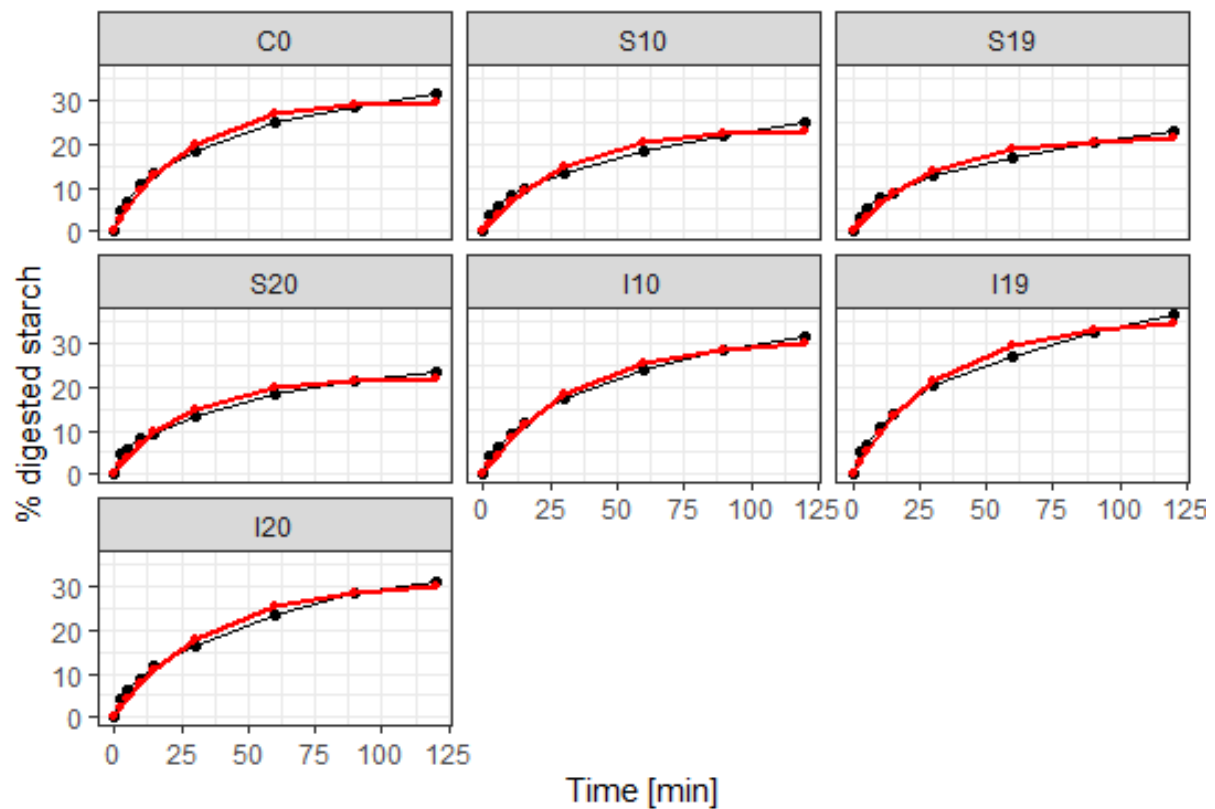
*Appendix figure A5.2 – Model fit comparison: mean values of % digested starch per recipe measured per timepoint in black vs predicted per timepoint according to the fitted model (Equation 5.2) in red.*

# Appendix to Chapter 6

## A6.1 Overnight hydration imaging with barley and oat bran particle

To investigate the hydration over time of barley and oat bran, a few particles of bran flour were mixed with calcofluor  stain (containing Evans blue) and immediately transferred onto a microscopy slide to image the start of the hydration (Appendix figure A6.1). Images were taken every minute over a time span of 150 min (not shown) as well as after an overnight hydration, as shown in Appendix figure A6.1. On the next day, oat bran had expanded and was surrounded by thicker layers of BG (stained in blue) as compared to BB. This indicated differences between the two cereal brans in the release of BG from the cell wall.
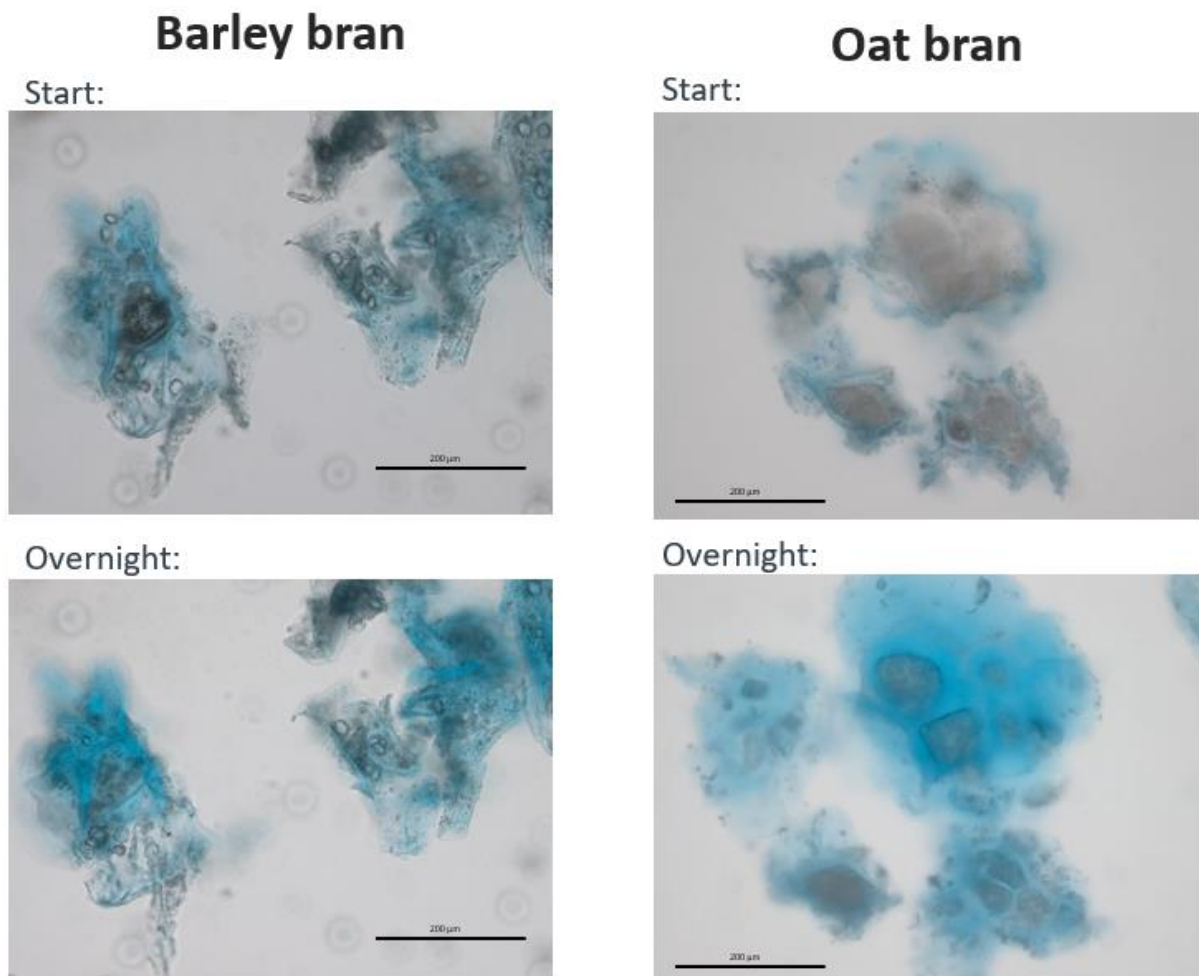
*Appendix figure A6.1 – Images taken at the start of the hydration (upper images) and after an overnight incubation (lower images) of barley bran (left) and oat bran (right) with a BX60 wide-field microscope, stain: calcofluor + Evans blue*